

UNIVERSIDAD COMPLUTENSE DE MADRID
FACULTAD DE MEDICINA
Departamento de Fisiología



TESIS DOCTORAL

Papel de la lipotoxicidad y la disfunción mitocondrial en las alteraciones cardiacas y metabólicas asociadas a la obesidad

Rol of lipotoxicity and mitochondrial dysfunction in cardiac and metabolic alterations associated with obesity

MEMORIA PARA OPTAR AL GRADO DE DOCTOR

PRESENTADA POR

Gema Marín Royo

Directores

Victoria Cachafeiro Ramos
María Luaces Méndez
Ernesto Martínez Martínez

Madrid 2019

Universidad Complutense de Madrid

Facultad de Medicina

Departamento de Fisiología



**PAPEL DE LA LIPOTOXICIDAD Y LA DISFUNCIÓN
MITOCONDRIAL EN LAS ALTERACIONES CARDIACAS Y
METABÓLICAS ASOCIADAS A LA OBESIDAD**

Memoria presentada por GEMA MARÍN ROYO, para optar al grado de doctor por la Universidad Complutense de Madrid, con mención internacional.

Directores de la tesis:

Dra. Victoria Cachofeiro Ramos

Dra. María Luaces Méndez

Dr. Ernesto Martínez Martínez

Madrid

2018

Universidad Complutense de Madrid

Facultad de Medicina

Departamento de Fisiología



**ROLE OF LIPOTOXICITY AND MITOCHONDRIAL
DYSFUNCTION IN CARDIAC AND METABOLIC ALTERATIONS
ASSOCIATED WITH OBESITY**

Memoria presentada por GEMA MARÍN ROYO, para optar al grado de doctor por la
Universidad Complutense de Madrid, con mención internacional.

Madrid

2018

La Dra. Victoria Cachafeiro Ramos, Catedrática de Fisiología, del Departamento de Fisiología, de la Facultad de Medicina de la Universidad Complutense de Madrid.

CERTIFICA:

Que la tesis doctoral: “PAPEL DE LA LIPOTOXICIDAD Y LA DISFUNCIÓN MITOCONDRIAL EN LAS ALTERACIONES CARDIACAS Y METABÓLICAS ASOCIADAS A LA OBESIDAD” ha sido realizada bajo su dirección, y se encuentra en condiciones para ser presentada como memoria para obtener el Grado de Doctor.

Y para que así conste firma la presente en Madrid, a 10 de Julio de 2018.

Fdo. Victoria Cachafeiro Ramos

La Dra. María Luaces Méndez, Médico Adjunto del Servicio de Cardiología, del Hospital Clínico San Carlos de Madrid.

CERTIFICA:

Que la tesis doctoral: “PAPEL DE LA LIPOTOXICIDAD Y LA DISFUNCIÓN MITOCONDRIAL EN LAS ALTERACIONES CARDIACAS Y METABÓLICAS ASOCIADAS A LA OBESIDAD” ha sido realizada bajo su dirección, y se encuentra en condiciones para ser presentada como memoria para obtener el Grado de Doctor.

Y para que así conste firma la presente en Madrid, a 10 de Julio de 2018.

Fdo: Dra. María Luaces Méndez

El Dr. Ernesto Martínez Martínez, Investigador postdoctoral del Departamento de Fisiología de la Facultad de Medicina de la Universidad Complutense de Madrid.

CERTIFICA:

Que la tesis doctoral: “PAPEL DE LA LIPOTOXICIDAD Y LA DISFUNCIÓN MITOCONDRIAL EN LAS ALTERACIONES CARDIACAS Y METABÓLICAS ASOCIADAS A LA OBESIDAD” ha sido realizada bajo su dirección, y se encuentra en condiciones para ser presentada como memoria para obtener el Grado de Doctor.

Y para que así conste firma la presente en Madrid, a 10 de Julio de 2018.

Fdo: Dr. Ernesto Martínez Martínez

Agradecimientos

“Individualmente, no somos más que una gota. Juntos, somos el océano”

Ryunosuke Satoro

Con esta frase quiero reflejar que esta tesis ha sido fruto del trabajo y apoyo de mucha gente y por ello quiero agradecer a todo el mundo que ha hecho posible que hoy esté yo aquí escribiendo estas páginas.

En primer lugar quiero agradecer a mis directores de tesis, Victoria, María y Ernesto. A Victoria, por darme un voto de confianza y haberme acogido desde el primer momento con los brazos abiertos en su laboratorio. Por ser para mí un ejemplo de trabajo y constancia, y por ser la mejor jefa de todas las jefas. A María, por tu apoyo y consejos. Me alegra haber tenido la oportunidad de haber aprendido un poquito de ti, eres una gran profesional. A Ernesto, por toda tu ayuda en estos últimos meses. Por estar siempre dispuesto a ayudar a todo el mundo aun cuando no tienes tiempo ni para ti. Porque me alucina lo trabajador que eres pero aún mas tu forma de ser. Ni te imaginas lo contenta que estoy de que hayas sido mi director y de haber podido coincidir contigo en este laboratorio. Ahora sí que si, espero por fin haberme ganado un abrazo tuyo ;)

Las siguientes personas a las que quiero agradecer son todas aquellas que en algún momento han formado parte de este laboratorio y han aportado su granito de arena para que esta tesis saliera adelante.

La primera personita (¿o tendría que decir gentuza?) a la que quiero agradecer es a Raquel, mi vallecana preferida. Porque para mí, TÚ eres mi tesis. Has estado de principio a fin. Desde el primer día a mi lado, enseñándome absolutamente todo. Porque si con Ernesto tuviste tu primera tesis, aquí va la segunda. Porque creo que todo el mundo debería aprender de ti. Me has alegrado cada mañana de western, cultivos o ratitas. Haciéndome reír millones de veces, y echándome mil broncas a las que nunca te hice caso ;). Gracias por estar ahí siempre y gracias por ser como eres.

A Roberto, por estar en el inicio de este camino y ayudarme a comenzar en este mundo. Por todas esas horas en cultivos para conseguir que nuestras queridas H9c2 llegaran a la confluencia perfecta. A los que habéis estado en el laboratorio en algún momento de estos tres años, Aliaume, Sara e Iván. A los que habéis estado acompañándome en estos últimos meses de escritura Rocío, Leonor, Marie y a los que continuáis en el

laboratorio, Francisco, Bea y Darío. Muchísimas gracias a todos por aguantarme y muchísima suerte en vuestras nuevas etapas. Solo me queda deciros, TRACATRÁ!

A Virginia y Avelina por estar siempre dispuestas a ayudar en lo que hiciera falta.

A nuestras vecinas de al lado, Elena, Belén y Sandra. Por los “martes locos” y por los ratitos de cafés (aunque siempre os hacíais de rogar para bajar). A Ana, por amenizarnos tantos cafés con el monotema. A Ricardo, porque aunque no me reconozcas cuando te llamo por teléfono seguiré avisándote para bajar a tomar café. Porque te mereces esa plaza de profe titular, lo vas a hacer genial.

A toda la gente del Departamento de Físio que de un modo u otro habéis hecho que me haya sentido muy a gusto estos años.

También quiero agradecer a todos los servicios que han hecho posible la realización de muchos de estos experimentos. Al CAI por los estudios PET, a la unidad de proteómica de NavarraBiomed y a la del CNIO, al servicio de cultivos del CIB y al animalario de la Complu.

A Mariví, por tus consejos y por estar siempre dispuesta a ayudarme en cualquier momento. A Marisa, por enseñarme a acomplejar el ácido palmítico y por toda tu ayuda con el análisis lipídómico. Al grupo de Mercedes Salaices y Ana Briones, por vuestro apoyo y colaboración. A Tony por todo tu tiempo invertido desinteresadamente para ayudarme con la escritura en inglés de la tesis.

Vorrei ringraziare pure a Massimiliano Caprio, per avermi dato l’opportunità di lavorare nel suo laboratorio. A Caterina, Andrea ed Alessandra, per tutto quello che mi avete insegnato in quei tre mesi a Roma. Per le escursioni allo stabulario e le piadine che abbiamo mangiato dopo. Grazie mille!

A Casa Lupita, mi familia madrileña, por ser una casa de científicos en la que prácticamente no se habla de ciencia, ayudándome así a desconectar siempre que lo he necesitado. Por haber sido los mejores compañeros de piso que podría haber tenido. Especialmente a Yosú, porque si he hecho esta tesis es por ti. Siempre te estaré agradecida. A Sara, por todo lo que hemos vivido juntas. Porque ya llevamos un Erasmus y una tesis, y lo que nos quedaa!! Por muchas más fritadas en nuestras vidas (aunque las tenemos un poco abandonadas últimamente). A Esther, por haber sido mi

descubrimiento soriano. Eres genial, menos mal que decidiste venirte con nosotros aunque fuera a la habita peque ;) A los tres, por todas las horas de Sing Star, 4 en raya, OT y Paquita Salas. Gracias, gracias y gracias!

A Aitana, otro de mis apoyos madrileños. Gracias por aguantarme estos años, por contagiarme tu alegría y por iniciarnos juntas en el mundo de la salsa. Fue genial conocerte en la resi pero más aún que nuestros caminos se volvieran a juntar en Madrid. Y como no, gracias también a mis salseros. Habéis hecho que este tiempo en Madrid sea mucho más divertido gracias a vosotros.

A mis salmantinas prefes, porque a pesar de haber acabado tras el máster cada una en un lugar diferente, os habéis hecho sentir muy cerca. Siempre os voy a estar agradecidas por el buen año que pasamos y por haber seguido conmigo desde entonces.

A Henar y Ester, porque si dicen que los amigos de la uni son para toda la vida, imagínate si a eso encima le tenemos que sumar las horas vividas en la residencia. Nunca me cansaré de pasar momentos, viajes y aventuras con vosotras.

A mi familia, por llevar toda una vida cuidándome y enseñándome a ser lo que soy hoy. A mi hermano, por ser la alegría y el cariñosico de la casa. No sé qué haríamos sin ti. Porque aunque no te lo diga mucho, sabes que te quiero como el que más. A mis padres, porque a pesar de las dificultades habéis dejado en todo momento que siguiera mi camino. Gracias por apoyarme siempre!!

Y por último, quiero agradecer a mis amigas, a las de siempre, LAS DEL PUEBLO. Esta tesis va dedicada a todas vosotras. Porque os he tenido muy presentes en todo el periodo de escritura, porque estáis en mi mente desde mis primeros recuerdos y porque sé que vais a formar parte de mí, toda la vida. Por habernos unido más que nunca frente a las adversidades y porque os admiro a todas y cada una de vosotras. Y en especial a ti, SAN, porque estoy segura de que estarías orgullosísima de cada uno de nuestros pequeños y grandes logros.

¡ MUCHAS GRACIAS A TODOS !

Abbreviations

Abbreviations

4-HNE	4-hydroxy-2-nonenal
¹⁸ F-FDG	¹⁸ F-Fluorodeoxyglucose
ACS	Acyl-CoA synthetase
ACSL1	Acyl-CoA Synthetase Long Chain Family Member 1
AGE	Advanced glycation end-products
AHA	American Heart Association
ALCAT1	Lysocardiolipin acyltransferase 1
ANT	Adenine nucleotide translocator
ATGL	Acyl triglyceride lipase
ATP	Adenosine triphosphate
BAT	Brown adipose tissue
BMI	Body mass index
BSA	Bovine serum albumin
BTHS	Barth syndrome
CD36	Cluster of differentiation 36
CER	Ceramide
CL	Cardiolipin
CoA	Coenzyme A
Col I	Collagen I
CPT1	Carnitine palmitoyl transferase 1
CPT2	Carnitine palmitoyl transferase 2
CRD	Carbohydrate recognition domain
CT	Control
CTGF	Connective tissue growth factor
CVF	Collagen volume fraction
CycloF	Cyclophilin F
DDP4	Dipeptidylpeptidase 4
DG	Diacylglycerol
DHE	Dihydroetidium
DGAT	Diacylglycerol transferase
DMEM	Dulbecco's Modified Eagle's Medium
DRP1	Dynamin related protein 1
ECAR	Extracellular acidification rate

Abbreviations

ECM	Extracellular matrix
EDD	End-diastolic diameter
EF	Ejection fraction
ER	Endoplasmic reticulum
ESD	End-systolic diameter
ETC	Electron transport chain
FABP	Fatty acid binding protein
FATP	Fatty acid transport protein
FADH2	Flavin adenine dinucleotide
FBS	Fetal bovine serum
FCCP	Carbonyl cyanide p-(trifluoromethoxy) phenylhydrazone
FFA	Free fatty acid
FS	Fractional shortening
Gal-3	Galectin-3
GLP1	Glucagon-like peptide 1
GLUT	Glucose transporter
GP	Glutathione peroxidase
HCCS	Holocytochrome C synthase
HFD	High fat diet
HOMA	Homeostatic model assessment
IDH3A	Isocitrate dehydrogenase 3
IL-1 β	Interleukin 1 β
IL-6	Interleukin 6
IL-10	Interleukin 10
IMM	Inner mitochondrial membrane
ip	Intraperitoneal
IR	Insulin resistance
IRS-1	Insulin receptor substrate-1
IVT	Interventricular septum
LA	Left atrium
LOX	Lysyl oxidase
LPC	Lysophosphatidilcholine
LPE	Lysophosphatidilethanolamine

Abbreviations

LV	Left ventricle
LVEF	Left ventricular ejection fraction
LVH	Left ventricle hypertrophy
LVM	Left ventricle mass
MCD	Malonil-CoA decarboxylase
MCP	Modified citrus pectin
MFN1	Mitofusin 1
MFN2	Mitofusin 2
MMP	Matrix metalloprotein
MOMP	Mitochondrial outer membrane permeabilization
MPO	Myeloperoxidase
MPTP	Mitochondrial permeability transition pore
MRI	Magnetic resonance imaging
MTND2	NADH:Ubiquinone oxidoreductase core
MQ	MitoQ
NADH	Nicotinamide adenine dinucleotide
NIDDM	Non-insulin-dependent diabetes mellitus
O ₂ ⁻	Superoxide anion
OCR	Oxygen consumption rate
OPA1	Optic atrophy 1
OXPHOX	Oxidative phosphorylation
PA	Palmitic acid
PC	Phosphatidylcholine
PE	Phosphatidylethanolamine
PG	Phosphatidylglycerol
PI	Phosphatidylinositol
PGC1 α	Peroxisome proliferator-activated receptor-gamma coactivator-1-alpha
PKC	Protein kinase C
PLA ₂	Phospholipase A ₂
PPL	Phospholipid
PRDX4	Peroxiredoxin 4
PUFA	Polyunsaturated fatty acids
PWT	Posterior wall thickness

Abbreviations

PWTd	Posterior wall thickness in diastole
PWTs	posterior wall thickness in systole
RAAS	Renin-angiotensin-aldosterone system
RNS	Reactive nitrogen species
ROS	Reactive oxygen species
RV	Right ventricle
RWT	Relative wall thickness
SBP	Systolic blood pressure
SDS-PAGE	Sodium dodecyl sulfate polyacrylamide gel electrophoresis
SM	Sphingomyelin
SOCS3	Suppressor of cytokine signalling 3
SOD	Superoxide dismutase
SUV	Standardized uptake value
TAC	Total antioxidant capacity
TCA	Tricarboxilic acid
TEAB	Triethylamonium bicarbonate
TGF β	Transforming growth factor beta
TG	Triglyceride
TNF α	Tumor necrosis factor α
UCP	Uncoupling protein
UPLC-QToF-MS	Ultrahigh performance liquid chromatography coupled to time-of-flight mass spectroscopy
UPR	Unfolded protein response
UQCRCQ	Ubiquinol-cytochrome c reductase complex III subunit VII
UQCRC2	Ubiquinol-cytochrome c reductase complex III subunit II
VLDL	Very-low-density lipoproteins
WAT	White adipose tissue
WHO	World health organization

Index

RESUMEN	1
SUMMARY	9
INTRODUCTION	
<u><i>I.OBESITY</i></u>	15
<u><i>II.CARDIOVASCULAR ALTERATIONS IN OBESITY</i></u>	
1. Structural alterations	17
2. Functional alterations	19
<u><i>III.MECHANISMS CONTRIBUTING TO STRUCTURAL AND FUNCTIONAL CHANGES IN THE HEART IN OBESITY</i></u>	
1. Cardiac fibrosis	22
1.1 Mediators of extracellular matrix deposition	22
1.2 Role of Gal-3 in cardiac fibrosis	23
1.3 Inhibition of Gal-3	24
2. Cardiac lipotoxicity	24
2.1 Lipotoxic mediators	25
<i>Triglycerides (TGs)</i>	25
<i>Diacylglycerol (DAG)</i>	26
<i>Ceramides (CER)</i>	26
<i>Acylcarnitines</i>	27
<i>Cardiolipins</i>	27
<i>Phosphatidylethanolamine (PE) and phosphatidylcholine (PC) and its lyso forms</i>	28
3. Alterations in metabolic substrates use	28
3.1 Decreased glucose utilization	29
3.2 Increased FA utilization	29
<i>Fatty acid metabolism in the heart</i>	29
<i>Fatty acid metabolism in obese heart</i>	31
4. Mitochondrial dysfunction and oxidative stress	32
4.1 Inhibition of mitochondrial oxidative stress	37

<u>V, ADIPOSE TISSUE REMODELLING IN OBESITY</u>	37
HYPOTHESIS AND OBJECTIVES	47
MATERIALS AND METHODS	53
<u>I. ANIMAL STUDY</u>	53
1. Experimental design	53
1.1 Animal model of obesity treated with the Gal-3 activity inhibitor	53
1.2 Animal model of obesity treated with a mitochondrial antioxidant	54
2. Monitoring of the animal model	54
3. Evaluation of cardiac structure and function	55
4. Sacrifice	55
5. Adiposity index	57
6. HOMA index	57
7. Histological and morphological evaluation	57
7.1 Cardiac tissue	57
7.2 Adipose tissue	58
8. Detection of superoxide anion (O ₂ ^{•-}) production	58
8.1 Production of total O ₂ ^{•-} (DHE)	59
8.2 Production of mitochondrial O ₂ ^{•-} (MitoSOX)	59
9. Lipidomic analysis	60
10. In vivo PET–CT imaging to study ¹⁸ F- Fluorodeoxyglucose heart uptake	61
11. Proteomic analysis	62
11.1 Proteomic analysis from cardiac tissue samples	62
12. Tissue processing for protein extraction	63
12.1 Cardiac tissue	63
12.1.1 Total proteins	63
12.1.2 Mitochondrial proteins	64
12.2 Adipose tissue	64
12.2.1 Total proteins	64

13. Western blot	64
14. RNA extraction from adipose tissue	65
15. Reverse Transcription and Real-Time PCR	65

II. CELL CULTURE STUDY

1. Cell culture	66
2. Measurements of cellular respiration and estimation of the rate of glycolysis	66
3. Viability assay	68

III. CLINICAL STUDY

1. Patients	68
2. Anthropometric measurements	69
3. Circulating parameters	69
4. Proteomic analysis from human adipose tissue samples	70

IV. STATISTICAL ANALYSIS

1. Experimental model analysis	74
2. Clinical data analysis	75

V. ANNEX 76

RESULTS

THE EFFECT OF GALECTIN-3 ACTIVITY INHIBITION ON CARDIAC

LIPOTOXICITY ASSOCIATED WITH OBESITY

1. Effect of Gal-3 activity inhibition on general characteristics in HFD rats	83
2. Effect of Gal-3 activity inhibition on cardiac structure in HFD rats	85
3. Effect of Gal-3 activity inhibition on cardiac glucose uptake and insulin resistance in HFD rats	87
4. Effect of Gal-3 activity inhibition on cardiac lipid profile in HFD rats	88
5. Effect of Gal-3 activity inhibition on cardiac mitochondrial alterations in HFD rats	90

6. Effect of palmitic acid on mitochondrial function in cardiac myoblasts. Consequences of Gal-3 activity inhibition 92

II. EFFECT OF MITOCHONDRIAL OXIDATIVE STRESS INHIBITION ON CARDIAC ALTERATIONS ASSOCIATED WITH OBESITY

1. Effect of mitochondrial oxidative stress inhibition on general characteristics in HFD rats 96
2. Effect of mitochondrial oxidative stress inhibition on cardiac superoxide anion levels 97
3. Effect of mitochondrial oxidative stress inhibition on cardiac structure 98
4. Proteomic analysis of HFD rat hearts 101
5. Effect of mitochondrial oxidative stress inhibition on OXPHOS complexes in HFD rats 104
6. Effect of palmitic acid on mitochondrial function in cardiac myoblasts. Consequences of mitochondrial oxidative stress inhibition. 105
7. Effect of a mitochondrial antioxidant on lipid profile of cardiac mitochondria in HFD rats 106
8. Effect of mitochondrial oxidative stress on enzymes implicated in TG metabolism 109
9. Effect of mitochondrial oxidative stress inhibition on mitochondrial biogenesis, dynamics and permeability in HFD rats. 112
10. Effect of mitochondrial oxidative stress inhibition on cardiac glucose uptake and insulin resistance in HFD rats 113

III. EFFECT OF MITOCHONDRIAL OXIDATIVE STRESS INHIBITION IN ADIPOSE TISSUE DYSFUNCTION-REMODELLING ASSOCIATED WITH OBESITY

1. Effect of mitochondrial oxidative stress inhibition on oxidative stress levels in the epididymal adipose tissue of HFD rats 115
2. Effect of mitochondrial oxidative stress inhibition on adipose tissue remodelling 116

3. Effect of mitochondrial oxidative stress inhibition on proteins involved in insulin signalling in adipose tissue of HFD animals	119
4. Effect of mitochondrial oxidative stress inhibition on fatty acid uptake in epididymal adipose tissue of HFD rats	121
5. Effect of mitochondrial oxidative stress inhibition on mitochondria in epididymal adipose tissue of HFD rats	122
6. Effect of mitochondrial oxidative stress inhibition on browning of adipose tissue in HFD rats	123
 <u>IV. IMPACT OF OBESITY IN VISCERAL ADIPOSE TISSUE</u>	
<u>REMODELLING IN PATIENTS</u>	
1. Effect of obesity on metabolic and circulating parameters in patients	124
2. Effect of obesity on proteome of the adipose tissue of patients	125
3. Effect of obesity on adipocyte area and pericellular fibrosis in adipose tissue of patients	128
 DISCUSSION	
<u>I. ROLE OF GAL-3 IN THE CARDIOMETABOLIC ALTERATIONS IN OBESE RATS</u>	
	133
<u>II. ROLE OF MITOCHONDRIAL OXIDATIVE STRESS IN THE CARDIOMETABOLIC ALTERATIONS IN OBESE RATS</u>	
	139
<u>III. ROLE OF OXIDATIVE STRESS ON ADIPOSE TISSUE REMODELING IN OBESITY</u>	
	147
CONCLUSIONS	159
BIBLIOGRAPHY	163
APPENDIX	187

Resumen

La obesidad se define como una excesiva acumulación de grasa debido a un desequilibrio entre las calorías consumidas y gastadas. La obesidad mundial ha crecido dramáticamente en las últimas décadas por lo que no es sorprendente que numerosos estudios se hayan llevado a cabo para investigar su efecto dañino sobre la salud humana.

Una de las características de los pacientes obesos es la presencia de adipocitos más grandes los cuáles una vez alcanzado su límite de expansión tienen una menor capacidad de almacenamiento de grasa dando lugar a un aumento de los niveles de ácidos grasos circulantes los cuales se pueden depositar en tejidos no adiposos, incluido el corazón, ejerciendo efectos tóxicos en los mismos. Además, la obesidad se asocia con alteraciones estructurales y funcionales en el corazón las cuales pueden dar lugar a disfunción cardíaca. De hecho, las enfermedades cardiovasculares son la primera causa de muerte en individuos con obesidad o diabetes. Entre los mecanismos que contribuyen a la aparición de alteraciones estructurales y funcionales se encuentran la lipotoxicidad cardíaca, las alteraciones en el uso de sustratos metabólicos, mediadores profibróticos como Galectina 3 (Gal-3), la disfunción mitocondrial y el estrés oxidativo, los cuales facilitan el desarrollo de fibrosis cardíaca con consecuencias funcionales. Niveles patológicos de especies reactivas de oxígeno siendo la mitocondria la principal fuente de los mismos, se ha demostrado que tienen un efecto dañino en el corazón. Además, el estrés oxidativo también puede participar en el remodelado del tejido adiposo el cual puede ser una de las alteraciones metabólicas subyacentes asociadas a la obesidad.

Por lo tanto, el objetivo global del trabajo fue evaluar el papel de la lipotoxicidad y el estrés oxidativo mitocondrial en las alteraciones cardiometabólicas en el contexto de la obesidad así como los posibles mecanismos involucrados.

Para ello, un modelo de obesidad inducida por dieta se utilizó en el presente estudio el cual se comparó con un grupo de animales control. Ratas Macho Wistar de 150 g se alimentaron durante seis semanas con una dieta rica en grasa (OB, 35% grasa) o con una dieta estándar (CT, 3.5% grasa). Animales de ambos grupos recibieron un inhibidor de la actividad de Gal-3 (MCP; 100 mg/kg/día) o un antioxidante mitocondrial (MitoQ; 50 mg/kg/día) en el agua de bebida durante el mismo periodo que duró la dieta.

Las ratas obesas mostraron hipertrofia y fibrosis cardíaca en comparación con las ratas control. También mostraron alteraciones en el uso de sustratos metabólicos caracterizados por una disminución en el uso de glucosa por el corazón que se

Resumen

acompañó con un aumento en el índice HOMA indicando resistencia a la insulina sistémica. No se observaron cambios ni en la función cardíaca ni en la presión sanguínea sistémica en ratas obesas.

Como revela el análisis lipidómico realizado, en las ratas obesas se observaron alteraciones en el perfil lipídico cardíaco caracterizado por un aumento de los niveles de triglicéridos, principalmente de aquellos enriquecidos con ácido palmítico 16:0, ácido esteárico 18:0 y ácido araquidónico 20:4, un aumento en los niveles de diacilglicéridos y una reducción de los niveles de esfingomiélinas y ceramidas. Otro análisis lipidómico realizado específicamente para valorar los lípidos presentes en las mitocondrias cardíacas, además de mostrar un aumento en los niveles de triglicéridos, también mostró una reducción en los niveles de carnitinas y cardiolipinas cardíacas, especies lipídicas que son esenciales para un correcto funcionamiento de la mitocondria.

Los niveles proteicos de CD36 y CPT1A, responsables del transporte de ácidos grasos a través de la membrana plasmática y mitocondrial, respectivamente, y los de DGAT1, enzima que cataliza la conversión de un diacilglicérido y un ácido graso a triglicérido, se encontraron aumentados en el corazón de las ratas obesas.

Un estudio proteómico realizado en tejido cardíaco reveló alteraciones en gran cantidad de proteínas mitocondriales en ratas obesas en comparación con las control, principalmente en aquellas proteínas relacionadas con la cadena respiratoria mitocondrial y la fosforilación oxidativa. También observamos alteraciones en otras proteínas mitocondriales involucradas en dinámica mitocondrial, biogénesis y permeabilidad mediante western blot.

MCP fue capaz de prevenir la aparición de fibrosis, el aumento de triglicéridos y diacilglicéridos cardíacos totales así como algunas de las alteraciones mitocondriales observadas en el corazón de ratas obesas sugiriendo el papel de Gal-3 en la lipotoxicidad cardíaca asociada con obesidad. Sin embargo, MCP no tuvo efecto sobre la captación de glucosa cardíaca ni sobre el índice HOMA demostrando que Gal-3 no participa en el desarrollo de resistencia a la insulina en este contexto. Por el contrario, MitoQ fue capaz de prevenir ambos, la captación de glucosa y el índice HOMA en ratas obesas destacando el papel del estrés oxidativo mitocondrial en las alteraciones en el uso de sustratos metabólicos y en la resistencia a la insulina. MitoQ también previno la fibrosis y la hipertrofia cardíaca, el aumento de triglicéridos y la reducción de

cardiolipinas mitocondriales así como la mayoría de las alteraciones mitocondriales en el corazón de ratas obesas. Todos estos resultados demuestran el rol del estrés oxidativo mitocondrial en la disfunción de la mitocondria y en las alteraciones cardiometabólicas anteriores a la disfunción cardíaca.

Por otro lado, se observó también alteraciones en el tejido adiposo epididimal de ratas obesas caracterizadas por adipocitos hipertróficos, desregulación de proteínas involucradas en la vía de señalización de la insulina y alteraciones en proteínas mitocondriales las cuales se previnieron con el tratamiento con MitoQ. Además, un estudio proteómico realizado en el tejido adiposo de paciente obesos mostró alteraciones en proteínas mitocondriales, principalmente en aquellas involucradas en β -oxidación, ciclo de Krebs y fosforilación oxidativa reflejando parte de las alteraciones previamente observadas en el tejido adiposo epididimal de ratas obesas. Teniendo en cuenta todos estos resultados, las conclusiones de nuestro estudio son las siguientes:

1. La obesidad se asocia con lipotoxicidad cardíaca la cual no solo comprende una acumulación de lípidos sino también un remodelado de los mismos que se asocia con cambios metabólicos y el desarrollo de fibrosis cardíaca.
2. Gal-3 modula la lipotoxicidad cardíaca en el contexto de la obesidad a través de su capacidad para inducir daño mitocondrial aumentando el estrés oxidativo.
3. Las especies reactivas de oxígeno mitocondriales participan en las alteraciones estructurales cardíacas observadas en ratas obesas caracterizadas por fibrosis intersticial e hipertrofia cardíaca, eventos tempranos anteriores a la disfunción cardíaca.
4. Las especies reactivas de oxígeno mitocondriales participan en la modificación en el uso de sustratos metabólicos cardíacos en ratas obesas.
5. Las especies reactivas de oxígeno mitocondriales facilitan el remodelado del tejido adiposo el cual participan en las alteraciones metabólicas asociadas a la obesidad.
6. Las alteraciones metabólicas observadas en pacientes obesos se acompañaron con alteraciones mitocondriales en el tejido adiposo similares a aquellas que se habían encontrado en ratas obesas confirmando la relevancia clínica de nuestros resultados.

Resumen

Los resultados presentados en este estudio sugieren que la lipotoxicidad a través del estrés oxidativo mitocondrial juega un papel central en las alteraciones cardiometabólicas asociadas a la obesidad.

Summary

Obesity is defined as an abnormal or excessive fat accumulation due to an energy imbalance between calories consumed and expended. Worldwide obesity has grown dramatically in the last decades so it is not surprising that numerous studies have been performed to investigate its harmful effect on human health.

One of the characteristics of obese patients is the presence of larger adipocytes which reach a limit and have diminished capacity to store fat, thereby leading to elevation of circulating fatty acids which can deposit in non-adipose tissues, including the heart, exerting toxic effects. Moreover, obesity is associated with structural and functional alterations in the heart that can lead to cardiac dysfunction. In fact, cardiovascular disease is the primary cause of death in individuals with obesity and diabetes. Among the mechanisms that contribute to cardiac structural and functional alterations, cardiac lipotoxicity, alterations in the use of metabolic substrates, profibrotic mediators such as Galectin-3 (Gal-3), mitochondrial dysfunction and oxidative stress are some of these which facilitate the development of cardiac fibrosis with functional consequences. Pathological ROS levels have been demonstrated to have harmful effects in the heart, with the mitochondria being the main source of ROS. Moreover, oxidative stress can also participate in the adipose tissue remodelling which can be underlying metabolic alterations associated with obesity.

Therefore, the overall aim of the work was to evaluate the role of lipotoxicity and mitochondrial oxidative stress in the cardiometabolic alterations in the context of obesity, as well as the possible mechanisms involved.

For this purpose, a model of diet-induced obesity was used in the study which was compared with a group of control animals. Male Wistar rats of 150 g were fed for 6 weeks either, a high fat diet (HFD; 35% fat) or a standard diet (CT; 3.5% fat). Animals of each group were treated with either the inhibitor of Gal-3 activity (Modified citrus pectin, MCP; 100 mg/kg/day) or a mitochondrial antioxidant (MitoQ; 50 mg/kg/day) in the drinking water for the same period.

HFD rats showed increased cardiac hypertrophy and fibrosis as compared with controls. They also showed alterations in the use of metabolic substrates characterized by a decrease in the use of glucose by the heart that was accompanied by an increase in HOMA index indicating systemic insulin resistance. Neither cardiac function alterations nor systemic blood pressure changes were observed in obese rats.

Summary

HFD rats also showed alterations in the cardiac lipid profile, as the lipidomic analysis revealed, characterized by an increase in triglyceride (TG) levels, mainly in those enriched with palmitic acid 16:0, stearic acid 18:0 and arachidonic acid 20:4, an increase in DAG levels and a reduction in sphingomyelin (SM) and ceramide (CER) levels. Another lipidomic analysis was performed specifically in cardiac mitochondria. In addition to showing increased TG levels, it also showed decreased carnitine and cardiolipin (CL) levels, lipid classes that are essential for a correct mitochondria functioning.

Increased levels of CD36 and CPT1A, responsible for fatty acid transport through plasmatic and mitochondrial membrane, respectively, as well as the increase levels of DGAT1, an enzyme that catalyzes the conversion of DAG and fatty acyl CoA to TG, were observed in the heart of obese rats.

A proteomic study performed in cardiac tissue revealed alterations in several mitochondrial proteins in obese rats, mainly in those related with mitochondrial respiratory chain and oxidative phosphorylation. By western blot, we also observed alterations in other proteins involved in mitochondrial dynamics, biogenesis and permeability.

MCP was able to prevent fibrosis, the increase in total TG and DAG levels as well as some of the mitochondrial alterations observed in the heart of obese rats, suggesting a role of Gal-3 in cardiac lipotoxicity associated with obesity. However, MCP had no effect on glucose uptake by the heart and HOMA index in obese rats, showing that Gal-3 does not play a role in insulin resistance in this context. Conversely, MitoQ was able to prevent both glucose uptake by the heart and HOMA index in HFD rats, highlighting the role of mitochondrial oxidative stress in metabolic substrate use alterations and insulin resistance.

MitoQ also prevented cardiac fibrosis and cardiac hypertrophy, the increase in mitochondrial TG levels and the reduction in mitochondrial CL levels as well as most of the mitochondrial alterations in obese rats. All these data together demonstrate the role of mitochondrial oxidative stress in mitochondrial dysfunction and cardiometabolic alterations prior to cardiac dysfunction.

On the other hand, we found alterations in the epididymal adipose tissue of obese rats characterized by hypertrophic adipocytes, deregulation in proteins involved in insulin signalling pathway and alterations in mitochondrial proteins that were prevented by MitoQ. Furthermore, a proteomic study was performed in adipose tissue of obese patients showing alterations in mitochondrial proteins mainly in those involved in β -oxidation, Krebs cycle and oxidative phosphorylation reflecting the alterations observed in the epididymal adipose tissue of obese rats and suggesting the translationality of our results.

Taking together all these results, the conclusions of our study are as follows:

1. Obesity is associated with cardiac lipotoxicity, which not only involve lipid accumulation but also remodelling of different lipid species that is associated with metabolic changes and the development of cardiac fibrosis.
2. Gal-3 is able to modulate cardiac lipotoxicity in the context of obesity through its capacity to induce mitochondrial damage, increasing oxidative stress.
3. Mitochondrial ROS plays a role in the cardiac structure alterations observed in obese rats characterized by interstitial fibrosis and cardiac hypertrophy, early events prior to cardiac dysfunction.
4. Mitochondrial ROS is involved in the cardiac metabolic substrate use modification in obese rats.
5. Mitochondrial ROS facilitates the remodelling of adipose tissue which participates in the metabolic alterations associated with obesity.
6. The metabolic alterations observed in obese patients were accompanied by similar mitochondrial alterations in the adipose tissue than those found in obese rats supporting the clinical relevance of our findings.

The results present in this study altogether suggest that lipotoxicity through mitochondrial oxidative stress plays a central role in the cardiometabolic alterations associates with obesity.

Introduction

I. OBESITY

Obesity is defined as an abnormal or excessive fat accumulation due to an energy imbalance between calories consumed and calories expended. There have been global changes in dietary and physical activity patterns due to an increased intake of energy-dense foods that are high in fat and a decrease in physical activity due to the increasingly sedentary nature of many forms of work, changing modes of transportation, and increasing urbanization.

In fact, worldwide obesity has nearly tripled since 1975. Studies from the World Health Organization (WHO) shows that more than 1900 million adults (39%) 18 years and older in 2016 were overweight and over 650 million of these (13%) were obese. Over 340 million children and adolescents aged 5-19 were overweight or obese in 2016 and 41 million children under the age of 5 were overweight or obese in 2016. Therefore, as data shows, obesity seriously affects the entire world population even though it is more prevalent in adult populations.

The World Health Organization (WHO) classifies obesity based on body mass index (BMI).

$$BMI = \frac{\text{body weight (kg)}}{\text{height}^2 (\text{m})}$$

BMI-based the classification is as follows:

- underweight: BMI < 18.5 kg/m²
- normal weight: BMI 18.5–24.9 kg/m²
- overweight: BMI 25.0–29.9 kg/m²
- class I obesity: BMI 30.0–34.9 kg/m²
- class II obesity: BMI 35.0–39.9 kg/m²
- class III or morbid obesity: BMI ≥ 40.0 kg/m²
- The term super obesity is sometimes applied to those whose BMI is ≥ 50 kg/m².

The maps below depict the worldwide prevalence of overweightness (Figure 1) and obesity (Figure 2) in the adult population. As we can observe, more than 40-50 % of the

Introduction

population in most of the developed countries is overweight (BMI>25 kg/m²) and between 10-30% of the population is obese (BMI>30 kg/m²).

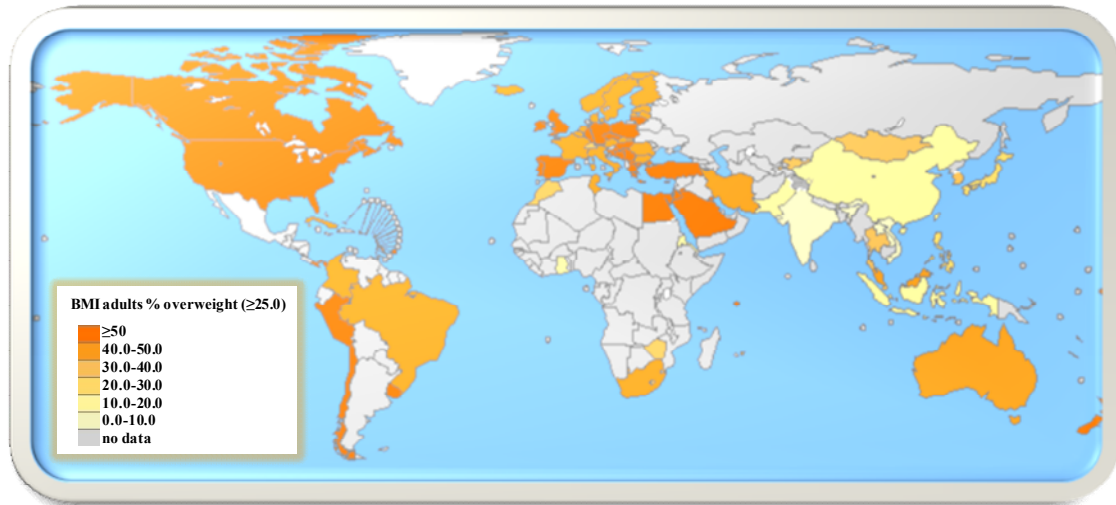


Figure 1. Prevalence of overweight adults (BMI≥25; +18 age) worldwide. Body mass index (BMI; kg/m²) adults % overweight. (Figure adapted from World Health Organisation,2016).

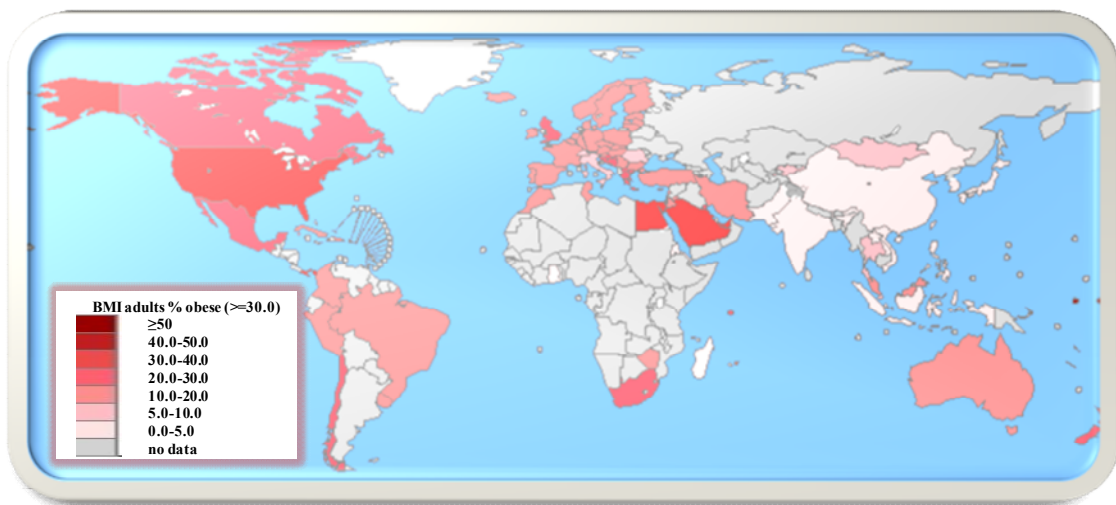


Figure 2. Prevalence of obese adults (BMI≥30; +18 age) worldwide. Body mass index (BMI; kg/m²) adults % overweight. (Figure adapted from World Health Organisation,2016).

Overweightness and obesity are associated with a major morbi-mortality. Moreover, has an association has been described between BMI and all cause-mortality, independently of sex (Figure 3).

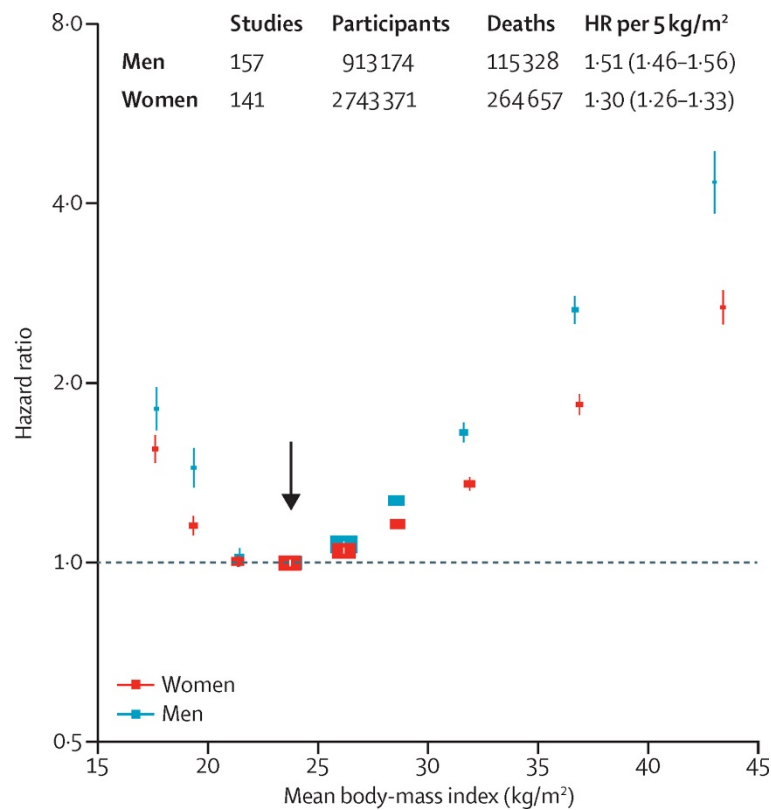


Figure 3. Association of BMI with all-cause mortality, by sex. (From Global BMI Mortality Collaboration, 2016) ¹.

Cardiovascular diseases are disorders of the heart and blood vessels that take the lives of 17.7 million people every year, which represents 31% of all global deaths. In the last years, the effort of the study in cardiovascular diseases has been intensified due to the high prevalence of obesity and its association with mortality –primarily cardiovascular in origin-.

II. CARDIOVASCULAR ALTERATIONS IN OBESITY

1. Structural alterations

One of the main alterations that occur in the heart associated with obesity is cardiac hypertrophy, which appears in response to hemodynamic overload as a mechanism for reducing the ventricular wall stress. Cardiac hypertrophy can be physiological or pathological. Physiological hypertrophy initially appears to be an adaptive response in the form of a mild cardiac mass increase (10-20%). It is reversible and it does not progress into heart failure, while pathological hypertrophy does have the ability to

Introduction

progress into heart failure. Obesity and diabetes have been associated with the development of pathological hypertrophy.² However, there are controversial opinions regarding left ventricle hypertrophy amongst different studies. Some authors suggest that the increase observed in left ventricle (LV) is proportional to increase in body size when considered not to be cardiac hypertrophy^{3,4} whereas other authors suggest that the increase in left ventricle size is independent of body size⁵⁻⁷. In order to minimise the interference of obesity in the estimate of ventricular mass, a specific body mass index for obese patients was developed and implemented for this clinical scenario⁸.

Cardiac hypertrophy is usually evaluated by the increase in left ventricle mass (LVM) due to an increase in both wall thickness and cavity size. Cardiac remodelling can thus be classified as follows: concentric remodelling, concentric hypertrophy and eccentric hypertrophy. Concentric remodelling is characterized by normal LV mass, an increase in relative wall thickness (RWT) and a decrease in LV cavity size. Concentric hypertrophy is characterized by an increase in LV mass, increased RWT and a normal cavity size, whereas eccentric hypertrophy is defined by an increase in LV mass, a normal RWT and increased cavity size⁹ (Figure 4).

According to the RWT and indexed mass for LV, geometric patterns were defined as:

1. Normal: RWT <0.45 and an indexed LV mass <51 g/m^{2.7}.
2. Concentric remodeling: RWT 0.45 and an indexed LV mass <51 g/m^{2.7}.
3. Concentric hypertrophy: RWT 0.45 and an indexed LV mass ≥51 g/m^{2.7}.
4. Eccentric hypertrophy: RWT <0.45 and an indexed LV mass ≥ 51 g/m^{2.7}.

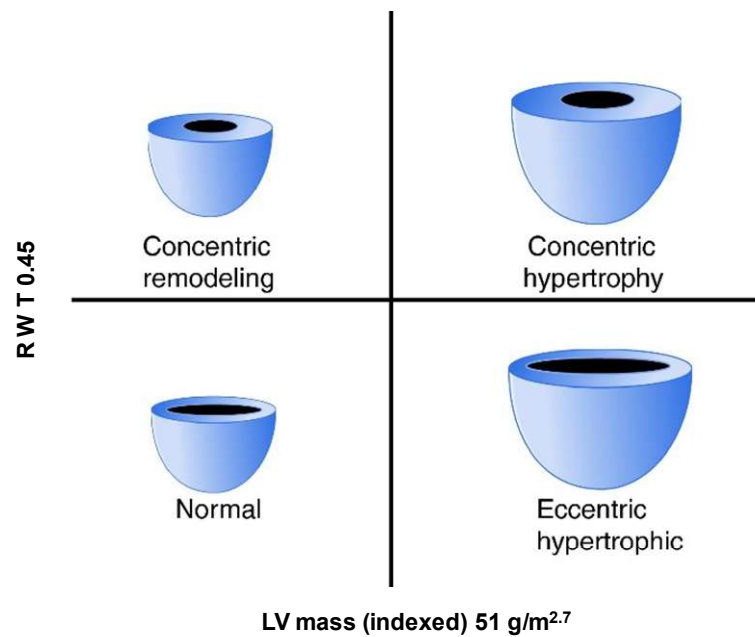


Figure 4. Left ventricle geometric patterns. LV, left ventricle; RWT; relative wall thickness; (From Luaces M et al, 2012)⁹.

Existing data on cardiac hypertrophy in obese patients show that obesity is associated with both eccentric^{9, 10} and concentric¹¹ patterns. Although concentric hypertrophy is associated with higher risk of cardiovascular event, both are associated with ischemic stroke risk¹².

In addition to changes in the left ventricle, alterations in left atrium and right ventricle have also been reported. Left atrial volume is commonly elevated in obese subjects, while right ventricular wall thickness and cavity size may also be augmented^{13,14}.

In animal models, left ventricle hypertrophy varies among species, type of animal model (genetic or diet induced obesity) and age of the animals. In addition, cardiac hypertrophy is related to interstitial and perivascular fibrosis in several animal models of obesity such as obese Zucker rats¹⁵, UCP1-DTA mice¹⁶, ob/ob mice¹⁷ and high-fat diet rats¹⁸.

2. Functional alterations

Several studies have shown that obesity is related to alterations in cardiac function. These alterations in cardiac function may be due to both systolic and diastolic dysfunction (Figure 5). However, it is sometimes difficult to know if the cardiac

Introduction

dysfunction is consequence of obesity per se or of the related comorbidities. The majority of the studies regarding cardiac dysfunction in obesity are focussed on both diastolic and systolic left ventricle (LV) function. Regarding LV diastolic function, impairment of LV filling has been observed in obese patients¹⁹. There are discrepancies amongst studies when considering systolic function. Some of them have shown no differences between obese and lean subjects in LV systolic function whereas others have shown reduced LV fractional shortening and LV ejection fraction in obese patients¹⁹. A recent study performed by Ng ACT et al, has showed that diabetes and increasing BMI category have an additive detrimental effect on both, LV myocardial systolic and diastolic function²⁰.

Some authors suggest that the degree of LV diastolic filling impairment seems to be related to the severity of obesity^{10, 21}. This is supported by a study showing an improvement in left ventricular diastolic function in young women with morbid obesity six months after bariatric surgery²². However, we have reported in a previous study of the group that morbidly obese patients after bariatric surgery had improved left ventricle geometry without improvement in systolic and diastolic function⁹.

Some studies have reported that critical LV dysfunction does not usually occur in obesity and that is due to co-morbidities. Conversely, a study performed in obese children without hypertension realized in order to evaluate left ventricular function by Tissue Doppler showed that obese children had impairment of longitudinal myocardial motion resulting in a reduction in LV systolic function as well as diastolic dysfunction due to damage in cardiac relaxation and compliance²³.

Relating to left atrium (LA) and right ventricle (RV) function in obesity, very little has been studied, mainly due to the limitations in non-invasive imaging techniques. Unusual LA strain and strain rate has been observed in obese patients²⁴. RV dysfunction has also been observed in obese patients due to decreased velocities in diastole and systole in the lateral tricuspid annulus²⁵.

In animal models of obesity, cardiac function has also been evaluated. However, we need to consider that these studies are performed in anesthetized animals and the different anesthetic agents used in each experiment may therefore affect the results. Most studies have shown systolic dysfunction in *db/db* and *ob/ob* mice between 12 and 20 weeks of age but no alteration in systolic function was found in younger animals²⁶⁻²⁸.

Conversely, a recent study has evaluated different types of HFD (Western diet (45% fat, 60% saturated), Surwit diet (60% fat, 90% saturated), milk-fat-based diet (60% fat, 60% saturated) or high-fat Western diet (HFWD, 60% fat, 32% saturated)) on cardiac function. None of the diets evaluated affected systolic function after 12 weeks in mice. However, HFWD induced diastolic dysfunction suggesting that composition of fatty acids may be determinant for diastolic dysfunction in diet-induced obesity animal models²⁹.

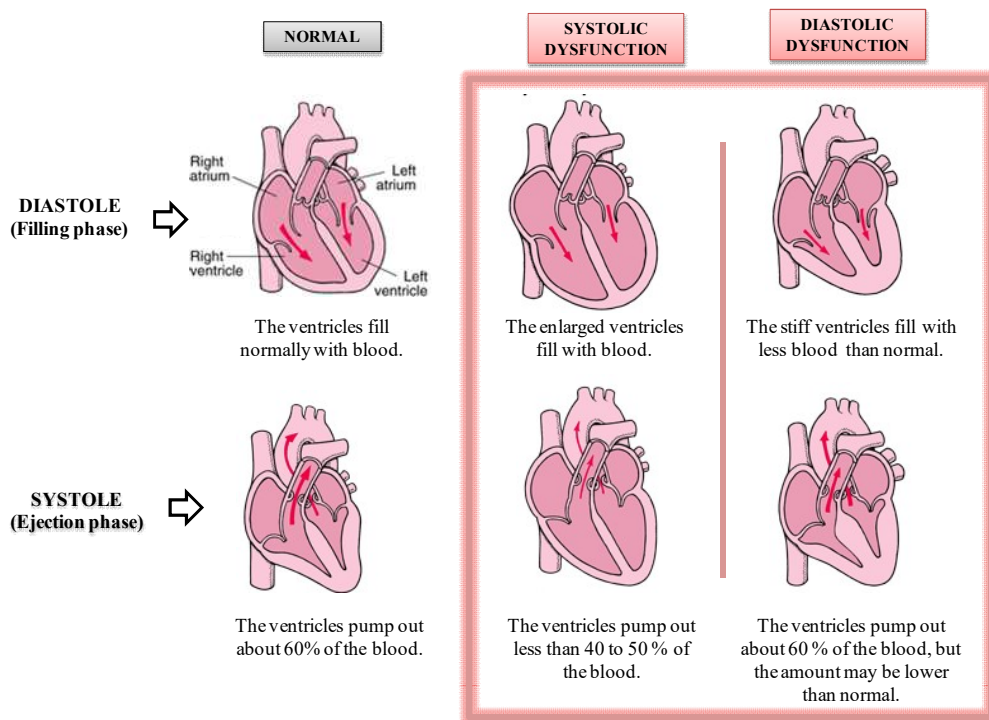


Figure 5. Normal heart function and systolic and diastolic dysfunction. (Adapted from The Merck Manual of Diagnosis and Therapy. 19 ed. New Jersey: Robert S. Porter; 2011)

III. MECHANISMS CONTRIBUTING TO STRUCTURAL AND FUNCTIONAL CHANGES IN THE HEART IN OBESITY

1. Cardiac fibrosis

1.1 Mediators of extracellular matrix deposition

Fibrosis is defined as an excessive extracellular matrix deposition. The extracellular matrix (ECM) is a network composed mainly by collagen fibers. Collagen monomers assemble by forming a triple helix called procollagen which maintains its stability through hydrogen bonds. N- and C-terminal regions are then cleaved by procollagen N- and C- proteinases, resulting in a molecule known as tropocollagen which self-assembles forming collagen microfibrils that undergoes crosslinking by lysyl oxidase (LOX) and thereby producing the collagen fibers³⁰. Along with collagen, proteoglycans, glycoproteins and glycosaminoglycans among others, are also components of the ECM³¹.

Different cell types such as cardiomyocytes and interstitial cells (cardiofibroblasts, vascular cells and immune cells) are continuously interacting with the matrix acting as sensors of the environment alterations. Cardiofibroblasts are the most abundant interstitial cells in the myocardium involved in cardiac fibrosis since they are the main cells responsible for matrix production. A correct preservation of the cardiac structure along with cardiac cells is necessary for the transmission of the cardiac contractile force. Experimental models in obesity have reported a loss of cardiomyocytes which are replaced by fibrotic tissue³¹. The production of collagen is mediated by several molecular signals such as activation of renin-angiotensin-aldosterone system (RAAS), TGF- β /Smad3 cascade, leptin, endothelin-1, matricellular proteins as thrombospondin and advanced glycation end-products (AGE), among others^{18, 31, 32}. Nevertheless, an increase in cardiac fibrosis may be due to both, an increase in ECM deposition or a reduction in ECM degradation. The proteins involved in ECM degradation are the matrix metalloproteins (MMPs) which are altered in obese hearts, favouring the development of cardiac fibrosis³³. In addition, increased levels of MMP-2, the main factor responsible for collagen degradation in the heart, have been associated with improvement of cardiac fibrosis in a rat model of cardiac hypertrophy³⁴.

1.2 Role of Gal-3 in cardiac fibrosis

Galectin-3 is member of the β -galactoside-binding lectin family with a N-terminal domain and a C-terminal carbohydrate recognition domain (CRD). It differs among the other members of the family because it is the only one with a single CRD and an intrinsically disordered sequence ,extra long and flexible, at the N-terminal domain that promotes oligomerization, it being the only one able to pentamerize³⁵. It is expressed in several tissues³⁶ including the heart¹⁸ as well as in many different type cells³⁵.

Galectin-3 (Gal-3) regulates basic cellular functions such as cell-cell and cell-matrix interactions, growth, proliferation, differentiation, and inflammation³⁵. Therefore, taking into consideration its participation in several processes and its distribution through different tissues, Gal-3 is involved in the pathogenesis of many relevant human diseases, including cancer, fibrosis, chronic inflammation and scarring³⁵.

Moreover, a study performed in two different cohorts of HF patients measured Gal-3 levels at baseline and at 3 months in patients from the Controlled Rosuvastatin Multinational Trial in Heart Failure (CORONA) trial (n=1329), and at baseline and at 6 months in patients from Coordinating Study Evaluating Outcomes of Advising and Counseling Failure (COACH) trial (n=324). This study showed that Gal-3 has prognostic value in identifying patients with HF at elevated risk for subsequent HF morbidity and mortality. In fact, Gal-3 has been described by the American Heart Association (AHA) as a biomarker predictive of hospitalization and death in patients with HF³⁷.

Moreover, Gal-3 is poorly expressed in the heart in normal conditions; however its expression may be enhanced under pathological conditions, and plays an important function³⁸. Previous studies from our laboratory have reported increased cardiac levels of Gal-3 in obese rats at mRNA and protein levels¹⁸.

Gal-3 has been extensively related to fibrosis. In fact, it is considered to be a potential mediator of fibrosis due to its ability to stimulate extracellular matrix (ECM) deposition. Several studies have shown that inhibition of Galectin-3 reduced the levels of cardiac, vascular and renal fibrosis by a reduction in collagen levels, as well as the levels of profibrotic factors such as transforming growth factor beta (TGF β), fibronectin and connective tissue growth factor (CTGF) in tissues such as heart¹⁸ , vessels³⁹ and

Introduction

kidney⁴⁰, suggesting that the increase of collagen deposition observed in obese rats could be due to the action that Gal-3 exerts in stimulating these factors.

1.3 Inhibition of Gal-3

The most studied Gal-3 inhibitor is Modified Citrus Pectin (MCP). MCP is a derivative of the citrus pectin essentially consisting of neutral sugar sequences with a low degree of branching. Pectin, present in plant cell walls, is a branched polysaccharide fiber rich in galactoside residues. In its native form, citrus pectin (CP) has a limited solubility in water and is unable to interact with Gal-3. On the other hand, it acts as a ligand for Gal-3⁴¹ in its modified form (MCP) after hydrolysis to form a smaller linear water-soluble fiber. Citrus pectin is obtained from the peel or pulp of citrus fruits and modified by means of high pH and temperature treatment⁴².

2. Cardiac lipotoxicity

Lipotoxicity is defined as the deleterious effects of lipid accumulation in non-adipose tissues leading to cellular dysfunction and death and, eventually resulting in whole organ dysfunction^{43, 44}. This term was first coined in 1994 by Roger Unger who developed the “lipotoxic hypothesis”, which attributes the beta cell dysfunction of adipogenic non-insulin-dependent diabetes mellitus (NIDDM) to an excessive accumulation of fat in the pancreatic islets⁴⁵. After this study, several new studies started to develop the hypothesis that cellular lipid accumulation in organs such as the muscle, liver, and pancreas cause deleterious effect in the organ themselves and that attenuation of this accumulation could protect against obesity-related metabolic disorders⁴⁶⁻⁴⁹.

The excess lipid accumulation in the heart is known as “cardiac lipotoxicity”. One of the first animal models of lipotoxicity in the heart was developed by Schaffer and colleagues who generated mice with Acyl-CoA Synthetase Long Chain Family Member 1 (ACSL1) overexpressed specifically in the heart. These animals showed a marked cardiac myocyte triglyceride accumulation that was associated with initial cardiac

hypertrophy, followed by the development of left-ventricular dysfunction and premature death⁵⁰.

2.1 Lipotoxic mediators

Triglycerides (TGs)

TGs are the main form of storage of fatty acid excess. They are stored in lipid droplets mainly constituted by a core of TG, cholesterol esters and a phospholipid free-cholesterol monolayer. This TG pool is in constant turnover in the heart in order to satisfy the cardiac energy demand. Two enzymes are the mainly implicated in this process (Figure 6). Diacylglycerol transferase (DGAT), implicated in TG metabolism, catalyzes the final step of TG synthesis. On the other hand, acyl triglyceride lipase (ATGL) is involved in the mobilization of TG and catalyzes the first step of hydrolysis. TGs are usually related directly to cardiac lipotoxicity and dysfunction. However, TGs are not directly toxic themselves because they are an inert neutral lipid form; however the increase in TGs is considered to be a biomarker of accumulation of other toxic lipid intermediates as DAG and ceramides (CER)⁴⁴.

DGAT may regulate toxic effects of lipids on tissue by converting DAG excess in TGs. In fact, there are studies that have shown beneficial effects of DGAT overexpression in cardiac lipotoxicity by increasing TG content⁵¹.

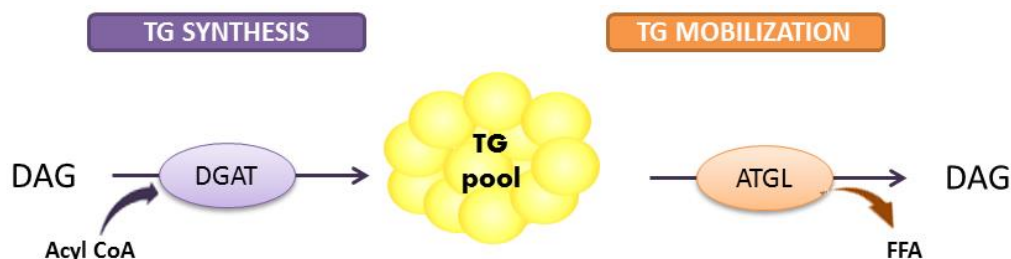


Figure 6. Enzymes involved in TG synthesis and degradation. DGAT, diacylglycerol acyltransferase; TG, triglyceride; ATGL, adipose triglyceride lipase.

Introduction

Diacylglycerol (DAG)

DAG, the lipid intermediary preceding the biosynthesis of TG, is considered to be a lipid much more harmful than TG. The potential underlying mechanisms are not well established but different data have linked DAG to cardiac lipotoxicity.

DAGs are involved in the activation of protein kinase C (PKC) isoforms, serine/threonine kinases that have been shown to phosphorylate the insulin receptor and/or the insulin receptor substrates and thereby impairing insulin resistance^{52, 53}.

They seem to also be a determinant factor for cardiac fibrosis⁵⁴. DAGs are intracellular second messengers capable of increasing the activity of protein kinase C (PKC), which promotes not only insulin resistance but also cardiac fibrosis and heart failure through the activation of galectin-3 and oxidative stress⁵⁵⁻⁵⁸. Studies from our laboratory have reported that Gal-3 and oxidative stress can participate in the cardiac fibrosis observed in rats fed a HFD³³ and could be a potential mediator through which DAG can participate in cardiac fibrosis in the context of obesity.

Ceramides (CER)

CER are structural elements found in cell membranes but have recently emerged as a bioactive lipid key player, involved in various cellular processes. Many of these cellular processes are related to mitochondria and mitochondrial respiratory chain⁵⁹⁻⁶¹. *In vitro* studies done in intact mitochondria extracted from rat heart showed that CER were able to inhibit electron transport and induce ROS formation^{60, 62}. An *in vivo* study also showed altered mitochondrial integrity due to CER accumulation. The study performed in a mouse mutant of *Cert* (gene that codified for CER transfer protein responsible for the CER transport from the endoplasmic reticulum (ER) to Golgi which is characterized by CER accumulation in the ER and by mislocalization of CER into the mitochondria showed a marked mitochondrial disorganization in the heart characterized by swollen mitochondria with fewer cristae. Moreover, these *Cert*^{-/-} mutant embryos had retarded growth and finally died around the embryonic day 11.5 as a result of cardiovascular insufficiency⁶³. Not only alterations in mitochondrial integrity but also increased ROS production induced by short and long chain CER was demonstrated in rat heart and liver mitochondria^{60, 62, 64}. The mechanisms by which these alterations occurred are not well elucidated but it is thought that the mitochondrial membrane lipid

milieu may be altered by introducing high levels of CER that would interfere with the structure of supercomplexes and the activity of mitochondrial respiratory chain⁶⁵ or by modifying the complexes activity acting as an allosteric effector directly binding to them⁶⁶. Moreover, CER are also related to mitochondrial outer membrane permeabilization, a critical step in apoptosis. CER activate the pro-apoptotic protein BAX by inducing BAX conformational change necessary to translocate it to mitochondria to form pores⁵⁹.

Acylcarnitines

Acylcarnitines are the result of the action of CPT1 that catalyze the transfer of the acyl group of a long-chain fatty acyl-CoA from coenzyme A to L-carnitine. Myocardial levels of acylcarnitines are higher⁶⁷⁻⁶⁹ in obesity and diabetes. On the one hand, acylcarnitines have been shown to disrupt sarcolemmal integrity and electrophysiologic functions, possibly leading to myocardial arrhythmias⁶⁹, which suggest that acylcarnitines are potent cardiolipotoxins. On the other hand, an accumulation of acylcarnitines may affect mitochondrial function by modulating mitochondrial protein acylation^{70, 71}. Hence, taking into consideration these studies, acylcarnitines may act as myocardial lipotoxic intermediates.

Cardiolipins

Cardiolipins (CLs) are the main phospholipid of the mitochondria predominantly present in the mitochondrial inner membrane and thus playing an important role in keeping optimal mitochondrial function^{72, 73}. CLs are dimeric phospholipids composed by four fatty acyl chains which can be different, generating a highly diversified pool of CL species. However in the heart, linoleic acid 18:2 is the predominant form of all the four fatty acids, with the tetralinoleoyl CL [(18:2)₄CL] being the predominant CL species.

A correct content and structure of CL is very important to cell maintenance due to its implication in mitochondrial protein transport, mitochondrial morphology and mitochondrial respiratory chain⁷⁴. However, CL are very sensitive to oxidative damage⁷⁵ due to the presence of double bond in the acyl chains. CL-induced mitochondrial damage is not only due to a drop in CL levels but also to a remodelling process⁷⁵. Barth syndrome (BTHS) is in fact, a rare genetic disorder caused by a

Introduction

mutation in TAF gene encoding for Tafazzin (a mitochondrial acyltransferase involved in the biogenesis of CL) is characterized by a remodelling in CL that results in a decrease of CL (18:2)₄ species⁷⁴. BTHS patients show greatly enlarged mitochondria with malformed cristae structures⁷⁶ and they have a high rate of mortality throughout infancy, which is primarily related to progressive cardiomyopathy and a severely weakened immune system.

Phosphatidylethanolamine (PE) and phosphatidylcholine (PC) and its lyso forms

Phospholipids such as phosphatidylethanolamine (PE) and phosphatidylcholine (PC) also have an influential role in mitochondrial function, although they are significantly less studied compared to CL⁷⁷. In fact, PE and PC are also altered in Barth syndrome and thus contribute to mitochondrial dysfunction⁷⁸.

Lysophospholipids are phospholipids that are missing an acyl chain due to the action of phospholipase enzyme. The phospholipase A₂ (PLA₂) family are lipolytic enzymes that catalyze the hydrolysis of the ester bond at the *sn*-2 position of phospholipids to yield free fatty acids (FFA) and lysophospholipids⁷⁹, which promote postprandial hyperglycemia by reducing glucose uptake by the liver, heart and muscle tissues, as well as suppressing insulin-stimulated glycogen synthesis in the liver⁸⁰. Moreover, lysophosphatidilcholine (LPC) can inhibit insulin signalling through the activation of JNK in fibroblasts which inhibit tyrosine phosphorylation of insulin receptor substrate-1 (IRS-1)⁸¹ or the activation of PKC- α , resulting in the inhibition of insulin-induced protein kinase B/Akt phosphorylation in vascular smooth muscle cells⁸².

3. Alterations in metabolic substrates use

The heart needs to continually generate ATP due to the very high energy demand to maintain contractile function and basal metabolic processes. 95% of ATP production in the heart derive from oxidative phosphorylation and 70 % is due to β -oxidation of fatty acids⁸³. Although the main substrates used for the heart to obtain energy are the fatty acids, they are not the alone. Glucose (~20–30%), ketone bodies, lactate and amino acids are also used for energy production. The heart is a very flexible organ and constantly switches between fatty acids and glucose in response to excess or deficiency of some of them⁵⁰. The heart is characterized by a decrease in the use of glucose during

obesity due to an excess of fatty acids and an increase in FA utilization. However, this shift could contribute to cardiac deficiency since fatty acid oxidation consumes more oxygen per ATP molecule produced than glucose⁸⁴.

3.1 Decreased glucose utilization

Glucose is uptaken by the cells through the glucose transporters (GLUT) family. In the heart, the predominant isoform is GLUT4⁸⁵ which is stored in intracellular vesicles and needs to be translocated to plasmatic membrane to mediate glucose uptake. Impaired glucose transport has been reported in diabetic hearts due to reduced expression and translocation of GLUT4⁸⁶. However, GLUT4 expression appeared unchanged or barely decreased specifically in these two types of diabetic model animals (*ob/ob* and *db/db* mice)^{87, 88}. Despite unaltered levels of GLUT4, glucose uptake by the cell could be altered in these animals since the translocation of GLUT4 has not been evaluated. In other animal models, such as male Wistar rats fed a high-fat diet, AKT phosphorylation and GLUT4 translocation to the plasmatic membrane were reduced⁸⁹. In addition, a study in H9C2 cells stimulated with palmitic acid to create a hyperlipidemia condition *in vitro* showed that proteins involved in GLUT4 metabolic pathway (p-PI3K and p-AKT) were decreased at high palmitic acid concentration⁹⁰.

3.2 Increased FA utilization

Fatty acid metabolism in the heart

Fatty acids must be uptaken by the cells before being oxidized. There are two sources of fatty acids to the heart. They can be supplied as free fatty acid bound to albumin or released by action of lipoprotein lipase from TGs contained in very-low-density lipoproteins (VLDL) or chylomicrones^{44, 83}.

The fatty acids pass through the plasmatic membrane via passive diffusion or via protein transporters such as cluster of differentiation 36 (CD36), fatty acid transport protein (FATP1/6) and fatty acid binding protein (FABPmp)^{44, 91}, with CD36 playing a major role in myocardial fatty acid translocation since 50 % of fatty acid uptake in the heart is due to mechanisms dependent on CD36⁹². Once in the cell, long-chain fatty acids before enter into the mitochondria need to be activated before entering into the

Introduction

mitochondria. This activation refers to thioesterification with coenzyme A, which is performed by an essential enzyme of lipid metabolism, the acyl-Coa synthetase (ACS)⁹³. Once activated, these long-chain acyl CoAs can be taken up into the mitochondria or used to synthesize intracellular lipid intermediates such as TG, DAG, and CER, which have been implicated in the development of insulin resistance, cardiac dysfunction, and heart failure⁹⁴⁻⁹⁷.

The mitochondrial membrane is impermeable to long-chain acyl CoA esters⁹⁸. Two enzymes are required for fatty acids being able to enter into the mitochondria, carnitine palmitoyl transferase 1 (CPT1) and carnitine palmitoyl transferase 2 (CPT2). Both, are localized in the mitochondrial membrane, with the difference that CPT1 is located in the outer mitochondrial membrane and CPT2 in the inner membrane⁹⁹. CPT1 converts an acyl CoA into its corresponding acylcarnitine that is transported by carnitine translocase into the mitochondrial matrix. CPT2 then converted the acyl-carnitine back into acyl CoA⁴⁴ (Figure 7).

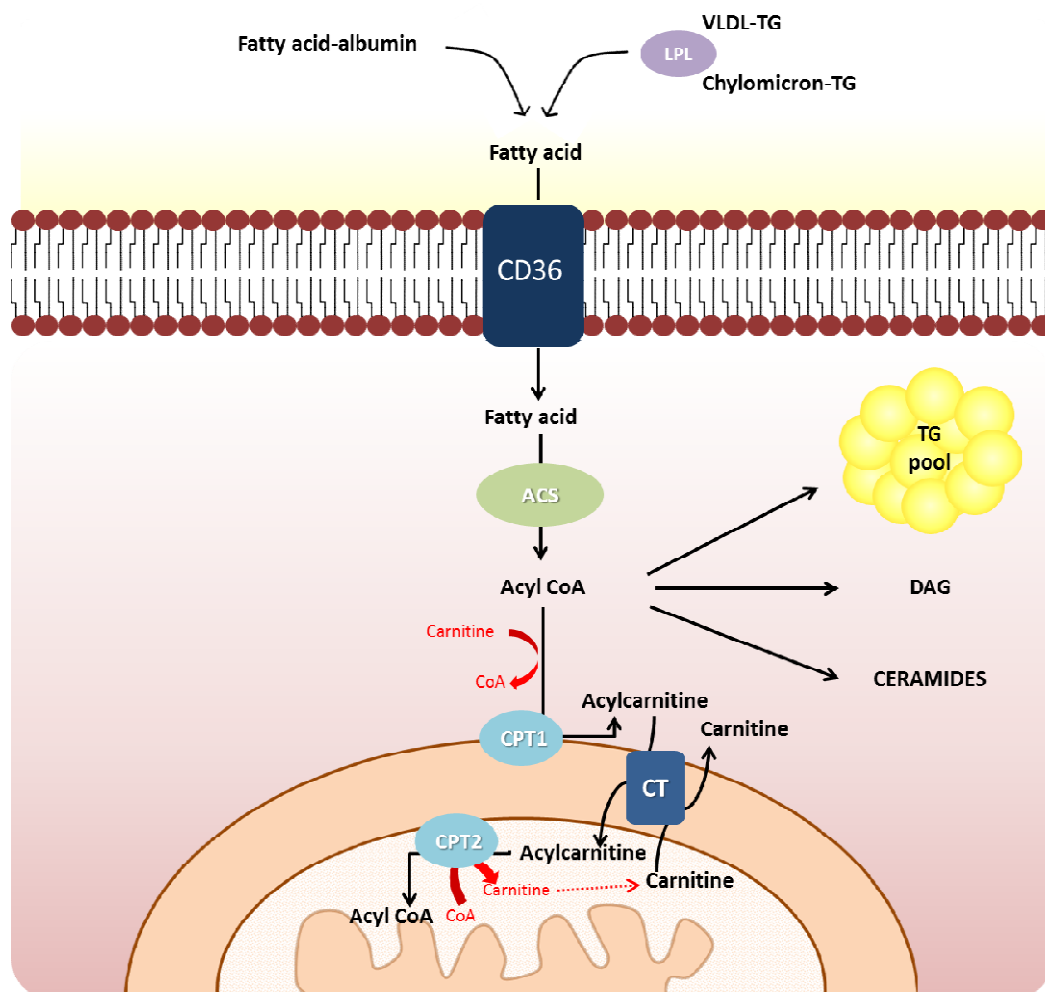


Figure 7. Fatty acid uptake by the cardiomyocyte and the mitochondria. VLDL, very-low-density lipoprotein; TG, triglyceride; LPL, lipoprotein lipase; CD36, cluster of differentiation 36; ACS, acetyl-CoA synthetase; CoA, coenzyme A; DAG, diacylglycerol; CPT1, carnitine palmitoyl transferase 1; CT, carnitine translocase; CPT2, carnitine palmitoyl transferase 2.

Once in the mitochondrial matrix, the acyl CoA is prepared to go under β -oxidation. This process envelops the sequential action of four enzymes (acyl-CoA dehydrogenase, enoyl-CoA hydratase, 3-hydroxyacyl-CoA dehydrogenase, and 3-ketoacyl-CoA thiolase) that results in the shortening of the acyl CoA by two carbons, as well as the production of acetyl CoA, flavin adenine dinucleotide (FADH₂) and nicotinamide adenine dinucleotide (NADH). The Acyl-Coa shortened by two carbons undergoes another round of β -oxidation, thereby producing more acetyl CoA, NADH and FADH₂. The acetyl CoA is subsequently metabolized in the tricarboxylic acid (TCA) cycle, also known as Krebs cycle, to produce GTP, FADH₂ and NADH which act as electron donors in the electron transport chain (ETC) to generate the proton gradient necessary to produce ATP via oxidative phosphorylation⁴⁴.

Fatty acid metabolism in obese heart

An imbalance between energy supply and energy expenditure is basically due to overconsumption of food, leading to an excess of lipids. When this occurs, the adipose tissue is the responsible to store the lipid excess as TG. However, at a certain point the adipocyte is unable for storing more lipids triggering an increase of circulating fatty acids that will be uptaken by the heart. This increase in the fatty acid uptake by cardiomyocytes may be dependent on higher expression of fatty acid transporters such as CD36. In fact, it has been reported that CD36 expression is increased in animal models of obesity^{91, 100}. Furthermore, its ablation protects the heart from dysfunction and lipotoxicity^{91, 101, 102}. This increase in fatty acids in the cell contributes to an increase in the mitochondrial fatty acid transporter (CPT1) through malonyl CoA regulation. Malonyl CoA inhibits CPT1, and a reduction in the levels of malonyl CoA during obesity has been demonstrated due to the action of Malonyl-CoA decarboxylase (MCD), the enzyme responsible for malonyl CoA degradation. However, the mechanism by which accumulation of intramyocardial fatty acids occurs is controversial. It is not clear if this is due to an excessive fatty acid supply, an impaired

Introduction

mitochondrial β -oxidation or both. Several studies have suggested that the accumulation of fatty acids in the myocardium is mainly due to a decrease in fatty acid oxidation¹⁰³⁻¹⁰⁶. Conversely, other studies have shown an increase in fatty acid β -oxidation in obese or insulin-resistant animal models^{26, 107}.

4. Mitochondrial dysfunction and oxidative stress

Mitochondria are organelles very important to the correct functioning of the cell since they are the responsible for energy production. Oxidative phosphorylation (OXPHOS) is a process that occurs in the mitochondria that involved electron transport, oxygen consumption and ATP production. In this process, substrates such as glucose and fatty acids are oxidized in the mitochondria and the resulting reducing equivalents (NADH and FADH_2) transfer electrons to the electron transport chain. The passage of electrons through the mitochondrial complex of the respiratory chain and its transfer to oxygen atoms produce energy, used to pump protons (H^+) from matrix to the mitochondrial space intermembrane, thus generating an electrochemical gradient. These protons return to the mitochondrial matrix passing through the mitochondrial complex V (or ATP synthase) generating ATP from ADP¹⁰⁸ (Figure 8).

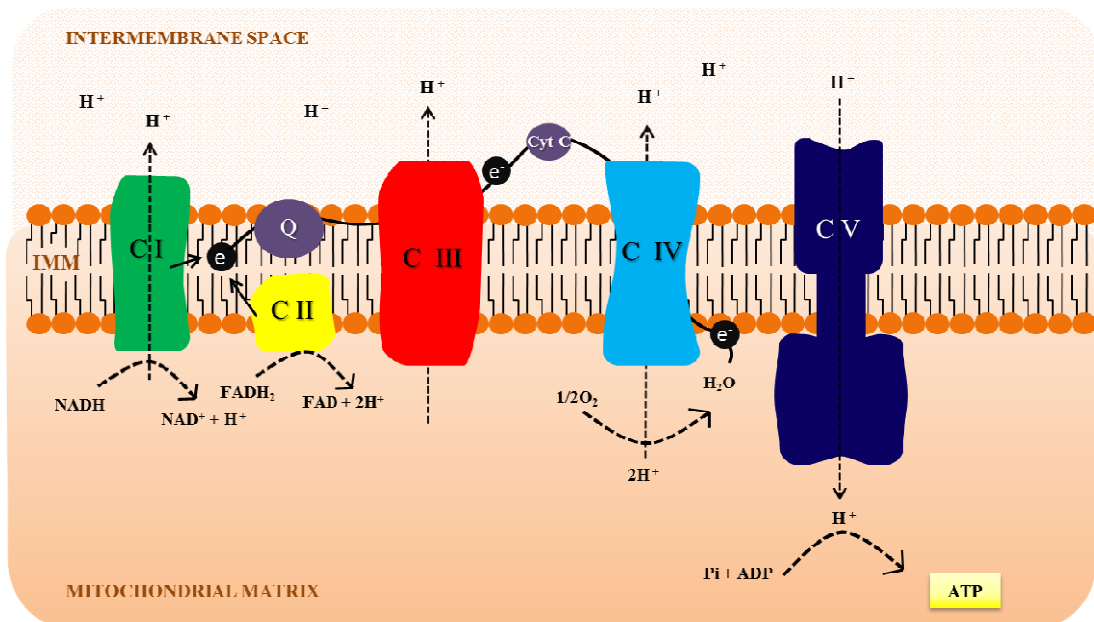


Figure 8. Mitochondrial oxidative phosphorylation (OXPHOS). CI, complex I; CII, complex II; CIII, complex III; CIV, complex IV; CV, complex V; Q, ubiquinone; CytC, cytochrome C; ADP, adenosine diphosphate; ATP, adenosine triphosphate.

Obesity is associated with changes in mitochondria. In different animal models of obesity there has been described increased mitochondrial number mediated by the upregulation of peroxisome proliferator-activated receptor-gamma coactivator-1-alpha (PGC1 α), the main transcription factor involved in mitochondrial biogenesis^{109, 110}. Nevertheless, there is evidence that mitochondrial dysfunction exists despite the increase in mitochondrial biogenesis. In fact, obese hearts are characterized by reduced ATP generation due to a reduction in the mitochondrial complexes as shown by studies in *ob/ob* mice and diet-induced obesity rats that reveal lower levels of cardiac mitochondrial complex I, II, III and V^{111, 112}.

Mitochondrial ROS are produced in physiological conditions as a product of the oxygen metabolism. However, the increase in the use of fatty acids to obtain ATP in some pathological situations and therefore the increase in the flux of electrons through the respiratory chain lead to hyperpolarization of the mitochondrial membrane and to inhibition of the electron flux through the mitochondrial complex III resulting in an excess of ROS production¹¹³. An increase in ROS levels may be due to an increase in ROS production, as well as to a decrease in the antioxidant system of the cell. The main enzymes involved in this system are superoxide dismutase (SOD), catalase and glutathione peroxidase (GP). SOD catalyzes the conversion of superoxide into H₂O₂ which is consequently converted into H₂O by the action of catalase and GP, respectively¹⁰⁸. Alterations in these enzymes may therefore contribute to an increase in oxidative stress. In addition, it is believed that ROS act close to their site of origin since they have a very short half-life. Consequently, not only is mitochondria the origin but it is also the target of ROS. Several studies have investigated the effect of ROS on mitochondrial function in diabetic and obesity rodent models. Although it is well known that obesity is related to cardiac deficiency the underlying mechanisms are not clearly elucidated. A study showed that 4-hydroxy-2-nonenal (4-HNE), a product of lipid peroxidation generated in the mitochondria due to ROS excess, appears increased in the heart of diabetic rats and is able to form adducts with mitochondrial complex II reducing its activity¹¹⁴. Another study demonstrated that reduction of oxidative stress by

Introduction

overexpressing the mitochondrial isoform of SOD in OVE26 cardiomyocytes was able to partially revert the impaired mitochondrial function¹¹⁵.

Another mechanism proposed to be responsible for this cardiac deficiency is an increase in ROS-induced mitochondrial uncoupling. Mitochondrial uncoupling refers to a process in which protons re-enter mitochondrial matrix through proteins with uncoupling action such as uncoupling protein (UCP) or adenine nucleotide translocase (ANT) instead of through ATP synthase, and thus, without contributing to ATP synthesis and dissipating energy as heat. A study performed by Boudina S et al, showed a reduction in mitochondrial oxidative capacity in *ob/on* mice hearts perfused with glucose and palmitate despite observing an increase in O₂ consumption, suggesting that the decrease in cardiac efficiency was due to mitochondrial uncoupling¹¹⁶. In a later study, they confirmed their hypothesis by demonstrating in *db/db* mice that mitochondrial uncoupling was mediated mainly by uncoupling proteins (UCPs) and to a lesser extent, by the adenine nucleotide translocator (ANT), independently of changes in expression levels¹¹¹.

Taking into consideration existing data which confirms that mitochondrial ROS and oxidative stress may be involved in mitochondrial dysfunction and cardiac deficiency in diabetes and obesity, a review by Bugger and Abel proposed a model in which mitochondrial uncoupling induced by ROS may favour cardiac deficiency¹⁰⁸. It suggests that in pathological situations such as obesity or metabolic syndrome, the increase in fatty acids in the heart leads to an increase in fatty acid uptake and oxidation by the mitochondria, triggering an excessive ROS production due to the increased activity of the respiratory chain. This excess of ROS may induce mitochondrial dysfunction in different ways. On the one hand, by reacting with lipid and proteins whose products may affect oxidative phosphorylation. On the other hand, activating UCPs and ANT leads to mitochondrial uncoupling. All these consequences drive to a reduction in ATP synthesis resulting in a deficiency in cardiac energy (Figure 9).

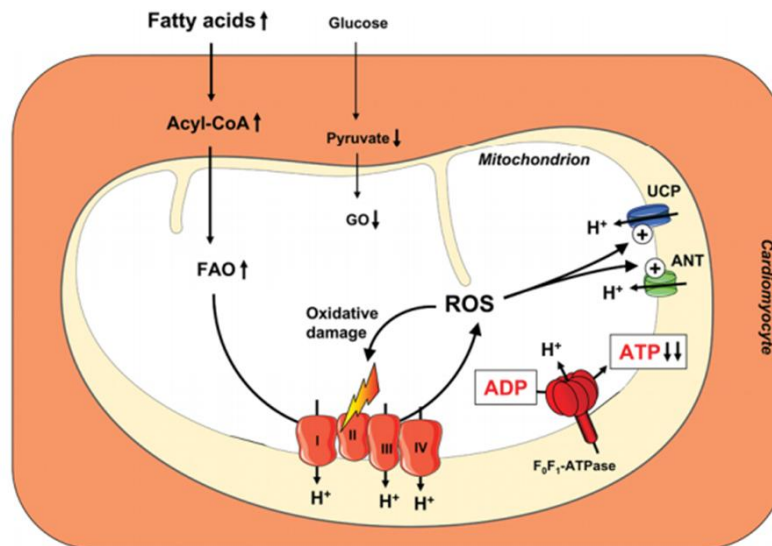


Figure 9. Effect of ROS excess on cardiac mitochondrial function in obesity. (From Bugger et al, 2008)¹⁰⁸. FAO, fatty acid oxidation; GO, glucose oxidation; ROS, reactive oxygen species; UCP, uncoupling protein; ANT, adenine nucleotide translocator; I, complex I; II, complex II; III, complex III; IV, complex IV.

Another mechanism that may be involved in mitochondrial dysfunction is an imbalance in mitochondrial dynamics. Mitochondria is a highly dynamic organelle that is constantly undergoing fusion and fission processes. In most cell types, it is able to change its morphology and localization depending on energy demands¹¹⁷. It is known that they can also move along the cytoskeleton to reach cellular regions of high ATP demand. Moreover, it has been shown that some mitochondrial aspects such as dynamic, morphology, intracellular organization, among others, can be tissue specific. In cardiomyocytes, the mitochondria have a very regular organization between myofibrils to ensure a correct cardiac contraction¹¹⁸. Therefore, an appropriate regulation of mitochondrial dynamics is essential for a great functioning of the heart.

The main proteins involved in mitochondrial fusion, a process that allows sharing mitochondrial DNA and machinery, are mitofusin 1 and 2 (MFN1 and MFN2) and the optic atrophy 1 (OPA1) protein. MFN1 and MFN2 are localized in the outer mitochondrial membrane whereas OPA1 is localized in the inner mitochondrial membrane. Therefore, mitochondrial fusion involved the fusion of two lipid membranes, an outer membrane regulated by mitofusins and an inner one mediated by OPA1. This process is required to maintain the respiratory capacity of the mitochondria.

Introduction

On the other hand, mitochondrial fission, which is the process that involves the fragmentation of one mitochondria into two or more, is regulated by dynamin-related protein 1 (DRP1) (Figure 10). Mitochondrial fission occurs during mitosis to ensure the mitotic segregation into the daughter cells but also occurs when mitochondria is damaged, allowing the elimination of the part of the mitochondria that is impaired in order to maintain a healthy mitochondrial network¹¹⁹.

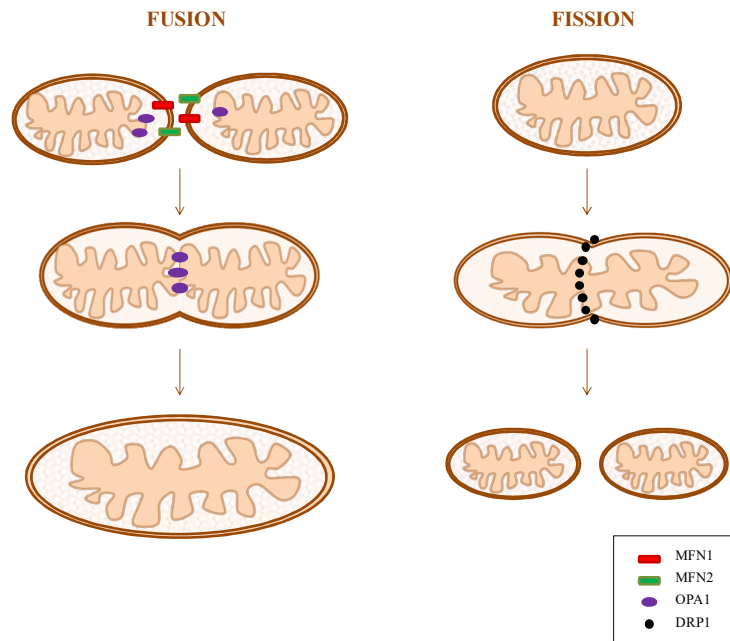


Figure 10. Proteins involved in mitochondrial dynamics. MFN1, mitofusin 1; MFN2, mitofusin 2; OPA1, optic atrophy 1; DRP1, dynamin related protein 1.

Several studies have showed the harmful effect of obesity and type 2 diabetes in mitochondrial dynamics. It has been amply reported that obesity is associated with a decrease in mitochondrial size mainly by a reduction in mitochondrial fusion proteins and an increase in mitochondrial fission proteins. In cardiomyocyte-specific FATP1 overexpression mice, which have increased cardiomyocyte FA uptake, the expression of MFN1, MFN2 and OPA1 are reduced¹²⁰. Similar results were observed in rats fed a HFD for 12 weeks in which MFN2 and OPA1 protein levels were reduced¹²¹. Reduced levels of MFN2 have also been found in patients with type 2 diabetes and obesity¹²². All these data suggest that obesity lead to a shift in mitochondrial dynamics toward mitochondrial fission resulting in mitochondrial dysfunction that may participate in insulin resistance and cardiometabolic alterations. That is the reason why the recent interest in drugs targeting mitochondrial dynamics has grown considerably.

4.1 Inhibition of mitochondrial oxidative stress

Because of the role of oxidative stress in cardiovascular diseases and other pathologies, several clinical trials have been performed with antioxidants such as vitamin E, trying to counteract the adverse effects of oxidative stress. However, most of them have failed in the results. One explanation of this could be that the antioxidants used are not targeted to mitochondria, the main source of ROS production. The development of mitochondria-targeted antioxidants has subsequently increased considerably in the last decades, with mitoquinone (mitoQ) being one of them¹²³.

MitoQ is a derivative of the natural antioxidant ubiquinone (also called coenzyme Q10). Coenzyme Q₁₀ is localized in the inner mitochondrial membrane and is involved in the electron transfer from dehydrogenases to complex III of ETC. Moreover, it also protects against lipid peroxidation by acting as free radical scavenger¹²⁴.

MitoQ is a ubiquinone derivative attached to a phosphonium cation [10-(6'-ubiquinonyl) decyltriphenyl phosphonium bromide]. The cation is accumulated within mitochondria due to the mitochondrial membrane potential, thus allowing the specificity of the antioxidant to the mitochondria. The ubiquinone moiety of MitoQ that is inserted into the lipid bilayer is reduced by the respiratory chain resulting in its reduced form ubiquinol, which has antioxidant effect. After detoxify, ROS antioxidant activity of ubiquinol can be recycled being regenerated by the respiratory chain¹²⁵.

IV. ADIPOSE TISSUE REMODELLING IN OBESITY

Obesity is characterized by an increase in adipose tissue as a result of a positive imbalance between food intake and energy expenditure¹²⁶. The adipose tissue is a metabolic organ involved in the regulation of whole-body energy homeostasis by acting as a caloric reservoir. Under conditions of constant energy surplus (such as obesity) adipocytes become larger since they store the lipid excess internally¹²⁷.

It is necessary to distinguish between the two main types of adipose tissue present in humans, white adipose tissue (WAT) and brown adipose tissue (BAT), which have

Introduction

different roles in the metabolism regulation. The function of WAT is mainly to act as energy store and it is divided into two types:

- Subcutaneous adipose tissue
- Visceral adipose tissue which is concentrated around internal organs

Rodents have gonadal (or epididymal) adipose tissue, which is considered part of the visceral adipose tissue. However, careful interpretation is required to extrapolate findings in rodents to humans because of lack of gonadal adipose tissue in humans.

On the other hand, BAT is responsible for cold-induced thermogenesis through lipid oxidation which would explain its very high mitochondrial content necessary for the heat production by lipid peroxidation. This specialization of BAT in heat production rather than ATP synthesis is due to the elevated expression of UCP-1 in BAT mitochondria (Figure 11).

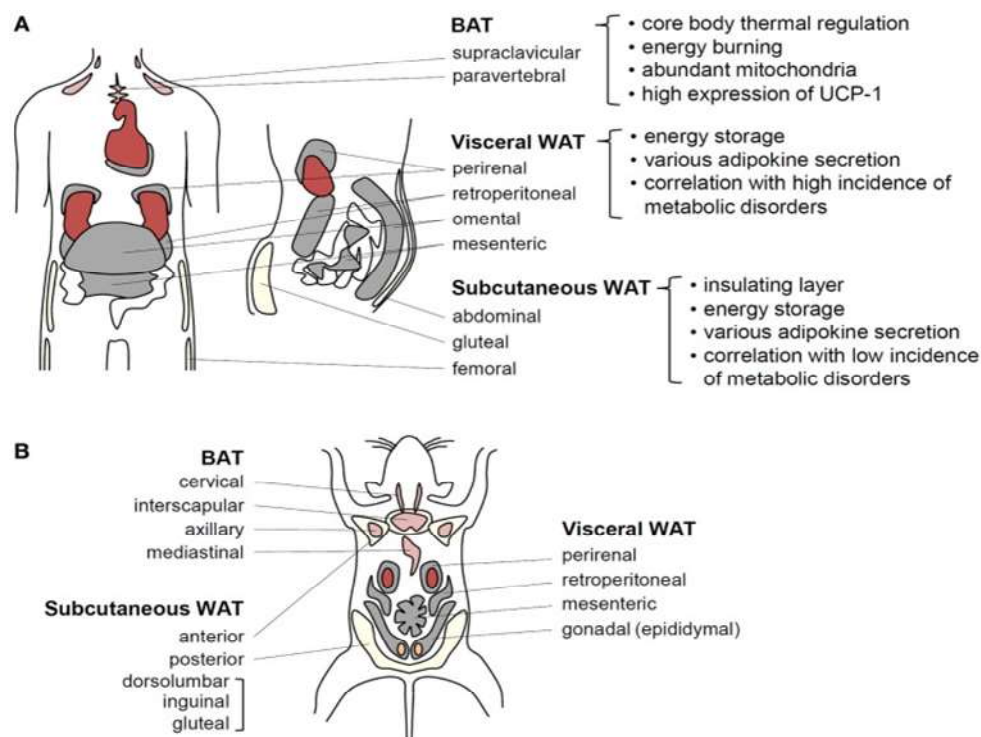


Figure 11. Adipose tissue function and distribution in human and rodents. BAT, brown adipose tissue; WAT, white adipose tissue. (From Choe SS et al, 2016)¹²⁷.

As we have mentioned, one of the most common characteristics of obesity is the adipose tissue expansion that is associated with adipocyte dysfunction. This increase in adipose tissue mass could be mediated by hyperplasia (increase number of adipocytes) or hypertrophy (enlargement of adipocytes). Adipose tissue dysfunction in adults is mainly due to adipocyte hypertrophy. Moreover, it has been shown that the number of

adipocytes is unaltered between obese and lean subjects¹²⁸, reinforcing the idea that hypertrophy rather than hyperplasia is responsible for adipose tissue expansion. Moreover, in the recent review of Tandon P et al, several studies are described that show the association in both subcutaneous and visceral adipose tissue, between hypertrophic adipocyte and insulin resistance, metabolic and cardiovascular diseases¹²⁹. Hypertrophic morphology appears mainly associated with increased circulating plasma insulin and glucose, total cholesterol and TG¹³⁰⁻¹³².

Extracellular matrix remodelling of adipose tissue along with inflammation are also common features of obesity. Some studies have shown that there is a negative correlation between adipocyte size and fibrosis¹³³⁻¹³⁵ suggesting that ECM deposition limits the capacity of store lipids by adipocytes, which results in ectopic deposition of fat in other tissues (Figure 12).

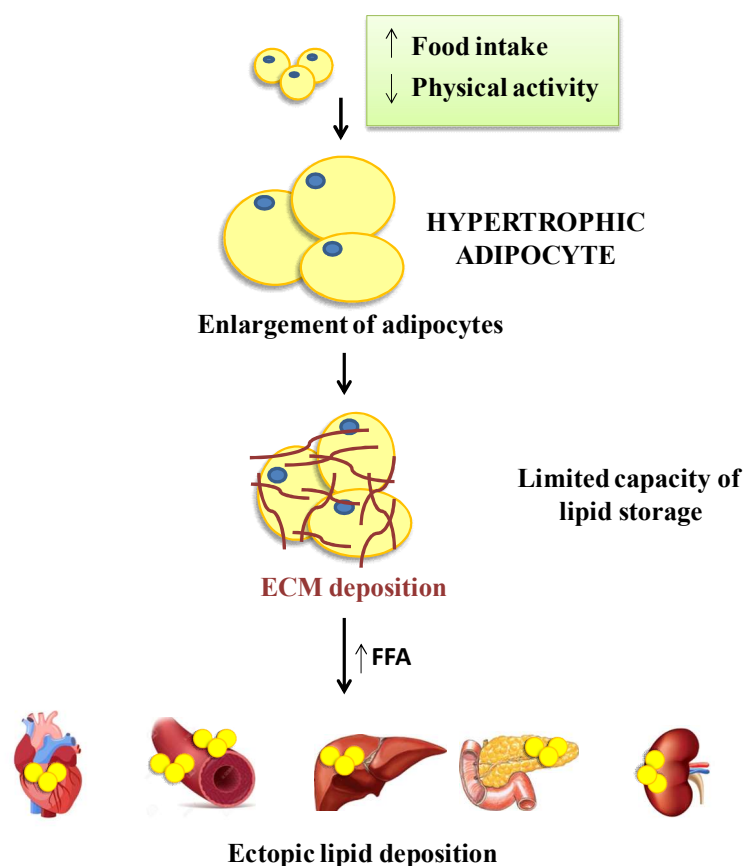


Figure 12. Effect of the adipose tissue fibrosis in ectopic fat deposition. ECM, extracellular matrix; FFA, free fatty acid.

Introduction

Adipose tissue has always been considered to be a reservoir organ. However, since the discovery of leptin (the first cytokine released by the adipocytes) in 1994 by Zhang et al¹³⁶, it has also begun to be considered an endocrine organ. Leptin is secreted after food intake by playing a role in inhibiting the appetite. Since leptin discovery, other cytokines delivered from adipose tissue have been found, these are termed “adypokines”. Adiponectin is another of them, which has anti-inflammatory and anti-obesity effects. In obese humans and animal models, adiponectin levels are reduced in both, plasma and adipose tissue, favouring an inflammatory response which is in agreement with the upregulation of pro-inflammatory cytokines, such as IL-1 β , IL-6, and MCP-1 observed in obese adipose tissue¹³⁷. Therefore, adipocyte hypertrophy is probably responsible, through activation of different mechanisms dependent or independent of inflammation, for the insulin resistance and impaired energy metabolism observed in the context of obesity.

On the other hand, some studies in the last years have demonstrated that human obesity¹³⁸⁻¹⁴² and mouse models of obesity^{143, 144} are also associated with low mitochondrial function in WAT. A study performed by Choo HJ et al, found reduced mitochondrial protein levels in *db/db* mice as well as abnormal mitochondrial morphology along with reduced fatty acid oxidation in *ob/ob* and mice¹⁴³. Similar results have been found in HFD mice in which genes associated with mitochondrial ATP production were decreased¹⁴⁴. In obese subjects a global downregulation of mitochondrial oxidative pathways mainly by a reduction in OXPHOS complex was also observed as compared with lean subjects¹³⁹. A study performed in visceral and subcutaneous adipose tissue of type 2 diabetic women showed that genes involved in electron transport and oxidative phosphorylation were downregulated independently of obesity¹⁴². All these alterations together are thought to contribute to the development of insulin resistance and adipocyte dysfunction observed in the context of obesity (Figure 13).

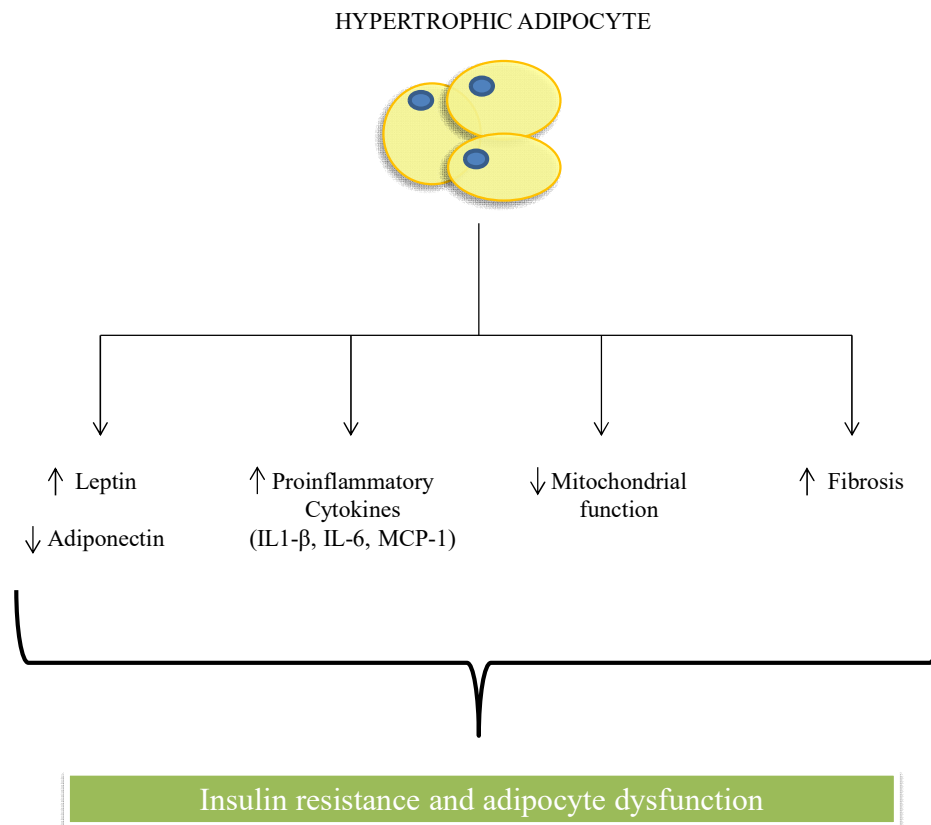


Figure 13. Adipose tissue remodelling contributing to adipocyte dysfunction.

As we have previously mentioned, the main characteristic of BAT is the increased expression of UCP-1 in their mitochondria. “Browning” is known as the phenomenon that refers to the transdifferentiation of white adipocytes into brown adipocytes, whose main characteristic is the appearance of UCP-1 positive adipocytes within WAT deposits¹⁴⁵. The presence of UCP-1 in white adipocytes mitochondria would grant them thermogenic capacity that could promote energy dissipation (Figure 14). This is the reason why browning, it has recently become an attractive target for counteracting the adverse metabolic consequences of obesity¹⁴⁶.

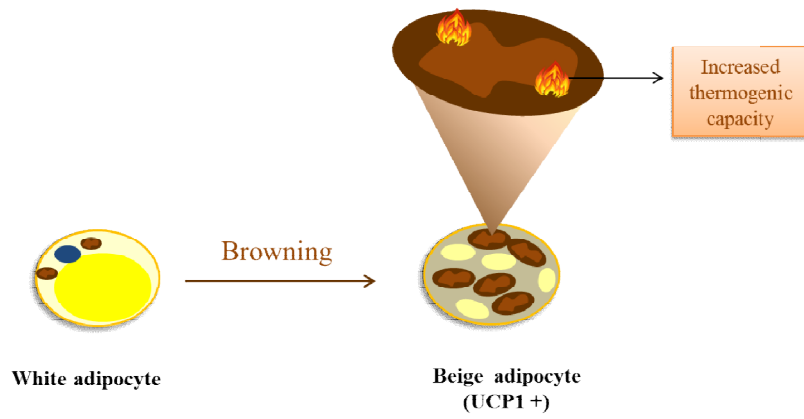


Figure 14. Transdifferentiation of white adipocyte into beige adipocyte (browning). UCP1, uncoupling protein 1.

Hypothesis and objectives

HYPOTHESIS

Cardiac lipotoxicity and mitochondrial oxidative stress participates in the development of cardiometabolic alterations associated with obesity.

HYPOTHESIS FOUNDATION

1. Larger adipocytes in obese adipose tissue have diminished capacity to store fat leading to elevation of circulating fatty acids which can be toxic in non-adipose tissues, including the heart.
2. Obesity is associated with cardiac alterations characterized by fibrosis and an increase in oxidative stress.
3. Pathological ROS levels have harmful effects in the heart, with the mitochondria being the main source of ROS.
4. Oxidative stress can participate in the adipose tissue remodelling which can be underlying metabolic alterations associated with obesity.

GENERAL OBJECTIVE

The overall aim of the work was to evaluate the role of lipotoxicity and mitochondrial oxidative stress in the cardiometabolic alterations in the context of obesity as well as the possible mechanisms involved.

SPECIFIC OBJECTIVES

1. To evaluate the impact of obesity in the cardiac lipid profile and its functional consequences in cardiac damage as well as the potential role of Gal-3.
2. To determine the role of mitochondrial oxidative stress in cardiac structural and functional alterations and in the metabolic substrate use modifications in the heart of obese rats.
3. To evaluate the interaction between mitochondrial oxidative stress and cardiac lipid profile in obese rats and its role in cardiac damage.
4. To assess the role of mitochondrial oxidative stress in adipose tissue remodelling in obese rats and its consequences in metabolic alterations.
5. To evaluate adipose tissue remodelling and metabolic alterations in obese patients.

Material and methods

I. ANIMAL STUDY

1. Experimental design

The study utilized a model of diet-induced obesity in comparison to a group of control animals.

Male Wistar rats of 150 g (Harlan Ibérica, Barcelona, Spain) were fed for 6 weeks either of the following:

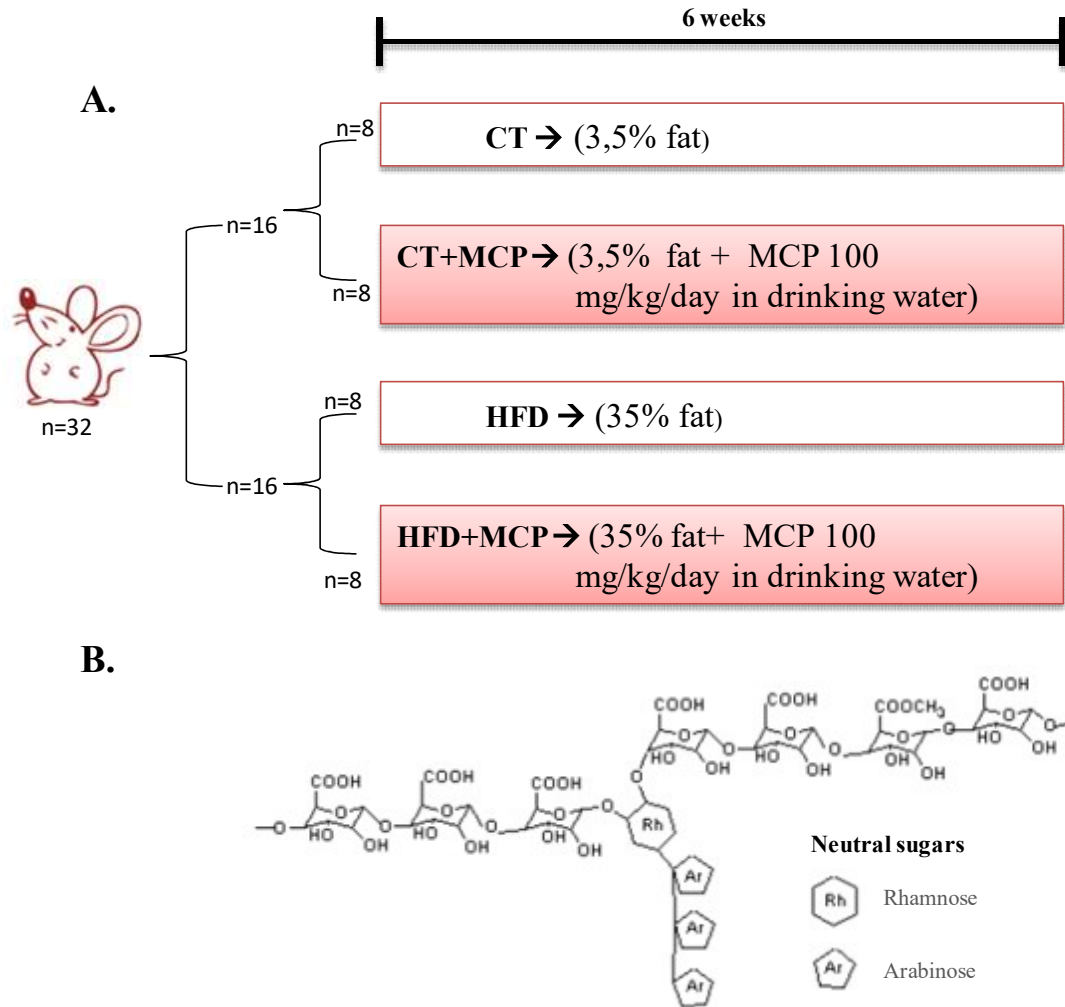
- High fat diet (HFD; 35% fat; Harlan Teklad no. TD.03307, Haslett, MI, USA)
- Standard diet (CT; 3.5% fat; Harlan Teklad no. TD.2014, Haslett, MI, USA)

The Animal Care and Use Committee of Universidad Complutense de Madrid approved all experimental procedures according to the Spanish Policy for Animal Protection RD53/2013, which meets the European Union Directive 2010/63/UE.

1.1 Animal model of obesity treated with the Gal-3 activity inhibitor

Animals of each group were treated with either vehicle or the inhibitor of galectin 3 activity (Modified citrus pectin, MCP; 100 mg/kg/day) in the drinking water for the same period (Figure 15A).

MCP is a derivative of the citrus pectin essentially consisting of neutral sugar sequences with a low degree of branching. MCP has been developed by depolymerizing the pectin polymer by interrupting the rhamnogalacturan backbone of the pectin molecule and then breaking down the side chains of neutral sugars into oligomers of neutral sugars. The molecular structure is shown in Figure (15B).



15. Animal model of diet induced obesity and inhibition of Galectin-3. (A) Development and evolution of animal model. **(B)** Molecular structure of MCP.

1.2 Animal model of obesity treated with a mitochondrial antioxidant

Animals of each group were treated with either vehicle or the mitochondrial antioxidant MitoQ (50 mg/kg/day) in the drinking water for the same period (Figure 16A).

MitoQ is a derivative of the natural antioxidant ubiquinol (also called coenzyme Q10). It is an ubiquinol derivative attached to a phosphonium cation [10-(6'-ubiquinonyl) decyltriphenyl phosphonium bromide]. The structure is shown in Figure 16B.

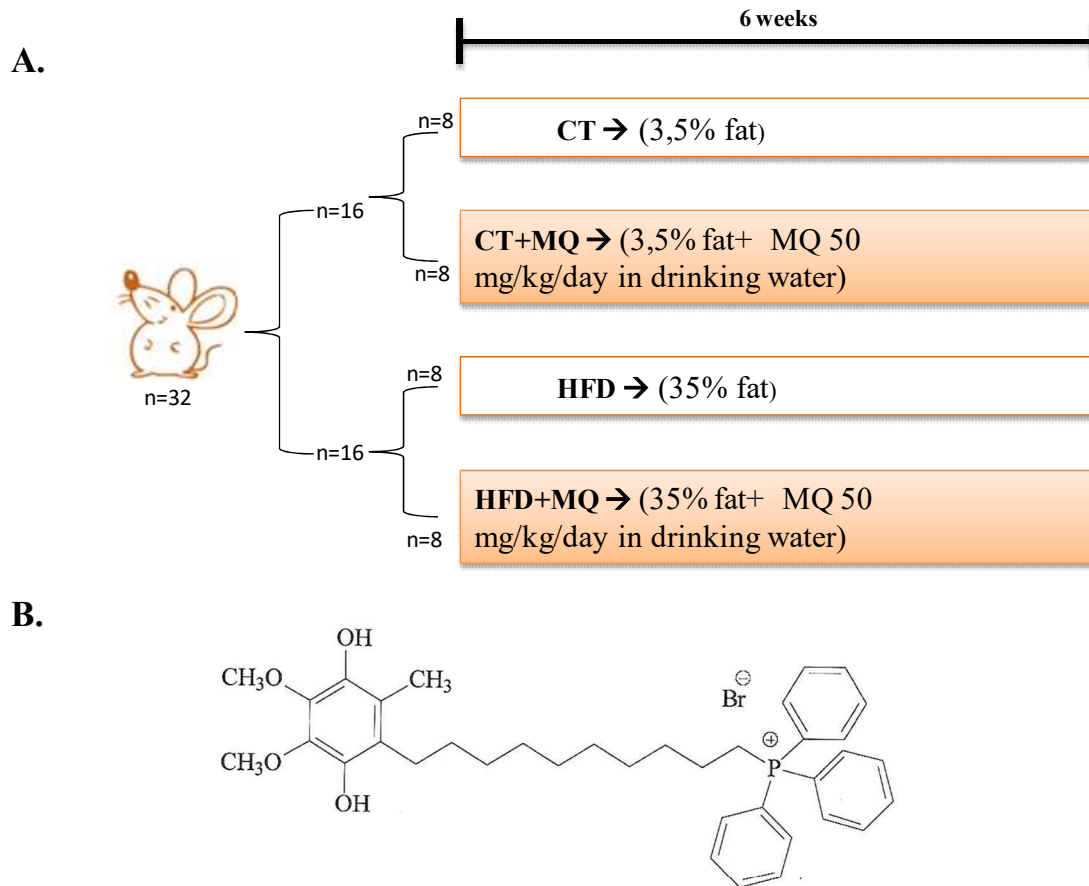


Figure 16. Animal model of diet induced obesity and inhibition of mitochondrial oxidative stress. (A) Fevelopment and evolution of animal model. (B) Molecular structure of MitoQ.

2. Monitoring of the animal model

Body weight was measured once a week. The intake of food and drink was determined throughout the experimental period. The amount of MCP and MitoQ taken daily per animal was calculated from the amount of water consumed on a daily basis. The systolic blood pressure (SBP) was determined three times throughout the entire experiment (at the beginning, at the middle and at the end of the study) by using a plethysmographic method (Narco Bio-Systems, Houston, TX, EEUU). The rats were kept in a room at 28°C for 2 hours. After this time, blood pressure was measured and the arithmetic mean of eight successive measurements was used as a final value on two consecutive days. On the days before the initial measurement of the pressure, simulations of the procedure were carried out to habituate the rats and to avoid alterations that could be distorting the experimental data.

3. Evaluation of cardiac structure and function

Cardiac structure and function were evaluated by transthoracic echocardiography with a Philips CX50 (Philips, Netherlands) connected to a L12-3 MHz linear transducer in rats anesthetized with isoflurane (2%; Esteve, Barcelona, Spain). 2D-guided M-mode recordings made from short axis views in order to measure LV chamber dimensions, interventricular septum (IVT) and posterior wall thickness (PWT) were measured from the bidimensional parasternal long-axis view. The mean measurements from several consecutive beats were used for data analysis.

Left ventricular ejection fraction (LVEF) was calculated according to the Teicholz Formula: $(EDD^3 \times 7) / (2.4 + EDD)$ and LV systolic chamber function (pump function) was determined from LV endocardial fractional shortening (FS) = $(EDD - ESD) / EDD \times 100$ and LV midwall fraction (MWFS) = $(EDD/2 + PWT_d/2) - (ESD/2 + PWT_s/2) / (EDD + PWT_d + IVT/2)$, where EDD is end-diastolic diameter in left ventricle, ESD is end-systolic diameter in LV, PWT_d is posterior wall thickness in diastole and PWT_s is posterior wall thickness in systole.

4. Sacrifice

Fasting animals were anesthetized (Ketamine 70mg/kg and xylazine 6mg/kg) and subsequently sacrificed by decapitation using a guillotine.

The blood was collected in two different tubes, one for obtaining serum and the other, in which an anticoagulant, EDTA, had previously been added to obtain plasma. They were subsequently they were centrifuged at 3000 rpm for 15 minutes, the supernatant was collected, aliquoted and stored at -80 ° C.

The heart was removed, the blood was eliminated and the heart was weighed before being cut into several parts. The section of the heart for molecular biology studies was immediately frozen in liquid nitrogen and stored at -80°C until use. Samples for histological studies were stored in two different ways. A heart section was stored in 35% v / v formaldehyde and another section was placed in a 30% (w / v) sucrose solution and left in for approximately 3-4 hours. It was then embedded in OCT, a tissue-freezing medium, and frozen in liquid nitrogen and stored at -80 ° C.

The fat depots (epididymal, mesenteric, lumbar and brown fat) were extracted and weighed. The epididymal fat, the main deposit used in this study, was sectioned in three pieces. One of them was stored in formaldehyde, another one was embedded in OCT and the last one was immediately frozen in liquid nitrogen and stored at -80°C for molecular biology.

5. Adiposity index

The adiposity index was calculated by the following formula:

$$\frac{\text{sum of fat pads}(g)}{\text{body weight}(g) - \text{fat pad weight}} \times 100$$

(*sum of fat pads= epididymal fat+ mesenteric fat+ lumbar fat)

6. HOMA index

Homeostatic model assessment (HOMA) is a method for assessing insulin resistance (IR) from basal (fasting) glucose and insulin concentrations. Glucose and insulin levels from blood samples were measured in our rats in order to make the calculation. Serum glucose levels were measured using the VITROS Chemistry Products GLU Slides Kit (VITROS Chemistry Products). Serum insulin levels were measured by ELISA (Mouse and rat leptin ELISA, Biovendor).

The formula used to calculate it is the following:

$$HOMA\ index = \frac{\text{Plasmatic glucose (mmol/L)} \times \text{plasmatic insulin (mU/L)}}{22.5}$$

7. Histological and morphological evaluation

7.1 Cardiac tissue

Heart samples kept in formaldehyde at the time of sacrifice were dehydrated in increasing solutions of ethyl alcohol, embedded in paraffin and cut with a microtome

Materials and methods

(Leica 1512, IMEB INC, CH, EEUU) in 4 μ -thick sections. Sections were stained with picosirius red in order to detect collagen fibers.

The area of cardiac interstitial fibrosis was identified as the ratio of collagen deposition to the total tissue area after excluding the vessel area from the region of interest. For each sample, 10-15 fields were analysed with a 40x objective.

Myocytes (60-80 per animal) with visible nucleus and intact cellular membranes were chosen for determination of cross-sectional area in cardiac sections stained with hematoxylin and eosin.

The photographs were made with an optical microscope (Leica DM 2000, Leica Camera AG, Wetzlar, Germany) and the quantification was performed by an image analyzer (LEICA Q550 IWB).

7.2 Adipose tissue

Epididymal adipose tissue samples were dehydrated in increasing solutions of ethyl alcohol, embedded in paraffin and cut into 5 μ m-thick sections with a microtome (Leica 1512, IMEB Inc, Chicago, EEUU) and stained with picosirius red in order to detect collagen fibers. The area of pericellular fibrosis was identified as the ratio of collagen deposition to the total tissue area after excluding the vessel area from the region of interest. This value was normalised by the number of adipocytes. Adipocytes (80-100 per subject or animal) with intact cellular membranes were chosen for determination of the cross-sectional area in hematoxylin-eosin stained sections. For each sample, 10-15 fields were analysed using a 40 \times objective (Leica DM 2000; Leica Camera AG, Wetzlar, Germany) and quantified (Leica Q550 IWB; Leica Camera AG, Wetzlar, Germany).

8. Detection of superoxide anion ($O_2^{\cdot-}$) production

For the in situ detection of superoxide anion ($O_2^{\cdot-}$) production, two different techniques were used. The dihydroetidium (DHE) technique that permits the measurement

production of total $O_2^{\cdot-}$ radicals in the cell and the mitoSOX technique that allows measuring the mitochondrial superoxide radicals.

8.1 Production of total $O_2^{\cdot-}$ (DHE)

We used the cardiac tissue samples that had been embedded in tissue-freezing medium for the detection of superoxide anion. 14 μm -thick sections were cut with a cryostat, placed onto glass microscope slides treated with APS and stored at -80°C until use. On the day of the experiment the slides were placed at least 1 hour at 37°C to fix the sample and prevent it from taking off. After that, they were washed in Krebs-HEPES buffer (see composition in annex I) for 30 minutes and then, incubated with DHE ($5\mu\text{M}$) for 30 minutes at 37°C in a light-protected humidified chamber. DHE is a fluorogenic dye that is useful for the detection of reactive oxygen species (ROS). DHE has been shown to be oxidized by superoxide anion to form 2-hydroxyethidium (2-OH-E^+). After the incubation with DHE, the slides were washed with warm phosphate-buffered. Cardiac images were viewed by fluorescent laser scanning microscope (40x objective in Leica DMI 3000 microscope) (Ex561nm and Em610 nm). Three histological sections and four different fields in each section per animal were quantified. The conditions of the microscope and the camera were kept constant to photograph all the preparations. The intensity of the fluorescence was quantified using the software Leica Application Suite Version4.7.0 (Switzerland).

8.2 Production of mitochondrial $O_2^{\cdot-}$ (MitoSOX)

The procedure to be followed and the method of analysis is the same as for the DHE technique. The only difference is the time for mitoSOX ($5\mu\text{M}$; Molecular probes, Invitrogen) incubation, being only 10 minutes.

MitoSOX Red reagent is live-cell permeant and is rapidly and selectively targeted to mitochondria. Once in the mitochondria, mitoSOX is oxidized by superoxide anion and exhibits red fluorescence. It is oxidized by superoxide but not by other ROS or reactive nitrogen species (RNS). The oxidation product becomes highly fluorescent upon binding to nucleic acids.

9. Lipidomic analysis

Myocardial lipids were extracted and analyzed by ultrahigh performance liquid chromatography coupled to time-of-flight mass spectroscopy (UPLC-QToF-MS) using an Acquity UPLC System and a SYNAPT HDMS G2 (Waters, Manchester, UK) with electrospray ionization. For the mitochondria-specific myocardial lipid analysis, mitochondria were first isolated from cardiac tissue with the *Mitochondria Isolation Kit for Tissue (Thermo Scientific)*. Extraction of lipids was carried out from cardiac homogenates (or isolated mitochondria in the case of mitochondria-specific analysis) in methanol:chloroform mixture (1:2, v/v) and split into two aliquots. One aliquot was evaporated to dryness and the pellet re-suspended in acetone:2-propanol:ethanol (3:4:3,v/v/v) and used for TGs measurement. The other aliquot was evaporated to dryness and the pellet re-suspended in methanol:water (9:1, v/v/v) and used for phospholipids (PPLs) measurement. Extracts were kept at -80°C until analysis. Mass spectrometric analysis of TGs was performed in positive mode (ESI+) using the parameters that follow: capillary, 0.8 kV; sampling cone, 15 V; source temperature, 90°C ; desolvation temperature, 280°C ; cone gas, 40 L/h; and desolvation gas, 700 L/h. Data were acquired with the software MassLynx at a rate of 5 scans/s within the range 0---18 min, and m/z 100---1200 Da for the low-energy function and m/z 100---900 Da for the high-energy function (MSE method, trap collision energy 30 V). LC and MS methods were optimized using the commercial standards TG (18:2/18:2/18:2) and TG (16:0/16:0/16:0). These standards were also used to draw calibration curves for quantification. Mass spectrometric analysis of PPLs was fitted as follows: capillary, 0.9 kV; sampling cone, 18 V; source temperature, 90°C ; desolvation temperature, 320°C ; cone gas, 45 L/h; and desolvation gas, 900 L/h. Data were acquired with the software MassLynx at a rate of 5 scans/s within the range 0---12 min and 100--1200 Da m/z for the low-energy function, and 50---900 Da m/z for the high-energy function (MSE method, trap collision energy 30 V), with ionization in positive mode (ESI+) for detection of diacylphosphatidylcholines (PCs), ceramides (CER) and sphingomyelins (SM), and with ionization in negative mode (ESI-) for detection of other phospholipids, which were diacyl phosphatidylethanolamine (PE), diacyl phosphatidylinositol (PI), diacyl phosphatidylglycerol (PG), and phosphatidicacids (PA). External commercial standards, namely PI (8:0/8:0), PG (14:0/14:0), PE (12:0/12:0), PC (10:0/10:0) and PA (14:0/14:0) were purchased from Cayman Chemical

(Michigan, USA) and used for method optimization and quantification. Up to three different chromatograms were manually checked for mass spectral peak identification where possible. Within each chromatographic point, m/z values with an intensity ≥ 700 were also checked for it in order to afford a defined chromatographic peak (Extracted Ion Chromatogram, EIC); if positive, the elemental composition tool was then used to determine all the possible chemical compositions ($C_nH_mO_pN_sPrSt$) that were compatible with the isotopic distribution (M , $M+1$, $M+2$ and $M+3$ peaks) of a given m/z value. Using LipidMaps, Metlin, CheBI, LipidBank and KEGG databases, a certain elemental composition was examined for possible known compounds. Acyl chains were identified where possible by data from the high energy function (fragmentation). Moreover, specific fragments in the high energy function (MSE) were considered for identification, in particular m/z 184.07 for PCs and SMs in positive ionization mode.

10. In vivo PET–CT imaging to study ^{18}F -Fluorodeoxyglucose heart uptake

Myocardial metabolic activity was evaluated by means of a small-animal dedicated dual scanner (Albira PET/CT scanner, Bruker NMI, Valencia Spain). One week before the end of the evolution period, animals were fasted for 18 hours and they were intraperitoneal (ip) injected with ^{18}F -Fluorodeoxyglucose (FDG; $12.99 \pm 0.04 \text{ MBq}$ in 0.2 ml of 0.9% NaCl; Instituto Tecnológico PET, Madrid, Spain). Twenty minutes later, rats underwent PET and computed tomography (CT) acquisitions under isoflurane anesthesia. The acquired tomographic images were then reconstructed using the maximum likelihood expectation maximization and filtered back projection algorithms for the PET and CT images, respectively. In order to account for the different rat weights and ^{18}F - injected FDG doses, we calculated the standardized uptake value (SUV). The semi-quantitative SUV measurement is the most widely used in both small animal and human ^{18}F -FDG PET studies ^{147, 148}. The software used was the PMOD 3.6 software (PMOD Technologies Ltd., Zurich, Switzerland).

11. Proteomic analysis

11.1 Proteomic analysis from cardiac tissue samples

Sample preparation. Tissue samples were homogenized in lysis buffer (7 M urea, 2 M thiourea, 50 mM DTT) and protein concentration was quantified with the Bradford assay kit (Bio-Rad) and then precipitated with the ReadyPrep 2-D cleanup kit (BioRad). The protein extract for each sample was diluted in Laemmli buffer and loaded into a 1.5 mm thick polyacrylamide gel with a 4% stacking gel casted over a 15% resolving gel. The run was stopped as soon as the front entered 3 mm into the resolving gel to concentrate the whole proteome in the stacking/resolving gel interface. Bands were stained with Coomassie Brilliant Blue and excised from the gel. Purification and concentration of peptides was performed using C18 Zip Tip Solid Phase Extraction (Millipore).

Mass Spectrometry analysis. Peptides mixtures were separated by reverse phase chromatography using an Eksigent nanoLC ultra 2D pump fitted with a 75 μ m ID column (Eksigent 0.075 \times 250). Samples were first loaded for desalting and concentration into a 0.5 cm length 100 μ m ID precolumn packed with the same chemistry as the separating column. Mobile phases were 100% water 0.1% formic acid (FA) (buffer A) and 100% Acetonitrile 0.1% FA (buffer B). Column gradient was developed in a 200 min two step gradient from 5% B to 25% B in 160 min and 25%B to 40% B in 21 min. Column was equilibrated in 95% B for 8 min and 5% B for 11 min. Precolumn was in line with column during the enter process and flow maintained all along the gradient at 300 nl/min. Eluting peptides from the column were analyzed using a Sciex 5600 Triple-TOF system. Information data acquisition was acquired upon a survey scan performed in a mass range from 350 m/z up to 1250 m/z in a scan time of 250 ms. Top 35 peaks were selected for fragmentation. Minimum accumulation time for MS/MS was set to 100 ms, resulting in a total cycle time of 3.8 s. Product ions were scanned in a mass range from 230 m/z up to 1500 m/z and excluded for further fragmentation during 15 s.

Data Analysis. The MS/MS data acquisition was performed using Analyst 1.7.1 (Sciex) and spectra files were processed through Protein Pilot Software (v 5.0.1-Sciex) using Paragon™ algorithm (v 5.0.1) for database search¹⁴⁹, Progroup™ for data grouping, and searched against the concatenated target-decoy UniProt proteome database (*rat*

norvegicus). False discovery rate was performed using a non-linear fitting method¹⁵⁰ and displayed results were those reporting a 1% Global false discovery rate or better.

The peptide quantification was performed using the Progenesis LC–MS software (ver. 2.0.5556.29015, Nonlinear Dynamics). Runs were aligned to compensate for between-run variations in our nanoLC separation system by using the accurate mass measurements from full survey scans in the TOF detector and the observed retention times. To this end, all runs were aligned to a reference run automatically chosen by the software, and a master list of features considering m/z values and retention times was generated. The quality of these alignments was manually supervised with the help of quality scores provided by the software. The peptide identifications were exported from Protein Pilot software and imported in Progenesis LC–MS software where they were matched to the respective features. Output data files were managed for subsequent statistical analyses and representation. Proteins identified by site (identification based only on a modification), reverse proteins (identified by decoy database) and potential contaminants were filtered out. Proteins quantified with at least two unique peptides, p-value lower than 0.05, and an absolute fold change of <0,7 or >1,3 in linear scale were considered significantly differentially expressed.

12. Tissue processing for protein extraction

12.1 Cardiac tissue

12.1.1 Total proteins

300 µl of buffer extraction (see annex I) and 150 mg of SSB14B 1.4mm Stainless Blend (0.9-2.00 mm) beads were added to 150 mg of cardiac tissue. Tissue was homogenized using a bullet blender (BBY24M Storm, Next Advance) according to the Bullet Blender® User Guide. The homogenate was incubated for 30 min on ice prior to centrifugation at 14.000 rpm for 10 min at 4 °C. The supernatant was extracted and stored at -80 °C until use. The protein contents of supernatant were measured using Comassie Brilliant Blue method.

12.1.2 Mitochondrial proteins

We must first isolate mitochondria to extract mitochondrial protein. For the isolation, frozen hearts were placed and washed in cold homogenization medium (see composition in annex I) containing 0.075mol/L sucrose, 1mmol/l EDTA, 10mmol/l Tris-HCl, pH 7.4. Briefly, heart tissue was homogenized (1/10w/v) at 800 rpm in a homogenizer (T 10 basic Ultra-turrax, Ika-Werke; Germany). The homogenates were centrifuged at 1,300 g for 5 min at 4°C to remove nuclei and debris. Supernatants were separated and centrifuged at 12,000 g for 10 min at 4°C. The resulting pellets were resuspended in 1ml homogenization medium and centrifuged twice at 14,400 g for 3 min at 4°C to wash the mitochondrial fraction. The supernatant was removed and the pellet was resuspended in 100 µl of homogenization medium. Protein concentration was determined by the Bradford method, and then it was stored at -80°C until use.

12.2 Adipose tissue

12.2.1 Total proteins

150 µl of commercial buffer extraction (2-D Rehydration/sample buffer, BIORAD including protease inhibitor cocktail added previously) and 150 mg of ZrOB05 0.5 mm Zirconium Oxide Beads were added to the same mass of epididymal adipose tissue. From this step, adipose tissue was homogenized following the same procedure as for the heart.

13. Western blot

Aliquots of 25 µg of proteins were denatured by heating at 95 °C for 5 minutes in presence of β-mercaptoethanol, a denaturing agent which cleaves the disulphide bonds. Proteins were separated by sodium dodecyl sulfate polyacrylamide gel electrophoresis (SDS-PAGE) on gradient gels (4–20% Mini-PROTEAN® TGX™ Precast Protein Gels, BIO-RAD) for 30 minutes at 100 mA. After the electrophoresis, which was used to separate the proteins according to molecular weight, the proteins were transferred to nitrocellulose membranes (Transblot® Turbo™ Midisize

Nitrocellulose, BIO-RAD, Germany) with the Trans-Blot Turbo Transfer System. The running buffer and transfer buffer are detailed in annex I.

For the immunodetection, the membranes were blocked with 7,5% milk in PBST for 1 hour at room temperature. The incubation conditions of each primary and secondary antibody are detailed in the table 1 (Annex I). Signals were detected using the ECL system (Amersham Pharmacia Biotech). Results are expressed as an n-fold increase over the values of the control group in densitometric arbitrary units.

14. RNA extraction from adipose tissue

100 mg of epididymal adipose tissue was disrupted and homogenized with a TissueRuptor in 1mL of QIAzol Lysis Reagent. After addition of chloroform, the homogenate is separated into aqueous and organic phases by centrifugation. The upper, aqueous phase is collected, and ethanol is added to provide appropriate binding conditions. The sample is then applied to an RNeasy spin column, where the total RNA binds to the membrane, and phenol and other contaminants are efficiently washed away. High-quality RNA is then eluted in RNase-free water. The extraction was carried out with the RNeasy Lipid Tissue Kit according to the manufacturer's instructions (Qiagen).

15. Reverse Transcription and Real-Time PCR

First, strand cDNA was synthesized according to the manufacturer's instructions (Go Script Reverse Transcription System, Promega). Quantitative PCR analysis was then performed with SYBR green PCR technology (GoTaq Real-Time PCR Systems, Promega). Relative quantification was achieved with MxPro-Mx3000P software. Data were normalized by 18S levels and expressed as percentage relative to controls. All PCRs were performed at least in triplicate for each experimental condition. Primer sequences are detailed in table 2 (Annex I).

II. CELL CULTURE STUDY

1. Cell culture

Cells of the H9c2 rat cardiomyoblast cell line (Merck, Darmstadt, Germany) were maintained in Dulbecco's modified Eagle's medium (DMEM)-high glucose (Merck, Darmstadt, Germany) supplemented with Fetal Bovine Serum (FBS) 10%, penicillin/streptomycin 1% and L-glutamine 1%. Cells were cultured according to the manufacturer's instructions and were used until passages 20-22. The cells were maintained at a temperature of 37 °C, 95% sterile air and 5% CO₂ in a saturation humidified incubator.

After 24 hours in medium without serum, cells were stimulated with 100, 200 or 300 µmol/l of palmitate conjugated with 10% free fatty acids (FFA)- BSA for 24 h in order to choose the dose appropriate for performing the experiments. The dose of 200 µmol/l was finally used in all analyses in the presence or absence of MPC (0.01%) or in the presence or absence of MitoQ (10⁻⁷M).

2. Measurements of cellular respiration and estimation of the rate of glycolysis

An XF24-3 extracellular flux analyzer (Seahorse Biosciences, North Billerica, MA) was used for determining the bioenergetic profile of the H9c2 cardiac myoblasts. 40x10³ cells were seeded per well in Seahorse XF24 plates. After 24 hours in medium without serum, cells were stimulated with 100, 200 or 300 µmol/l of palmitate conjugated with 10% free fatty acids (FFA)- BSA for 24 h in order to choose the dose appropriate for performing the experiments. The dose of 200 µmol/l was finally used in all analyses in the presence or absence of MPC (0.01%) or in the presence or absence of MitoQ (10⁻⁷ M).

For the XF24-3 assays, DMEM growth media was replaced by unbuffered DMEM supplemented with 5.5 mmol/L glucose, 1mmol/L pyruvate and 10 mmol/L L-glutamine, stimuli were re-added and cells incubated at 37 °C in a CO₂-free incubator for 1 h. Subsequently, the oxygen consumption rate (OCR) and extracellular acidification rate (ECAR), a proxy for lactate production, were recorded to assess the

mitochondrial respiratory activity and glycolytic activity, respectively. After four measurements under basal conditions, cells were treated sequentially with 1 $\mu\text{mol/L}$ oligomycin, 0.6 $\mu\text{mol/L}$ carbonyl cyanide p-(trifluoromethoxy) phenylhydrazone (FCCP) and 0.4 $\mu\text{mol/L}$ FCCP with three consecutive determinations under each condition that were averaged during data evaluation. At the end of the run, 1 $\mu\text{mol/L}$ rotenone and 1 $\mu\text{mol/L}$ antimycin A were added to determine the mitochondria-independent oxygen consumption and the value subtracted from all OCR measurements. ATP turnover was estimated from the difference between the basal and the oligomycin-inhibited respiration, and maximum respiratory capacity was the rate in the presence of the uncoupler FCCP (Figure 17). A scheme showing at which level the modulators of ETC act is represented in Figure 18. Protein concentration in each well was determined using the BCA method and results were normalized according to protein content. Experiments were repeated four times with similar results.

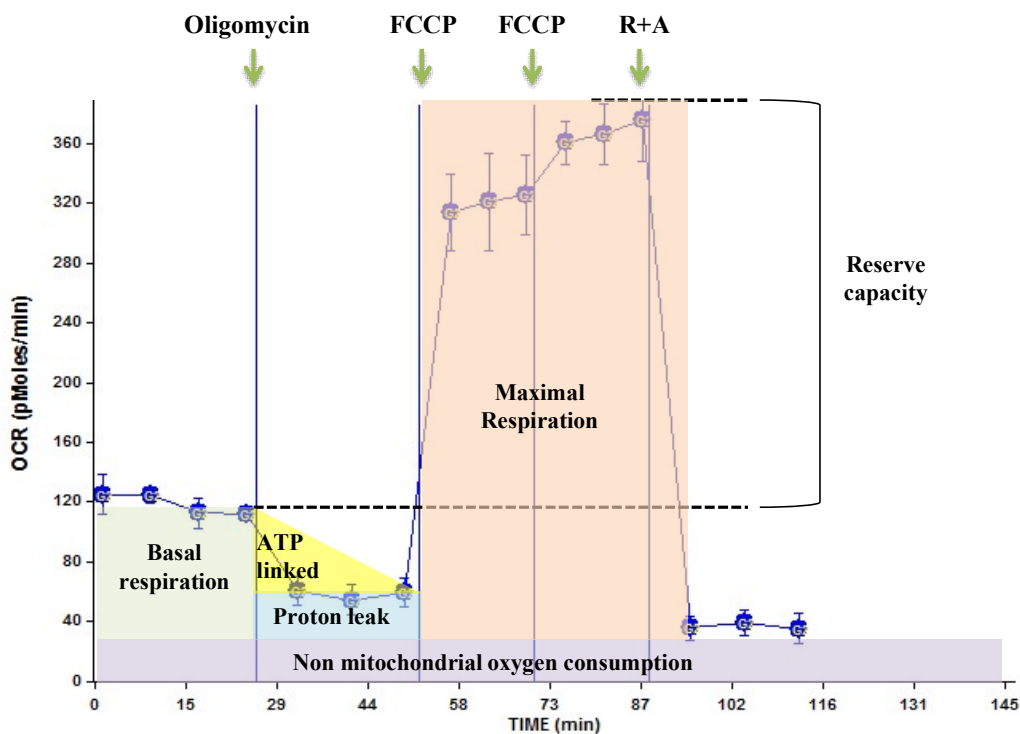


Figure 17. Representative XF assay and diagram of how mitochondrial measurements were calculated. R, rotenone; A, antimycin A.

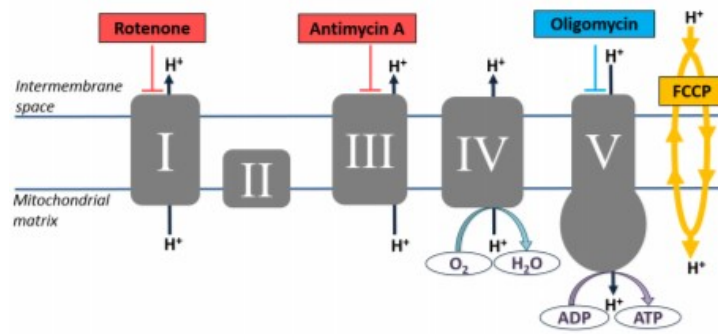


Figure 18. Scheme of Seahorse XF Cell Mito Stress Test modulators of the ETC. Figure from Agilent Seahorse XF Cell Mito Stress Test Kit User Guide.

3. Viability assay

H9c2 cell proliferation was evaluated by using the Promega kit (Madison, WI), Cell Titer 96® Aqueous One Solution Cell Proliferation Assay, according to the manufacturer's recommendations. Briefly, cells were seeded in 96-well plates and serum-starved for 24 h. Cells were then stimulated with 100, 200 or 300 $\mu\text{mol/l}$ of palmitate-BSA or 20% of fetal bovine serum (FBS). After 24 h of incubation, formazan product formation was assayed by recording the absorbance at 490 nm in a 96-well plate reader (OD value). Formazan is measured as an assessment of the number of metabolically active cells and expressed in percentages relative to unstimulated cells.

III. CLINICAL STUDY

1. Patients

Morbidly obese patients who were referred to bariatric surgery were consecutively recruited from the Obesity Care Unit of Fuenlabrada University Hospital, Spain. The selection of the patients was performed by a multidisciplinary committee, which includes personnel from endocrinology, general and upper gastroenterology surgery, and internal medicine and cardiology services.

Inclusion criteria were age ≥ 18 years and universally accepted indications for bariatric surgery: long-term obesity (>4 years), body mass index ≥ 40 kg/m^2 despite other weight

loss strategies, or body mass index ≥ 35 kg/m² in the presence of obesity-related comorbidities (diabetes mellitus, obesity hypoventilation syndrome, obstructive sleep apnea syndrome, and hypertension). Exclusion criteria were age >60 years and unacceptable surgical risk because of concomitant comorbidities. ~

Non-obese volunteers (body mass index, ≤ 25 kg/m²) were recruited from staff of the hospital.

The study protocol was approved by the ethics committee, and all participants signed the informed consent. This study was conducted in compliance with Good Clinical Practice Guidelines and the ethical principles stated in the Declaration of Helsinki.

2. Anthropometric measurements

Body mass index (BMI) was measured using the following calculation:

$$BMI = \frac{\text{body weight (kg)}}{\text{height}^2 \text{ (m}^2\text{)}}$$

Only those bariatric patients with a BMI < 25 (as controls) and those with BMI > 25

Of all the subjects who underwent bariatric surgery, for the data analysis presented in this thesis only those with a BMI < 25 (as controls) and those with BMI > 25 in absence of obesity-related diabetes were selected for the analysis presented in this thesis.

3. Circulating parameters

Blood samples were obtained following the clinical protocol approved for bariatric surgery. Briefly, venous blood samples (20 mL) were collected after an overnight fast (>10 hours) between 7:00 a.m. and 9:00 a.m. into vacutainers Rapid Serum Tubes. Serum was separated from whole blood by centrifugation (20 minutes at 300g) and stored at -80°C until analysis.

Serum concentrations of the different circulating parameters were analysed by ELISA kit according to the manufacturer's instructions (Milliplex® Map Kit, MA, USA).

4. Proteomic analysis from human adipose tissue samples

The proteomic analysis comprises several steps: sample preparation, isoelectrofocusing separation, mass spectrometry and data analysis (Figure 19).

Sample preparation. Tissue samples pools were lysed in a Precellys 24 Bead Mill Homogenizer (Bertin Technologies) (15 x 2 s, power set to 5500 w) using 5 mM EDTA, 0.1% Triton X-100, 1% glycerol in 30 mM Hepes pH 7.4, supplemented with 1:1000 (v/v) of benzonase (Novagen) and 1:100 (v/v) of Halt™ phosphatase and protease inhibitor cocktail 100x (Thermo Fisher Scientific). Lysates were clarified by centrifugation at 4 °C and 16000 rpm for 15 min. Recovered supernatants were cleaned-up by methanol-chloroform extraction¹⁵¹.

Pellets were dissolved in 8 M urea in 0.1 M Triethylammonium bicarbonate (TEAB) buffer. Protein concentration was determined using the Bradford Protein Assay Kit (Bio-Rad) using BSA as standard. Samples were then digested by means of the standard FASP protocol¹⁵². Briefly, proteins were reduced (10 mM DTT, 30 min, RT), alkylated (50 mM IA, 20 min in the dark, RT) and sequentially digested with Lys-C (Wako) (protein:enzyme ratio 1:50, o/n at RT) and trypsin (Promega) (protein:enzyme ratio 1:100, 6 h at 37°C). Resulting peptides were desalted using C₁₈ stage-tips.

Samples (110 µg) were labeled using iTRAQ® reagent 4-plex following the manufacturer's instructions. Labeling scheme was as follows: Control (114), Insulin resistant obese (115). Samples were mixed in 1:1 ratios based on total peptide amount, which was determined from an aliquot by comparing overall signal intensities on a regular LC-MS/MS run. The final mixture was finally desalted using a Sep-Pak C18 cartridge (Waters) and dried. The sample was reconstituted in OFFGEL solution (5% glycerol, 1% ampholytes pH 3-10) prior to electrofocusing.

Isoelectrofocusing separation. Peptides were pre-fractionated offline by means of IEF using a 3100 OFFGEL Fractionator system (Agilent Technologies, Böblingen, Germany) with a 24-well set-up. The IPG gel strips of 24 cm-long (GE Healthcare, München, Germany) with a 3–10 linear pH range were rehydrated according to the protocol provided by the manufacturer. Subsequently, 150 µL of sample was loaded in each well. Electrofocusing of the peptides was performed at 20°C and 50 µA until the 50 kVh level was reached. The 24 peptide fractions were withdrawn after focusing and

the wells rinsed with 100 μ L of a solution of 0.1%TFA. Rinsing solutions were pooled with their corresponding peptide fraction. All fractions were evaporated by centrifugation under vacuum. Solid phase extraction and salt removal was performed with home-made columns based on Stage Tips with C8 Empore Disks (3M, Minneapolis, MN) filled with Poros Oligo R3 resin (Life Technologies). Eluates were evaporated to dryness and maintained at 4°C. Just prior nano-LC, the fractions were resuspended in H₂O with 0.1% (v/v) formic acid (FA).

Mass spectrometry. LC-MS/MS was done by coupling a nanoLC-Ultra 1D+ system (Eksigent) to a LTQ Orbitrap Velos mass spectrometer (Thermo Fisher Scientific) via a Nanospray Flex source (Thermo Fisher Scientific). Peptides were loaded into a trap column (ReproSil Pur C18-AQ 5 μ m, 10 mm length and 0.3 mm ID, SGE Analytical) for 10 min at a flow rate of 2.5 μ L/min in 0.1% FA. Then peptides were transferred to an analytical column (ReproSil Pur C18-AQ 3 μ m, 200 mm length and 0.075 mm ID, SGE Analytical) and separated using a 117 min effective linear gradient (buffer A: 4% ACN, 0.1% FA; buffer B: 100% ACN, 0.1% FA) at a flow rate of 300 nL/min. The gradient used was: 0-3 min 2% B, 3-120 min 40% B, 120-131 min 98% B and 131-140 min 2% B. The peptides were electrosprayed (1.7 kV) into the mass spectrometer with a PicoTip emitter (360/20 Tube OD/ID μ m, tip ID 10 μ m) (New Objective), a heated capillary temperature of 240°C and S-Lens RF level of 60%. The mass spectrometer was operated in a data-dependent mode, with an automatic switch between MS and MS/MS scans using a top 15 method (threshold signal \geq 1000 counts and dynamic exclusion of 45 sec). MS spectra (250-1750 m/z) were acquired in the Orbitrap with a resolution of 60,000 FWHM (400 m/z). Peptides were isolated using a 2 Th window and fragmented using higher-energy collisional dissociation (HCD) with Orbitrap readout at a NCE of 42% (0.25 Q-value and 0.1 ms activation time). The ion target values were 1E6 for MS (500 ms max injection time) and 2E5 for MS/MS (200 ms max injection time). Samples were injected in duplicates.

Data analysis. Raw files were processed with Proteome Discoverer 1.3.0.339 software suite (Thermo Fisher Scientific). The fragmentation spectra were searched against a human protein database (UniProtKB/Swiss-Prot with isoforms, January 2013, 20,232 sequences) supplemented with contaminants. MASCOT was the preferred search engine (v2.2.7) with the precursor and fragment mass tolerances set to 10 ppm and 0.025 Da, respectively, and with up to two missed cleavages. Lysine and peptide N-termini

Materials and methods

labeling with iTRAQ-4plex reagent as well as carbamidomethylation of cysteine were considered to be fixed modifications, while oxidation of methionine was chosen as variable modification for database searching. Minimal peptide length was set to 6 amino acids and Mascot ion score > 20 . Peptide identification false discovery rate (FDR) was less than 1%. In case that identified peptides were shared by two or more proteins (homologs or isoforms), they were reported by Proteome Discoverer as one protein group. The results were then exported into Excel for manual data interpretation. Although relative quantification and some statistical data were provided by the Proteome Discoverer software, an additional 1.3-fold change cutoff for all iTRAQ ratios was selected to classify proteins as up- or down-regulated (ratio >1.3 or <0.77 , respectively) (Figure 20). Protein classification (biological process and protein class) was performed by PANTHER software, using the entire list of identified proteins as the reference data set to analyse the regulated proteins.

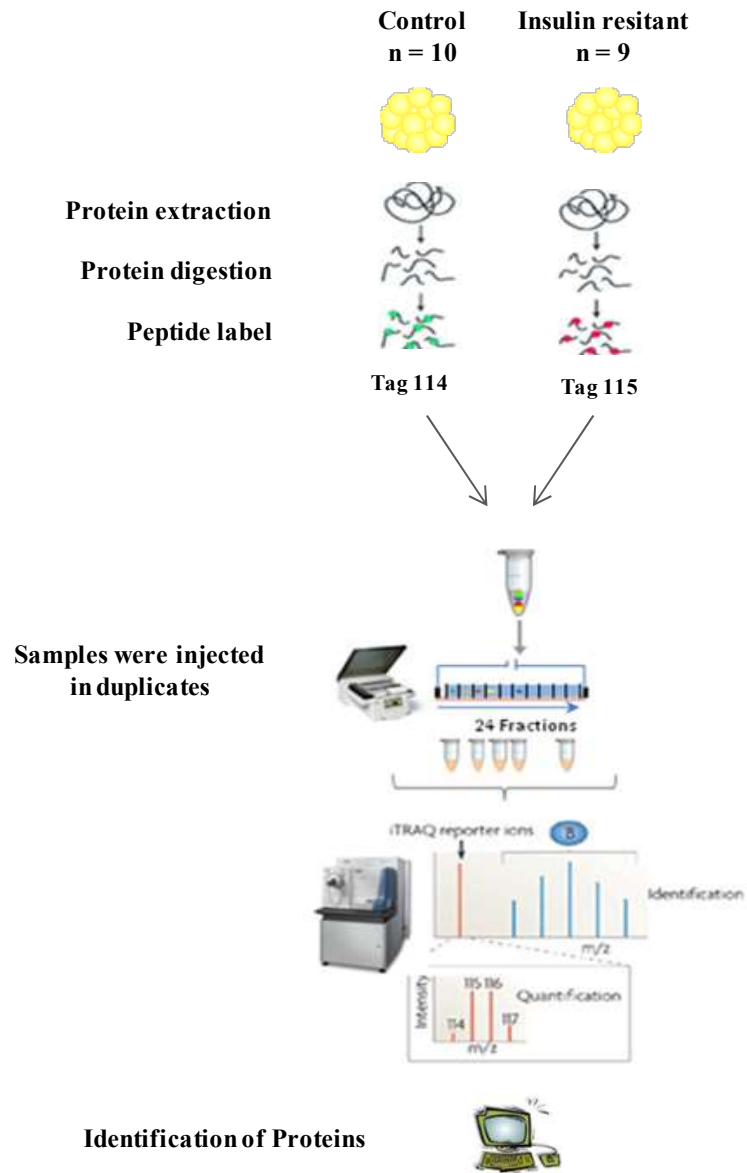


Figure 19. Representative scheme of the proteomic study from adipose tissue of patients.

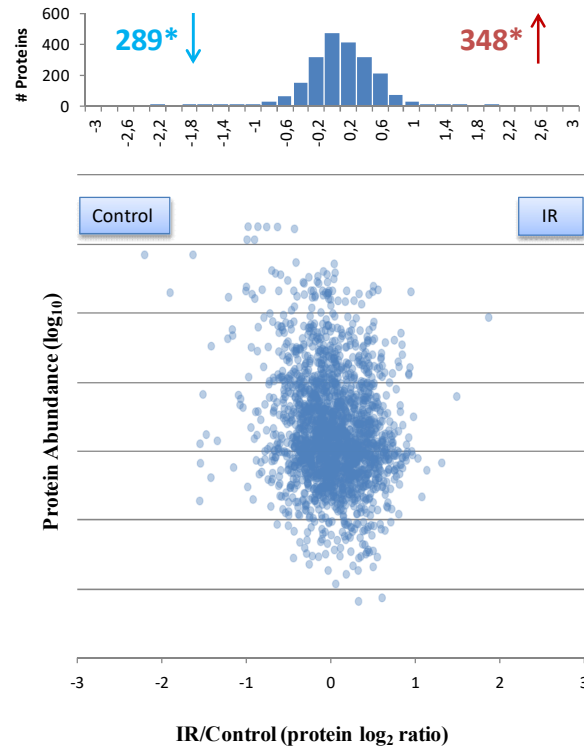


Figure 20. Data analysis of differentially regulated proteins between control and IR obese patients using a protein Log₂ ratio=0.378. (<> Fold Change = 1.3). IR, insulin resistant.

IV. STATISTICAL ANALYSIS

1. Experimental model analysis

Normality of distributions was verified by means of the Kolmogorov–Smirnov test. One-way ANOVA was used and followed by Newman-Keuls test. Continuous variables are expressed as mean±s.e.m.

In case the data did not follow a normal distribution, a non parametric test (Kruskal-Wallis tets) was performed followed by a Dunns post-test to compared selected pairs of columns.

Either Pearson or Spearman correlation analysis were used to examine association among different variables according to whether they are normally distributed.

A value of $p < 0.05$ was used as the cutoff value for defining statistical significance. Data analysis was performed using the statistical program GraphPad Software Inc. (San Diego, CA, USA).

2. Clinical data analysis

Continuous variables are expressed as mean \pm standard deviation. Normality of distributions of the data was verified by means of the Kolmogorov–Smirnov test. Levene’s test was used to assess the equality of variances and a Student’s t test was performed to determine if two sets of data were significantly different from each other. A value of $p < 0.05$ was used as the cutoff value for defining statistical significance. Data analysis was performed using the statistical program SPSS 22.0 (SPSS Inc., Chicago, IL, EE. UU).

Materials and methods

V. ANNEX

Protein analysis

Cardiac mitochondrial protein extraction buffer

Homogenization medium

Sucrose.....	75 mM	} pH=7.4
EDTA.....	1mM	
Tris-HCl.....	10mM	

Cardiac total protein extraction buffer

Complete Lysis-M buffer
(Roche; REF 04719956001).....10 ml

Complete Tablets (protease
inhibitor cocktail, Roche;
Ref 04639124001).....1 tablet

Adipose tissue total protein extraction buffer

ReadyPREP™ 2-D Starter
Kit Rehydration/Sample buffer
(BIORAD).....10 ml

Complete Tablets (protease
inhibitor cocktail, Roche;
Ref 04639124001).....1 tablet

Running buffer

Tris.....50 mM
Glycine.....192 mM
SDS.....0.3 %

Transfer buffer (1L)

5x transfer buffer (BIORAD).....200 mL
Ethanol.....200 mL

H₂O distilled.....600 mL

Detection of superoxide anion

Krebs-HEPES buffer

CaCl₂·2H₂O.....2mM

NaCl.....130 mM

KCl.....5.6 mM

MgCl₂·6H₂O.....250μM

Hepes.....8.4 mM

Glucose.....10 mM

pH=7.4

Table 1. Immunodetection conditions for each protein measured by western blot.

Antibody	Molecular weight	Dilution	Secondary antibody and dilution	Commercial reference
Primary antibodies				
ACS	79 kDa	1:1000	α -rabbit (1:1000)	abcam
ATGL	54 kDa	1:1000	α -rabbit (1:1000)	abcam
Adiponectin	32 kDa	1:1000	α -rabbit (1:1000)	abcam
CD36	78-88 kDa	1:1000	α -rabbit (1:1000)	abcam
CPT1A	88 kDa	1:1000	α -mouse (1:1000)	abcam
CTGF	45 kDa	1:1000	α -rabbit (1:1000)	Sigma-aldrich
Cyclophilin F	18 kDa	1:1000	α -mouse (1:1000)	Santa Cruz Biotechnology
Cytochrome C	12 kDa	1:1000	α -mouse (1:1000)	abcam
DGAT1	55 kDa	1:500	α -goat (1:1000)	abcam
DRP1	82 kDa	1:500	α -mouse (1:1000)	abcam
Fumarate hydratase	46 kDa	1:1000	α -mouse (1:1000)	Santa Cruz Biotechnology
Galectin 3	30 kDa	1:1000	α -mouse (1:1000)	Thermo
GLP1	21 kDa	1:1000	α -mouse (1:1000)	abcam
GLUT 4	50-63 kDa	1:1000	α -mouse (1:1000)	Santa Cruz Biotechnology
HCCS	31 kDa	1:1000	α -rabbit (1:1000)	abcam
4-HNE	52-76 kDa	1:100	α -rabbit (1:100)	abcam
IDH3A	40 kDa	1:1000	α -rabbit (1:1000)	abcam
IRS-1(Ab-636)	180 kDa	1:1000	α -rabbit (1:1000)	Signalway
IRS-1(PhosphoSer636)	180 kDa	1:1000	α -rabbit (1:1000)	Signalway
MFN1	84 kDa	1:1000	α -mouse (1:1000)	abcam
OXPPOS cocktail				
CV-ATP5A	55 kDa			
CIII-UQCRC2	48 kDa	1:1000	α -mouse (1:1000)	abcam
CIV-MTCO1	40 kDa			
CII-SDHB	30 kDa			
CI-NDUFB8	20 kDa			
PDIA6	48 kDa	1:1000	α -rabbit (1:1000)	abcam
PGC1 α	91 kDa	1:500	α -goat (1:1000)	abcam
PRX IV	31 kDa	1:1000	α -mouse (1:1000)	Santa Cruz Biotechnology
TGF β	13 kDa	1:1000	α -rabbit (1:1000)	abcam
α -tubulin (constitutive)	50 kDa	1:10000	α -mouse (1:5000)	Sigma-aldrich
β -actin (constitutive)	42 kDa	1:10000	α -mouse (1:5000)	Sigma-aldrich
GAPDH (constitutive)	37 kDa	1:5000	α -rabbit (1:5000)	Cell signaling

<i>Secondary antibodies</i>				
α -goat	-----	-----	-----	Santa Cruz Biotechnology
α -mouse	-----	-----	-----	GE Healthcare
α -rabbit	-----	-----	-----	GE Healthcare

Table 2. Primer sequences.

Gene	Forward primer	Reverse primer
UCP-1	CCCTGCCATTTACTGTCA	CAGCTGGGTACACTTGGGTA
18S	CGGCTACCACATCCAAGGAA	GCTGGAATTACCGCCGCT

Results

I. EFFECT OF GALECTIN-3 ACTIVITY INHIBITION ON CARDIAC LIPOTOXICITY ASSOCIATED WITH OBESITY

Previous data of our group have demonstrated that Gal-3 is higher in plasma of obese patients and that it plays a role in cardiac remodelling in obese rats. We herein study the cardiac lipotoxicity in the context of obesity and the implication of Gal-3 as well as the possible mechanisms involved.

We thus developed a model animal of diet-induced obesity where Gal-3 activity was inhibited through the administration of the pharmacological Gal-3 inhibitor (MCP, 100mg/kg/day) in the drinking water.

1. Effect of Gal-3 activity inhibition on general characteristics in HFD rats

Rats fed a high-fat diet showed an increase in body weight as compared with controls from the third week on (Figure 21). The inhibition of Gal-3 through MCP treatment did not affect this increase.

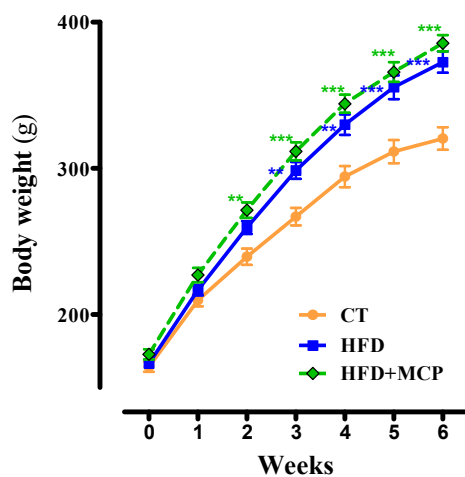


Figure 21. Pharmacological inhibition of Gal-3 activity on body weight evolution in obese rats. Body weight (g) evolution of rats fed either a standard diet (CT) or high-fat diet (HFD) treated with the inhibitor of Gal-3 activity (MCP, 100 mg/kg/day). Values are mean±SEM of 6-8 animals. ** $p < 0.01$, *** $p < 0.001$ vs control group.

Results

Obese animals also showed cardiac hypertrophy, as suggested by the increased relative heart weight and although no changes in cardiac function or blood pressure were found as compared with control rats after 6 weeks of HFD intake. MCP treatment did not modify cardiac hypertrophy, nor did it affect any of the other parameters (Table 3).

Our results showed increased Gal-3 protein levels in the heart of HFD rats, which was prevented by MCP treatment (Table 3).

Table 3. Effect of Gal-3 activity inhibition on body weight, cardiac hypertrophy, echocardiographic parameters and systolic blood pressure in obese rats.

Parameters	CT	CT+MCP	HFD	HFD+MCP
Body weight (g)	320.5±8	321.4±13.8	370.4±7.8***	385.5±6.1***
SBP, mm Hg	124.7±3.3	119.3±2.5	127.1±2.8	126.0±2.6
HW/TL, g/cm	0.21±0.008	0.22±0.008	0.25±0.007*	0.25±0.013*
IVT, mm	1.47±0.05	1.39±0.05	1.46±0.06	1.50±0.05
PWT, mm	1.70±0.1	1.60±0.06	1.51±0.04	1.64±0.07
EDD, mm	6.17±0.16	6.05±0.12	6.41±0.06	6.09±0.09
ESD, mm	2.71±0.18	3.08±0.16	3.11±0.15	2.96±0.10
EF, %	89.6±1.2	84.6±1.4	86.9±1.6	86.1±1.4
FS, %	54.9±1.5	47.9±1.4	52.1±2.0	51.4±1.81
Cardiac Gal-3 levels (% vs CT)	100±5.4	112.5±6.3	143.8±10.1*	95.1±12.1†

SBP: systolic blood pressure; HW: heart weight; TL: tibia length; IVT: interventricular septum thickness; PWT: posterior wall thickness; EDD: end-diastolic diameter; ESD: end-systolic diameter; EF: ejection fraction; FS: fractional shortening; Gal-3: galectin-3. Rats fed either a standard diet (CT) or high-fat diet (HFD) treated with the inhibitor of Gal-3 activity (MCP, 100 mg/kg/day). Data values represent mean±SEM; n= 8 animals per group. *p<0.05, ** p < 0.01, *** p < 0.001 vs control group. †p<0.05 vs HFD group.

The results present only rats fed standard diet (CT) or HFD treated with vehicle or MCP in order to simplify the data, since MCP did not affect any of these parameters in control animals (Table 3).

2. Effect of Gal-3 activity inhibition on cardiac structure in HFD rats

Cardiac interstitial collagen levels were higher in HFD rats compared with controls ones. Interstitial fibrosis was reduced in HFD rats treated with MCP, confirming our previous results and showing the reproducibility of the model¹⁸ (Figure 22).

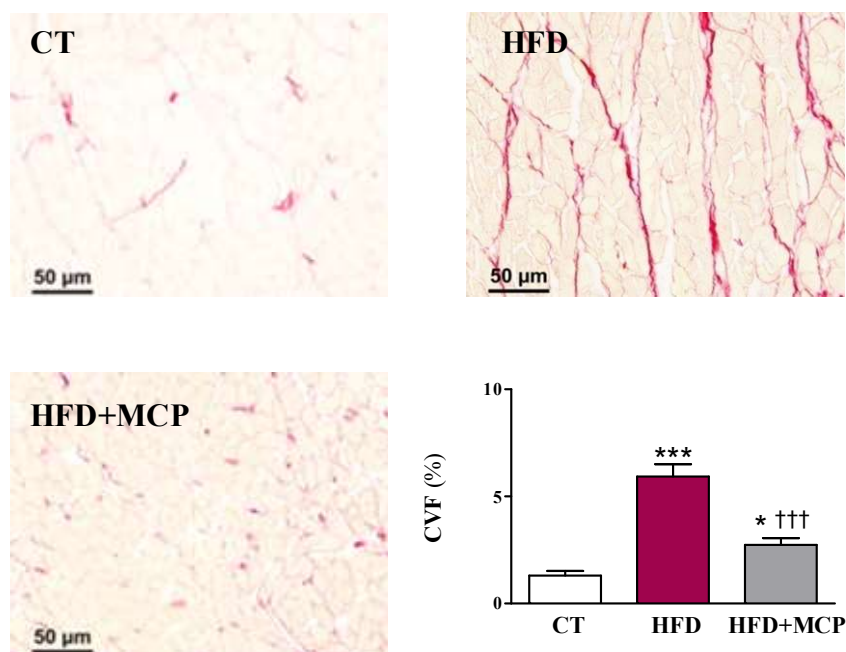


Figure 22. Pharmacological inhibition of Gal-3 activity blocked cardiac fibrosis in obese rats. Representative microphotographs of cardiac sections stained with picrosirius red and quantification of collagen volume fraction (CVF) in the heart of rats fed either a standard diet (CT) or a high-fat diet (HFD) treated with the inhibitor of Gal-3 activity (MCP, 100 mg/kg/day). Magnification: 40x. Scale bar: 50 μ m. Bar graphs represent the mean \pm SEM of 6–8 animals. * $p < 0.05$, *** $p < 0.001$ vs CT group. ††† $p < 0.001$ vs HFD group.

We also determined the levels of ECM components. Diet-induced obese rats showed enhanced protein levels of collagen I (Col I), as well as the two profibrotic mediators, CTGF and TGF- β . MCP was able to prevent these alterations (Figure 23).

Results

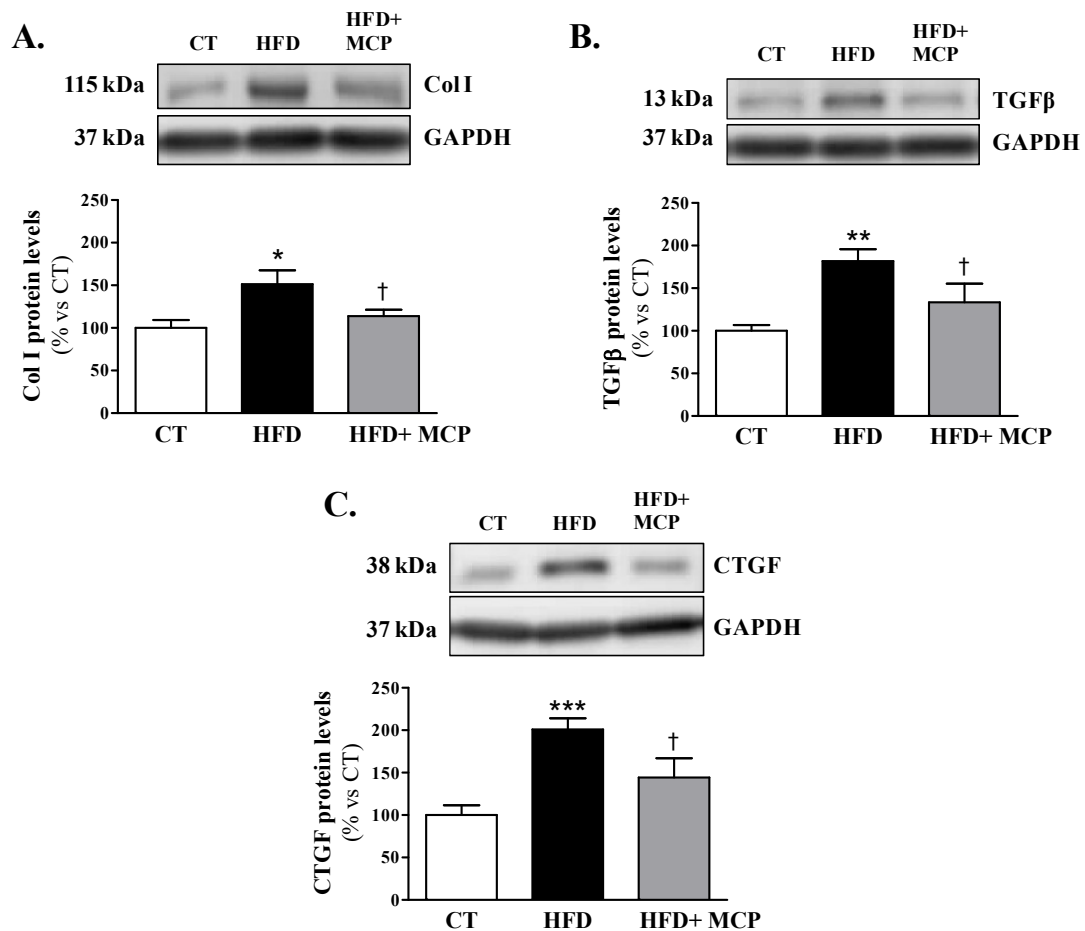


Figure 23. Pharmacological inhibition of Gal-3 activity reduced profibrotic makers in obese rats. Protein levels of (A) collagen I, (B) TGF-β and (C) CTGF in the heart from rats fed either a standard diet (CT) or a high-fat diet (HFD) treated with the inhibitor of Gal-3 activity (MCP, 100 mg/kg/day). Bar graphs represent the mean ± SEM of 6–8 animals. *p < 0.05, **p < 0.01, ***p < 0.001 vs CT group. †p < 0.05 vs HFD group.

In agreement with the results regarding hypertrophy, we observed an increase in the area of cardiomyocytes in HFD rats that was not prevented by MCP treatment (Figure 24).

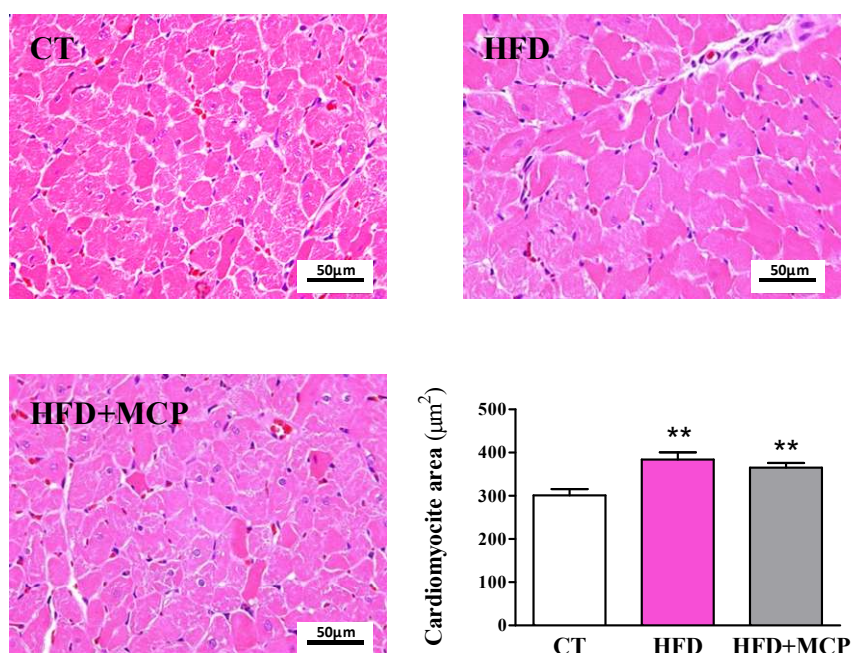


Figure 24. Pharmacological inhibition of Gal-3 activity had no effect on the increase in cardiomyocyte area observed in obese rats. Representative microphotographs of cardiac sections stained with hematoxylin-eosin and quantification of cardiomyocyte area (μm^2) from rats fed either a standard diet (CT) or high-fat diet (HFD) rats treated with the inhibitor of Gal-3 activity (MCP, 100 mg/kg/day). Magnification: 40x. Scale bar: 50 μm . Bar graphs represent the mean \pm SEM of 6-8 animals. **p<0.01 vs CT group.

3. Effect of Gal-3 activity inhibition on cardiac glucose uptake and insulin resistance in HFD rats

In order to determine a possible mechanism involved in the development of cardiac alterations, as well as a possible the role of Gal-3, we evaluated metabolic substrate-use changes that occur in obesity. HFD rats showed a decrease in ^{18}F - Fluorodeoxyglucose (FDG) uptake at cardiac level accompanied by an increase in HOMA index as compared with control group. MCP was unable to affect both the increase in HOMA index and myocardial ^{18}F -FDG uptake in obese rats, supporting that Gal-3 activity did not affect glucose homeostasis (Figure 25).

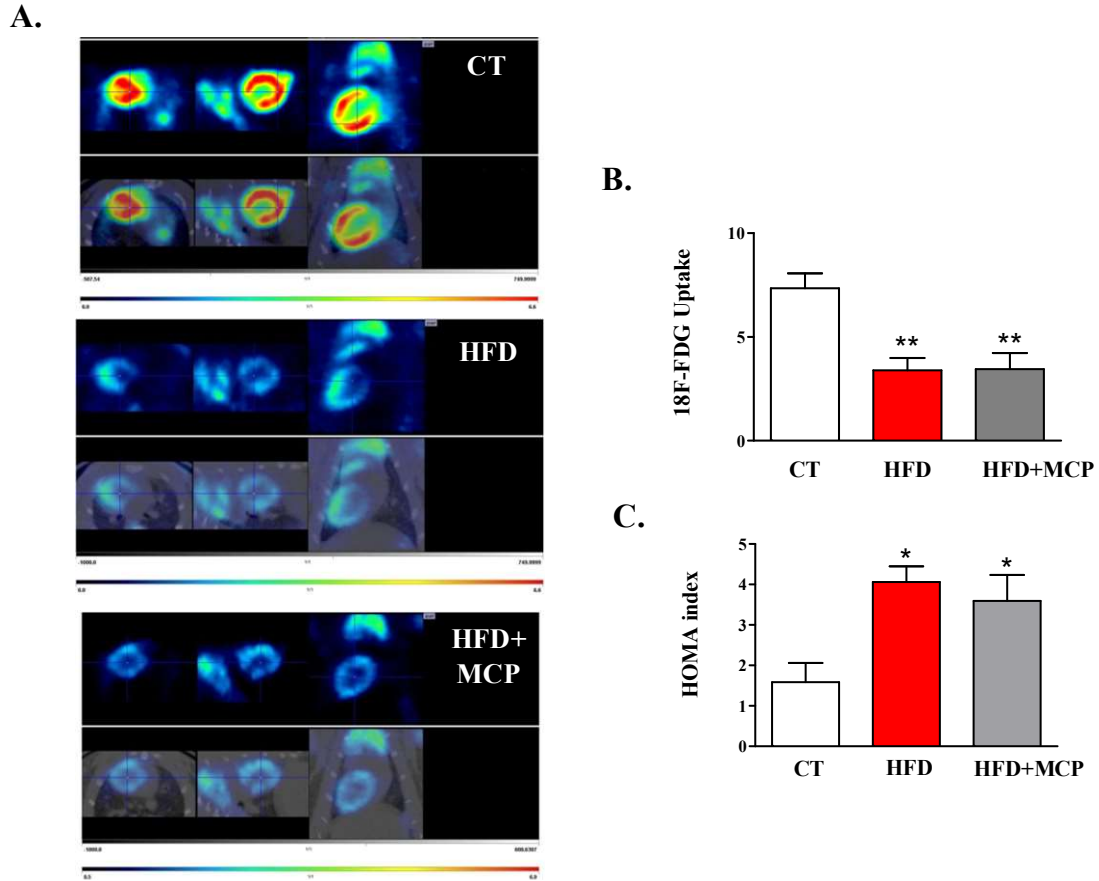


Figure 25. Pharmacological inhibition of Gal-3 activity on cardiac ^{18}F -FDG-uptake and HOMA index in obese rats. (A) Representative images of ^{18}F -Fluorodeoxyglucose PET/CT scans of the heart, (B) quantification of ^{18}F -FDG-uptake and (C) homeostasis model assessment (HOMA) index of rats fed either a standard diet (CT) or a high-fat diet (HFD) treated with the inhibitor of Gal-3 activity (MCP, 100 mg/kg/day). Bar graphs represent the mean \pm SEM of 6-8 animals. * p <0.05, ** p <0.01 vs CT group.

4. Effect of Gal-3 activity inhibition on cardiac lipid profile in HFD rats

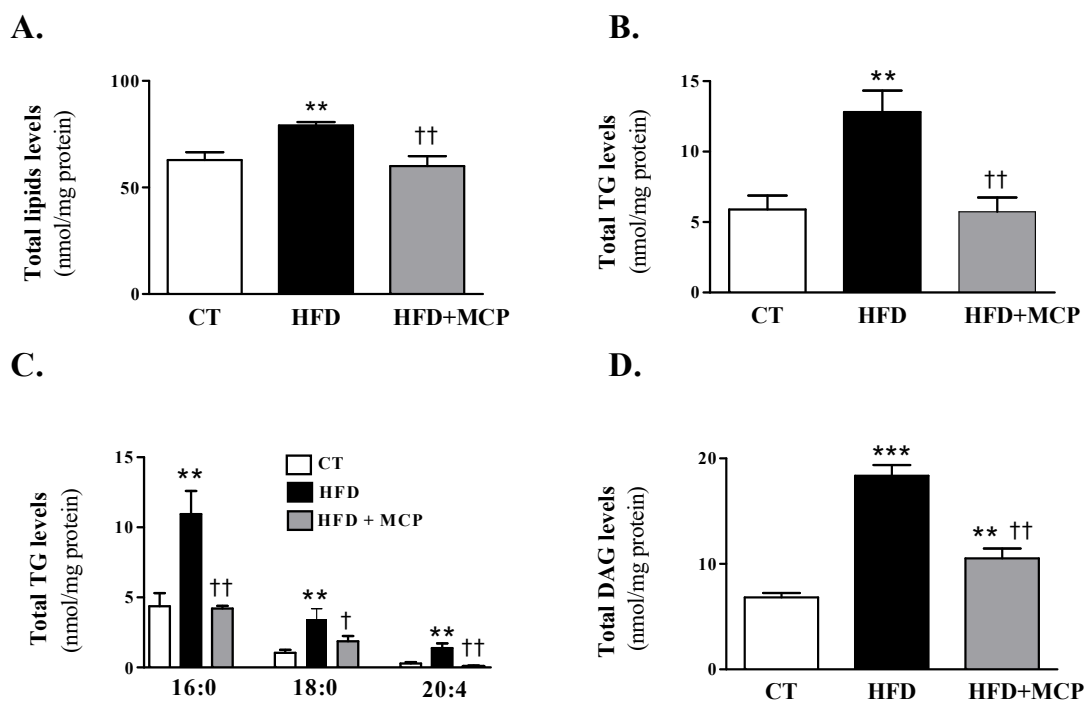
HFD animals showed an increase in total cardiac lipids content, although all lipid components were not affected in the same manner (Figure 26A). Obese rats showed an increase in total TG content in the heart mainly due to an accumulation of those enriched with palmitic acid (16:0), and to a minor extent of those enriched with stearic acid (18:0) and arachidonic acid (20:4). Obese rats presented a global increase in TGs enriched with saturated fatty acids (4-fold; p <0.001), although no significant changes were observed in overall polyunsaturated fatty acids (data not shown). The inhibition of Gal-3 was able to normalize this rise observed in HFD animals (Figure 26B and C).

There was also observed an increase in total DAG content in obese rats which was partially prevented with MCP (Figure 26D).

A reduction in total sphingomyelins (SM) was observed in HFD rats. MCP was unable to prevent this reduction (Figure 26E). A positive correlation was observed between total SM levels and ^{18}F -FDG cardiac uptake levels ($r=0.6220$; $p=0.0175$) suggesting a possible role of SM in glucose metabolism.

Regarding ceramides (Cer), we observed increased levels in obese rats as compared with control ones but MCP was unable to revert this increase (Figure 26F). A negative correlation was observed between Cer and SM levels ($r= -0.5274$; $p=0.0433$) and between Cer and ^{18}F -FDG cardiac levels ($r=-0.668$; $p=0.0065$) in obese rats.

None of the groups presented modifications in total phosphatidylcholine (PC) (Figure 26G) or phosphatidylethanolamine (PE) levels in the heart (Figure 26H); however, obese rats showed an increase in both lyso forms (LPC and LPE), an effect that was prevented by the pharmacological inhibition of Gal-3 (Figure 26I and J). Total LPC levels were correlated to those TGs enriched with palmitic acid ($r=0.6841$; $p=0.0048$).



Results

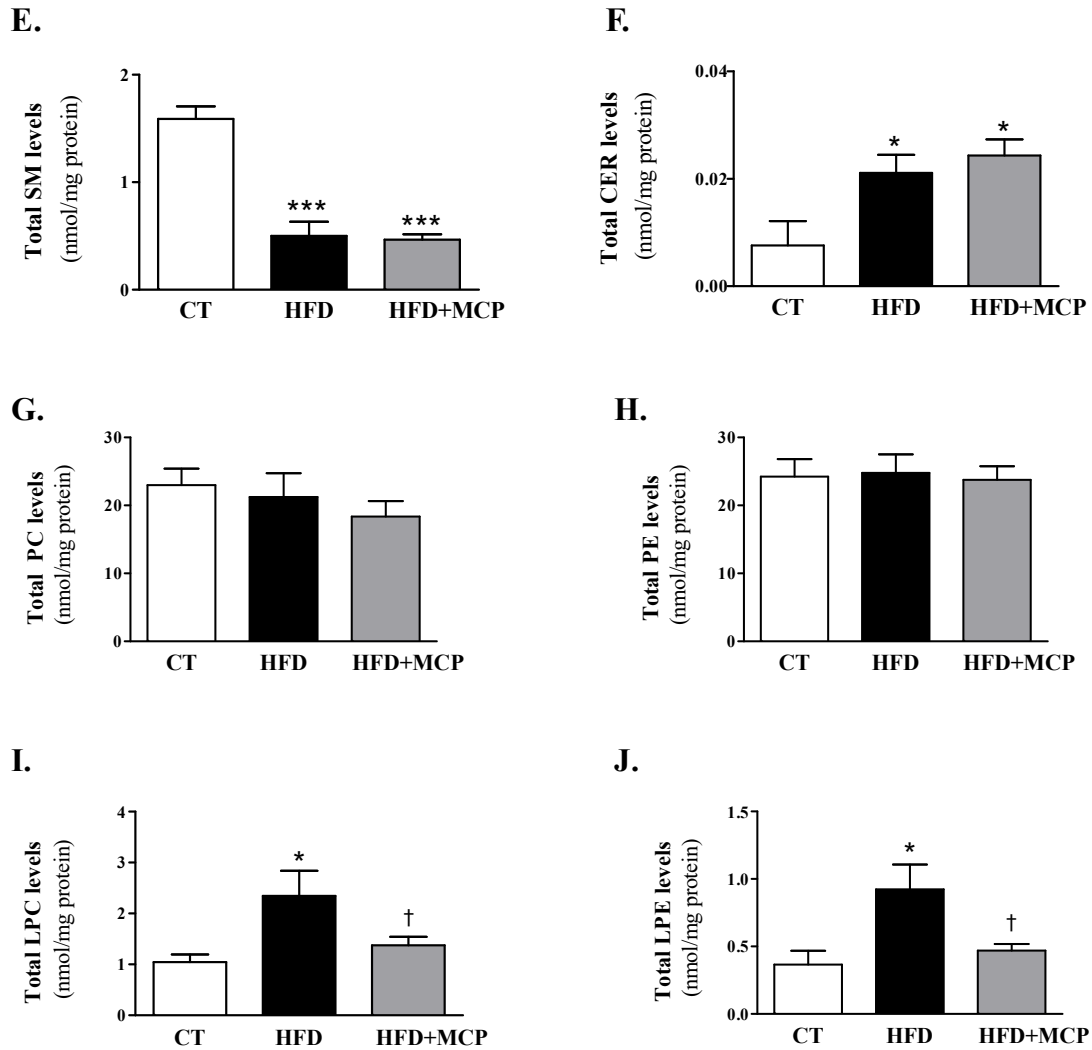


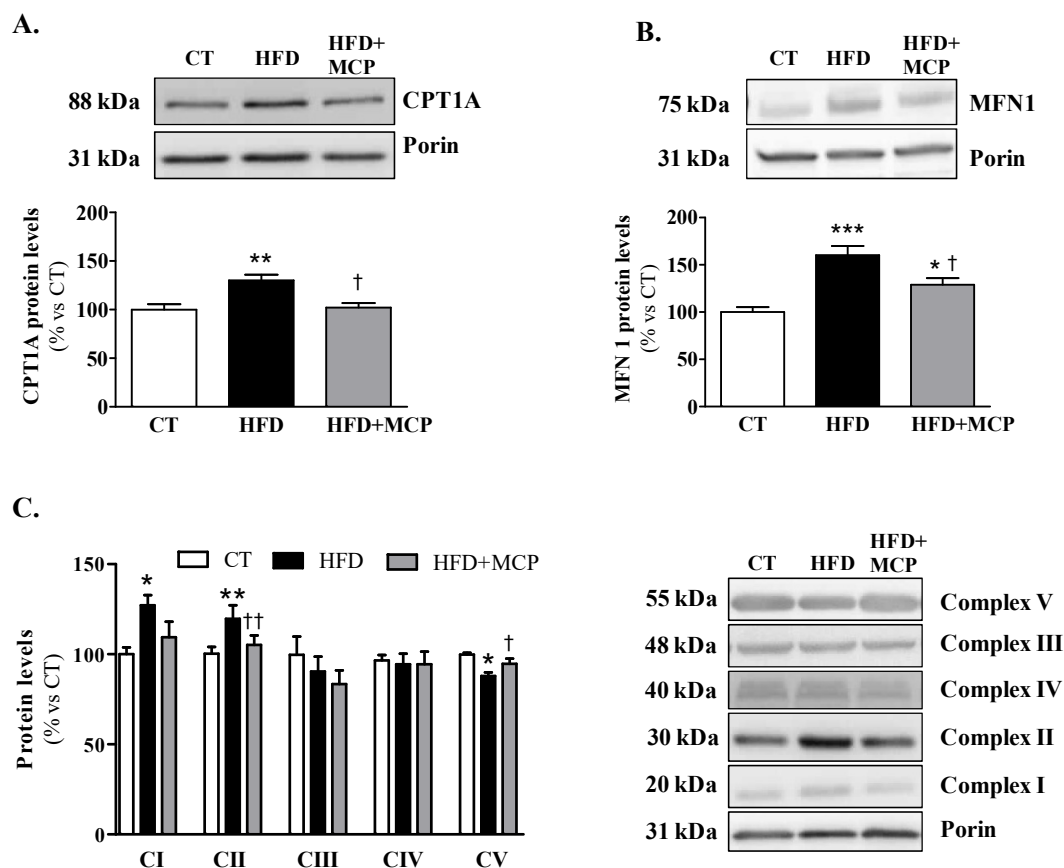
Figure 26. Effect of pharmacological inhibition of Gal-3 activity on cardiac lipid profile in obese rats. Quantification of (A) total lipids, (B) total TGs, (C) TGs enriched with saturated (palmitic acid 16:0, stearic acid 18:0) and unsaturated acids (arachidonic acid 20:4), (D) total DAGs, (E) total sphingomyelins, (F) total ceramides, (G) total phosphatidylcholine (PC), (H) total phosphatidylethanolamine (PE), (I) total lyso phosphatidylcholine (LPC) and (J) total lyso phosphatidylethanolamine (LPE) in the heart of rats fed either a standard diet (CT) or a high-fat diet (HFD) treated with the inhibitor of Gal-3 activity (MCP, 100 mg/kg/day). Bar graphs represent the mean \pm SEM of 6-8 animals. * p <0.05, ** p <0.01, *** p <0.001 vs CT group. † p <0.05, †† p <0.01 vs HFD group.

5. Effect of Gal-3 activity inhibition on cardiac mitochondrial alterations in HFD rats

Considering that there is an accumulation of fatty acids in the heart, we explored whether this increase could be reflected in the mitochondria by exploring fatty acid

transport. Higher protein levels of CPT1A, the transporter of fatty acids inside the mitochondria, were observed in obese rats as compared with controls. Treatment with MCP was able to normalize this increase in HFD rats (Figure 27A). The increase in CPT1A suggests that the entrance of FFA inside the mitochondria in HFD rats is enhanced. Therefore, we explored the consequences that this could cause on the mitochondrial dynamic. For this purpose, we evaluated the levels of two proteins involved in the process of mitochondrial fusion and fission, mitofusin 1 (MFN1) and dynamin-related protein 1 (DRP1), respectively. The protein levels of MFN1 were increased in HFD animals and MCP treatment was able to reduce these high levels (Figure 27B). Nevertheless, the levels of DRP1 were unchanged among all the groups (data not shown).

We also evaluated the protein levels of the components of mitochondrial respiratory chain complexes and we observed that obesity exerts a different impact on these. Complex I and II were increased in HFD rats, whereas complex V was reduced. The pharmacological inhibition of Gal-3 was able to ameliorate these alterations. Neither obesity nor MCP were able to affect complex III and IV (Figure 27C).



Results

Figure 27. Pharmacological inhibition of Gal-3 activity ameliorated the alterations in mitochondrial proteins in the heart of obese rats. Protein levels of (A) CPT1A, (B) MFN1 and (C) mitochondrial complex I, II, III, IV and V in the heart of rats fed either a standard diet (CT) or a high-fat diet (HFD) treated with the inhibitor of Gal-3 activity (MCP, 100 mg/kg/day). Bar graphs represent the mean±SEM of 6-8 animals. * $p < 0.05$, ** $p < 0.01$, *** $p < 0.001$ vs control group. † $p < 0.05$, †† $p < 0.01$ vs HFD group.

Moreover, HFD-fed animals showed higher levels in cardiac mitochondrial superoxide anion levels. MCP treatment was able to reduce the increase observed in HFD rats (Figure 28). In addition, a correlation between mitochondrial ROS and TG levels was found ($r = 0.6523$; $p < 0.004$)

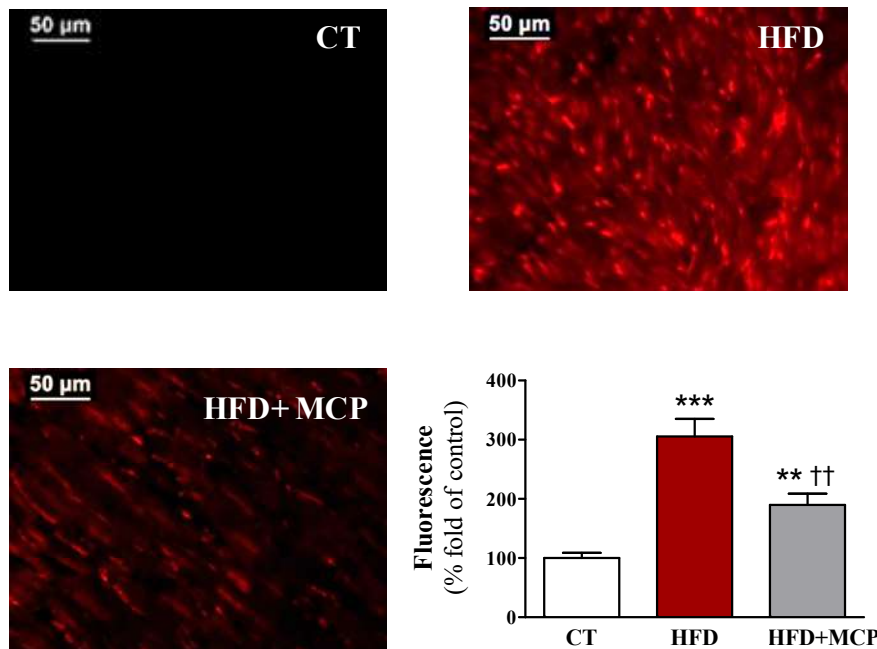


Figure 28. Pharmacological inhibition of Gal-3 activity blocked cardiac superoxide anion production in obese rats. Representative microphotographs of cardiac sections and quantification of superoxide anion in the heart of rats fed either a standard diet (CT) or a high-fat diet (HFD) treated with the inhibitor of Gal-3 activity (MCP, 100 mg/kg/day). Magnification: 40x. Scale bar: 50µm. Bar graphs represent the mean±SEM of 6-8 animals. ** $p < 0.01$, *** $p < 0.001$ vs CT group. †† $p < 0.01$ vs HFD group.

6. Effect of palmitic acid on mitochondrial function in cardiac myoblasts. Consequences of Gal-3 activity inhibition

Considering that palmitic acid is the main fatty acid accumulated in the heart of obese rats, we decided to explore its effect on mitochondrial function by using cultured rat

cardiomyoblasts. H9C2 cells were stimulated in a dose-dependent manner (100-300 $\mu\text{mol/l}$) with palmitic acid for 24 hours. We then performed a “mitochondrial stress test” in order to assess parameters of mitochondrial function by directly measuring the oxygen consumption rate (OCR) of cells. Palmitic acid produced a dose-dependent increase in the basal rate of respiration (OCR), in the proton leak and in the extracellular acidification rate (ECAR) indicating an uncoupling of mitochondrial membrane that trigger to OXPHOS deficiency (Figure 29).

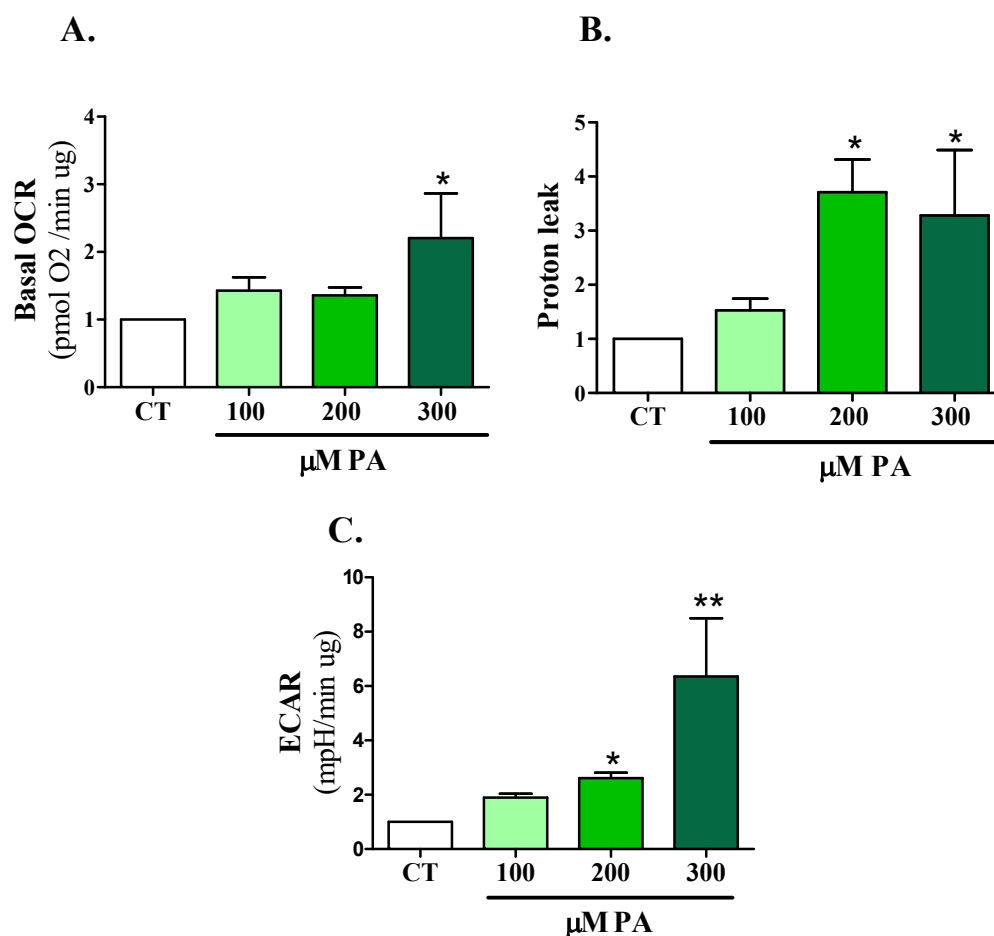


Figure 29. Dose response of palmitic acid on parameters of mitochondrial function in cardiac myoblasts. H9C2 cardiomyoblasts were stimulated with palmitic acid 100- 300 μM for 24 hours and (A) oxygen consumption rate (OCR), (B) proton leak and (C) extracellular acidification rate (ECAR) were quantified using the XF24 seahorse technology. Bar graphs represent the mean \pm SEM of 3 assays. *p<0.05, **p<0.01 vs CT.

Results

Palmitic acid was unable to affect cell viability at the doses used (100-300 $\mu\text{mol/l}$) (Figure 30).

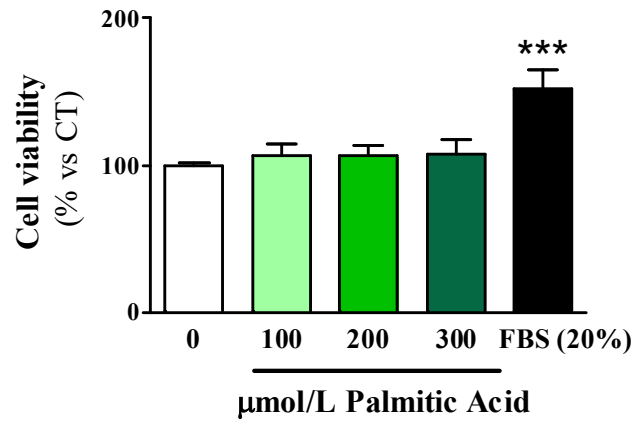


Figure 30. Effect of palmitic acid on cell viability in cardiac myoblasts. H9C2 were stimulated with palmitic acid (100-300 μM) or 20 % of fetal bovine serum (FBS) for 24 hours. Viability was determined by an MTT assay. Data are expressed as percent of control cells. Values are mean \pm SEM of three assays. *** p <0.001 vs CT.

H9C2 cells were stimulated with palmitic acid (200 μM) in absence or presence of MCP (10 mg/ml) for 24 hours. Neither palmitic acid nor MCP affected basal respiration (OCR) (Figure 31A). Palmitic acid at a dose of 200 μM increased proton leak and ECAR, however, MCP was unable to prevent this increase (Figure 31B and C).

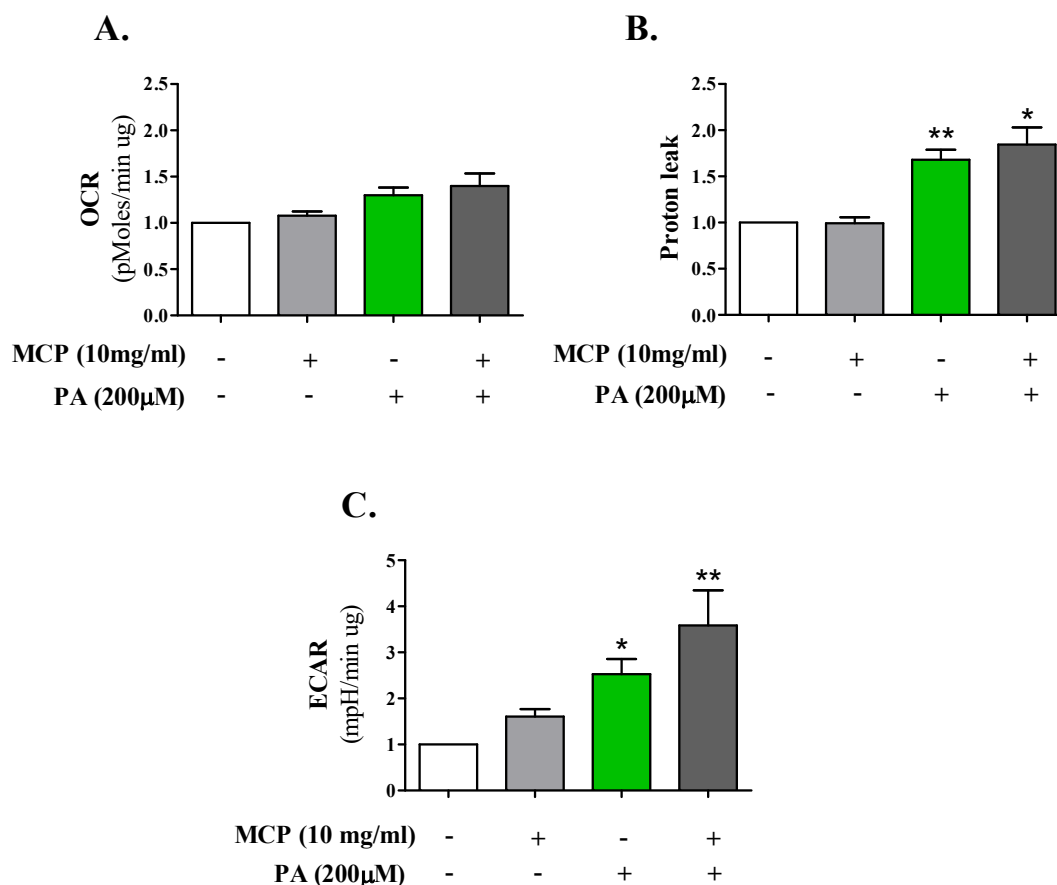


Figure 31. Effect of palmitic acid on mitochondrial function. Consequences of Gal-3 activity inhibition. H9C2 cardiomyoblasts were stimulated with palmitic acid (200 μM) in presence or absence of the inhibitor of Gal-3, MCP, for 24 hours. (A) Oxygen consumption rate (OCR), (B) proton leak and (C) extracellular acidification rate (ECAR) were quantified using the XF24 seahorse analyser. Bar graphs represent the mean ± SEM of 3 assays. *p<0.05, **p<0.01, ***p<0.001 vs CT.

II. EFFECT OF MITOCHONDRIAL OXIDATIVE STRESS INHIBITION ON CARDIAC ALTERATIONS ASSOCIATED WITH OBESITY

Due to the observed effects of the high-fat diet on the mitochondria, we decided to study the role of mitochondrial oxidative stress on the cardiac alterations associated with obesity.

1. Effect of mitochondrial oxidative stress inhibition on general characteristics in HFD rats

HFD-fed rats showed an increase in body weight that reached a significant difference from the fourth week. This difference was maintained until the end of the study. The administration of MitoQ attenuated the increase in body weight of HFD rats, although it did not reach the levels of control animals (Figure 32A). Animals fed a high fat diet showed a reduction in food intake as compared with CT animals (Figure 32B).

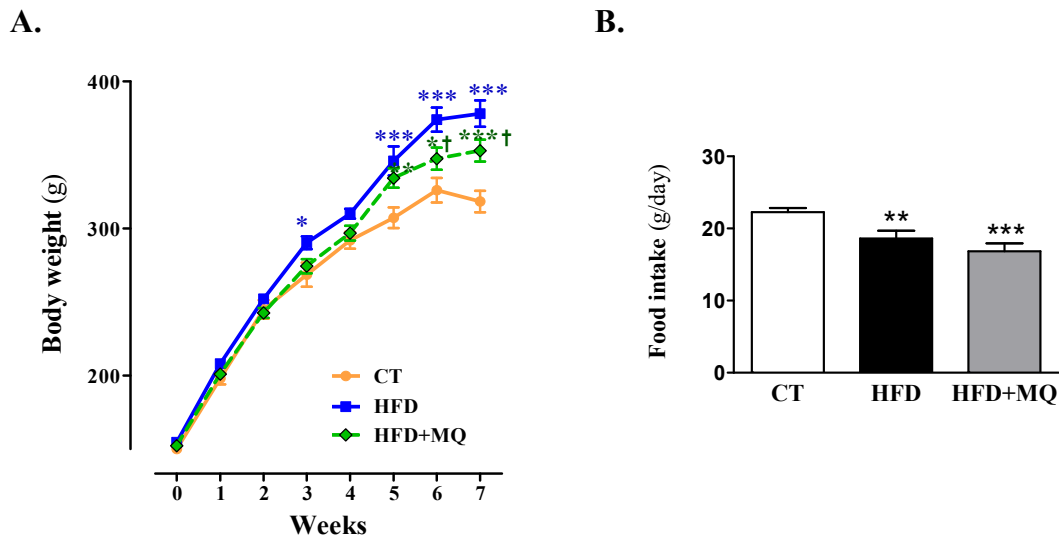


Figure 32. Effect of the administration of a mitochondrial antioxidant on body weight evolution and food intake in obese rats. (A) Body weight evolution and (B) amount of food intake (g/day) from rats fed either a standard diet (CT) or a high-fat diet (HFD) treated with the inhibitor of mitochondrial oxidative stress (MQ, 50 mg/kg/day). Values are mean±SEM of 6-8 animals. * $p < 0.05$, ** $p < 0.01$, *** $p < 0.001$ vs control group. † $p < 0.05$ vs HFD group.

No changes in cardiac function or blood pressure were found at the end of the experiment among any group (Table 4).

HFD animals showed cardiac hypertrophy characterized by higher relative cardiac weight than control animals (Table 4), an effect that was prevented with MitoQ.

Table 4. Effect of the administration of a mitochondrial antioxidant on body weight, cardiac hypertrophy, echocardiographic parameters and systolic blood pressure in rats fed either a standard diet (CT) or a high-fat diet (HFD) rats treated with the inhibitor of mitochondrial oxidative stress (MQ, 50 mg/kg/day).

Parameters	CT	CT+MQ	HFD	HFD+MQ
HW/TL (g/cm tibia)	0.20 ±0.03	0.21±0.06	0.24±0.02*	0.22±0.02 †
IVT (mm)	1.3±0.08	1.37±0.06	1.43±0.2	1.35±0.08
PWT(mm)	1.9±0.13	1.33±0.05	1.71±0.2	1.67±0.16
EDD (mm)	6.5±0.43	6.7±0.22	6.15±0.23	6.13±0.19
ESD (mm)	3.5±0.34	4.03±0.12	2.93±0.3	3.49±0.32
EF (%)	75.3±5.6	73.2±2.7	80.9±8.5	77.3±5.3
FS (%)	40.6±4.4	35.6±3.07	55.7±3.8	43.2±4.7
E/A	1.05±0.08	1.2±0.02	1.06±0.06	1.2±0.02
SBP (mmHg)	126.5±4.7	130.6±3.9	121.0±2.5	128.4±3.4

HW: heart weight; TL: tibia length; IVT: interventricular septum thickness; PWT: posterior wall thickness; EDD: end-diastolic diameter; ESD: end-systolic diameter; EF: ejection fraction; FS: fractional shortening; SBP: systolic blood pressure. Data values represent mean± SEM; n= 8 animals per group. * p < 0.05, vs CT group. †p<0.05 vs HFD group.

Since MQ did not affect any of these parameters in control animals (Table), to simplify the data only rats fed with a standard diet (CT) and with HFD treated with vehicle or MitoQ will be presented in the results.

2. Effect of mitochondrial oxidative stress inhibition on cardiac superoxide anion levels

As we expected, HFD-fed animals showed higher levels of oxidative stress, as suggested by the increase in red fluorescence staining induced by the total superoxide indicator DHE. MitoQ treatment was able to reduce the superoxide anion levels to the control levels (Figure 33). These data support the effectiveness of the treatment.

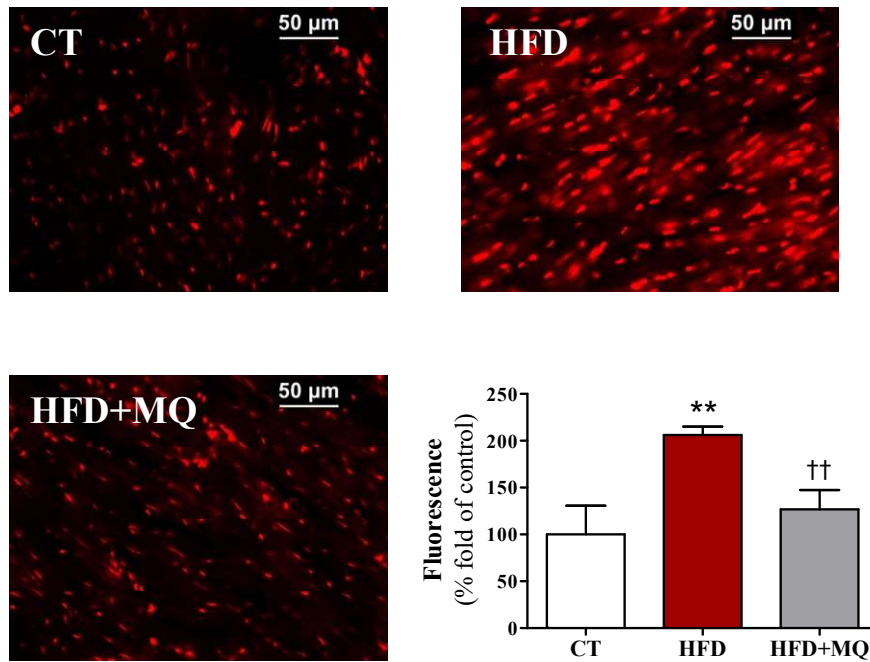


Figure 33. Effect of the administration of a mitochondrial antioxidant on total superoxide anion levels in the heart of obese rats. Representative microphotographs of cardiac sections and quantification of superoxide anion in the heart from rats fed either a standard diet (CT) or a high-fat diet (HFD) treated with the inhibitor of mitochondrial oxidative stress (MQ, 50 mg/kg/day). Magnification: 40x. Scale bar: 50μm. Bar graphs represent the mean±SEM of 6-8 animals. ** $p < 0.01$ vs CT group. †† $p < 0.01$ vs HFD group.

3. Effect of mitochondrial oxidative stress inhibition on cardiac structure

We evaluated the role of mitochondrial oxidative stress in cardiac remodelling. The HFD rats showed an increase in cardiac interstitial fibrosis, as shown by the increase in total collagen content. MitoQ treatment reduced this increase (Figure 34).

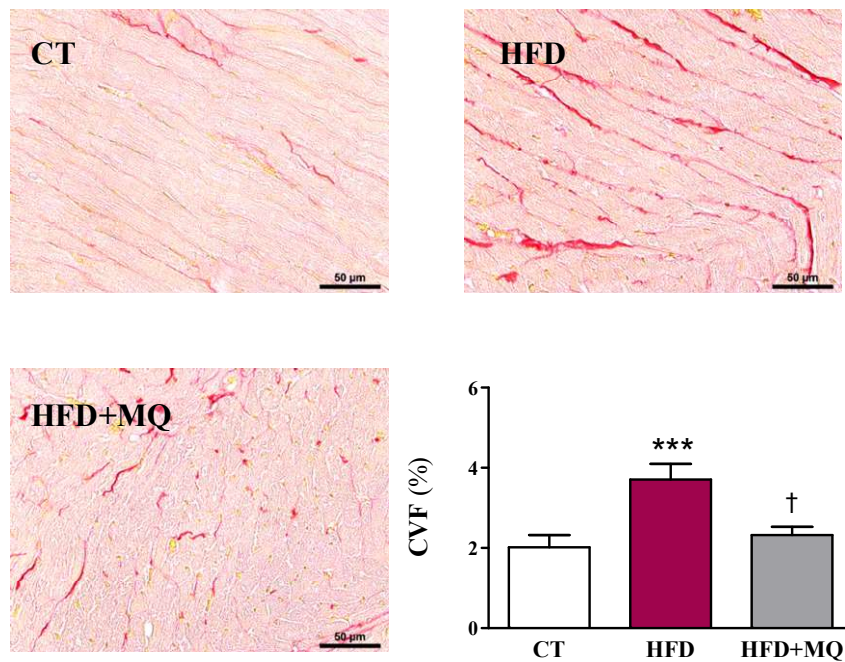


Figure 34. Effect of the administration of a mitochondrial antioxidant on cardiac fibrosis in obese rats. Representative microphotographs of sections stained with picosirius red and quantification of collagen volume fraction (CVF) in the heart of rats fed either a standard diet (CT) or a high-fat diet (HFD) treated with the inhibitor of mitochondrial oxidative stress (MQ, 50 mg/kg/day). Magnification: 40x. Scale bar: 50 μ m. Bar graphs represent the mean \pm SEM of 6–8 animals. *** p < 0.001 vs CT group. † p < 0.05 vs HFD group.

We also evaluated the protein levels of the extracellular matrix component collagen I and the profibrotic mediators TGF β and CTGF. All of them were increased in the heart of obese rats. MitoQ normalised the levels of collagen I and TGF β in obese rats (Figure 35).

Results

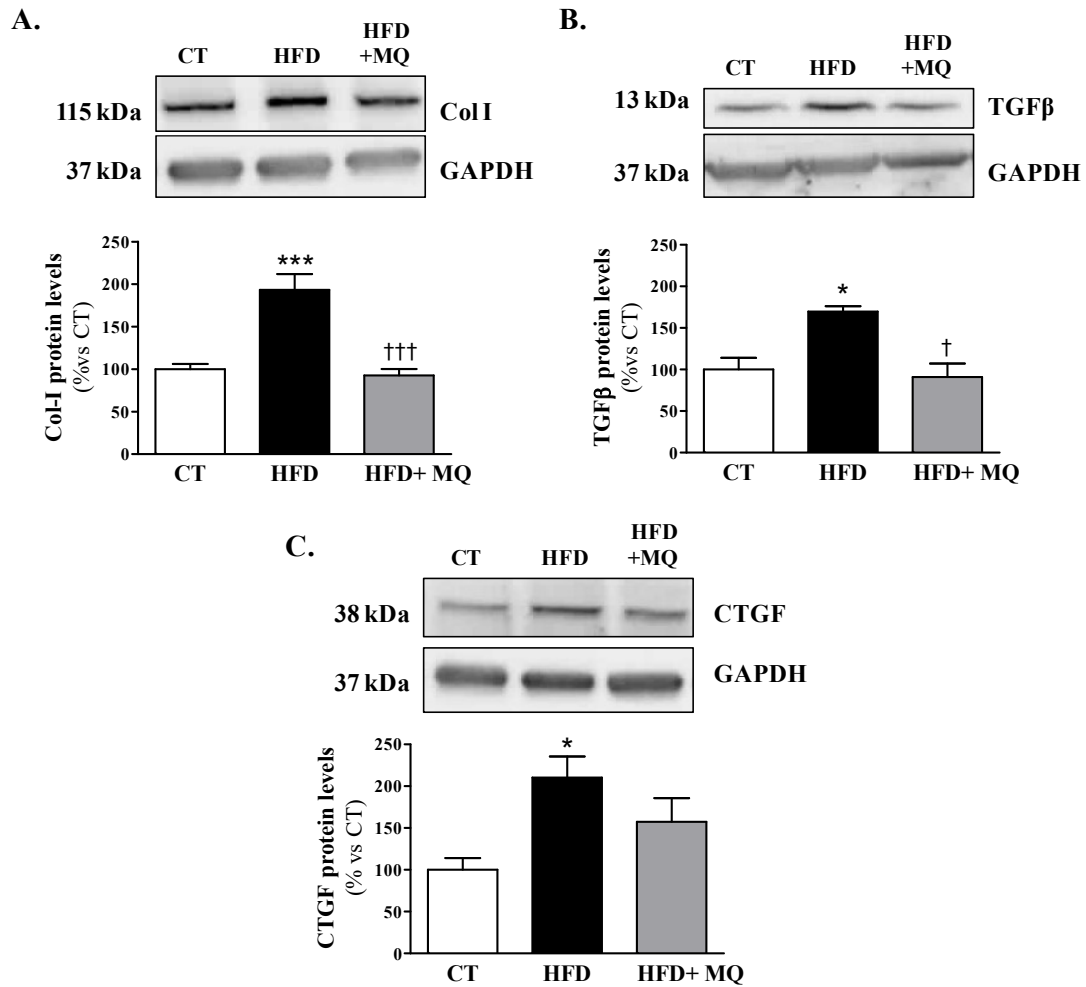


Figure 35. Effect of the administration of a mitochondrial antioxidant on profibrotic mediators in the heart of obese rats. Protein expression of (A) collagen I, (B) TGFβ and (C) CTGF in the heart of rats fed either a standard diet (CT) or a high-fat diet (HFD) treated with the inhibitor of mitochondrial oxidative stress (MQ, 50 mg/kg/day). Bar graphs represent the mean ± SEM of 6–8 animals. *p<0.05, ***p < 0.001 vs CT group. † p < 0.05, ††† p < 0.001 vs HFD group.

MitoQ was also able to prevent the increase in cardiomyocyte area observed in HFD rats (Figure 36).

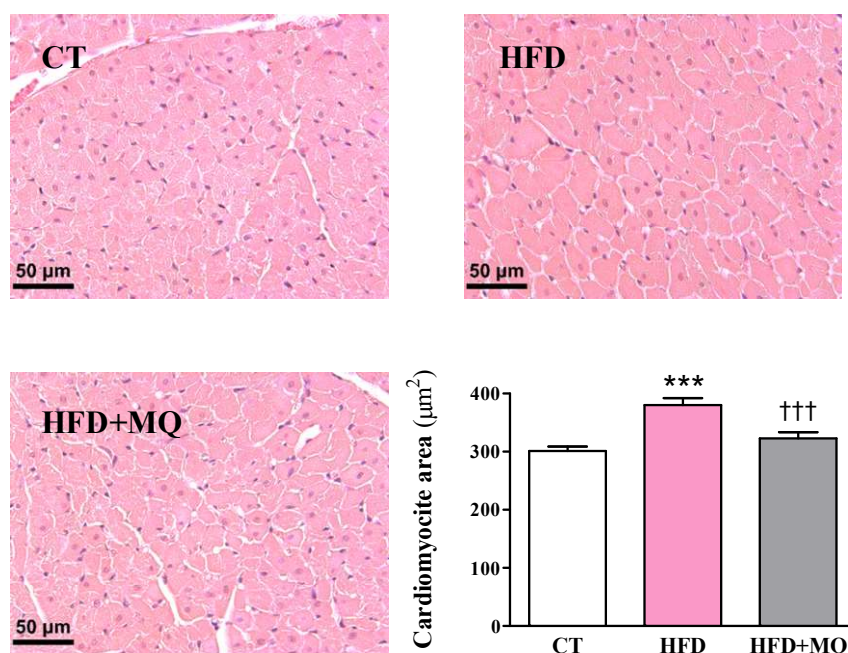


Figure 36. Effect of the administration of a mitochondrial antioxidant on cardiomyocyte area in obese rats. Representative microphotographs cardiomyocytes from cardiac sections embedded in paraffin stained with hematoxylin-eosin and quantification of cardiomyocyte area from the heart of rats fed either a standard diet (CT) or a high-fat diet (HFD) treated with the inhibitor of mitochondrial oxidative stress (MQ, 50 mg/kg/day). Magnification: 40x). Scale bar: 50µm. Bar graphs represent the mean±SEM of 6-8 animals. ***p<0.001 vs CT group. †††p<0.001 vs HFD group.

4. Proteomic analysis of HFD rat hearts

In order to identify molecules or pathways that could be altered by the effect of a high fat diet in the heart and in turn the impact of MitoQ on these, a proteomic analysis of cardiac tissue was performed using iTRAQ (isobaric Tags for Relative and Absolute Quantitation) approach coupled to 2D nano-liquid chromatography tandem mass spectrometry.

1367 proteins were detected in the study. 1.3-fold change cutoff (ratio <0.77 or >1.3) and a p-value lower than 0.05 were selected to classify proteins as up- or down-regulated. Changes of expression were found in 33 proteins in the hearts of HFD rats as compared to controls (18 up- and 15 down-regulated) and in 23 proteins of HFD+MQ group as compared to HFD (15 up- and 8 down-regulated).

A subcellular distribution analysis was performed using DAVID software¹⁵³ with the proteins that had showed changes of expression among the different groups. Of the 33

Results

proteins modified in the heart of HFD rats, 11 were localized in the mitochondria and three of them were related with oxidative phosphorylation (OXPHOS) (Table 5). There was observed an increase in ubiquinol-cytochrome c reductase complex III subunit VII (UQCRCQ), a subunit of the complex III of respiratory chain, in HFD rats as compared to control group. On the other hand, a reduction in mitochondrially encoded NADH:Ubiquinone oxidoreductase core (MTND2), a subunit of the complex I, was observed. There was also observed a reduction in holocytochrome C synthase (HCCS), an enzyme that covalently links a heme group to the apoprotein of cytochrome c, which is necessary for the electron transfer in the respiratory chain. These data show alterations in proteins involved in respiratory chain, suggesting damage in the oxidative phosphorylation and subsequently in ATP production.

Table 5. Mitochondrial proteins identified by a proteomic analysis altered in the heart of obese rats as compared to controls. 1.3-fold change cut-off for all iTRAQ ratios (ratio<0.77 or >1.3) and a p-value lower than 0.05 were selected to classify proteins as up- or down-regulated; ratio <0.77 was considered underexpressed (green color) and >1.3 was considered overexpressed (red color).

Protein	CT	HFD	Fold change CT/HFD	Pvalue
Lysine-tRNA ligase	13,10	12,72	0,62	0,018
Isocitrate dehydrogenase [NAD] subunit	12,60	12,14	0,54	0,019
Mitochondrial pyruvate carrier 2	11,14	12,08	1,94	0,033
Peroxisomal multifunctional enzyme type 2	11,03	11,86	1,82	0,003
Cysteine conjugate-beta lyase 1, isoform CRA_a	10,00	9,36	0,36	0,043
Valine-tRNA ligase	10,04	9,63	0,59	0,023
Serine hydroxymethyltransferase	9,82	9,34	0,53	0,041
Hccs	9,01	8,17	0,17	0,001
Cytochrome b-c1 complex subunit 8	10,20	9,38	0,19	0,003
NADH-ubiquinone oxidoreductase chain 2	9,59	10,76	2,17	0,016
Cathepsin B	9,60	9,12	0,52	0,025

CT: control; HFD: high fat diet; HCCS: holocytochrome c synthase.

Indeed, a protein interactome network that measures proteome-wide physical connections between protein pairs was extracted for the three proteins mentioned above using STRING tool. As we can observe in Figure 37 the proteins that show an interaction with our queries proteins are also related to the respiratory chain, showing that oxidative phosphorylation is damaged in HFD rats.

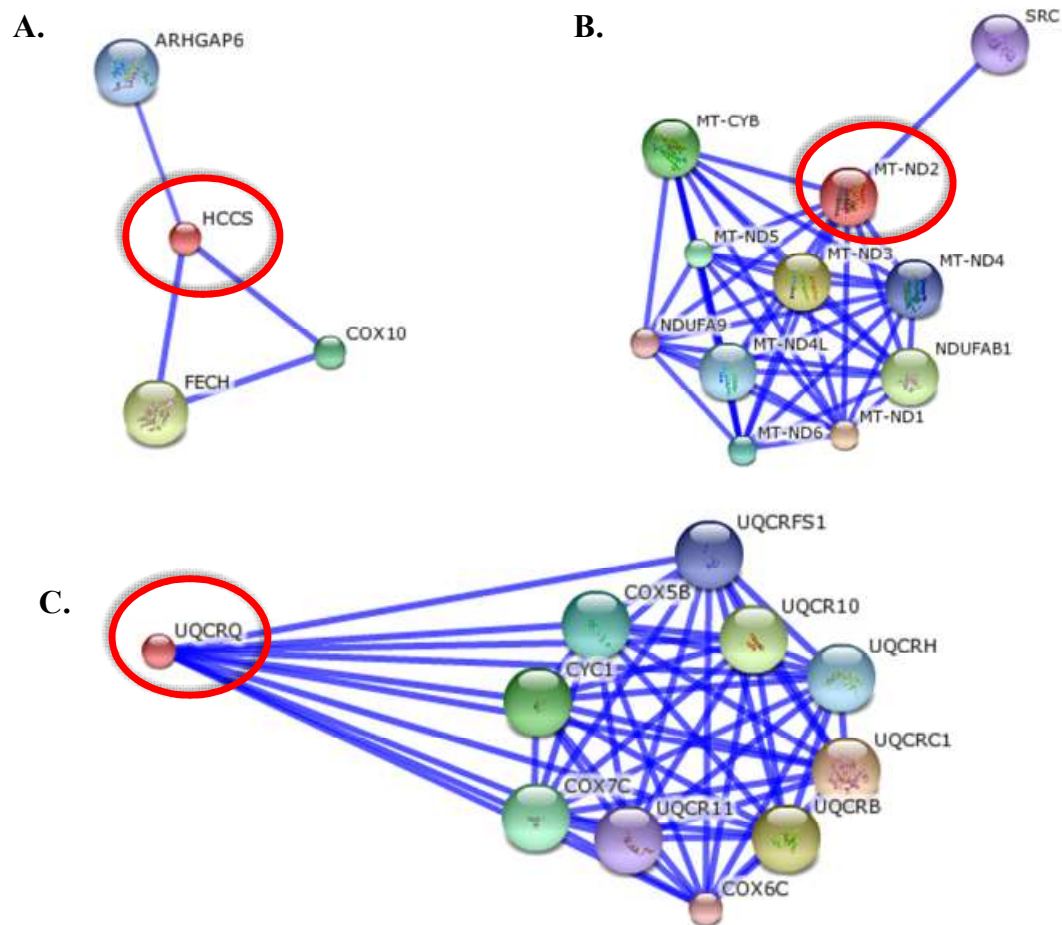


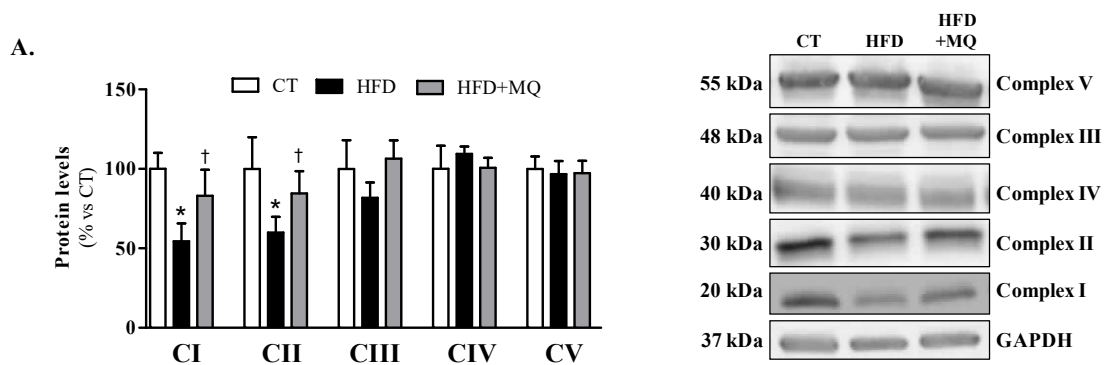
Figure 37. Protein interactome network for three proteins involved in oxidative phosphorylation. Protein of interest are surrounded by a red circle. (A) holocytochrome C synthase (HCCS), (B) mitochondrially Encoded NADH:Ubiquinone oxidoreductase Core Subunit 2 (MT-ND2) and (C) ubiquinol-cytochrome C reductase Complex III Subunit VII (UQCRQ).

5. Effect of mitochondrial oxidative stress inhibition on OXPHOS complexes in HFD rats

In order to validate the proteomic analysis data, protein level measurements were performed by western blotting. First of all, we analysed the five mitochondrial complexes involved in the respiratory chain. The NADH:ubiquinone oxidoreductase, or complex I, was reduced in HFD rats, confirming proteomic results. There is a tendency to reverse these reductions by MitoQ, although it did not reach significant levels. The same results were observed concerning complex II, or succinate:ubiquinone oxidoreductase. The rest of the complex (ubiquinol:cytochrome c oxidoreductase or complex III, cytochrome c oxidase or complex IV and ATP synthase or complex V) were unaffected in obese rats (Figure 38A). In the proteomic analysis, complex III was conversely increased. However, these differences are due to the subunit measured in both experiments being different. In the proteomic analysis UQCRQ (subunit VIII) was detected, whereas we measured UQCRC2 (subunit II) by western blot.

HCCS was also evaluated by western blot. However, the individual measurements of the protein levels did not show differences among groups (Figure 38B). This difference between proteomic and western blot analysis could be explained by the fact that the proteomic analysis was performed from a pool of animals that could be distorting the overall results.

Since HCCS is an enzyme that links a heme group to cytochrome c, we also decided to measure cytochrome c levels. As those observed with HCCS, the levels of cytochrome c were unchanged (Figure 38C).



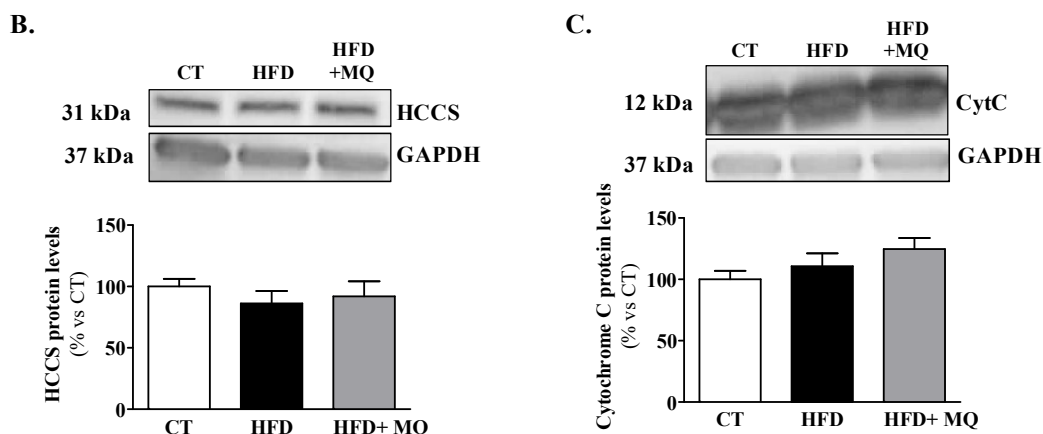


Figure 38. Effect of the administration of a mitochondrial antioxidant on OXPHOS complexes in the heart of obese rats. Protein levels of (A) mitochondrial chain respiratory complexes, (B) holocytochrome C synthase (HCCS) and (C) cytochrome c in the heart from a standard diet (CT) and high-fat diet (HFD) rats treated with the inhibitor of mitochondrial oxidative stress (MQ, 50 mg/kg/day). Bar graphs represent the mean±SEM of 6-8 animals. * $p < 0.05$ vs control group. † $p < 0.05$ vs HFD group.

6. Effect of palmitic acid on mitochondrial function in cardiac myoblasts. Consequences of mitochondrial oxidative stress inhibition.

As we have showed in the previous section, palmitic acid has an effect on mitochondrial bioenergetics in cultured rat cardiomyoblasts. Given the beneficial effect of MitoQ in the heart of obese rats, we decided to explore whether the inhibition of mitochondrial oxidative stress was able to improve the palmitic acid-induced mitochondrial damage in H9C2 cells.

H9C2 cells were stimulated with palmitic acid (200 μ M) in absence or presence of MitoQ (10⁻⁷ M) for 24 hours. We then performed a “mitochondrial stress test”. Neither palmitic acid nor MQ had effect on oxygen consumption rate (OCR) (Figure 39A).

Confirming previous results, cells stimulated with palmitic acid (200 μ M) showed an increase in proton leak and ECAR. Although MitoQ had no effect on ECAR in cells stimulated with palmitic acid, it was able to prevent this increase in proton leak. (Figure 39B and C).

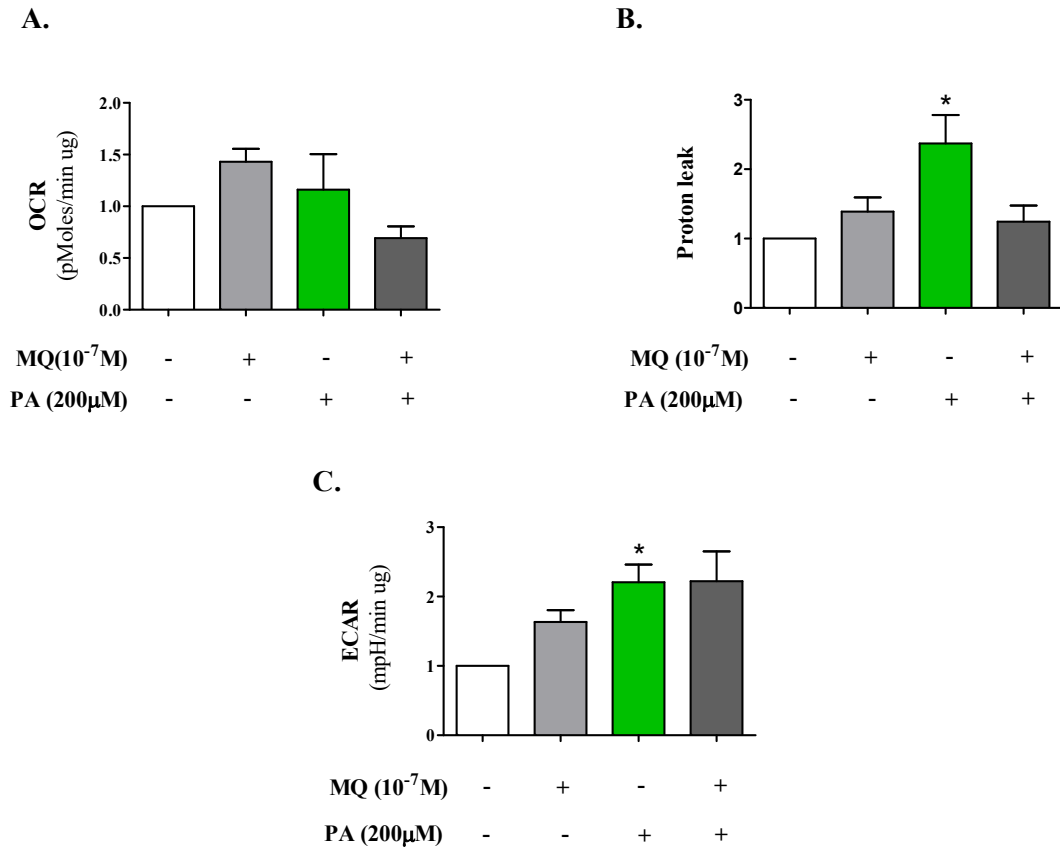


Figure 39. Effect of palmitic acid on mitochondrial function. Consequences of a mitochondrial antioxidant. H9C2 cardiomyoblasts were stimulated with palmitic acid (200 μ M) in presence or absence of MQ (10^{-7} M) for 24 hours. **(A)** Oxygen consumption rate (OCR), **(B)** proton leak and **(C)** extracellular acidification rate (ECAR) were quantified using the XF24 seahorse technology. Bar graphs represent the mean \pm SEM of 3 assays. * $p < 0.05$ vs CT.

7. Effect of a mitochondrial antioxidant on lipid profile of cardiac mitochondria in HFD rats

Taking into consideration the mitochondrial changes observed in HFD rats, a lipidomic analysis was performed to study the mitochondrial lipid content in the heart of obese rats treated with MitoQ.

Total mitochondrial TG levels were higher in obese rats (Figure 40A) mainly due to an accumulation of those enriched with palmitic acid (16:0) and stearic acid (18:0) (Figure 40B and C). Mitochondrial FFA levels were increased almost two-fold in HFD rats as compared to controls (Figure 40D). The inhibition of mitochondrial oxidative stress reduced the increase observed in HFD animals.

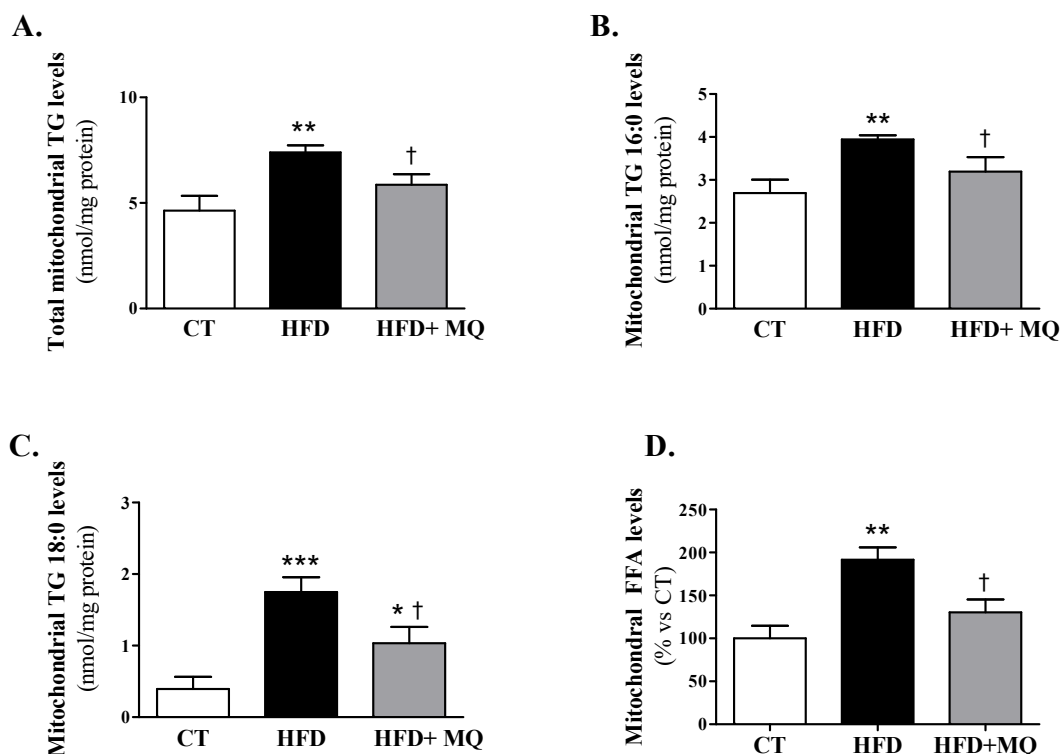


Figure 40. Effect of the administration of a mitochondrial antioxidant on mitochondrial cardiac TG and FFA of obese rats. Quantification of mitochondrial (A) total triglycerides (TG), (B) TG enriched with palmitic acid 16:0, (C) TG enriched with stearic acid 18:0 and (D) FFA levels in the heart from a standard diet (CT) and high-fat diet (HFD) rats treated with the inhibitor of mitochondrial oxidative stress (MQ, 50 mg/kg/day). Bar graphs represent the mean±SEM of 6-8 animals. * $p < 0.05$, ** $p < 0.01$ vs control group. † $p < 0.05$ vs HFD group,

No changes were observed in mitochondrial ceramide levels among any group (Figure 41).

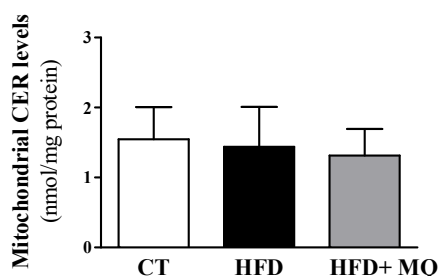


Figure 41. Effect of a mitochondrial antioxidant on mitochondrial cardiac CER levels in obese rats. Quantification of mitochondrial ceramides (CER) in the heart from a standard diet (CT) and high-fat diet (HFD) rats treated with the inhibitor of mitochondrial oxidative stress (MQ, 50 mg/kg/day). Bar graphs represent the mean±SEM of 6-8 animals.

Results

Regarding mitochondrial SM, these were not detected or detected at low levels in some animals, independently of the group (data not shown).

Obese rats presented an increase in PC and PE, as well as in LPC and LPE. MitoQ treatment, despite having no effect on PE and LPE, was able to prevent the rise in PC and LPC (Figure 42).

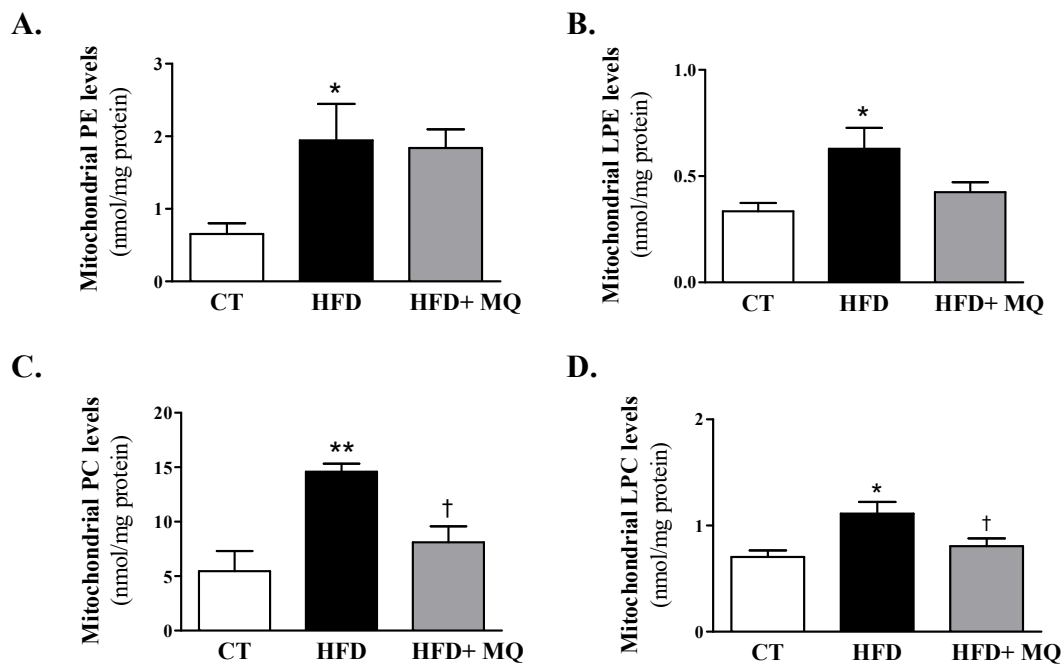


Figure 42. Effect of the administration of a mitochondrial antioxidant on mitochondrial cardiac PE, PC and its lyso forms levels in obese rats. Quantification of mitochondrial (A) phosphatidylethanolamine (PE), (B) lysophosphatidylethanolamine (LPE), (C) phosphatidylcholine (PC) and (D) lysophosphatidylcholine (LPC) in the heart from rats fed either a standard diet (CT) or a high-fat diet (HFD) treated with the inhibitor of mitochondrial oxidative stress (MQ, 50 mg/kg/day). Bar graphs represent the mean±SEM of 6-8 animals. * $p < 0.05$, ** $p < 0.01$ vs control group. † $p < 0.05$ vs HFD group.

A reduction in both carnitine and cardiolipin levels was observed in cardiac mitochondria of obese rats. MitoQ treatment was able to normalize the levels of cardiolipins. Regarding carnitines, there was a trend towards increase in obese rats treated with MQ, but this did not reach statistical significance as compared with obese animals, which received vehicle (only water) (Figure 43).

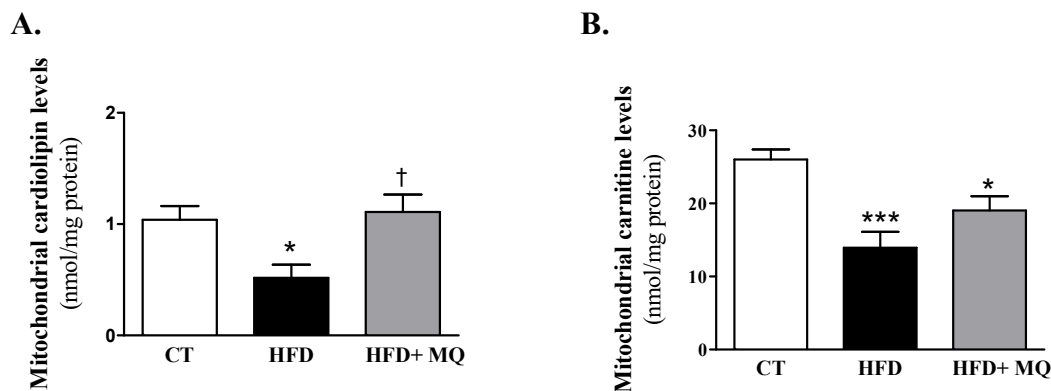


Figure 43. Effect of the administration of a mitochondrial antioxidant on mitochondrial cardiac cardiolipin and carnitine levels in obese rats. Quantification of mitochondrial (A) cardiolipin and (B) carnitine levels in the heart from rats fed either a standard diet (CT) or a high-fat diet (HFD) treated with the inhibitor of mitochondrial oxidative stress (MQ, 50 mg/kg/day). Bar graphs represent the mean \pm SEM of 6-8 animals. * $p < 0.05$, *** $p < 0.001$ vs control group. † $p < 0.05$ vs HFD group.

8. Effect of mitochondrial oxidative stress on enzymes implicated in TG metabolism

Due to the increase in total cardiac TGs, we decided to evaluate the protein levels in the heart of obese rats of adipose triglyceride lipase (ATGL) and diacylglycerol O-Acyltransferase 1 (DGAT1), two enzymes involved in TG catabolism and anabolism, respectively. ATGL selectively performs the first step in TG hydrolysis resulting in the formation of DAG and FFA. No differences were found in ATGL levels among any group (Figure 44A). However, DGAT1 that catalyzes the conversion of DAG and fatty acyl CoA to TG was increased in obese rats and MitoQ treatment was able to normalize this increase in obese rats (Figure 44B).

Results

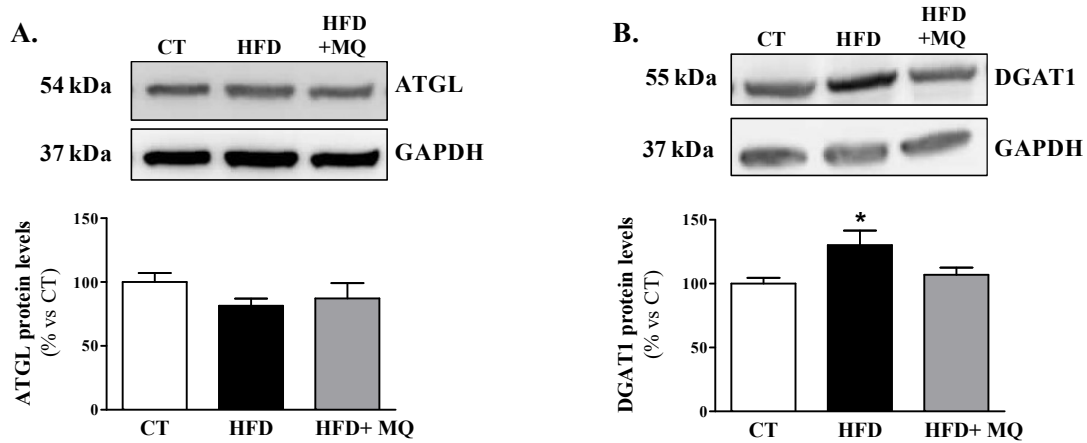


Figure 44. Effect of the administration of a mitochondrial antioxidant on TG metabolism in obese rats. Protein levels of (A) adipose triglyceride lipase (ATGL) and (B) diacylglycerol O-acyltransferase 1 (DGAT1) in the heart from rats fed either a standard diet (CT) or a high-fat diet (HFD) treated with the inhibitor of mitochondrial oxidative stress (MQ, 50 mg/kg/day). Bar graphs represent the mean \pm SEM of 6-8 animals. * $p < 0.05$ vs control group.

Given the accumulation of lipids observed in the heart of HFD rats, we explored whether this accumulation was due to an increase in the transport of fatty acids. The protein responsible for the entrance of long-chain fatty acyl-CoA in the cell is the fat transporter CD36 (cluster of differentiation 36). In the obese rats, higher protein levels of CD36 were observed supporting an increase in the inflow to the cell. In addition, an increase in the HFD group was also observed in the enzyme involved in the entry of long-chain fatty acyl CoA into mitochondria (CPT1A). MitoQ was able to normalize the increase in both proteins (Figure 45A and B)

Before entering the mitochondria and being oxidized, fatty acids must be uptaken by the cell and subsequently be activated in the cytosol. This activation is performed by the enzyme Acyl-Coa Synthetase (ACS), which is responsible for the addition of coenzyme A (CoA) to fatty acid. Surprisingly, the levels of ACS were not affected by obesity nor MitoQ (Figure 45C).

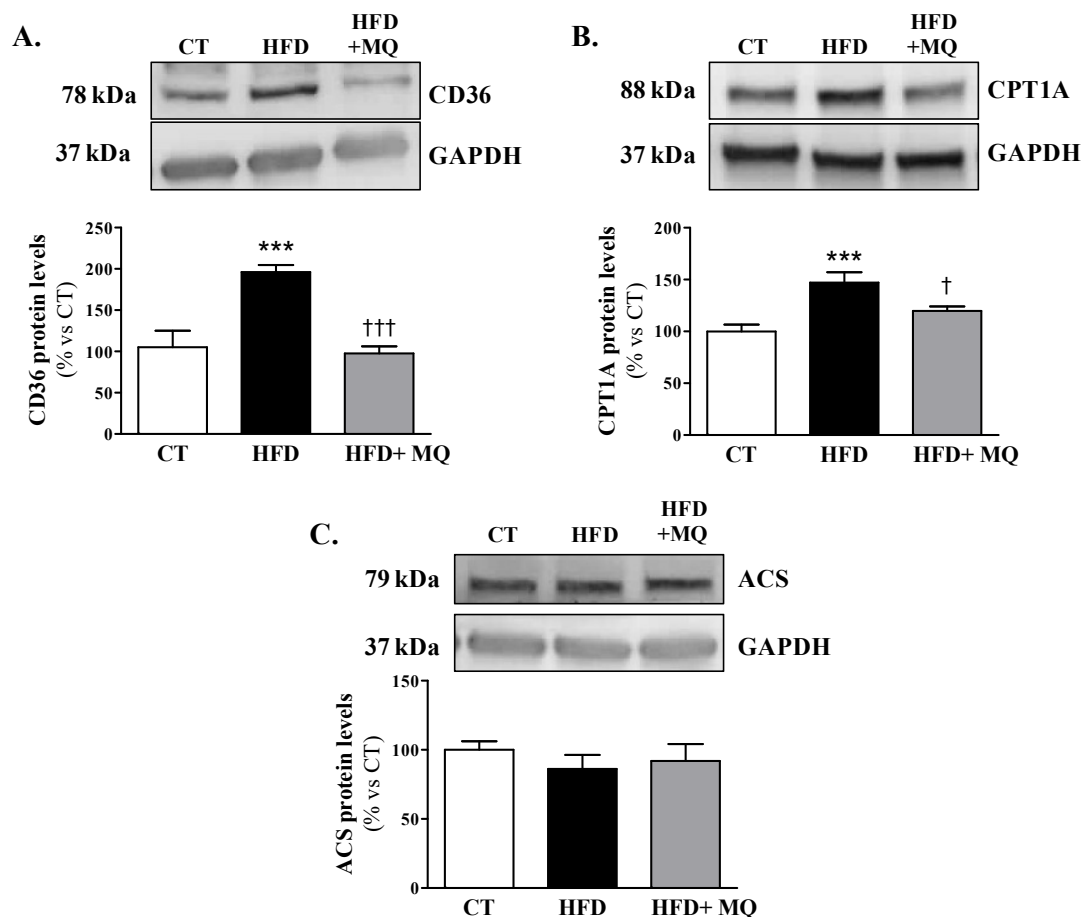


Figure 45. Effect of the administration of a mitochondrial antioxidant on cardiac fatty acid uptake in obese rats. Protein levels of (A) cluster of differentiation 36 (CD36), (B) carnitine plamitoyl transferase 1A (CPT1A) and (C) *acetyl—CoA synthetase (ACS)* in the heart from rats fed either a standard diet (CT) or a high-fat diet (HFD) treated with the inhibitor of mitochondrial oxidative stress (MQ, 50 mg/kg/day). Bar graphs represent the mean±SEM of 6-8 animals. *** $p < 0.001$ vs control group. † $p < 0.05$, ††† $p < 0.001$ vs HFD group.

We determined the levels of two enzymes that are involved in Krebs cycle, isocitrate dehydrogenase 3 (IDH3A) and fumarase, implicated in the third and seventh step of Krebs cycle, respectively. IDH3A was not affected by obesity nor MitoQ treatment. However, fumarase was reduced in obese rats, suggesting a decrease in Krebs cycle activity which was prevented by MitoQ treatment (Figure 46).

Results

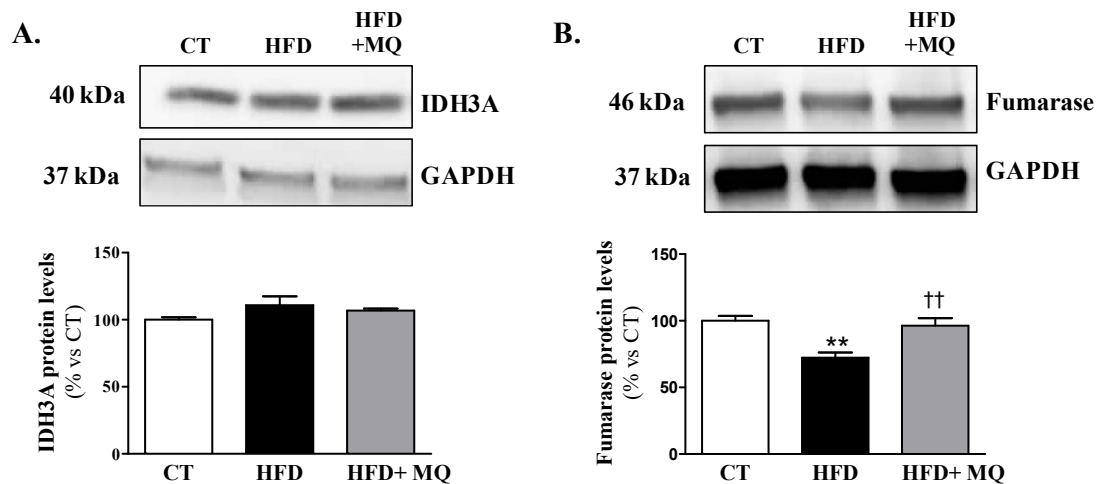


Figure 46. Effect of mitochondrial oxidative stress inhibition on enzymes of Krebs cycle in obese rats. Protein levels of (A) isocitrate dehydrogenase 3 (IDH3A) and (B) fumarase in the heart from standard diet (CT) and high-fat diet (HFD) rats treated with the inhibitor of mitochondrial oxidative stress (MQ, 50 mg/kg/day). Bar graphs represent the mean \pm SEM of 6-8 animals. ** p <0.01 vs control group. †† p <0.01 vs HFD group.

9. Effect of mitochondrial oxidative stress inhibition on mitochondrial biogenesis, dynamics and permeability in HFD rats.

Considering all these changes concerning mitochondrial complexes and Krebs cycle enzyme at mitochondrial level, we decide to evaluate other mitochondrial aspects such as biogenesis, dynamics and permeability.

First of all, protein levels of peroxisome proliferator-activated receptor gamma coactivator 1-alpha (PGC1 α), a protein that plays a central role in the regulation of cellular energy metabolism by stimulating biogenesis mitochondrial, were measured. Obese rats showed an increase in the levels of this transcription coactivator, which were normalized in MitoQ-treated obese animals (Figure 47A).

Mitochondrial dynamics was also evaluated by measuring MFN1 and DRP1, two proteins implicated in mitochondrial fusion and fission, respectively. The protein levels of MFN1 are higher in obese animals as compared with control ones. MitoQ treatment was able to reduce these levels. By contrast, the levels of DRP1 were unaffected by either obesity or the mitochondrial antioxidant (Figure 47B and C).

Finally, we evaluated the levels of cycloF, a protein that acts as a major regulator of the opening mitochondrial permeability transition pore (MPTP). In obese rats cycloF was higher than in control ones. The MitoQ treatment in obese rats prevented the increase in cycloF and therefore the uncoupling of OXPHOS (Figure 47D).

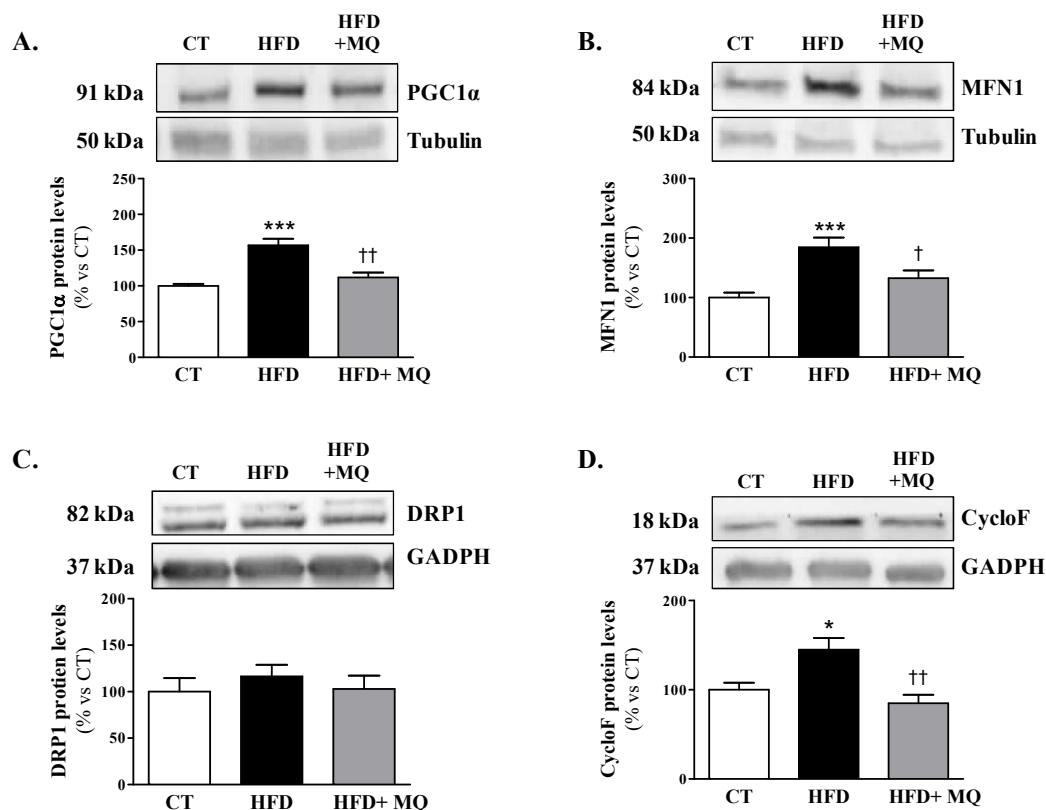


Figure 47. Effect of the administration of a mitochondrial antioxidant on mitochondrial biogenesis, dynamics and permeability in obese rats. Protein levels of (A) peroxisome proliferator-activated receptor- γ coactivator 1-alpha (PGC1 α), (B) mitofusin 1 (MFN1), (C) dynamin-related protein 1 (DRP1) and (D) cyclophilin F (cycloF) in the heart from rats fed either a standard diet (CT) or a high-fat diet (HFD) treated with the inhibitor of mitochondrial oxidative stress (MQ, 50 mg/kg/day). Bar graphs represent the mean \pm SEM of 6-8 animals. * p <0.05, *** p <0.05 vs control group. † p <0.05, †† p <0.01 vs HFD group.

10. Effect of mitochondrial oxidative stress inhibition on cardiac glucose uptake and insulin resistance in HFD rats

To assess whether the mitochondrial oxidative stress was involved in the changes in metabolic substrate utilization observed in obese rats, PET studies were performed to evaluate the use of glucose by the heart. HFD rats showed reduced ^{18}F -FDG uptake suggesting a lower use of glucose by the heart of obese rats (Figure 48A and B). HOMA

Results

index was also increased in obese rats as compared to controls, suggesting a systemic insulin resistance (Figure 48C). MitoQ was able to ameliorate both of these, suggesting an improvement in glucose utilization and insulin resistance.

A negative correlation was found between mitochondrial TG levels and cardiac ^{18}F -FDG uptake ($r=-0.6233$; $p=0.0025$).

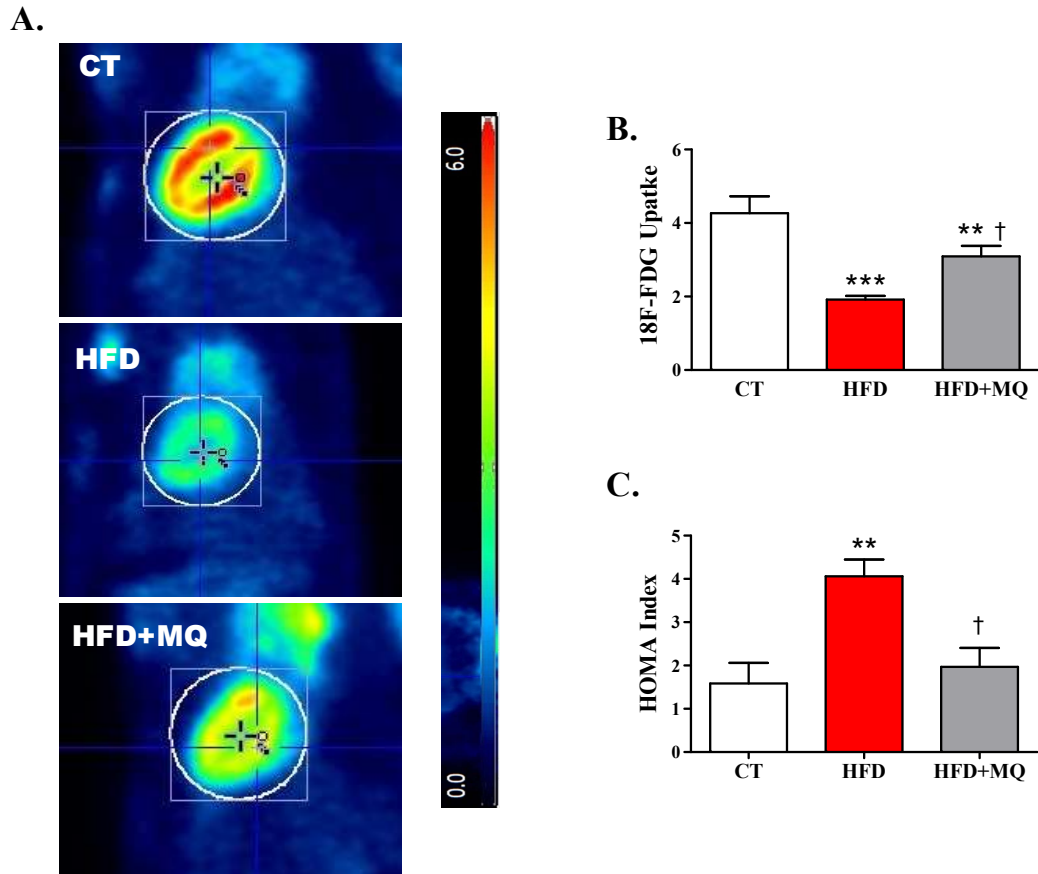


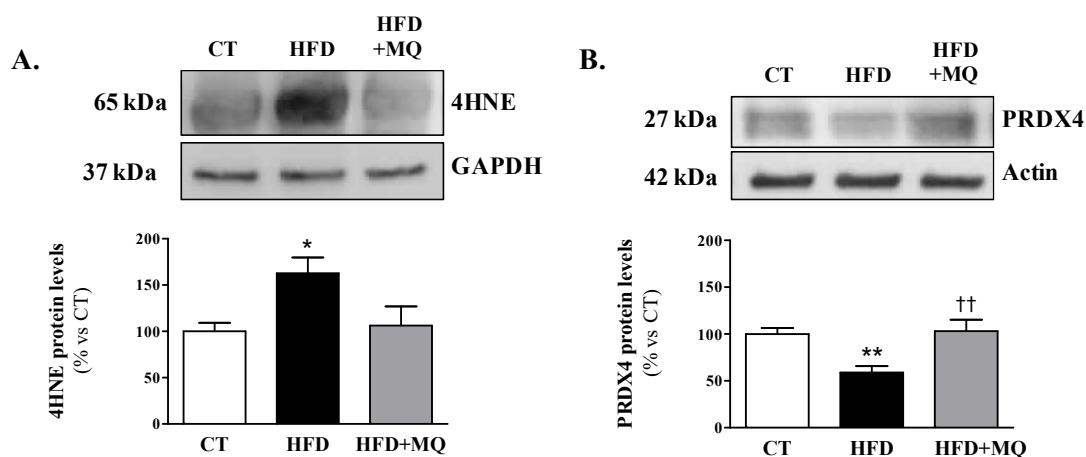
Figure 48. Effect of the administration of a mitochondrial antioxidant on cardiac ^{18}F -FDG-uptake and HOMA index in obese rats. (A) Representative images of ^{18}F -Fluorodeoxyglucose PET/CT scans of the heart, (B) quantification of cardiac ^{18}F -FDG-uptake and (C) homeostasis model assessment (HOMA) index from rats fed either a standard diet (CT) or a high-fat diet (HFD) treated with the inhibitor of mitochondrial oxidative stress (MQ, 50 mg/kg/day). Bar graphs represent the mean \pm SEM of 6-8 animals. ** $p<0.01$, *** $P<0.001$ vs CT group. † $p<0.05$ vs HFD group.

III. EFFECT OF MITOCHONDRIAL OXIDATIVE STRESS INHIBITION IN ADIPOSE TISSUE DYSFUNCTION-REMODELLING ASSOCIATED WITH OBESITY

Given the observed effect of MitoQ administration on body weight of HFD rats, we decided to evaluate its impact on adipose tissue.

1. Effect of mitochondrial oxidative stress inhibition on oxidative stress levels in the epididymal adipose tissue of HFD rats

The protein expression of 4-HNE, derived from lipid peroxidation, is used as biomarker of oxidative stress. In obese rats higher levels of 4-HNE were found elevated, which indicates an increase in oxidative stress (Figure 49A). We also determined the protein levels of the antioxidant enzyme peroxiredoxin 4 (PRDX4). We observed a decrease in the HFD rats, indicating a reduction in the antioxidant defense and thus an imbalance between production and elimination of ROS (Figure 49B). The protein levels of PRDX4 and 4-HNE were normalised with the MitoQ treatment, suggesting a reduction in ROS levels and hence an improvement in the mitochondrial damage. We also assessed the levels of PDIA6, a marker of endoplasmic reticulum (ER) stress showing an increase in HFD rats that was prevented in those HFD rats treated with MitoQ (Figure 49C).



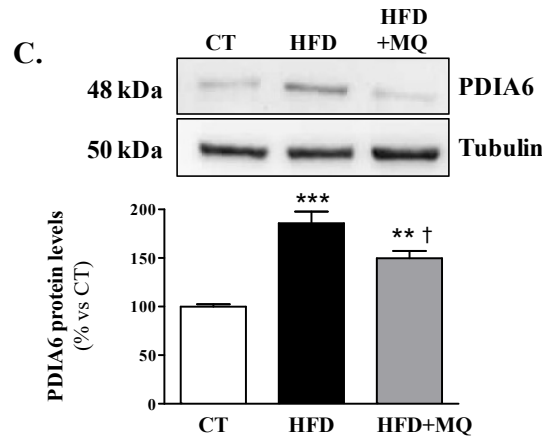


Figure 49. Effect of the administration of a mitochondrial antioxidant on oxidative stress biomarkers in epididymal adipose tissue of HFD rats. Protein levels of (A) the lipid peroxidation product 4-HNE, (B) the antioxidant enzyme PRDX4 and (C) the RE stress marker PDIA6 in epididymal adipose tissue from control rats fed a normal diet (CT) and rats fed a high-fat diet (HFD) treated with the inhibitor of mitochondrial oxidative stress (MitoQ, 50 mg/kg/day). Bars graphs represent the mean \pm SEM of 6-8 animals. ** $p < 0.01$, *** $p < 0.001$ vs CT group. † $p < 0.05$, †† $p < 0.01$ vs HFD group.

2. Effect of mitochondrial oxidative stress inhibition on adipose tissue remodelling

MitoQ was able to mitigate the increased weight of the epididymal, mesenteric and lumbar adipose tissue observed in HFD rats. Accordingly, obese animals showed an increase in adiposity index which was reduced in those treated with MitoQ (Figure 50).

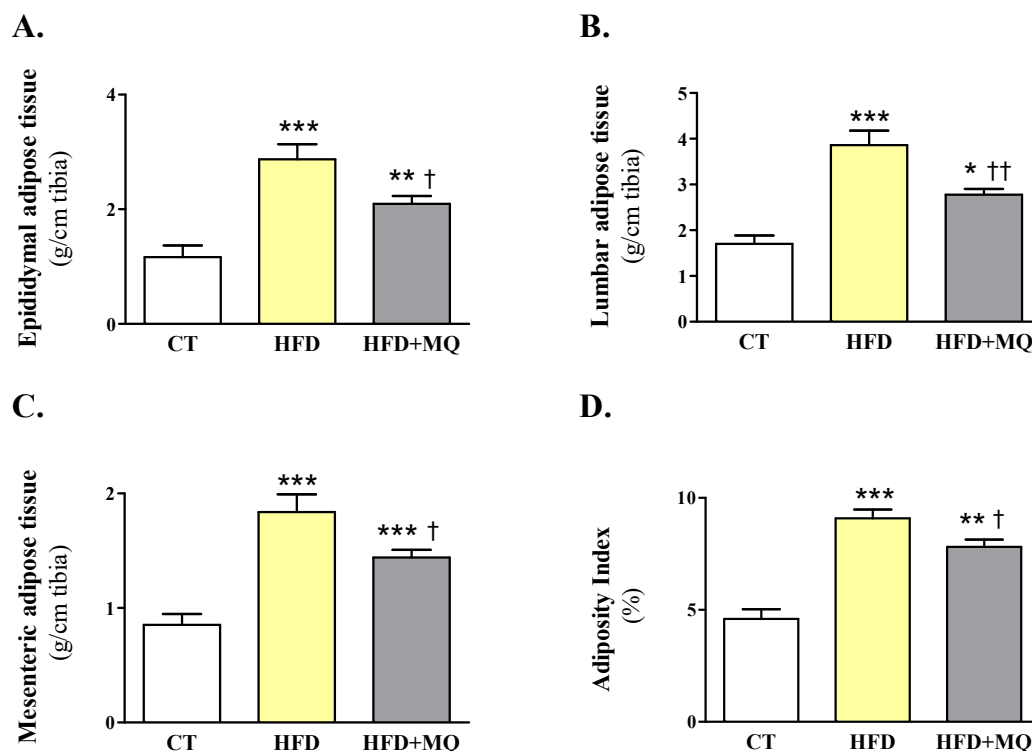


Figure 50. Effect of the administration of a mitochondrial antioxidant on fat depots and adiposity index in obese rats. Weight of (A) epididymal adipose tissue, (B) lumbar adipose tissue, (C) mesenteric adipose tissue, and (D) adiposity index from rats fed either a standard diet (CT) or a high-fat diet (HFD) treated with the inhibitor of mitochondrial oxidative stress (MitoQ, 50 mg/kg/day). Values are mean \pm SEM of 6-8 animals. * p <0.05, ** p <0.01, *** p <0.001 vs CT group. † p <0.05, †† p <0.01 vs HFD group.

Histological analysis of epididymal adipose tissue revealed an increased adipocyte area in the HFD group. A trend towards a reduction in adipocyte size was observed in obese animals that had been treated with MitoQ, although it did not reach statistical significance. Furthermore, a shift toward smaller adipocytes was detected in MitoQ-treated obese animals compared with HFD rats (Figure 51).

Results

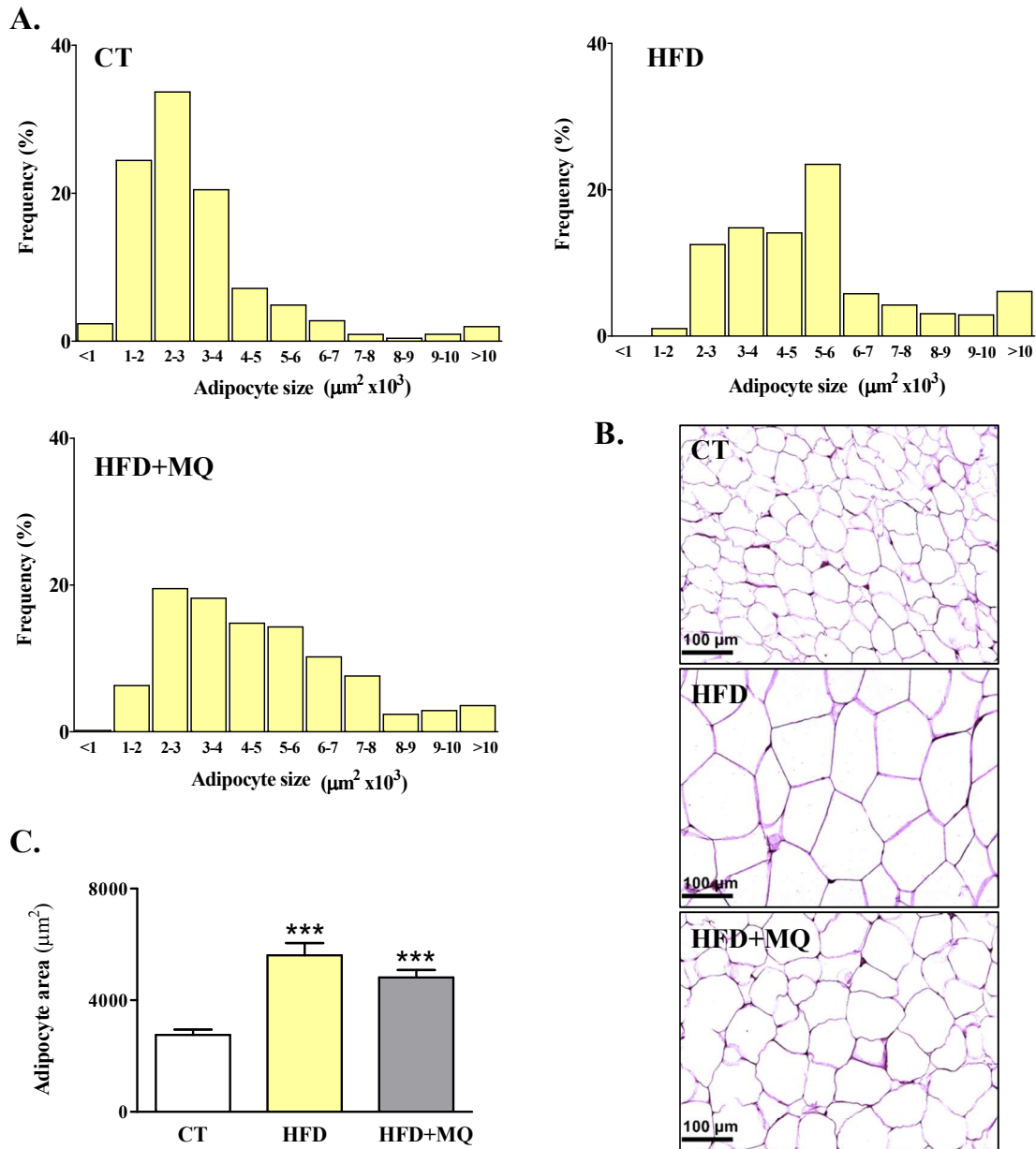


Figure 51. Effect of the administration of a mitochondrial antioxidant on adipocyte size and distribution in epididymal adipose tissue from obese rats. (A) Size distribution, (B) representative microphotographs sections stained with haematoxylin and eosin and (C) adipocyte area of epididymal adipose tissue from control rats fed either a standard diet (CT) or a high-fat diet (HFD) treated with the inhibitor of mitochondrial oxidative stress (MitoQ, 50 mg/kg/day). Magnification: 20x. Scale bar: 100 μm . Values are mean \pm SEM of 6-8 animals. * p <0.001 vs CT group.**

In addition, we have evaluated pericellular collagen content in epididymal adipose tissue sections stained with picrosirius red. HFD rats showed an increase in collagen content that was reduced by MitoQ (Figure 52).

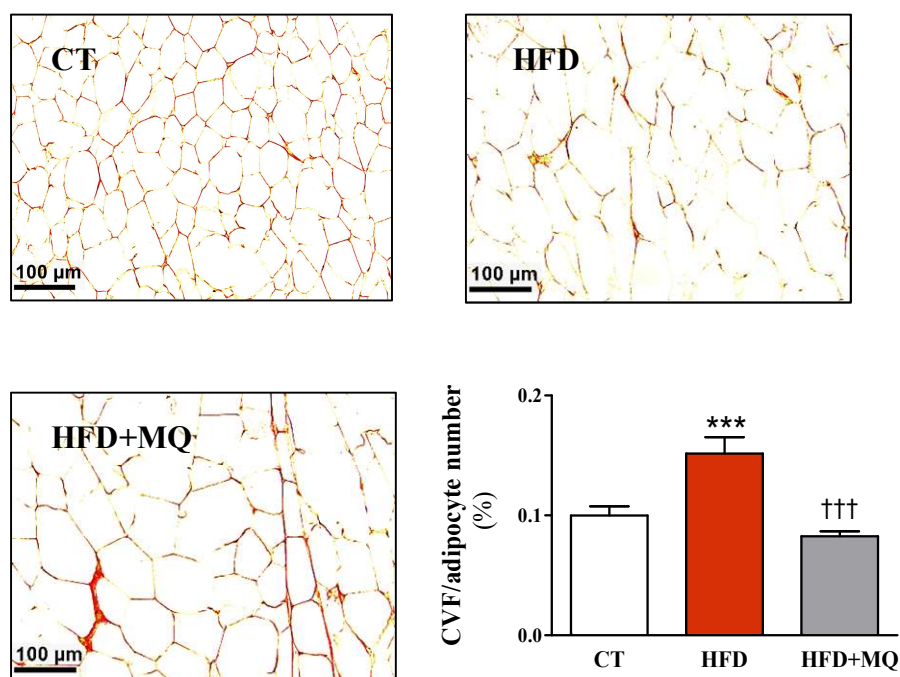


Figure 52. Effect of the administration of a mitochondrial antioxidant on pericellular fibrosis in epididymal adipose tissue of obese rats. Representative microphotographs of sections stained with picrosirius Red and quantification of collagen volume fraction (CVF) normalised by the number of adipocytes analysed in epididymal adipose tissue from control rats fed a normal diet (CT) and rats fed a high-fat diet (HFD) treated with the inhibitor of mitochondrial oxidative stress (MitoQ, 50 mg/kg/day). Magnification: 20x. Scale bar: 100 μ m. Values are mean \pm SD of 6-8 animals. *** p <0.001 vs CT group. ††† p <0.001 vs HFD group.

3. Effect of mitochondrial oxidative stress inhibition on proteins involved in insulin signalling in adipose tissue of HFD animals.

As we have described previously, the increase in HOMA index observed in HFD rats was ameliorated by MitoQ. In order to understand the effect of MitoQ on insulin sensitivity in HFD rats, we analysed proteins involved in the control of insulin sensitivity in epididymal adipose tissue. The decrease observed in adiponectin and glucose transporter 4 (GLUT4) levels in HFD rats was normalised by MitoQ (Figure 53A and B). The increase in dipeptidylpeptidase 4 (DPP4) and suppressor of cytokine signalling 3 (SOCS3) was improved as well (Figure 53C and D). SOCS 3 is involved in glucagon-like peptide 1 (GLP1) degradation and, in accordance with this, the levels of

Results

GLP1 were reduced in HFD rats (Figure 53E). There was also observed an increase in the phosphorylation of insulin receptor substrate-1 (IRS-1) that was ameliorated by MitoQ treatment (Figure 53F).

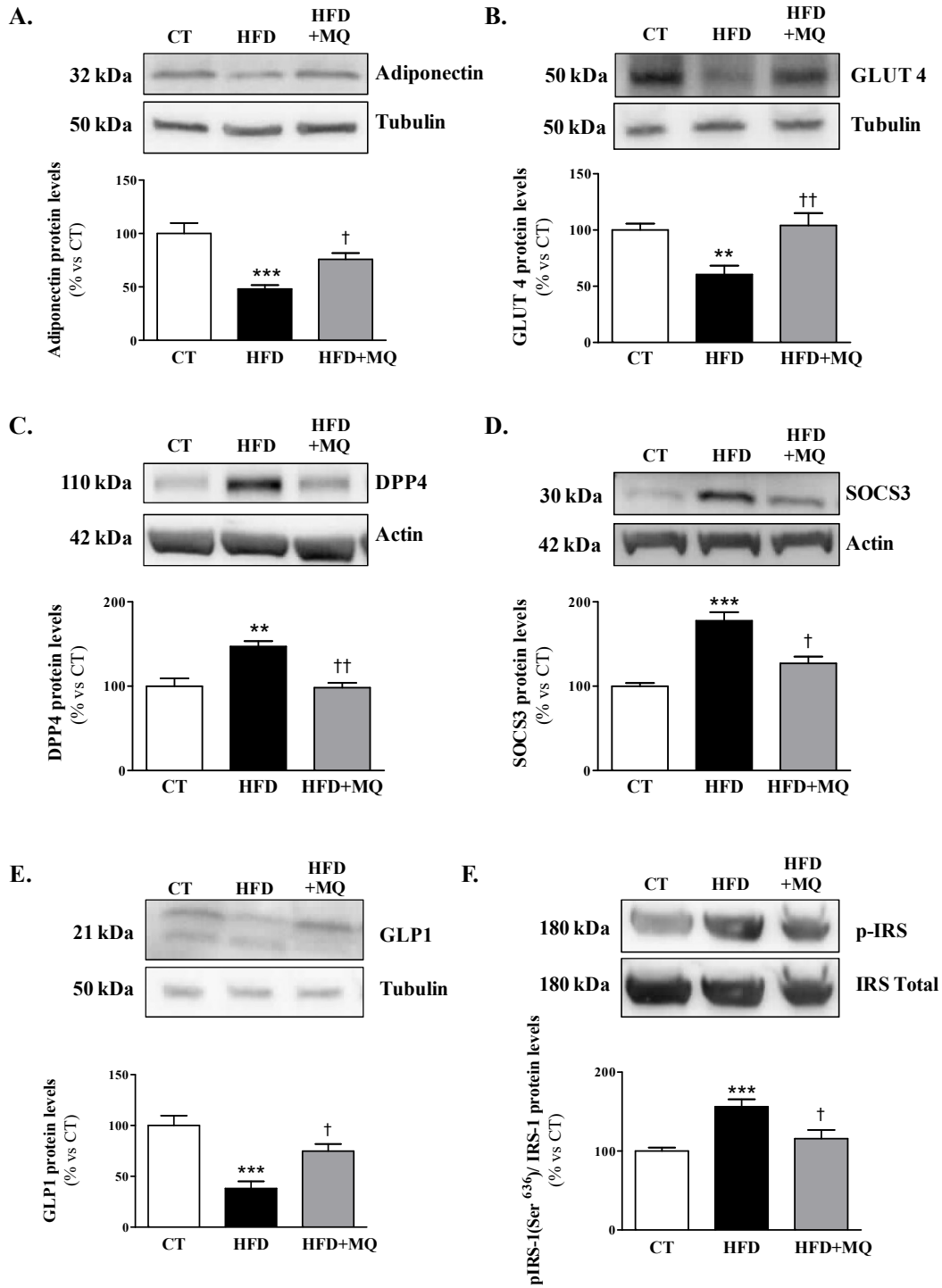


Figure 53. Effect of the administration of a mitochondrial antioxidant on insulin signalling in the epididymal adipose tissue of obese rats. Protein levels of (A) adiponectin, (B) GLUT4, (C) dipeptidyl peptidase-4 (DDP4), (D) *suppressor of cytokine signalling 3* (SOCS3) and (E) glucagon like peptide 1 (GLP1) and (F) phospho-insulin receptor substrate 1 (p-IRS1) in epididymal adipose from control rats fed a normal diet (CT) and rats fed a high-fat diet (HFD) treated with the inhibitor of mitochondrial oxidative stress (MitoQ, 50 mg/kg/day). Bars graphs represent the mean \pm SEM of 6-8 animals. ** $p < 0.01$, *** $p < 0.001$ vs CT group. † $p < 0.05$, †† $p < 0.01$ vs HFD group.

4. Effect of mitochondrial oxidative stress inhibition on fatty acid uptake in epididymal adipose tissue of HFD rats

In epididymal adipose tissue of HFD rats, CD36 was reduced and MitoQ was unable to prevent this reduction. However, MitoQ treatment was able to prevent the increase in CPT1A observed in HFD rats (Figure 54).

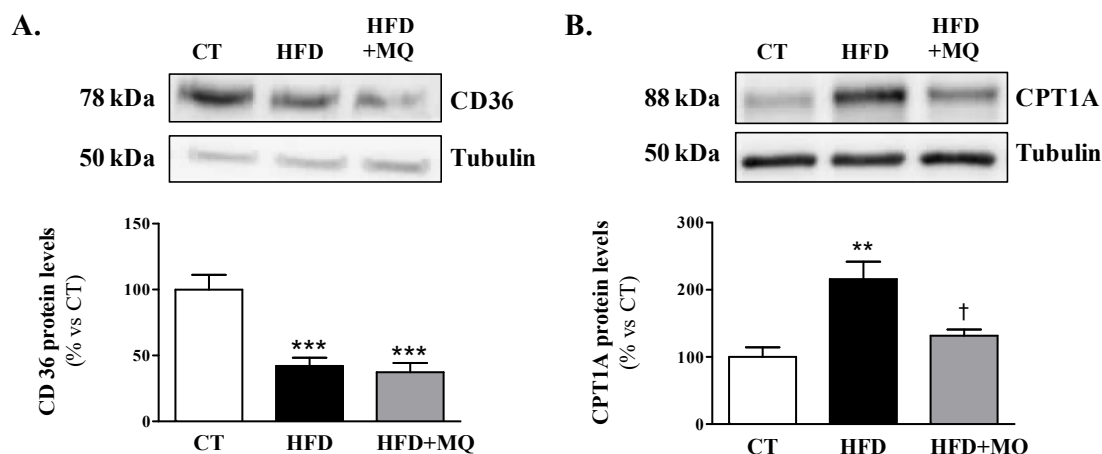


Figure 54. Effect of the administration of a mitochondrial antioxidant on fatty acid transporters in epididymal adipose tissue of obese rats. Protein levels of (A) the cell fatty acid transporter CD36 and (B) the mitochondrial fatty acid transporter CPT1A in epididymal adipose tissue from control rats fed a normal diet (CT) and rats fed a high-fat diet (HFD) treated with the inhibitor of mitochondrial oxidative stress (MitoQ, 50 mg/kg/day). Bars graphs represent the mean \pm SEM of 6-8 animals. ** $p < 0.01$, *** $p < 0.001$ vs CT group. † $p < 0.05$ vs HFD group.

5. Effect of mitochondrial oxidative stress inhibition on mitochondria in epididymal adipose tissue of HFD rats

To investigate whether the increase of fatty acid content has an impact on mitochondria, we evaluated the protein expression of all mitochondrial complexes implicated in the ATP production through the electron transport chain. As shown in Figure 55, complexes I, II and IV were reduced in HFD rats but MitoQ had no effect on them. Complex III was not altered either in HFD or HFD+MQ rats. However, complex V was increased in HFD rats and the MitoQ treatment attenuated this increase.

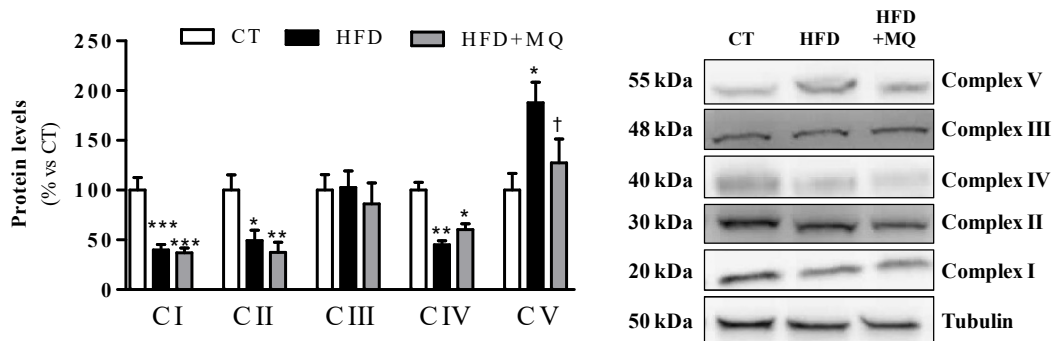


Figure 55. Effect of the administration of a mitochondrial antioxidant on mitochondrial complex in epididymal adipose tissue of HFD rats. Protein levels of the five mitochondrial respiratory chain complex in epididymal adipose tissue from control rats fed a normal diet (CT) and rats fed a high-fat diet (HFD) treated with the inhibitor of mitochondrial oxidative stress (MitoQ, 50 mg/kg/day). Bars graphs represent the mean \pm SEM of 6-8 animals. ** $p < 0.01$, *** $p < 0.001$ vs CT group. † $p < 0.05$ vs HFD group.

To further investigate the consequences of the accumulation of fatty acids inside the mitochondria, we evaluated some mitochondrial characteristics such as permeability and dynamics, among others. CycloF was increased in obese rats, suggesting the opening of the mitochondrial permeability transition pore (MPTP). This marker of mitochondrial permeability is normalized with MitoQ treatment (Figure 56A).

We also determined the protein levels of fumarase, an enzyme of the Krebs cycle necessary to mitochondrial metabolism. MitoQ treatment in HFD rats was able to prevent the reduction in FH observed in HFD rats (Figure 56B).

MFN1, a protein involved in the mitochondrial fusion process, was reduced in HFD rats but this reduction was prevented in HFD rats treated with MitoQ (Figure 56C).

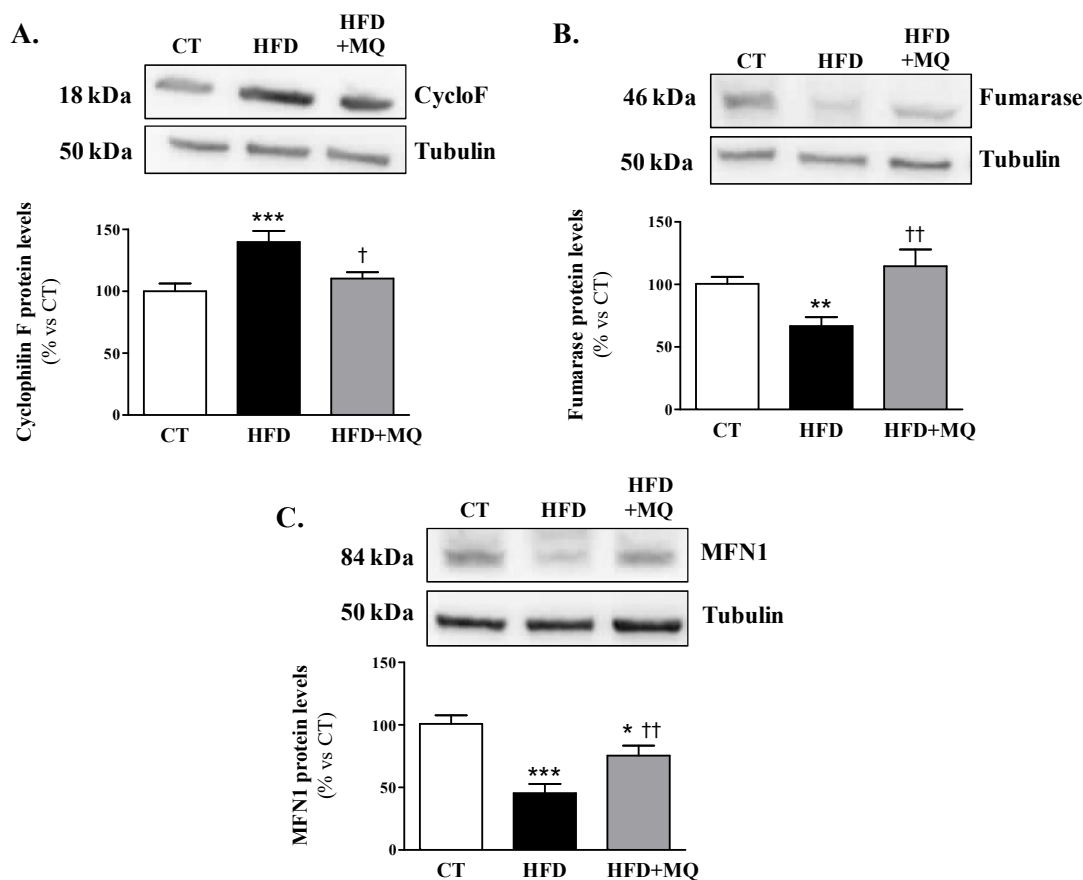


Figure 56. Effect of the administration of a mitochondrial antioxidant on mitochondrial characteristics in epididymal adipose tissue of HFD rats. Protein levels of (A) cyclophilin F, (B) Fumarase and (C) Mitofusin 1 in epididymal adipose tissue from control rats fed a normal diet (CT) and rats fed a high-fat diet (HFD) treated with the inhibitor of mitochondrial oxidative stress (MitoQ, 50 mg/kg/day). Bars graphs represent the mean \pm SEM of 6-8 animals. ** $p < 0.01$, *** $p < 0.001$ vs CT group. † $p < 0.05$, †† $p < 0.01$ vs HFD group.

6. Effect of mitochondrial oxidative stress inhibition on browning of adipose tissue in HFD rats

Due to the lower body weight observed in HFD rats treated with MQ as compared to HFD rats, we decided to evaluate whether browning of white adipose tissue could be the mechanism by which MitoQ prevented the body weight gain.

Results

We analysed mRNA expression of UCP1, the main protein involved in the browning process, in epididymal and mesenteric adipose tissue. Neither diet nor MitoQ administration were able to increase UCP1 expression in white adipose tissue which was not expressed in any animal group (data not shown). Therefore, the browning process seems not to be responsible for body weight reduction observed in HFD treated with MitoQ.

IV. IMPACT OF OBESITY IN VISCERAL ADIPOSE TISSUE REMODELLING IN PATIENTS

1. Effect of obesity on metabolic and circulating parameters in patients

As summarized in table 6, obesity was associated with an increase in insulin plasma levels. This increase was also reflected in the HOMA index, which was almost twice that in the obese patients. Likewise, increased levels of inflammation mediators such as IL-1 β , IL-6 and TNF α were observed, except for IL-10, another inflammatory cytokine that was not modified. Gal-3 was also increased in obese patients, as well as the marker of oxidative stress and cardiac damage MPO. Adiponectin levels were also reduced in obese patients, in accordance with our previous data that showed reduced levels of adiponectin protein levels in the adipose tissue of obese patients and in the epididymal adipose tissue of obese rats.

Table 6. Metabolic and circulating parameters in lean control subjects and obese patients.

Parameter	Lean subjects n=67	Obese subjects n=36	p value
Insulin (pg/mL)	163,51 \pm 62,92	256,46 \pm 71,73	<0,001
HOMA index	0,79 \pm 0,32	1,34 \pm 0,38	<0,001
Adiponectin (pg/mL)	41,87 \pm 43,95	17,61 \pm 11,17	<0,01
Gal-3 (ng/mL)	10,24 \pm 2,83	16,89 \pm 7,56	<0,001

MMP9	140,8±85,9	221,8 ±159,2	<0,01
MPO (pg/mL)	44,20±36,42	108,71±153,88	<0,001
IL-1β (pg/mL)	0,58±0,52	1,33±1,57	0,001
IL-6 (pg/mL)	3,34±3,42	11,26±11,8	<0,001
IL-10 (pg/mL)	38,89±26,73	37,58±22,89	0,790
TNFα (pg/mL)	8,68±3,83	16,92±6,86	<0,001

Data are expressed as mean ± SD. Glucagon like peptide 1 (GLP1); Galectin-3 (Gal-3); Matrix Metalloproteinase 9 (MMP9); Myeloperoxidase (MPO); Interleukin 1β (IL-1β); Interleukin 6 (IL-6); Interleukin 10 (IL-10); Tumor necrosis factor α (TNFα).

2. Effect of obesity on proteome of the adipose tissue of patients

In order to verify whether the adipose tissue remodelling occurs not only in an obese animal model but also in obese patients, we performed a proteomic study of adipose tissue from control and obese (non-diabetic) subjects. These patients, despite not being diabetic, are insulin-resistant as are our HFD rats. Therefore, they are excellent patients for the translational approach, since both patients and rats have insulin resistance but they have not developed diabetes.

2119 proteins were identified in the analysis, of which 53 were related to mitochondria. Those proteins with a fold change > 1.3 (over expression) or <0.769 (down regulation) between obese and control group were selected. According to these criteria, 23 of the 53 mitochondrial proteins were modified in the obese patients (Table 7).

Results

Table 7. Mitochondrial proteins altered in the adipose tissue of obese patients as compared with controls identified by a proteomic analysis. 1.3-fold change cut-off for all iTRAQ ratios was selected to classify proteins as up- or down-regulated; ratio <0.77 was considered underexpressed (green color) and >1.3 was considered overexpressed (red color).

Protein	Fold change OB/CT
<i>Mitochondrial proteins</i>	
10 kDa heat shock protein	0,745
Microsomal glutathione S-transferase	1,482
Aconitate hydratase	0,735
Enoyl-CoA hydratase	0,697
Electron transfer flavoprotein subunit alpha	0,662
Isoform Short of ES1 protein homolog	0,711
NADP-dependent malic enzyme	0,738
Protein NipSnap homolog 3A	0,767
Cytochrome c (Fragment)	0,691
T-complex protein 1 subunit zeta	1,303
Ras-related protein Rab-5A	0,618
NADH dehydrogenase [ubiquinone] flavoprotein 2	0,698
NADH dehydrogenase [ubiquinone] flavoprotein 1	0,727
Phosphoenolpyruvate carboxykinase [GTP]	0,740
Isoform 3 of Ethylmalonyl-CoA decarboxylase	0,766
Aspartate aminotransferase	0,576
ATPase inhibitor, mitochondrial	1,469
T-complex protein 1 subunit gamma	1,369
Branched-chain-amino-acid aminotransferase	0,558

Ubiquinone biosynthesis protein COQ9	0,736
Isoform 4 of Glutathione S-transferase kappa	1,470
Enoyl-CoA delta isomerase 1	0,601
ATP synthase lipid-binding protein	1,363
<i>Other proteins</i>	
Adiponectin	0,681
Collagen VI (alpha-3)	1,359

Most of the modified mitochondrial proteins were involved in fatty acid β -oxidation, Krebs cycle or OXPHOS. Regarding fatty acid β -oxidation and Krebs cycle, three proteins appeared reduced in each process in obese patients as compared with controls. Concerning OXPHOS seven proteins were altered (five reduced and two increased) in obese patients (Figure 57). Other processes such as protein folding and transport, oxidative stress and aminotransferase reactions were also altered.

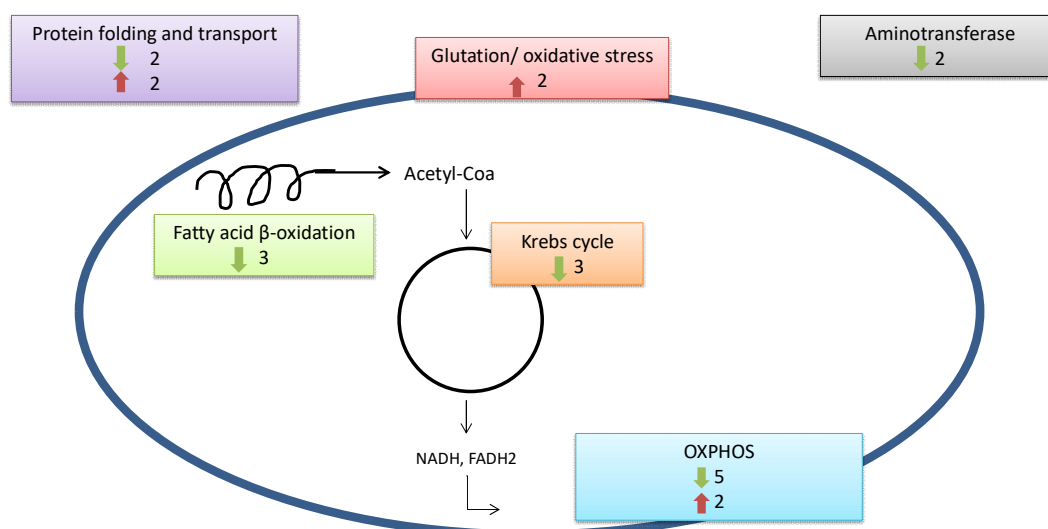


Figure 57. Scheme of the processes in which are involved the modified mitochondrial proteins in the adipose tissue of obese patients. Green arrow indicates downregulated proteins in HFD rats as compared with controls. Red arrow indicates upregulated proteins in HFD rats as compared with controls.

Results

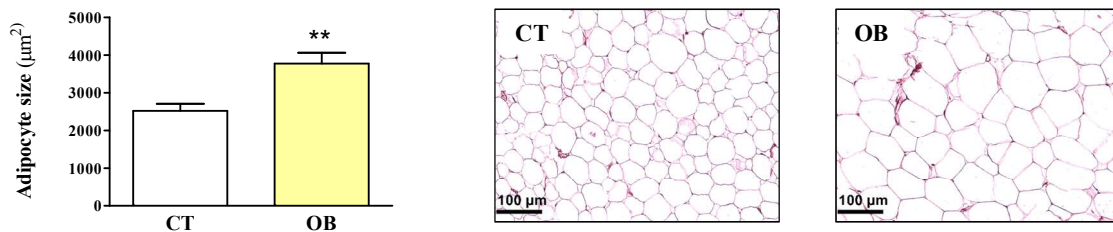
These results agree with the previous data (showed above) regarding mitochondrial dysfunction in the adipose tissue of obese rats. Some of the proteins showed in the table 7 had been evaluated by western blot in the epididymal adipose tissue of HFD rats and showed a similar pattern of expression. Two subunits of the mitochondrial complex I (described in table 7 as NADH dehydrogenase [ubiquinone] flavoprotein 1 and NADH dehydrogenase [ubiquinone] flavoprotein 2) were reduced in obese patients, as well cytochrome c levels. Both complex I and cytochrome C were also reduced in the epididymal adipose tissue of HFD rats. On the other hand, a subunit of mitochondrial complex V or ATPase (described in table 7 as ATP synthase lipid-binding protein) was increased in obese patients as compared with controls, coinciding with the higher levels of complex V observed in the epididymal adipose tissue of obese rats.

In addition, other proteins that are not related to mitochondria also showed the same expression pattern in the adipose tissue of patients and rats such as, for example, adiponectin, which is reduced in both during obesity. Another protein that was evaluated in both analyses was collagen. We observed increased levels of collagen VI in patients (table 7) and increased levels of collagen I and total collagen in the epididymal adipose tissue of rats.

3. Effect of obesity on adipocyte area and pericellular fibrosis in adipose tissue of patients

The obese patients showed increased adipocyte size as compared with controls (Figure 58A), as well as increased levels of pericellular fibrosis (Figure 58B).

A.



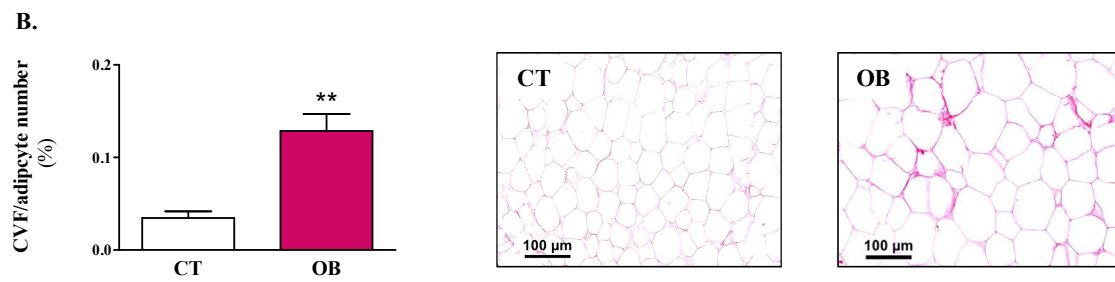


Figure 58. Adipocyte size and pericellular fibrosis in adipose tissue in obese patients. (A) Representative microphotographs of sections stained with haematoxylin and eosin and quantification of adipocyte area from control and obese patients and **(B)** representative microphotographs of sections stained with picrosirius red and quantification of collagen volume fraction (CVF) normalised for the number of adipocytes analysed in adipose tissue from control and obese patients. Magnification: 20x. Scale bars: 50 μm . Values are mean \pm SEM of 8 patients. ** $p < 0.01$ vs CT group.

Discussion

Worldwide obesity has nearly tripled in the last forty years, so it is not surprising that numerous studies have been performed to investigate its harmful effect on human health. Obesity is associated with structural and functional alterations in the heart that can lead to cardiac dysfunction. In fact, cardiovascular disease is the primary cause of death in individuals with obesity and diabetes.

It has been suggested that altered cardiac metabolism may play an important role in cardiac damage associated with obesity since obese heart is characterized by increased fatty acid oxidation, increased myocardial oxygen consumption and decreased use of glucose. Cardiac remodelling, characterized by an inflammatory response that triggers to extracellular matrix accumulation and development of fibrosis, is also involved in cardiac damage. However, the underlying mechanisms for cardiac dysfunction are partially understood. Therefore, it is necessary to explore in depth the possible mechanisms that reduce cardiac efficiency in obesity in order to focus on new therapeutic targets.

Many animal models have been studied in attempts to clarify the mechanisms that contribute to cardiac injury and dysfunction in obesity. The animal obesity models are of two types: transgenic mice and rats with genetic mutations that result in obesity, commonly through mutations in leptin gene or leptin receptor, and a diet- induced animal obesity model achieved by feeding animals a HFD. Since human obesity is mainly caused by a combination of physical inactivity and excessive food intake more than by mutations and endocrine disorders, the animal model used in the development of this study is a diet-induced obesity model.

I. ROLE OF GAL-3 IN THE CARDIOMETABOLIC ALTERATIONS IN OBESE RATS

A previous study of the group showed higher Gal-3 circulating levels in morbidly obese patients. Interestingly, these elevated levels were independent predicting factors of diastolic dysfunction. The study also showed that Gal-3 was upregulated in the cardiovascular system since increased levels of Gal-3 were found in the heart and aorta of obese rats¹⁸.

Discussion

The results herein presented show that Gal-3 is over-expressed in the heart of obese rats and that the pharmacological inhibition of Gal-3 activity decreased cardiac fibrosis in obese rats without affecting body weight gain. The animals fed a high-fat diet did not develop cardiac dysfunction and were normotensive, confirming previous studies and showing model reproducibility¹⁸.

The role played by Gal-3 in cardiovascular fibrosis and inflammation has been amply showed in diverse pathologies such as obesity, hypertension, hyperaldosteronism, aortic stenosis and renal damage^{18, 39, 154-156}. In our study we show that the administration of the Gal-3 activity inhibitor, MCP, ameliorated cardiac fibrosis as well as cardiac lipotoxicity. This was accompanied by an improvement in mitochondrial damage, suggesting that mitochondrial dysfunction could participate in the cardiac damage associated with obesity. The main source of energy in the heart is lipids but glucose is also needed to satisfy the elevated cardiac energy demand. Since both lipids and glucose are oxidized in the mitochondria to produce ATP⁷³, a correct functioning of mitochondria seems to be indispensable for healthy heart maintenance. This is the reason why we have focused on this organelle in the present study.

As we have mentioned above, lipids are the main energy substrate for cardiac mitochondrial oxidation but they also act as signalling molecules and play an important role in membrane structure^{157, 158}. Therefore, alterations in the cardiac lipid profile may contribute to cardiac lipotoxicity associated with obesity.

Our results show an increase in TG levels in the heart of obese rats, confirming previous experimental and clinical studies that have also found increased myocardial TG levels in obese Zucker rats and obese patients^{44, 159}. The increase in TG observed in the myocardium of our HFD rats was mainly a consequence of the rise in the levels of TGs enriched with palmitic acid 16:0 and stearic acid 18:0 (saturated fatty acids) and arachidonic acid 20:4 (polyunsaturated fatty acid), reflecting the fat composition of the diet. Recent evidence indicates that saturated fatty acid-induced lipotoxicity contributes to the pathogenesis of cardiovascular and metabolic diseases. It is important to know that saturated and unsaturated fatty acids play different roles in the lipotoxic context^{160, 161} since saturated fatty acids are considered more prone to induce cardiovascular complications than unsaturated ones. Moreover, several studies show the beneficial effect of polyunsaturated fatty acids in the prevention and treatment of cardiovascular

diseases¹⁶²⁻¹⁶⁴. In fact, WHO Dietary Guidelines advise substituting saturated fatty acids in the diet for monounsaturated and polyunsaturated fatty acids (PUFA) in order to reduce cardiovascular risk¹⁶⁵. One of the mechanisms that explain this difference between saturated and unsaturated fatty acids is their ability to promote TG accumulation¹⁶⁶. TG-enriched lipid droplets accumulation was thought to be the cause of insulin resistance and toxicity in tissues but it has recently been suggested that the accumulation of TG in lipid droplets may play a protective role. Saturated fatty acids, such as palmitic acid are deficiently incorporated into TG and cause apoptosis by increasing CER synthesis and reactive intermediates. However, unsaturated fatty acids such as oleic acid trend toward TG accumulation as DGAT1, the enzyme that catalyzes TG synthesis, preferentially incorporates unsaturated fatty acids. Moreover, unsaturated fatty acids rather than saturated ones activate PPAR α and PPAR γ promoting fatty acid oxidation^{166, 167}.

Although TGs are not directly toxic themselves because they are an inert neutral lipid form, the increase in TGs is considered to be a biomarker of accumulation of other toxic lipid intermediates such as DAG and CER. Therefore, an increase in TGs is associated with cardiac lipotoxicity⁴⁴. Our data showed that treatment with MCP was able to prevent the increase in TG observed in the heart of HFD rats indicating that Gal-3 is involved in cardiac lipotoxicity.

In a previous study of our group, we found that cardiac SM levels could modulate GLUT4 levels in HFD rats¹¹² that may facilitate changes in the use of metabolic substrates by the myocardium during obesity. Our present results show decreased SM levels in the heart of obese rats. Moreover, a direct correlation between cardiac levels of SM and ¹⁸F-FDG cardiac uptake has been found, suggesting that the reduced SM levels in the heart of obese rats might participate in the cardiac insulin resistance observed in these animals. On the other hand, CER levels result from both de novo synthesis and hydrolysis of SM, suggesting a link between both lipids. We have observed increased CER levels in HFD rats. In fact, a negative correlation between CER and SM levels was observed. We have also observed a negative correlation between CER levels and ¹⁸F-FDG uptake pointing out the participation of this lipid class in insulin resistance. However, MCP treatment was able to ameliorate neither SM and CER levels nor ¹⁸F-FDG cardiac uptake and HOMA index, demonstrating that Gal-3 does not play a role in insulin resistance associated with obesity. Conversely, a recent study showed that Gal-3

Discussion

administration in mice is associated with insulin resistance, whereas Gal-3 loss of function, pharmacological and genetic, improved insulin sensitivity in obese mice¹⁶⁸. However, previous data have reported that Gal-3 knockout mice fed a HFD for 12 or 18 weeks presented dysregulated glucose metabolism^{169, 170}. Therefore, further studies are needed to assess the specific role of Gal-3 in metabolic disorders and insulin resistance.

Regarding DAGs, we found in a previous study of the group that these were independent predictors of cardiac fibrosis⁵⁴. DAGs activate protein kinase C (PKC), a family of serine/threonine kinases, which is involved in cardiac hypertrophy and heart failure. However, differences in fatty acid DAG composition are involved in the activation of different PKC isoforms¹⁷¹. DAG enriched with 20:4 ω 6 are more efficient in activating PKC α , PKC ϵ and PKC δ than other fatty acids such as 20:5 ω 3 and 22:6 ω 3. Conversely, PKC β I is less activated by DAG 20:4 ω 6 than by DAG enriched in ω 3 polyunsaturated fatty acids. The three PKC isoforms activated by 20:4 ω 6 are involved in cardiofibroblast proliferation and collagen production^{172, 173}. PKC δ , specifically, has been associated with cardiac damage¹⁷⁴. Our results showed an increase in DAG enriched with 20:4 ω 6 in the heart of HFD rats, supporting the idea that DAG could be involved in the cardiac fibrosis observed in obese rats. In addition, a study performed by Song X et al. showed that PKC stimulated Gal-3, collagen I and fibronectin production and that the inhibition of Gal-3 blocked collagen production in mouse cardiomyocyte HL-1 cells. They also showed that rats with heart failure induced by pulmonary artery banding presented increased levels of PKC α , Gal-3 and collagen I suggesting that, *in vivo*, PKC α mediates cardiac fibrosis through Gal-3⁵⁵. We have gone further in our studies by showing that the inhibitor of Gal-3 activity, MCP, reduced cardiac fibrosis and DAG levels in the heart of obese rats, demonstrating the role of Gal-3 in cardiac lipotoxicity.

Our results showed that lysophosphatidylcholine (LPC), mainly LPC18:0 and LPC 20:4, and lysophosphatidylethanolamine (LPE) were increased in the heart of HFD rats. Moreover, in a previous study of our group, we found that cardiac LPC levels correlated with adiposity index⁵⁴. A similar increase has been reported for circulating LPC levels in obese patients and in experimental models of obesity^{175, 176}, even proposing LPC 18:0 as a biomarker of obesity¹⁷⁷. However, reduction of LPC has been found in other studies. This could be explained by the fact that the main LPCs detected in our study are LPCs enriched in stearic acid 18:0 and arachidonic acid 20:4 and the studies performed

by Tulipani¹⁷⁸ and Pickens¹⁷⁹ particularly observed reduced levels of LPC acylated with margaric, oleic and linoleic acids. Therefore, our data support the idea that cardiac lipotoxicity involves not only variations in the type of lipid but is also due to differences in their fatty acid composition.

Unlike SM and CER, treatment with MCP was able to normalize both cardiac TG and LPC levels without altering the abnormal ¹⁸F-FDG cardiac uptake. Therefore, neither TG nor LPC levels seem to be major determinants of the altered cardiac glucose use observed in HFD animals because no correlation was found amongst these parameters. These data confirm previous observations that found no link between either TG or LPC circulating levels and insulin resistance in the context of obesity^{175, 178, 180, 181}. Conversely, what we have found is a correlation between the cardiac levels of TGs enriched with palmitic acid and LPC, and those of mitochondrial ROS in MCP-treated and untreated HFD rats, suggesting that excess of some lipid class are associated with increased ROS levels, supporting a previous study of our group that show that palmitic acid, the most elevated fatty acid in TGs, was able to stimulate mitochondrial ROS production in H9c2 cells¹¹².

ROS are essential in physiological conditions since they are signalling molecules that regulate cell function. However, overproduction of ROS in pathological conditions has harmful consequences, causing organelle stress and cell death¹⁸². Our results showed higher levels of mitochondrial oxidative stress in the heart of obese rats that could itself be damaging mitochondria. This increase in mitochondrial oxidative stress is accompanied by an increase in CPT1A, suggesting an accumulation of fatty acids inside the mitochondria that could be altering other mitochondrial components. In fact, alterations in respiratory chain complexes were observed. Complex I and II were increased in the heart of HFD rats whereas complex V, which is responsible for providing energy for the cell through the synthesis of ATP, was reduced. This suggests that oxidative phosphorylation (OXPHOS) is damaged. We also observed an increase in MFN1 cardiac protein levels in obese rats, indicating that changes not only occur at mitochondrial machinery levels but also at morphological level. This increase in MFN1 indicates a rise in mitochondrial fusion, a process that is considered to be an adaptive pro-survival response against stress¹⁸³. Different studies support the idea that during obesity there is an increase in ROS production that triggers mitochondrial dysfunction. The study from Tsushima et al, suggest that prolonged lipid overload enhances

Discussion

mitochondrial ROS generation followed by reduced mitochondrial respiration and ATP synthesis¹⁸⁴. Another study performed in right atrial cardiomyocytes isolated from type-2 diabetic patients also showed an increase in mitochondrial ROS accompanied by damaged mitochondrial bioenergetics¹⁸⁵. Our results showed that treatment with MCP reduced the mitochondrial oxidative stress in the heart of obese rats and normalized CPT1A, MFN1 and respiratory chain complex levels, supporting this link between oxidative stress and mitochondrial dysfunction in the context of obesity and highlighting a role for Gal-3.

H9c2 cells stimulated with palmitic acid, the main fatty acid accumulated in the heart of HFD rats, showed an increase in the proton leak, suggesting a reduced capacity of the mitochondria to accomplish oxidative phosphorylation. Palmitic acid stimulation also induced an increase in glycolysis in H9c2 cells, which is thought as a compensatory mechanism to satisfy the energy demand of the cell. However, ATP production through this pathway might be limited in the HFD animals since the cardiac glucose uptake is reduced. In the palmitic acid stimulated cells, MCP in the incubation media did not prevent these alterations, suggesting that Gal-3 does not have a direct effect on mitochondrial function. However, we have then seen that Gal-3 production was not induced by palmitic acid in this cell line, so we cannot discard a possible role of Gal-3 in mitochondrial dysfunction.

In summary, the inhibition of Gal-3 activity through MCP was able to prevent some of the changes in cardiac lipid profile in HFD rats, supporting a role of Gal-3 in cardiac lipotoxicity. In fact, it was able to reduce the total lipids in the heart mainly due to a reduction in TG, DAG and LPC levels, although it was not able to improve insulin resistance. Gal-3 inhibition was also accompanied by a reduction in mitochondrial oxidative stress and an improvement in the mitochondrial damage observed in obese rats. The mechanism by which Gal-3 is involved in cardiac lipotoxicity remains unclear but one option might be its capacity to induce oxidative stress that finally triggers mitochondrial dysfunction. Supporting this idea, a recent published paper has shown that Gal-3 decreases the antioxidant enzyme PRDX 4 in cardiac fibroblasts, altering the antioxidant capacity of the cell and leading to increase of mediators of oxidative stress¹⁸⁶.

II. ROLE OF MITOCHONDRIAL OXIDATIVE STRESS IN THE CARDIOMETABOLIC ALTERATIONS IN OBESE RATS

As we have reported in the previous section, the high fat diet rats showed an accumulation of fatty acids in the heart that trigger cardiac lipotoxicity. There is evidence that the accumulation of fatty acids leads to an increase in the production of ROS, thereby causing oxidative stress that participates in the cardiac damage associated with obesity. As aforementioned, the heart is able to produce ATP from diverse substrates but 60-70% of the ATP is obtained from mitochondrial fatty acid oxidation, whereas the remaining 30-40% is obtained from other substrates such as glucose and lactate. In a normal situation the electrons derived from substrate oxidation are transported through the respiratory chain by electron carriers and during this transport the electrons can leak from the respiratory chain and react with oxygen generating ROS as superoxide and hydroxyl anions. Diabetic and obese hearts even further increase the use of fatty acids to obtain ATP^{26, 88} increasing the electron transport through the respiratory chain, favouring a greater leakage of electrons and therefore the generation of ROS. Moreover, fatty acid oxidation consume more oxygen than glucose oxidation per ATP molecule produced, so an increase in fatty acid use in diabetic and obese hearts contribute to a greater O₂ consumption, resulting in further deterioration of the heart and in a state of energy deficiency⁸⁴. Since mitochondria is the main source of ROS that plays a central role in the energy production essential in maintaining cardiac activity, we decided to explore the role of mitochondrial oxidative stress on the cardiometabolic alterations, changes in cardiac structure and changes in the use of metabolic substrates as well as on the mitochondrial alterations associated with obesity. For this purpose, we developed a rat model of diet-induced obesity in which mitochondrial oxidative stress was inhibited through the administration of the mitochondrial antioxidant MitoQ (50mg/kg/day) in the drinking water.

As we have shown in the previous section, our results demonstrated increased collagen content in the heart of obese rats as well as higher levels of CTGF and TGF β , which were prevented by the Gal-3 inhibitor. Since we proposed that Gal-3 could exert its action by inducing oxidative stress and alterations of mitochondrial function, we explored whether the inhibition of mitochondrial oxidative stress was also able to prevent this increase in ECM as well as cardiac hypertrophy and the increase in the cardiomyocyte area of the HFD rats.

Discussion

Cardiac hypertrophy is initially a compensatory physiological mechanism to reduce ventricular wall stress and maintain a correct efficiency of the heart. However, this initial adaptation finally results in heart failure². Cardiac hypertrophy, mainly left ventricular hypertrophy (LVH), is associated with changes in cardiac tissue architecture by myocardial and perivascular fibrosis, arterial and myocardial wall thickness and myocyte hypertrophy. In addition, LVH is an independent predictor of adverse cardiovascular outcomes such as coronary heart disease, heart failure and stroke¹⁸⁷. A previous study of the group performed in obese patients that are undergoing bariatric surgery showed that body weight reduction normalized LVH in 36,5 % of the patients and improved in 51,2%, demonstrating that obesity is associated with LVH. Our results showed reduced levels of interstitial fibrosis in obese rats treated with MitoQ as well as a reduced cardiomyocyte size, which was accompanied by a reduction in relative heart weight indicating an improvement in cardiomyocyte hypertrophy. These data support a role for mitochondrial oxidative stress in the development of fibrosis and hypertrophy in the context of obesity. Supporting our data, some studies have suggested the role of oxidative stress in cardiac fibrosis and hypertrophy. The study performed by Qian Y and colleagues showed that the inhibition of inflammation with X22, a derivative of imidazopyridine that is a compound with different activities --including anti-inflammatory, antioxidant and anti-cancer-- reduced oxidative stress, cardiac fibrosis and hypertrophy in the heart of high-fat diet fed rats¹⁸⁸. Another study carried out by Xu W et al. demonstrated that the ubiquitin-modifying enzyme A20, an anti-inflammatory protein, ameliorated HFD-induced ROS, hypertrophy, fibrosis and cardiac dysfunction¹⁸⁹. Both studies show that the inhibition of the inflammation leads to a reduction of oxidative stress and cardiac fibrosis. However, we have acted directly on the oxidative stress and we have demonstrated that a mitochondria-targeted antioxidant was able to prevent cardiac fibrosis and hypertrophy in HFD rats.

Nevertheless, fibrosis and hypertrophy are not the only cardiac consequences of obesity. As we have shown in the previous section, HFD rats show an accumulation of cardiac lipids. This myocardial accumulation may be due to an imbalance between cardiomyocyte fatty acid uptake and fatty acid oxidation that contributes to the increase of cardiotoxic metabolites. The fatty acid uptake is mediated by several fatty acid transporters localized in the plasmatic membrane of the cell as fatty acid-binding protein (FABPpm), fatty acid transport proteins 1–6 (FATP1–6) and caveolin-1. However,

CD36 seems to be the predominant fatty acid transporter in adipocytes, enterocytes, cardiac myocytes and skeletal myocytes. In fact, CD36 contribute approximately 70% to the fatty acid uptake in cardiomyocytes¹⁹⁰. We have reported increased levels of CD36 in the heart of HFD rats, suggesting that cardiomyocyte fatty acid uptake is increased in our HFD rats. Once inside the cell, the fatty acids can be stored for future use as triglycerides in the TG pool or can be uptaken by the mitochondria to be consequently oxidized. Our results demonstrate that both processes are reinforced in the heart of obese rats. On the one hand, our HFD rats showed increased levels of diacylglycerol O-Acyltransferase 1 (DGAT1), the enzyme involved in the last step of TG synthesis. On the other hand, CPT1A protein levels are also increased in the HFD rats, suggesting an increase in the fatty acid uptake inside the mitochondria to be consequently oxidized. MitoQ was able to prevent the increase in both CD36 and CPT1A. These results lead us to think that oxidative stress may be involved in the enhancing of fatty acid uptake inside the mitochondria as a compensatory mechanism to counteract the excess of lipids in the heart.

Considering the increase of fatty acid uptake by mitochondria in obese rats, we decided to perform a lipidomic analysis specifically of the lipids present in the mitochondria of the heart to assess whether changes in lipid profile may be involved in mitochondrial damage and the development of cardiac dysfunction. Our data showed a reduction in cardiolipin (CL) levels in the cardiac mitochondria of obese rats. CL is a mitochondrial specific phospholipid that reside in the inner mitochondrial membrane (IMM) and is necessary for maintaining the structural integrity of mitochondrial membranes as well as the function of chain respiratory complexes¹⁹¹. CL-induced mitochondrial damage is not only due to a drop in CL levels but also by a remodelling process that is responsible for generating CL species which causes oxidative stress and mitochondrial dysfunction⁷⁵. Actually, although we observed a reduction in the total CL levels in the cardiac mitochondria of obese rats, HFD had a diverse impact on different CL species, diminishing CL enriched with 18:2 and 22:6 fatty acids and increasing those enriched with 20:4. Specifically, we observed a reduction in CL enriched with linoleic acid 18:2 (an essential ω 6 fatty acid), which represents 75–80% of the total CL content in both rat and human cardiac mitochondria. Several studies have shown that loss of tetralinoleoyl CL [(18:2)₄CL] occurs in different states of cardiac diseases. Barth syndrome, characterized by dilated cardiomyopathy, is caused by a mutation in the tafazzin gene

Discussion

that results in loss of (18:2)₄CL and lower CL abundance¹⁹². Moreover, reduced levels of (18:2)₄CL have been observed in ischemic heart failure^{193, 194} and diabetes¹⁹⁵. MitoQ was able to prevent the reduction in CL levels (CL18:2 and CL22:6) showing the important role played by mitochondrial oxidative stress in CL remodelling in the context of obesity. Moreover, CLs are highly sensitive to ROS due to its high content in double bonds of the polyunsaturated fatty acids and its location near ROS production sites⁷⁵.

CER are also components of the mitochondrial membrane and they have been reported to be involved in mitochondrial function and OXPHOS since they are associated with decreased mitochondrial respiratory chain activity, increased ROS production and oxidative stress, mitochondrial outer membrane permeabilization (MOMP), reduced mitochondrial membrane potential, mitophagy and apoptosis⁶⁵. However, we have observed no changes in CER levels in the cardiac mitochondria of our obese rats. This difference may be explained because not all CER are implicated in mitochondrial function; it depends on the acyl chain length. In fact, most of these studies that show harmful effects for CER have been carried out using short chain CER (C2 and C6) (23933096). Nevertheless, the CER that we were able to detect in our experiment were enriched with long chain fatty acids, mainly CER (d18:1/16:0), CER (d18:1/18:1) and CER (d18:1/20:0), so we cannot discard that with a more exhaustive analysis regarding CER we could find a reduction in short chain CER and therefore its possible implication in mitochondrial dysfunction in our obese rats.

Our results show that PC, PE, LPC and LPE were increased in the mitochondria of the heart of obese rats. A remodelling in phospholipids of cardiac mitochondria of HFD mice have been reported by Sullivan EM et al⁷⁷, who demonstrate that PE and PC remodelling are involved in membrane-packing reduction in cardiac tissue, although these have no effect on super complex formation and respiratory enzymatic activity. Phospholipids remodelling involves changes in the fatty acid containing phospholipids as a result of the action of a group of enzymes called phospholipases, which hydrolyze the fatty acid esterified to the first or second carbon of glycerol backbone. The membrane phospholipid diversity is important for the fluidity of the bilipidic membrane. The increased levels of LPE and LPC observed in obese rats might be a sign of failure of the mechanism responsible for promoting remodelling of the mitochondrial phospholipids (the deacylation-reacylation cycle), which may result in a mitochondrial

membrane structure defect contributing to mitochondrial dysfunction. MitoQ treatment was able to prevent the increase in PC and LPC levels of obese rats, although it did not modify the increased in PE and LPE levels in HFD rats.

Another lipid class that was modified in the heart of our HFD rats as compared with CT was carnitine, which was observed to be reduced in obese rats. This could be explained by the fact that we have previously seen enhanced fatty acid uptake by the mitochondria in HFD rats. For this to happen, the fatty acyl CoA need to be conjugated with carnitine, therefore reducing the levels of carnitine and increasing those of acylcarnitines. MitoQ was able to improve this reduction in carnitine levels of HFD rats, concordantly with the improvement in CPT1A levels.

Our results show elevated levels of mitochondrial FFA and mitochondrial TGs in the heart of obese rats mainly due to an increase in saturated acids as palmitic acid (16:0) and stearic acid (18:0). MitoQ was able to ameliorate both TG and FFA levels.

In conclusion, obesity has an important impact on mitochondrial lipid profile of the heart. On the one hand, it reduces or modifies the acyl chain of some lipid classes required for a correct functioning of the mitochondria, such as CL and carnitine. On the other hand, it increases FFA, TG, phospholipids and lysophospholipids which contribute to creating a lipotoxic environment. The inhibition of mitochondrial oxidative stress in obese rats by MitoQ was able to prevent these alterations on the lipid profile suggesting, that an excess in ROS drives to mitochondrial cardiac lipid remodelling and contributes to cardiac lipotoxicity.

The changes in the mitochondrial lipid profile in the heart of obese rats, along with the increase in ROS, leads us to think that the function of mitochondria could likely be affected. We confirmed this hypothesis with the observation that proteomic analysis of the 33 proteins modified in the heart of HFD rats, as compared to control ones, 11 were localized in the mitochondria and 3 were specifically related to respiratory chain, suggesting alterations in oxidative phosphorylation, ATP production and mitochondrial function. The data showed a reduction in a subunit of the complex I, as well as an increase in a subunit of the complex III. There was also observed a reduction in Holocytochrome C Synthase (HCCS), an enzyme that covalently links a heme group to the cytochrome c, which is necessary for the electron transfer in the respiratory chain. The reduction in protein levels of complex I was confirmed by western blot and we also

Discussion

found a reduction in complex II, which had not been found in the proteomic analysis, likely because it is a more restrictive method. On the other hand, no differences were observed in the protein levels of HCCS or complex III by western blot. This discordance regarding proteomic analysis could be because the measured subunits are not the same. OXPHOS antibody cocktail allows us to assess UQCRC2 (subunit II) by Western Blot, whereas we observed differences in the UQCRQ (subunit VII) by proteomic analysis. Proteomic analysis is performed from pooling of samples. Moreover, the protein expression in a pool usually matches the mean expression of the individuals, although pool expression is sometimes different.

Complex I and II are both involved in the electron transfer to quinol. The only difference between them is that complex I transfer electrons from NADH to quinol and the energy released in the electron transfer reaction are utilized for pumping four protons from the matrix into the crista lumen, whereas complex II transfers electrons from succinate directly to quinol and does not contribute to the proton gradient¹⁹⁶. Our data suggest that obesity affects mainly the first two mitochondrial complexes by reducing the electron transfer to quinol, which is necessary for the subsequent transfer to cytochrome. In addition, as we have previously mentioned, mitochondria are the main source of ROS production since there are electron transfer steps in the electron transport chain (ETC) where electrons before reaching complex IV can escape and react with oxygen and produce ROS¹⁹⁷. Therefore, our results suggest that the alteration in complex I and II observed in obese rats may contribute to a deregulation in the electron transfer favouring ROS production. ROS, in turn, could alter complex activity by establishing a vicious circle of oxidative stress and mitochondrial respiration decline. Supporting our data, reduced protein levels of complex I and III have been reported in the heart of ob/ob mice¹¹⁶ and reduced mitochondrial respiration activity has been reported in the skeletal muscle of diabetic patients¹⁹⁸ as well as in the liver mitochondria of murine diet-induced obesity⁷⁷. Our results showed that MitoQ treatment was able to improve the reduction in both complexes in the HFD rats, suggesting that mitochondrial oxidative stress is involved in respiratory chain deficiency. Indeed, it has been previously reported that increased mitochondrial oxidative stress due to coenzyme Q₁₀ deficiency in fibroblast leads to mitochondrial bioenergetic deficiency¹⁹⁹. Conversely, another study shows activity deficiency in mitochondrial complex in the heart without

alterations in ROS levels. Therefore, further studies need to be performed in order to clarify the specific role of ROS in mitochondrial complex activity²⁰⁰.

Nevertheless, respiratory chain components are not the only ones involved in ROS formation. Enzymes of the Krebs cycle are also involved in its production, such as α -ketoglutarate dehydrogenase^{201, 202} or reduced levels of FH, which has been demonstrated to lead to fumarate accumulation and finally to ROS production²⁰³. Supporting these data, we have found decreased levels of FH in the heart of our obese rats, suggesting that this reduction could be contributing to the accumulation of fumarate and the consequent production of ROS.

Our data also showed that palmitic acid, the most abundant fatty acid found in the heart of obese rats, impaired mitochondrial function in a cell line of cardiomyoblasts (H9C2). Although no significant changes were observed in oxygen consumption (at the dose of 200 μ M PA), the proton leak was increased, thereby showing mitochondria uncoupling. In addition, extracellular acidification rate (ECAR), which is considered in the mitochondrial stress test to be a measure of glycolysis, is increased in palmitic acid stimulated cells, reflecting an attempt by the mitochondria to maintain the production of energy in these conditions. MitoQ was able to prevent the increase in proton leak and ECAR in palmitic-stimulated cells suggesting that this improvement in the mitochondrial function is due to a reduction in ROS levels.

Mitochondria are continuously changing in respond to energy request²⁰⁴. Since our data suggest that there is an energetic deficiency in the heart of obese rats due to the alterations in mitochondrial respiratory chain, we hypothesized that mitochondrial pathways involved in the response to energy shifts should be enhanced. These pathways could include both mitochondrial biogenesis and mitochondrial dynamics, which involved processes of fusion and fission. Supporting our hypothesis, we have observed increased levels of PPAR gamma co-activator 1 α (PGC1 α) in the heart of our HFD rats, a transcription coactivator that plays a key role in mitochondrial biogenesis and oxidative phosphorylation²⁰⁵. Regarding mitochondrial dynamics, we observed increased levels of MFN1 in obese rats, indicating an increase in mitochondrial fusion. Such fusion is thought to be a compensatory mechanism for trying to maintain energy metabolism, as is the case for the increase in mitochondrial biogenesis. It has thus been proposed that fusion helps sharing of mitochondrial machinery, thereby improving

Discussion

mitochondrial network by allowing healthy mitochondria to complement deficiencies of other mitochondria²⁰⁶. In addition, the levels of the mitochondrial fission protein DRP1 were unchanged in obese rats. MitoQ prevented these alterations in HFD rats, suggesting that the reduction of ROS improved mitochondrial function, and therefore the activation of alternative pathways to obtain energy, was not necessary.

Cyclophilin F has been extensively reported for its role in cell-death due to the opening of MPTP. By contrast, a recent study has mentioned a possible role in cell survival in oxidative stress conditions, showing that overexpression of CycloF in HEK293 cell line increases the membrane potential of the mitochondria and improves cell survival by the enhancement of electron transfer through the respiratory chain²⁰⁷. The authors emphasize that the results are obtained by overexpression experiments and highlight the possibility that a similar increase under pathological conditions may be used to enhance the transport of electrons through the respiratory chain in order to maintain the energy demand of the cell, as occurs in the heart of our HFD rats where CycloF levels were increased. However, we do not totally agree with this idea, since an enhancement of the electron transfer would increase the production of ROS, thereby aggravating the situation. In fact, our results showed an improvement by MitoQ, probably due to the fact that it is able to reduce ROS levels.

In addition to mitochondrial alterations, as we have shown in the previous section, the use of glucose was reduced in the heart of obese rats. MCP treatment was not able to prevent this reduction. However, MitoQ treatment ameliorated the uptake of ¹⁸F-FDG in the heart of obese rats, suggesting a role for mitochondrial oxidative stress in the alterations in the use of metabolic substrates in the context of obesity. According to these results, inhibition of mitochondrial oxidative stress was also able to improve the HOMA index that was increased in obese rats. Moreover, mitochondrial TG correlated negatively with ¹⁸F-FDG uptake in the heart of obese rats, unlike total cardiac TG levels that did not show any correlation, showing the relevance of mitochondria in the alterations in the use of metabolic substrate in obese rats.

In summary, our results show that the mitochondrial oxidative stress inhibition by MitoQ treatment was able to prevent cardiac fibrosis and hypertrophy, thereby demonstrating a role for oxidative stress in the alterations in cardiac structure in the context of obesity. The reduction in the levels of the fatty acid transporters observed in

the obese rats treated with MitoQ was accompanied by an improvement in the alterations of the mitochondrial lipid profile, suggesting that ROS reduction ameliorated cardiac lipotoxicity in obese rats. Moreover, alterations in mitochondrial proteins, such as respiratory chain complex and Krebs cycle enzymes, as well as those involved in mitochondrial biogenesis and dynamics, were also ameliorated by MitoQ. Indeed, glucose uptake by the heart in obese rats was improved by MitoQ showing the role of oxidative stress in glucose homeostasis. Therefore, our results showed that MitoQ was able to improve mitochondrial alterations and modification in the use of metabolic substrates in the heart of obese rats, supporting a role for mitochondrial oxidative stress in the cardiometabolic alterations associated with obesity prior to cardiac dysfunction.

III. ROLE OF OXIDATIVE STRESS ON ADIPOSE TISSUE REMODELING IN OBESITY

An aspect that we have to take into consideration is the reduction of body weight observed in the HFD rats treated with MitoQ. HFD rats presented a reduction in food intake as compared to control ones probably due to the satiating effect of a HFD. However, in spite of the food intake reduction, the body weight and adiposity index were higher in HFD rats than CT rats. HFD+MQ group presented the same values of food intake than HFD. Therefore, the reduction in body weight observed in HFD+MQ rats should involve other modifications which are not present in HFD rats.

Given that a minor food intake seems not to be the cause of the decreased body weight, the need to propose some mechanism by which MitoQ may be acting on body weight reduction arises. One of the characteristics of MitoQ, which has been developed mainly for antioxidant purposes, is its role as mitochondrial uncoupling²⁰⁸, which means a loss of coupling between the rate electron transport in the respiratory chain and ATP production. Therefore, uncoupling is considered to be an energy-dissipating pathway, which increases non-productive energy expenditure in mitochondria²⁰⁹. We have thus hypothesized that MitoQ may be acting at this level by increasing non-productive energy expenditure which would contribute to a reduction in body weight.

The process of uncoupling is mediated by uncoupling proteins (UCPs), membrane integral proteins that function as transporters allowing proton leak and altering proton gradient necessary to ATP production²¹⁰. The first UCP discovered was UCP1, found in

Discussion

the mitochondria of brown adipose tissue²¹⁰. This is why browning, the phenomenon that refers to the transdifferentiation of white adipocytes into brown adipocytes, whose main characteristic is the appearance of UCP-1 positive adipocytes within WAT deposits, has recently become an attractive target for counteracting the adverse metabolic consequences of obesity¹⁴⁶. Therefore, we hypothesized that browning could be responsible for the body weight reduction observed in obese rats treated with mitoQ. We measured UCP1 mRNA expression in the epididymal adipose tissue but, surprisingly, UCP1 was not expressed in any of the groups. These results surprised us due to the numerous studies in mice that propose a role for browning as a means of counteracting the effects of obesity^{211, 212}. However, a study performed by Oliver P. in 2001²¹³ showed a rare and occasional pattern of mRNA expression of UCP1 in the different depots of WAT in rats. Regarding epididymal and inguinal adipose tissue, they found expression of UCP1 in 10-month adult rats. However, a more detailed study at different ages showed expression of UCP1 in suckling rats (at 18 days) and adult rats (from 7 months on), without expression between these two periods of time. This study confirms our results regarding epididymal adipose tissue not expressing UCP1, taking into account that the rats used in our experiment are approximately two-and-a-half months old. In conclusion, browning is not involved in the reduction of body weight in the HFD rats treated with MitoQ, thus prompting the need to find another mechanism that could be involved.

On the other hand, considering the findings regarding cardiac metabolic alterations and knowing the role that the adipose tissue remodelling plays in metabolic disorders such as insulin resistance, we decided to explore in depth the alterations occurring in the epididymal adipose tissue of the obesity diet-induced animal model treated with MitoQ. The adipose tissue is a metabolic organ involved in the regulation of whole-body energy homeostasis by acting as a caloric reservoir. During conditions of overconsumption of nutrients, such as occurs in obesity, adipose tissue stores the excess nutrients as TG and during situations of nutrient deficient conditions release these fatty acids stored through lipolysis²¹⁴. Therefore, in response to nutrient availability, the adipose tissue undergoes dynamic remodelling, including quantitative and qualitative alterations in adipocytes²¹⁴. In pathological situations such as obesity, chronic overnutrition triggers uncontrolled adipose tissue remodelling, leading to metabolic disorders, such as insulin resistance¹²⁷.

One of the characteristics of adipose tissue remodelling is the adipose tissue expansion that could be mediated by hyperplasia (increased numbers of adipocytes), hypertrophy (enlarged adipocytes) or both. Accordingly, our results showed enlarged adipocytes in the epididymal adipose tissue of our HFD rats indicating, adipocyte hypertrophy and therefore adipose tissue remodelling in obese rats.

Several studies suggest that an excess of fibrosis restrict the capacity of the adipocytes to store lipids leading to ectopic deposition of fat in other tissues¹³³⁻¹³⁵. In accordance with this, our results showed ectopic deposition of fat in the heart of obese rats, suggesting that the adipose tissue remodelling that contributes to fibrosis could be one of the causes of the ectopic deposition of fat in HFD rats.

As we have mentioned before, hypertrophic adipocytes are characterized by enlarged adipocytes that could be consequence of an internal accumulation of fatty acids. This leads us to think that one of the mechanisms by which this accumulation could occur is through an increase in the fatty acid uptake by the cell due to an increase in the fatty acid transporter; hence we expected an increase in CD36 but our results surprisingly showed the opposite. The CD36 protein levels in the epididymal adipose tissue of our HFD rats were reduced as compared with controls. There is a study that shows reduced expression of genes involved in FA trafficking in abdominal adipose tissue of obese patients; however, the only gene of all those measured that was not significantly reduced was CD36, although it also showed a tendency to diminish despite not reaching statistical significance¹³⁵. One of the causes of this difference regarding CD36 between this study and our results may be due to the fact that they measured mRNA levels and we measured protein levels. There are other studies suggesting that lower CD36 expression in adipose tissue is metabolically protective²¹⁵. Taking these data as a whole, we surmised that the reduction in CD36 expression could be a protection mechanism of the adipocyte to counteract the intracellular accumulation of fatty acid. Both a decrease in fatty acid uptake by the cell and an increase in fatty acid oxidation may be used by the cell as protective mechanism. In fact, we observed in support of this idea increased levels of CPT1A in the epididymal adipose tissue of HFD rats, which allow the entrance of fatty acids inside the mitochondria to subsequently be oxidized. MitoQ partially reduced the levels of CPT1A in HFD rats, although this had no effect on CD36 protein levels. The exact role of the oxidation of fatty acids in adipose tissue has not yet been elucidated. On the other hand, beneficial effects of FA oxidation through the

Discussion

overexpression of CPT1A have been proposed, since such overexpression improves insulin sensitivity and inflammation^{216, 217}. However, whether the increase in FA oxidation may contribute to reduce the fatty acid-induced ROS production remains unclear. Further studies need to be performed to clarify the role of fatty acid transporters in adipose tissue in the context of obesity.

As we have previously mentioned, the obese rats presented systemic insulin resistance as shown by the increase in HOMA index, which improved in the obese rats treated with MitoQ. In accordance with this, our results showed a deregulation in proteins involved in insulin signalling pathway in the epididymal adipose tissue of HFD rats, as suggested by an increase in the phosphorylation of insulin receptor substrate 1 (IRS1), as well as a decrease in the levels of GLUT4, responsible for the insulin-dependent glucose uptake in the cell. Our data are supported by numerous studies demonstrating that increased serine phosphorylation of IRS1 results in diminished glucose uptake and utilization leading to insulin resistance due to the reduced capacity of phosphorylated IRS1 to activate PI3K²¹⁸ and due to the accelerated capacity to degraded the IRS1 protein itself²¹⁹. We also observed increased levels of suppressor of cytokine signalling 3 (SOCS3) in the epididymal adipose tissue of our HFD rats, which is known to bind to IRS1 and thereby promoting its ubiquitination and degradation²²⁰. We also observed reduced levels of glucagon like peptide 1 (GLP1) in the epididymal adipose tissue of HFD rats, which is an incretin secreted after meals that induces insulin secretion to regulate postprandial glucose levels, as well as increased levels of dipeptidil peptidasa-4 (DDP4), which is in turn responsible for the degradation of GLP1. Therefore, the increase in DDP4 and the consequent reduction in GLP1 both contribute to the development of insulin resistance. As Figure 59 shows, insulin resistance observed in HFD rats involved alterations at different levels. MitoQ was able to prevent all these alterations in HFD rats suggesting that mitochondrial oxidative stress is involved in the development of insulin resistance. This is supported by a study that suggests that the superoxide originating as byproduct of electron transport through respiratory chain activates the uncoupling UCP2 protein that triggers proton leak in the mitochondria, thereby resulting in reduced glucose uptake by the mitochondria and impairing the glucose-dependent insulin secretion²²¹. For this reason, the study performed by Lowell suggests that insulin resistance is in part, due to mitochondrial dysfunction. Taking this study together with our results, we hypothesize that MitoQ

could be able to ameliorate mitochondrial function through its capacity to reduced superoxide levels, and consequently curtail insulin resistance, as well.

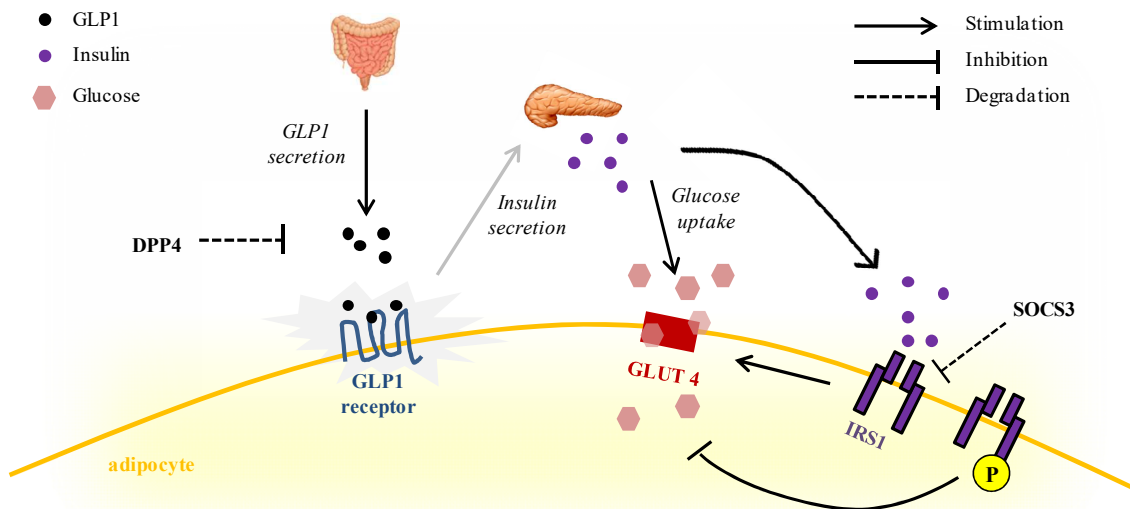


Figure 59. Representative scheme of proteins involved in insulin signalling pathway in the epididymal adipose tissue of obese rats. GLP1, glucagon like peptide-1; DPP4, dipeptidyl peptidase 4; GLUT4, glucose transporter 4; IRS1, insulin receptor substrate 1; SOCS3, suppressor of cytokine signaling 3.

Supporting our hypothesis, we have observed altered mitochondrial proteins in the epididymal adipose tissue of the HFD rats, as compared to controls that may trigger mitochondrial dysfunction. Our results showed a reduction in the mitochondrial complex protein levels I, II and IV and an increase in the complex V of the epididymal adipose tissue from HFD rats as compared to controls. Confirming our results, previous studies have reported that obesity modifies respiratory chain complexes both, at protein²²² and activity levels²⁰⁰, altering oxidative phosphorylation (OXPHOS). This alteration in OXPHOS could facilitate the production of more ROS and thus accelerating the mitochondrial and adipocyte dysfunction. On the other hand, we also found reduced protein levels of MFN1 in the epididymal adipose tissue of HFD rats. Regarding white adipose tissue little has been studied regarding MFN1 but there is a study carried out by Meng-Ting Wu and colleagues²²³ showing that high fat diet in mice decreased MFN1 mRNA levels in inguinal white adipose tissue but not in epididymal

Discussion

white adipose tissue. The difference regarding MFN1 levels in epididymal adipose tissue between this study and our experiment could be due to the difference in diet duration (5 weeks instead of 6) or because of the percentage of fat (23% instead of 35%) as well as due to the different technique (mRNA measurement instead of protein levels) which was employed. Our results also showed that cycloF was increased in the adipose tissue of HFD rat model facilitating the opening of the mPTP and thereby accelerating adipocyte dysfunction and facilitating cell death. In those animals treated with MitoQ the protein levels of CycloF were reduced until normal levels, which suggests an improvement in the mitochondrial function. Moreover, we observed a reduction in FH, which, as mentioned before, causes the accumulation of fumarate and the production of ROS. MitoQ was able to prevent the increase in complex V, although it had no effect on the rest of the complex in addition to ameliorated MFN1, CycloF and FH protein levels. All these improvements, could contribute to an improvements, in mitochondrial function and consequently in insulin resistance.

We suggest that the improvement by MitoQ is due to a reduction in ROS levels. However, we were not able to measure ROS levels in the epididymal adipose tissue with the DHE technique as we did with the heart due to tissue characteristics, we measured other markers of oxidative stress in order to assess the efficiency of MitoQ in reducing ROS in the epididymal adipose tissue. First of all, we measured 4-HNE, a product of lipid peroxidation that appeared to rise in situations of overproduction of ROS and is directly related to mitochondria dysfunction²²⁴. As we expected, 4-HNE was increased in the epididymal adipose tissue of our HFD rats and this increase was prevented by MitoQ. Since increased oxidative stress could be due to both an increase in ROS production or a reduction in the antioxidant defense. We also assessed the levels of PRDX4, an antioxidant enzyme that we found diminished in the epididymal adipose tissue of obese rats promoting an imbalance between ROS production and scavenging, favoring the increase in ROS levels. Supporting our data, the ATTICA study assessed the association between obesity and total serum antioxidant capacity (TAC) in 3042 adults (1514 men and 1528 women with an age between 18-89 years old) and found reduced TAC in both, obese and overweight men and female as compared to healthy patients²²⁵. Moreover, PRDX4 has been also associated with the maintenance of the redox potential of the ER lumen²²⁶. In fact, PDIA6, a marker of ER stress that function as a chaperone that inhibits aggregation of misfolded proteins²²⁷ and that negatively

regulates the unfolded protein response (UPR)²²⁸, was increased in the epididymal adipose tissue of HFD rats. Both, PRDX4 and PDIA6 levels were ameliorated by MitoQ, suggesting an improvement in the oxidant environment of the cell.

In summary, obesity exerts a negative impact on epididymal adipose tissue through the increase in ROS, thereby resulting in adipose tissue remodelling and mitochondrial dysfunction that favors insulin resistance in obese rats.

To obtain a clinical perspective of our animal results, a group of obese patients with insulin resistance undergoing bariatric surgery was selected. These patients were an ideal study group to compare with the HFD-induced obesity rat model used in our experiments, since these patients (like the rats) were insulin resistant but they are not diabetic. To extrapolate the results obtained with the animal model to humans, we evaluated the visceral adipose tissue of these patients, which was obtained from bariatric surgery.

The obese patients presented adipocyte hypertrophy as indicated by the increased size of the adipocyte that was accompanied by an increase in pericellular fibrosis. These data revealed that an adipose tissue remodelling also occurs in the context of obesity in humans. As we have previously mentioned, adipose tissue fibrosis is associated with limited capacity of the adipocytes to store lipid excess, which may contribute to ectopic fat deposition and cardiometabolic alterations. In fact, the patients of our study show higher epicardial fat before bariatric surgery than after bariatric surgery, which was accompanied by a reduction in BMI (unpublished data). Supporting our hypothesis, a study performed by Levelt et al, showed cardiac and hepatic fat deposition in diabetic subjects that was more pronounced in obese-diabetic subjects than in lean-diabetic subjects, thus showing the association between obesity and ectopic fat deposition²²⁹. Another study showed that obese patients with a BMI > 30 kg/m² presented liver and pancreatic fat deposition, with the visceral adipose tissue size being the main predictor of ectopic fat deposition²³⁰.

Adipose tissue is an endocrine tissue in which there is a dysregulation of adipokines production/secretion in obesity. In this regard, we observed in obese patients in the present study an increase in leptin circulating levels accompanied by a decrease in adiponectin ones. Previous studies in our group have demonstrated the potential role of leptin in fibrotic process in the cardiovascular system^{33,231}. In addition, the circulating

Discussion

levels of MMP-9 which is involved in ECM degradation were altered in obese patients. Our group has also demonstrated that inflammation contributes to cardiovascular remodelling¹⁸. Regarding inflammation, the obese patients showed increased levels of the inflammatory cytokines IL-1 β , IL-6 and TNF α as compared to controls. Moreover, the marker of oxidative stress MPO was also increased in obese patients. Taken together, these results reveal alterations in fibrosis, inflammation and oxidative stress. All of these mechanisms have been demonstrated to contribute to cardiovascular alterations associated with obesity^{18, 231}.

A proteomic study showed that in adipose tissue 23 of 53 mitochondrial proteins identified in the analysis were altered in obese patients as compared with control ones. Moreover, most of the altered mitochondrial proteins were associated with FA oxidation, Krebs cycle and OXPHOS, which all suggest mitochondrial dysfunction in the adipose tissue of these patients. In agreement with our data, some studies have also reported mitochondrial dysfunction in adipose tissue of obese patients. The recent study performed by Urbanova et al, has shown reduced mRNA expression of most of the mitochondrial genes measured as well as decreased activity of respiratory chain enzymatic complexes in the subcutaneous adipose tissue of obese subjects and obese subjects with type 2 diabetes mellitus²³². Moreover, mitochondrial dysfunction in adipose tissue has also been reported in childhood obesity by Zamora-Mendoza et al, showing altered mitochondrial biogenesis and structure in the abdominal adipose tissue of obese children (8-12 years old; percentile ≥ 95)²³³.

The proteomic results also showed reduced levels of adiponectin in the visceral adipose tissue of obese patients in accordance with the reduction in adiponectin observed by western blot in the epididymal adipose tissue of rats, suggesting a deregulation in glucose levels that triggers insulin resistance.

In a previous study of the group it has been demonstrated that inflammation markers, enhanced by Gal-3, were involved in adipose tissue remodelling in HFD rats²³⁴. Although we have not measured Gal-3 and inflammation marker levels in the visceral adipose tissue of obese patients, the increased levels observed in plasma suggest that an adipose tissue remodelling in obese patients may be driven by Gal-3 and inflammation. Moreover, we have also observed in plasma of obese patients increased levels of MPO, a marker of oxidative stress that along with Gal-3 and inflammation could regulate the

adipose tissue remodelling and cardiovascular alterations in the context of obesity. Supporting these data observed in obese patients, it has been demonstrated in previous studies of the group that Gal-3, inflammation and oxidative stress are important mechanisms underlying cardiovascular remodelling in HFD rats¹⁸.

Therefore, these results reveal how most of the alterations observed in the epididymal adipose tissue of obese rats are also reflected in adipose tissue of obese patients suggesting the translationality of our results.

In summary, this study highlights the role of mitochondrial dysfunction in the development of cardiac lipotoxicity and metabolic alterations associated with obesity and pointing out ROS as the main cause of that mitochondrial dysfunction. Therefore, we propose targeting mitochondrial oxidative stress as a possible therapeutic approach in obesity-induced cardiometabolic alterations.

Conclusions

1. Obesity is associated with cardiac lipotoxicity which not only involve lipid accumulation but also remodelling of different lipid species that is associated with metabolic changes and the development of cardiac fibrosis.
2. Gal-3 is able to modulate cardiac lipotoxicity in the context of obesity through its capacity to induce mitochondrial damage and thereby increasing oxidative stress.
3. Mitochondrial ROS plays a role in the cardiac structure alterations observed in obese rats characterized by interstitial fibrosis and cardiac hypertrophy, early events prior to cardiac dysfunction.
4. Mitochondrial ROS is involved in the cardiac metabolic substrate use modification in obese rats.
5. Mitochondrial ROS facilitates the remodelling of adipose tissue which participates in the metabolic alterations associated with obesity.
6. The metabolic alterations observed in obese patients were accompanied by similar mitochondrial alterations in the adipose tissue to those found in obese rats, thus supporting the clinical relevance of our findings.

The conglomeration of results present in this study suggests that lipotoxicity through mitochondrial oxidative stress plays a central role in the cardiometabolic alterations associated with obesity.

Bibliography

1. Global BMIMC, Di Angelantonio E, Bhupathiraju Sh N, Wormser D, Gao P, Kaptoge S, Berrington de Gonzalez A, Cairns BJ, Huxley R, Jackson Ch L, Joshy G, Lewington S, Manson JE, Murphy N, Patel AV, Samet JM, Woodward M, Zheng W, Zhou M, Bansal N, Barricarte A, Carter B, Cerhan JR, Smith GD, Fang X, Franco OH, Green J, Halsey J, Hildebrand JS, Jung KJ, Korda RJ, McLerran DF, Moore SC, O'Keefe LM, Paige E, Ramond A, Reeves GK, Rolland B, Sacerdote C, Sattar N, Sofianopoulou E, Stevens J, Thun M, Ueshima H, Yang L, Yun YD, Willeit P, Banks E, Beral V, Chen Z, Gapstur SM, Gunter MJ, Hartge P, Jee SH, Lam TH, Peto R, Potter JD, Willett WC, Thompson SG, Danesh J, Hu FB. Body-mass index and all-cause mortality: individual-participant-data meta-analysis of 239 prospective studies in four continents. *Lancet*. 2016;388:776-786.
2. Nakamura M, Sadoshima J. Mechanisms of physiological and pathological cardiac hypertrophy. *Nat Rev Cardiol*. 2018;15:387-407.
3. Iacobellis G. True uncomplicated obesity is not related to increased left ventricular mass and systolic dysfunction. *J Am Coll Cardiol*. 2004;44:2257; author reply 2258.
4. Iacobellis G, Ribaldo MC, Zappaterreno A, Iannucci CV, Di Mario U, Leonetti F. Adapted changes in left ventricular structure and function in severe uncomplicated obesity. *Obes Res*. 2004;12:1616-1621.
5. Avelar E, Cloward TV, Walker JM, Farney RJ, Strong M, Pendleton RC, Segerson N, Adams TD, Gress RE, Hunt SC, Litwin SE. Left ventricular hypertrophy in severe obesity: interactions among blood pressure, nocturnal hypoxemia, and body mass. *Hypertension*. 2007;49:34-39.
6. Berkalp B, Cesur V, Corapcioglu D, Erol C, Baskal N. Obesity and left ventricular diastolic dysfunction. *Int J Cardiol*. 1995;52:23-26.
7. de Simone G, Devereux RB, Roman MJ, Alderman MH, Laragh JH. Relation of obesity and gender to left ventricular hypertrophy in normotensive and hypertensive adults. *Hypertension*. 1994;23:600-606.
8. de Simone G, Daniels SR, Devereux RB, Meyer RA, Roman MJ, de Divitiis O, Alderman MH. Left ventricular mass and body size in normotensive children and adults: assessment of allometric relations and impact of overweight. *J Am Coll Cardiol*. 1992;20:1251-1260.
9. Luaces M, Cachafeiro V, Garcia-Munoz-Najar A, Medina M, Gonzalez N, Cancer E, Rodriguez-Robles A, Canovas G, Antequera-Perez A. Anatomical and

Bibliography

functional alterations of the heart in morbid obesity. Changes after bariatric surgery. *Rev Esp Cardiol (Engl Ed)*. 2012;65:14-21.

10. Alpert MA, Terry BE, Mulekar M, Cohen MV, Massey CV, Fan TM, Panayiotou H, Mukerji V. Cardiac morphology and left ventricular function in normotensive morbidly obese patients with and without congestive heart failure, and effect of weight loss. *Am J Cardiol*. 1997;80:736-740.

11. Turkbey EB, McClelland RL, Kronmal RA, Burke GL, Bild DE, Tracy RP, Arai AE, Lima JA, Bluemke DA. The impact of obesity on the left ventricle: the Multi-Ethnic Study of Atherosclerosis (MESA). *JACC Cardiovasc Imaging*. 2010;3:266-274.

12. Di Tullio MR, Zwas DR, Sacco RL, Sciacca RR, Homma S. Left ventricular mass and geometry and the risk of ischemic stroke. *Stroke*. 2003;34:2380-2384.

13. Wong CY, O'Moore-Sullivan T, Leano R, Hukins C, Jenkins C, Marwick TH. Association of subclinical right ventricular dysfunction with obesity. *J Am Coll Cardiol*. 2006;47:611-616.

14. Antonini-Canterin F, Di Nora C, Poli S, Sparacino L, Cosei I, Ravasel A, Popescu AC, Popescu BA. Obesity, Cardiac Remodeling, and Metabolic Profile: Validation of a New Simple Index beyond Body Mass Index. *J Cardiovasc Echogr*. 2018;28:18-25.

15. Toblli JE, Cao G, DeRosa G, Forcada P. Reduced cardiac expression of plasminogen activator inhibitor 1 and transforming growth factor beta1 in obese Zucker rats by perindopril. *Heart*. 2005;91:80-86.

16. Cittadini A, Mantzoros CS, Hampton TG, Travers KE, Katz SE, Morgan JP, Flier JS, Douglas PS. Cardiovascular abnormalities in transgenic mice with reduced brown fat: an animal model of human obesity. *Circulation*. 1999;100:2177-2183.

17. Zaman AK, Fujii S, Goto D, Furumoto T, Mishima T, Nakai Y, Dong J, Imagawa S, Sobel BE, Kitabatake A. Salutary effects of attenuation of angiotensin II on coronary perivascular fibrosis associated with insulin resistance and obesity. *J Mol Cell Cardiol*. 2004;37:525-535.

18. Martinez-Martinez E, Lopez-Andres N, Jurado-Lopez R, Rousseau E, Bartolome MV, Fernandez-Celis A, Rossignol P, Islas F, Antequera A, Prieto S, Luaces M, Cachofeiro V. Galectin-3 Participates in Cardiovascular Remodeling Associated With Obesity. *Hypertension*. 2015;66:961-969.

19. Alpert MA, Agrawal H, Aggarwal K, Kumar SA, Kumar A. Heart failure and obesity in adults: pathophysiology, clinical manifestations and management. *Curr Heart Fail Rep.* 2014;11:156-165.
20. Ng ACT, Prevedello F, Dolci G, Roos CJ, Djaberi R, Bertini M, Ewe SH, Allman C, Leung DY, Marsan NA, Delgado V, Bax JJ. Impact of Diabetes and Increasing Body Mass Index Category on Left Ventricular Systolic and Diastolic Function. *J Am Soc Echocardiogr.* 2018.
21. Alpert MA, Lambert CR, Terry BE, Cohen MV, Mulekar M, Massey CV, Hashimi MW, Panayiotou H, Mukerji V. Effect of weight loss on left ventricular diastolic filling in morbid obesity. *Am J Cardiol.* 1995;76:1198-1201.
22. Kurnicka K, Domienik-Karłowicz J, Lichodziejewska B, Bielecki M, Kozłowska M, Goliszek S, Dzikowska-Diduch O, Lisik W, Kosieradzki M, Pruszczyk P. Improvement of left ventricular diastolic function and left heart morphology in young women with morbid obesity six months after bariatric surgery. *Cardiol J.* 2018;25:97-105.
23. Ghandi Y, Sharifi M, Habibi D, Dorreh F, Hashemi M. Evaluation of left ventricular function in obese children without hypertension by a tissue Doppler imaging study. *Ann Pediatr Cardiol.* 2018;11:28-33.
24. Gulel O, Yuksel S, Soylu K, Kaplan O, Yilmaz O, Kahraman H, Sahin M. Evaluation of left atrial functions by color tissue Doppler imaging in adults with body mass indexes ≥ 30 kg/m² versus those < 30 kg/m². *Int J Cardiovasc Imaging.* 2009;25:371-377.
25. Otto ME, Belohlavek M, Khandheria B, Gilman G, Svatikova A, Somers V. Comparison of right and left ventricular function in obese and nonobese men. *Am J Cardiol.* 2004;93:1569-1572.
26. Buchanan J, Mazumder PK, Hu P, Chakrabarti G, Roberts MW, Yun UJ, Cooksey RC, Litwin SE, Abel ED. Reduced cardiac efficiency and altered substrate metabolism precedes the onset of hyperglycemia and contractile dysfunction in two mouse models of insulin resistance and obesity. *Endocrinology.* 2005;146:5341-5349.
27. Semeniuk LM, Kryski AJ, Severson DL. Echocardiographic assessment of cardiac function in diabetic db/db and transgenic db/db-hGLUT4 mice. *Am J Physiol Heart Circ Physiol.* 2002;283:H976-982.
28. Yue P, Arai T, Terashima M, Sheikh AY, Cao F, Charo D, Hoyt G, Robbins RC, Ashley EA, Wu J, Yang PC, Tsao PS. Magnetic resonance imaging of progressive

Bibliography

cardiomyopathic changes in the db/db mouse. *Am J Physiol Heart Circ Physiol*. 2007;292:H2106-2118.

29. Nguyen S, Shao D, Tomasi LC, Braun A, de Mattos ABM, Choi YS, Villet O, Roe N, Halterman CR, Tian R, Kolwicz SC, Jr. The effects of fatty acid composition on cardiac hypertrophy and function in mouse models of diet-induced obesity. *J Nutr Biochem*. 2017;46:137-142.

30. Shoulders MD, Raines RT. Collagen structure and stability. *Annu Rev Biochem*. 2009;78:929-958.

31. Cavalera M, Wang J, Frangogiannis NG. Obesity, metabolic dysfunction, and cardiac fibrosis: pathophysiological pathways, molecular mechanisms, and therapeutic opportunities. *Transl Res*. 2014;164:323-335.

32. Gutierrez-Tenorio J, Marin-Royo G, Martinez-Martinez E, Martin R, Miana M, Lopez-Andres N, Jurado-Lopez R, Gallardo I, Luaces M, San Roman JA, Gonzalez-Amor M, Salaices M, Nieto ML, Cachofeiro V. The role of oxidative stress in the crosstalk between leptin and mineralocorticoid receptor in the cardiac fibrosis associated with obesity. *Sci Rep*. 2017;7:16802.

33. Martinez-Martinez E, Jurado-Lopez R, Valero-Munoz M, Bartolome MV, Ballesteros S, Luaces M, Briones AM, Lopez-Andres N, Miana M, Cachofeiro V. Leptin induces cardiac fibrosis through galectin-3, mTOR and oxidative stress: potential role in obesity. *J Hypertens*. 2014;32:1104-1114; discussion 1114.

34. Liu Y, Xiao Y, Liu J, Feng L, Kang YJ. Copper-induced reduction in myocardial fibrosis is associated with increased matrix metalloproteins in a rat model of cardiac hypertrophy. *Metallomics*. 2018;10:201-208.

35. Sciacchitano S, Lavra L, Morgante A, Ulivieri A, Magi F, De Francesco GP, Bellotti C, Salehi LB, Ricci A. Galectin-3: One Molecule for an Alphabet of Diseases, from A to Z. *Int J Mol Sci*. 2018;19.

36. Kim H, Lee J, Hyun JW, Park JW, Joo HG, Shin T. Expression and immunohistochemical localization of galectin-3 in various mouse tissues. *Cell Biol Int*. 2007;31:655-662.

37. Writing Committee M, Yancy CW, Jessup M, Bozkurt B, Butler J, Casey DE, Jr., Drazner MH, Fonarow GC, Geraci SA, Horwich T, Januzzi JL, Johnson MR, Kasper EK, Levy WC, Masoudi FA, McBride PE, McMurray JJ, Mitchell JE, Peterson PN, Riegel B, Sam F, Stevenson LW, Tang WH, Tsai EJ, Wilkoff BL, American College of Cardiology Foundation/American Heart Association Task Force on Practice

- G. 2013 ACCF/AHA guideline for the management of heart failure: a report of the American College of Cardiology Foundation/American Heart Association Task Force on practice guidelines. *Circulation*. 2013;128:e240-327.
38. Sharma UC, Pokharel S, van Brakel TJ, van Berlo JH, Cleutjens JP, Schroen B, Andre S, Crijns HJ, Gabius HJ, Maessen J, Pinto YM. Galectin-3 marks activated macrophages in failure-prone hypertrophied hearts and contributes to cardiac dysfunction. *Circulation*. 2004;110:3121-3128.
39. Calvier L, Miana M, Reboul P, Cachofeiro V, Martinez-Martinez E, de Boer RA, Poirier F, Lacolley P, Zannad F, Rossignol P, Lopez-Andres N. Galectin-3 mediates aldosterone-induced vascular fibrosis. *Arterioscler Thromb Vasc Biol*. 2013;33:67-75.
40. Martinez-Martinez E, Ibarrola J, Calvier L, Fernandez-Celis A, Leroy C, Cachofeiro V, Rossignol P, Lopez-Andres N. Galectin-3 Blockade Reduces Renal Fibrosis in Two Normotensive Experimental Models of Renal Damage. *PLoS One*. 2016;11:e0166272.
41. Nangia-Makker P, Hogan V, Honjo Y, Baccarini S, Tait L, Bresalier R, Raz A. Inhibition of human cancer cell growth and metastasis in nude mice by oral intake of modified citrus pectin. *J Natl Cancer Inst*. 2002;94:1854-1862.
42. Glinsky VV, Raz A. Modified citrus pectin anti-metastatic properties: one bullet, multiple targets. *Carbohydr Res*. 2009;344:1788-1791.
43. Engin AB. What Is Lipotoxicity? *Adv Exp Med Biol*. 2017;960:197-220.
44. Zlobine I, Gopal K, Ussher JR. Lipotoxicity in obesity and diabetes-related cardiac dysfunction. *Biochim Biophys Acta*. 2016;1861:1555-1568.
45. Lee Y, Hirose H, Ohneda M, Johnson JH, McGarry JD, Unger RH. Beta-cell lipotoxicity in the pathogenesis of non-insulin-dependent diabetes mellitus of obese rats: impairment in adipocyte-beta-cell relationships. *Proc Natl Acad Sci U S A*. 1994;91:10878-10882.
46. Holland WL, Brozinick JT, Wang LP, Hawkins ED, Sargent KM, Liu Y, Narra K, Hoehn KL, Knotts TA, Siesky A, Nelson DH, Karathanasis SK, Fontenot GK, Birnbaum MJ, Summers SA. Inhibition of ceramide synthesis ameliorates glucocorticoid-, saturated-fat-, and obesity-induced insulin resistance. *Cell Metab*. 2007;5:167-179.

Bibliography

47. Shimabukuro M, Higa M, Zhou YT, Wang MY, Newgard CB, Unger RH. Lipoapoptosis in beta-cells of obese prediabetic fa/fa rats. Role of serine palmitoyltransferase overexpression. *J Biol Chem*. 1998;273:32487-32490.
48. Ussher JR, Koves TR, Cadete VJ, Zhang L, Jaswal JS, Swyrd SJ, Lopaschuk DG, Proctor SD, Keung W, Muoio DM, Lopaschuk GD. Inhibition of de novo ceramide synthesis reverses diet-induced insulin resistance and enhances whole-body oxygen consumption. *Diabetes*. 2010;59:2453-2464.
49. Choi CS, Savage DB, Abu-Elheiga L, Liu ZX, Kim S, Kulkarni A, Distefano A, Hwang YJ, Reznick RM, Codella R, Zhang D, Cline GW, Wakil SJ, Shulman GI. Continuous fat oxidation in acetyl-CoA carboxylase 2 knockout mice increases total energy expenditure, reduces fat mass, and improves insulin sensitivity. *Proc Natl Acad Sci U S A*. 2007;104:16480-16485.
50. Chiu HC, Kovacs A, Ford DA, Hsu FF, Garcia R, Herrero P, Saffitz JE, Schaffer JE. A novel mouse model of lipotoxic cardiomyopathy. *J Clin Invest*. 2001;107:813-822.
51. Liu L, Shi X, Bharadwaj KG, Ikeda S, Yamashita H, Yagyu H, Schaffer JE, Yu YH, Goldberg IJ. DGAT1 expression increases heart triglyceride content but ameliorates lipotoxicity. *J Biol Chem*. 2009;284:36312-36323.
52. Kraegen EW, Bruce C, Hegarty BD, Ye JM, Turner N, Cooney G. AMP-activated protein kinase and muscle insulin resistance. *Front Biosci (Landmark Ed)*. 2009;14:4658-4672.
53. Taegtmeyer H, McNulty P, Young ME. Adaptation and maladaptation of the heart in diabetes: Part I: general concepts. *Circulation*. 2002;105:1727-1733.
54. Marin-Royo G, Martinez-Martinez E, Gutierrez B, Jurado-Lopez R, Gallardo I, Montero O, Bartolome MV, Roman JAS, Salaices M, Nieto ML, Cachofeiro V. The impact of obesity in the cardiac lipidome and its consequences in the cardiac damage observed in obese rats. *Clin Investig Arterioscler*. 2018;30:10-20.
55. Song X, Qian X, Shen M, Jiang R, Wagner MB, Ding G, Chen G, Shen B. Protein kinase C promotes cardiac fibrosis and heart failure by modulating galectin-3 expression. *Biochim Biophys Acta*. 2015;1853:513-521.
56. Connelly KA, Kelly DJ, Zhang Y, Prior DL, Advani A, Cox AJ, Thai K, Krum H, Gilbert RE. Inhibition of protein kinase C-beta by ruboxistaurin preserves cardiac function and reduces extracellular matrix production in diabetic cardiomyopathy. *Circ Heart Fail*. 2009;2:129-137.

57. Adebisi OA, Adebisi OO, Owira PM. Naringin Reduces Hyperglycemia-Induced Cardiac Fibrosis by Relieving Oxidative Stress. *PLoS One*. 2016;11:e0149890.
58. George M, Vijayakumar A, Dhanesh SB, James J, Shivakumar K. Molecular basis and functional significance of Angiotensin II-induced increase in Discoidin Domain Receptor 2 gene expression in cardiac fibroblasts. *J Mol Cell Cardiol*. 2016;90:59-69.
59. Ganesan V, Perera MN, Colombini D, Datskovskiy D, Chadha K, Colombini M. Ceramide and activated Bax act synergistically to permeabilize the mitochondrial outer membrane. *Apoptosis*. 2010;15:553-562.
60. Gudz TI, Tserng KY, Hoppel CL. Direct inhibition of mitochondrial respiratory chain complex III by cell-permeable ceramide. *J Biol Chem*. 1997;272:24154-24158.
61. Yu J, Novgorodov SA, Chudakova D, Zhu H, Bielawska A, Bielawski J, Obeid LM, Kindy MS, Gudz TI. JNK3 signaling pathway activates ceramide synthase leading to mitochondrial dysfunction. *J Biol Chem*. 2007;282:25940-25949.
62. Di Paola M, Cocco T, Lorusso M. Ceramide interaction with the respiratory chain of heart mitochondria. *Biochemistry*. 2000;39:6660-6668.
63. Wang X, Rao RP, Kosakowska-Cholody T, Masood MA, Southon E, Zhang H, Berthet C, Nagashim K, Veenstra TK, Tessarollo L, Acharya U, Acharya JK. Mitochondrial degeneration and not apoptosis is the primary cause of embryonic lethality in ceramide transfer protein mutant mice. *J Cell Biol*. 2009;184:143-158.
64. Garcia-Ruiz C, Colell A, Mari M, Morales A, Fernandez-Checa JC. Direct effect of ceramide on the mitochondrial electron transport chain leads to generation of reactive oxygen species. Role of mitochondrial glutathione. *J Biol Chem*. 1997;272:11369-11377.
65. Kogot-Levin A, Saada A. Ceramide and the mitochondrial respiratory chain. *Biochimie*. 2014;100:88-94.
66. Kota V, Szulc ZM, Hama H. Identification of C(6) -ceramide-interacting proteins in D6P2T Schwannoma cells. *Proteomics*. 2012;12:2179-2184.
67. Sanchez-Pintos P, de Castro MJ, Roca I, Rite S, Lopez M, Couce ML. Similarities between acylcarnitine profiles in large for gestational age newborns and obesity. *Sci Rep*. 2017;7:16267.
68. Ussher JR, Koves TR, Jaswal JS, Zhang L, Ilkayeva O, Dyck JR, Muoio DM, Lopaschuk GD. Insulin-stimulated cardiac glucose oxidation is increased in high-fat

Bibliography

- diet-induced obese mice lacking malonyl CoA decarboxylase. *Diabetes*. 2009;58:1766-1775.
69. Su X, Han X, Mancuso DJ, Abendschein DR, Gross RW. Accumulation of long-chain acylcarnitine and 3-hydroxy acylcarnitine molecular species in diabetic myocardium: identification of alterations in mitochondrial fatty acid processing in diabetic myocardium by shotgun lipidomics. *Biochemistry*. 2005;44:5234-5245.
70. Lin H, Su X, He B. Protein lysine acylation and cysteine succination by intermediates of energy metabolism. *ACS Chem Biol*. 2012;7:947-960.
71. Chamberlain LH, Shipston MJ. The physiology of protein S-acylation. *Physiol Rev*. 2015;95:341-376.
72. He Q, Han X. Cardiolipin remodeling in diabetic heart. *Chem Phys Lipids*. 2014;179:75-81.
73. Anupama N, Sindhu G, Raghu KG. Significance of mitochondria on cardiometabolic syndromes. *Fundam Clin Pharmacol*. 2018.
74. Dudek J, Maack C. Barth syndrome cardiomyopathy. *Cardiovasc Res*. 2017.
75. Shi Y. Emerging roles of cardiolipin remodeling in mitochondrial dysfunction associated with diabetes, obesity, and cardiovascular diseases. *J Biomed Res*. 2010;24:6-15.
76. Bissler JJ, Tsoras M, Goring HH, Hug P, Chuck G, Tombragel E, McGraw C, Schlotman J, Ralston MA, Hug G. Infantile dilated X-linked cardiomyopathy, G4.5 mutations, altered lipids, and ultrastructural malformations of mitochondria in heart, liver, and skeletal muscle. *Lab Invest*. 2002;82:335-344.
77. Sullivan EM, Fix A, Crouch MJ, Sparagna GC, Zeczycki TN, Brown DA, Shaikh SR. Murine diet-induced obesity remodels cardiac and liver mitochondrial phospholipid acyl chains with differential effects on respiratory enzyme activity. *J Nutr Biochem*. 2017;45:94-103.
78. Xu Y, Sutachan JJ, Plesken H, Kelley RI, Schlame M. Characterization of lymphoblast mitochondria from patients with Barth syndrome. *Lab Invest*. 2005;85:823-830.
79. Hui DY. Phospholipase A(2) enzymes in metabolic and cardiovascular diseases. *Curr Opin Lipidol*. 2012;23:235-240.
80. Labonte ED, Kirby RJ, Schildmeyer NM, Cannon AM, Huggins KW, Hui DY. Group 1B phospholipase A2-mediated lysophospholipid absorption directly contributes to postprandial hyperglycemia. *Diabetes*. 2006;55:935-941.

81. Fang X, Gibson S, Flowers M, Furui T, Bast RC, Jr., Mills GB. Lysophosphatidylcholine stimulates activator protein 1 and the c-Jun N-terminal kinase activity. *J Biol Chem.* 1997;272:13683-13689.
82. Motley ED, Kabir SM, Gardner CD, Eguchi K, Frank GD, Kuroki T, Ohba M, Yamakawa T, Eguchi S. Lysophosphatidylcholine inhibits insulin-induced Akt activation through protein kinase C-alpha in vascular smooth muscle cells. *Hypertension.* 2002;39:508-512.
83. Lopaschuk GD, Ussher JR, Folmes CD, Jaswal JS, Stanley WC. Myocardial fatty acid metabolism in health and disease. *Physiol Rev.* 2010;90:207-258.
84. Lionetti V, Stanley WC, Recchia FA. Modulating fatty acid oxidation in heart failure. *Cardiovasc Res.* 2011;90:202-209.
85. Shao D, Tian R. Glucose Transporters in Cardiac Metabolism and Hypertrophy. *Compr Physiol.* 2015;6:331-351.
86. Szablewski L. Glucose transporters in healthy heart and in cardiac disease. *Int J Cardiol.* 2017;230:70-75.
87. Koranyi L, James D, Mueckler M, Permutt MA. Glucose transporter levels in spontaneously obese (db/db) insulin-resistant mice. *J Clin Invest.* 1990;85:962-967.
88. Mazumder PK, O'Neill BT, Roberts MW, Buchanan J, Yun UJ, Cooksey RC, Boudina S, Abel ED. Impaired cardiac efficiency and increased fatty acid oxidation in insulin-resistant ob/ob mouse hearts. *Diabetes.* 2004;53:2366-2374.
89. Zafirovic S, Obradovic M, Sudar-Milovanovic E, Jovanovic A, Stanimirovic J, Stewart AJ, Pitt SJ, Isenovic ER. 17beta-Estradiol protects against the effects of a high fat diet on cardiac glucose, lipid and nitric oxide metabolism in rats. *Mol Cell Endocrinol.* 2017;446:12-20.
90. Wen SY, Velmurugan BK, Day CH, Shen CY, Chun LC, Tsai YC, Lin YM, Chen RJ, Kuo CH, Huang CY. High density lipoprotein (HDL) reverses palmitic acid induced energy metabolism imbalance by switching CD36 and GLUT4 signaling pathways in cardiomyocyte. *J Cell Physiol.* 2017;232:3020-3029.
91. Gharib M, Tao H, Fungwe TV, Hajri T. Cluster Differentiating 36 (CD36) Deficiency Attenuates Obesity-Associated Oxidative Stress in the Heart. *PLoS One.* 2016;11:e0155611.
92. Ibrahimi A, Abumrad NA. Role of CD36 in membrane transport of long-chain fatty acids. *Curr Opin Clin Nutr Metab Care.* 2002;5:139-145.

Bibliography

93. Fullekrug J, Poppelreuther M. Measurement of Long-Chain Fatty Acyl-CoA Synthetase Activity. *Methods Mol Biol.* 2016;1376:43-53.
94. Muoio DM, Newgard CB. Mechanisms of disease: Molecular and metabolic mechanisms of insulin resistance and beta-cell failure in type 2 diabetes. *Nat Rev Mol Cell Biol.* 2008;9:193-205.
95. Petersen KF, Shulman GI. Etiology of insulin resistance. *Am J Med.* 2006;119:S10-16.
96. Shulman GI. Cellular mechanisms of insulin resistance. *J Clin Invest.* 2000;106:171-176.
97. Law BA, Liao X, Moore KS, Southard A, Roddy P, Ji R, Szulc Z, Bielawska A, Schulze PC, Cowart LA. Lipotoxic very-long-chain ceramides cause mitochondrial dysfunction, oxidative stress, and cell death in cardiomyocytes. *FASEB J.* 2018;32:1403-1416.
98. Murthy MS, Pande SV. Mechanism of carnitine acylcarnitine translocase-catalyzed import of acylcarnitines into mitochondria. *J Biol Chem.* 1984;259:9082-9089.
99. Longo N, Amat di San Filippo C, Pasquali M. Disorders of carnitine transport and the carnitine cycle. *Am J Med Genet C Semin Med Genet.* 2006;142C:77-85.
100. Ouwens DM, Diamant M, Fodor M, Habets DDJ, Pelsers M, El Hasnaoui M, Dang ZC, van den Brom CE, Vlasblom R, Rietdijk A, Boer C, Coort SLM, Glatz JFC, Luiken J. Cardiac contractile dysfunction in insulin-resistant rats fed a high-fat diet is associated with elevated CD36-mediated fatty acid uptake and esterification. *Diabetologia.* 2007;50:1938-1948.
101. Sung MM, Byrne NJ, Kim TT, Levasseur J, Masson G, Boisvenue JJ, Febbraio M, Dyck JR. Cardiomyocyte-specific ablation of CD36 accelerates the progression from compensated cardiac hypertrophy to heart failure. *Am J Physiol Heart Circ Physiol.* 2017;312:H552-H560.
102. Zhang Y, Bao M, Dai M, Wang X, He W, Tan T, Lin D, Wang W, Wen Y, Zhang R. Cardiospecific CD36 suppression by lentivirus-mediated RNA interference prevents cardiac hypertrophy and systolic dysfunction in high-fat-diet induced obese mice. *Cardiovasc Diabetol.* 2015;14:69.
103. How OJ, Aasum E, Kunnathu S, Severson DL, Myhre ES, Larsen TS. Influence of substrate supply on cardiac efficiency, as measured by pressure-volume analysis in ex vivo mouse hearts. *Am J Physiol Heart Circ Physiol.* 2005;288:H2979-2985.

104. How OJ, Aasum E, Severson DL, Chan WY, Essop MF, Larsen TS. Increased myocardial oxygen consumption reduces cardiac efficiency in diabetic mice. *Diabetes*. 2006;55:466-473.
105. Sharma S, Adroque JV, Golfman L, Uray I, Lemm J, Youker K, Noon GP, Frazier OH, Taegtmeyer H. Intramyocardial lipid accumulation in the failing human heart resembles the lipotoxic rat heart. *FASEB J*. 2004;18:1692-1700.
106. Young ME, Guthrie PH, Razeghi P, Leighton B, Abbasi S, Patil S, Youker KA, Taegtmeyer H. Impaired long-chain fatty acid oxidation and contractile dysfunction in the obese Zucker rat heart. *Diabetes*. 2002;51:2587-2595.
107. Fujita M, Momose A, Ohtomo T, Nishinosono A, Tanonaka K, Toyoda H, Morikawa M, Yamada J. Upregulation of fatty acyl-CoA thioesterases in the heart and skeletal muscle of rats fed a high-fat diet. *Biol Pharm Bull*. 2011;34:87-91.
108. Bugger H, Abel ED. Molecular mechanisms for myocardial mitochondrial dysfunction in the metabolic syndrome. *Clin Sci (Lond)*. 2008;114:195-210.
109. Boudina S, Abel ED. Mitochondrial uncoupling: a key contributor to reduced cardiac efficiency in diabetes. *Physiology (Bethesda)*. 2006;21:250-258.
110. Duncan JG, Fong JL, Medeiros DM, Finck BN, Kelly DP. Insulin-resistant heart exhibits a mitochondrial biogenic response driven by the peroxisome proliferator-activated receptor-alpha/PGC-1alpha gene regulatory pathway. *Circulation*. 2007;115:909-917.
111. Boudina S, Sena S, Theobald H, Sheng X, Wright JJ, Hu XX, Aziz S, Johnson JI, Bugger H, Zaha VG, Abel ED. Mitochondrial energetics in the heart in obesity-related diabetes: direct evidence for increased uncoupled respiration and activation of uncoupling proteins. *Diabetes*. 2007;56:2457-2466.
112. Marin-Royo G, Gallardo I, Martinez-Martinez E, Gutierrez B, Jurado-Lopez R, Lopez-Andres N, Gutierrez-Tenorio J, Rial E, Bartolome MAV, Nieto ML, Cachofeiro V. Inhibition of galectin-3 ameliorates the consequences of cardiac lipotoxicity in a rat model of diet-induced obesity. *Dis Model Mech*. 2018;11.
113. Jia G, Hill MA, Sowers JR. Diabetic Cardiomyopathy: An Update of Mechanisms Contributing to This Clinical Entity. *Circ Res*. 2018;122:624-638.
114. Lashin OM, Szweda PA, Szweda LI, Romani AM. Decreased complex II respiration and HNE-modified SDH subunit in diabetic heart. *Free Radic Biol Med*. 2006;40:886-896.

Bibliography

115. Shen X, Zheng S, Metreveli NS, Epstein PN. Protection of cardiac mitochondria by overexpression of MnSOD reduces diabetic cardiomyopathy. *Diabetes*. 2006;55:798-805.
116. Boudina S, Sena S, O'Neill BT, Tathireddy P, Young ME, Abel ED. Reduced mitochondrial oxidative capacity and increased mitochondrial uncoupling impair myocardial energetics in obesity. *Circulation*. 2005;112:2686-2695.
117. Piquereau J, Caffin F, Novotova M, Lemaire C, Veksler V, Garnier A, Ventura-Clapier R, Joubert F. Mitochondrial dynamics in the adult cardiomyocytes: which roles for a highly specialized cell? *Front Physiol*. 2013;4:102.
118. Kuznetsov AV, Hermann M, Saks V, Hengster P, Margreiter R. The cell-type specificity of mitochondrial dynamics. *Int J Biochem Cell Biol*. 2009;41:1928-1939.
119. Hall AR, Burke N, Dongworth RK, Hausenloy DJ. Mitochondrial fusion and fission proteins: novel therapeutic targets for combating cardiovascular disease. *Br J Pharmacol*. 2014;171:1890-1906.
120. Elezaby A, Sverdlov AL, Tu VH, Soni K, Luptak I, Qin F, Liesa M, Shirihai OS, Rimer J, Schaffer JE, Colucci WS, Miller EJ. Mitochondrial remodeling in mice with cardiomyocyte-specific lipid overload. *J Mol Cell Cardiol*. 2015;79:275-283.
121. Apaijai N, Chunchai T, Jaiwongkam T, Kerdphoo S, Chattipakorn SC, Chattipakorn N. Testosterone Deprivation Aggravates Left-Ventricular Dysfunction in Male Obese Insulin-Resistant Rats via Impairing Cardiac Mitochondrial Function and Dynamics Proteins. *Gerontology*. 2018;64:333-343.
122. Zorzano A, Liesa M, Palacin M. Mitochondrial dynamics as a bridge between mitochondrial dysfunction and insulin resistance. *Arch Physiol Biochem*. 2009;115:1-12.
123. Sheu SS, Nauduri D, Anders MW. Targeting antioxidants to mitochondria: a new therapeutic direction. *Biochim Biophys Acta*. 2006;1762:256-265.
124. Shukla S, Dubey KK. CoQ10 a super-vitamin: review on application and biosynthesis. *3 Biotech*. 2018;8:249.
125. Kelso GF, Porteous CM, Coulter CV, Hughes G, Porteous WK, Ledgerwood EC, Smith RA, Murphy MP. Selective targeting of a redox-active ubiquinone to mitochondria within cells: antioxidant and antiapoptotic properties. *J Biol Chem*. 2001;276:4588-4596.
126. Doucet E, Tremblay A. Food intake, energy balance and body weight control. *Eur J Clin Nutr*. 1997;51:846-855.

127. Choe SS, Huh JY, Hwang IJ, Kim JI, Kim JB. Adipose Tissue Remodeling: Its Role in Energy Metabolism and Metabolic Disorders. *Front Endocrinol (Lausanne)*. 2016;7:30.
128. Spalding KL, Arner E, Westermark PO, Bernard S, Buchholz BA, Bergmann O, Blomqvist L, Hoffstedt J, Naslund E, Britton T, Concha H, Hassan M, Ryden M, Frisen J, Arner P. Dynamics of fat cell turnover in humans. *Nature*. 2008;453:783-787.
129. Tandon P, Wafer R, Minchin JEN. Adipose morphology and metabolic disease. *J Exp Biol*. 2018;221.
130. Arner E, Westermark PO, Spalding KL, Britton T, Ryden M, Frisen J, Bernard S, Arner P. Adipocyte turnover: relevance to human adipose tissue morphology. *Diabetes*. 2010;59:105-109.
131. Hoffstedt J, Arner E, Wahrenberg H, Andersson DP, Qvisth V, Lofgren P, Ryden M, Thorne A, Wiren M, Palmer M, Thorell A, Toft E, Arner P. Regional impact of adipose tissue morphology on the metabolic profile in morbid obesity. *Diabetologia*. 2010;53:2496-2503.
132. Lundgren M, Svensson M, Lindmark S, Renstrom F, Ruge T, Eriksson JW. Fat cell enlargement is an independent marker of insulin resistance and 'hyperleptinaemia'. *Diabetologia*. 2007;50:625-633.
133. Dankel SN, Svard J, Mattha S, Claussnitzer M, Kloting N, Glunk V, Fandalyuk Z, Grytten E, Solsvik MH, Nielsen HJ, Busch C, Hauner H, Bluher M, Skurk T, Sagen JV, Mellgren G. COL6A3 expression in adipocytes associates with insulin resistance and depends on PPARgamma and adipocyte size. *Obesity (Silver Spring)*. 2014;22:1807-1813.
134. Divoux A, Tordjman J, Lacasa D, Veyrie N, Hugol D, Aissat A, Basdevant A, Guerre-Millo M, Poitou C, Zucker JD, Bedossa P, Clement K. Fibrosis in human adipose tissue: composition, distribution, and link with lipid metabolism and fat mass loss. *Diabetes*. 2010;59:2817-2825.
135. Spencer M, Yao-Borengasser A, Unal R, Rasouli N, Gurley CM, Zhu B, Peterson CA, Kern PA. Adipose tissue macrophages in insulin-resistant subjects are associated with collagen VI and fibrosis and demonstrate alternative activation. *Am J Physiol Endocrinol Metab*. 2010;299:E1016-1027.
136. Zhang Y, Proenca R, Maffei M, Barone M, Leopold L, Friedman JM. Positional cloning of the mouse obese gene and its human homologue. *Nature*. 1994;372:425-432.

Bibliography

137. Gregor MF, Hotamisligil GS. Inflammatory mechanisms in obesity. *Annu Rev Immunol.* 2011;29:415-445.
138. Yin X, Lanza IR, Swain JM, Sarr MG, Nair KS, Jensen MD. Adipocyte mitochondrial function is reduced in human obesity independent of fat cell size. *J Clin Endocrinol Metab.* 2014;99:E209-216.
139. Heinonen S, Buzkova J, Muniandy M, Kaksonen R, Ollikainen M, Ismail K, Hakkarainen A, Lundbom J, Lundbom N, Vuolteenaho K, Moilanen E, Kaprio J, Rissanen A, Suomalainen A, Pietilainen KH. Impaired Mitochondrial Biogenesis in Adipose Tissue in Acquired Obesity. *Diabetes.* 2015;64:3135-3145.
140. Patti ME, Corvera S. The role of mitochondria in the pathogenesis of type 2 diabetes. *Endocr Rev.* 2010;31:364-395.
141. Pietilainen KH, Naukkarinen J, Rissanen A, Saharinen J, Ellonen P, Keranen H, Suomalainen A, Gotz A, Suortti T, Yki-Jarvinen H, Oresic M, Kaprio J, Peltonen L. Global transcript profiles of fat in monozygotic twins discordant for BMI: pathways behind acquired obesity. *PLoS Med.* 2008;5:e51.
142. Dahlman I, Forsgren M, Sjogren A, Nordstrom EA, Kaaman M, Naslund E, Attersand A, Arner P. Downregulation of electron transport chain genes in visceral adipose tissue in type 2 diabetes independent of obesity and possibly involving tumor necrosis factor-alpha. *Diabetes.* 2006;55:1792-1799.
143. Choo HJ, Kim JH, Kwon OB, Lee CS, Mun JY, Han SS, Yoon YS, Yoon G, Choi KM, Ko YG. Mitochondria are impaired in the adipocytes of type 2 diabetic mice. *Diabetologia.* 2006;49:784-791.
144. Rong JX, Qiu Y, Hansen MK, Zhu L, Zhang V, Xie M, Okamoto Y, Mattie MD, Higashiyama H, Asano S, Strum JC, Ryan TE. Adipose mitochondrial biogenesis is suppressed in db/db and high-fat diet-fed mice and improved by rosiglitazone. *Diabetes.* 2007;56:1751-1760.
145. Sepa-Kishi DM, Ceddia RB. White and beige adipocytes: are they metabolically distinct? *Horm Mol Biol Clin Investig.* 2018;33.
146. Vargas-Castillo A, Fuentes-Romero R, Rodriguez-Lopez LA, Torres N, Tovar AR. Understanding the Biology of Thermogenic Fat: Is Browning A New Approach to the Treatment of Obesity? *Arch Med Res.* 2017;48:401-413.
147. Byrnes TJ, Xie W, Al-Mukhailed O, D'Sa A, Novruzov F, Casey AT, House C, Bomanji JB. Evaluation of neck pain with (18)F-NaF PET/CT. *Nucl Med Commun.* 2014;35:298-302.

148. Deleye S, Verhaeghe J, wyffels L, Dedeurwaerdere S, Stroobants S, Staelens S. Towards a reproducible protocol for repetitive and semi-quantitative rat brain imaging with (18) F-FDG: exemplified in a memantine pharmacological challenge. *Neuroimage*. 2014;96:276-287.
149. Shilov IV, Seymour SL, Patel AA, Loboda A, Tang WH, Keating SP, Hunter CL, Nuwaysir LM, Schaeffer DA. The Paragon Algorithm, a next generation search engine that uses sequence temperature values and feature probabilities to identify peptides from tandem mass spectra. *Mol Cell Proteomics*. 2007;6:1638-1655.
150. Tang WH, Shilov IV, Seymour SL. Nonlinear fitting method for determining local false discovery rates from decoy database searches. *J Proteome Res*. 2008;7:3661-3667.
151. Kline KG, Frewen B, Bristow MR, Maccoss MJ, Wu CC. High quality catalog of proteotypic peptides from human heart. *J Proteome Res*. 2008;7:5055-5061.
152. Wisniewski JR, Zougman A, Nagaraj N, Mann M. Universal sample preparation method for proteome analysis. *Nat Methods*. 2009;6:359-362.
153. Huang da W, Sherman BT, Lempicki RA. Systematic and integrative analysis of large gene lists using DAVID bioinformatics resources. *Nat Protoc*. 2009;4:44-57.
154. Martinez-Martinez E, Calvier L, Fernandez-Celis A, Rousseau E, Jurado-Lopez R, Rossoni LV, Jaisser F, Zannad F, Rossignol P, Cachofeiro V, Lopez-Andres N. Galectin-3 blockade inhibits cardiac inflammation and fibrosis in experimental hyperaldosteronism and hypertension. *Hypertension*. 2015;66:767-775.
155. Arrieta V, Martinez-Martinez E, Ibarrola J, Alvarez V, Sadaba R, Garcia-Pena A, Fernandez-Celis A, Cachofeiro V, Rossignol P, Lopez-Andres N. A role for galectin-3 in the development of early molecular alterations in short-term aortic stenosis. *Clin Sci (Lond)*. 2017;131:935-949.
156. Calvier L, Martinez-Martinez E, Miana M, Cachofeiro V, Rousseau E, Sadaba JR, Zannad F, Rossignol P, Lopez-Andres N. The impact of galectin-3 inhibition on aldosterone-induced cardiac and renal injuries. *JACC Heart Fail*. 2015;3:59-67.
157. Lim HY, Wang W, Wessells RJ, Ocorr K, Bodmer R. Phospholipid homeostasis regulates lipid metabolism and cardiac function through SREBP signaling in *Drosophila*. *Genes Dev*. 2011;25:189-200.
158. Cedars A, Jenkins CM, Mancuso DJ, Gross RW. Calcium-independent phospholipases in the heart: mediators of cellular signaling, bioenergetics, and

Bibliography

ischemia-induced electrophysiologic dysfunction. *J Cardiovasc Pharmacol.* 2009;53:277-289.

159. Kroon T, Baccega T, Olsen A, Gabrielsson J, Oakes ND. Nicotinic acid timed to feeding reverses tissue lipid accumulation and improves glucose control in obese Zucker rats[S]. *J Lipid Res.* 2017;58:31-41.

160. Gehrman W, Wurdemann W, Plotz T, Jorns A, Lenzen S, Elsner M. Antagonism Between Saturated and Unsaturated Fatty Acids in ROS Mediated Lipotoxicity in Rat Insulin-Producing Cells. *Cell Physiol Biochem.* 2015;36:852-865.

161. Mei S, Ni HM, Manley S, Bockus A, Kassel KM, Luyendyk JP, Copple BL, Ding WX. Differential roles of unsaturated and saturated fatty acids on autophagy and apoptosis in hepatocytes. *J Pharmacol Exp Ther.* 2011;339:487-498.

162. Ander BP, Dupasquier CM, Prociuk MA, Pierce GN. Polyunsaturated fatty acids and their effects on cardiovascular disease. *Exp Clin Cardiol.* 2003;8:164-172.

163. Bowen KJ, Harris WS, Kris-Etherton PM. Omega-3 Fatty Acids and Cardiovascular Disease: Are There Benefits? *Curr Treat Options Cardiovasc Med.* 2016;18:69.

164. Szostak-Wegierek D, Klosiewicz-Latoszek L, Szostak WB, Cybulska B. The role of dietary fats for preventing cardiovascular disease. A review. *Rocz Panstw Zakl Hig.* 2013;64:263-269.

165. Briggs MA, Petersen KS, Kris-Etherton PM. Saturated Fatty Acids and Cardiovascular Disease: Replacements for Saturated Fat to Reduce Cardiovascular Risk. *Healthcare (Basel).* 2017;5.

166. Listenberger LL, Han X, Lewis SE, Cases S, Farese RV, Jr., Ory DS, Schaffer JE. Triglyceride accumulation protects against fatty acid-induced lipotoxicity. *Proc Natl Acad Sci U S A.* 2003;100:3077-3082.

167. Nolan CJ, Larter CZ. Lipotoxicity: why do saturated fatty acids cause and monounsaturates protect against it? *J Gastroenterol Hepatol.* 2009;24:703-706.

168. Li P, Liu S, Lu M, Bandyopadhyay G, Oh D, Imamura T, Johnson AMF, Sears D, Shen Z, Cui B, Kong L, Hou S, Liang X, Iovino S, Watkins SM, Ying W, Osborn O, Wollam J, Brenner M, Olefsky JM. Hematopoietic-Derived Galectin-3 Causes Cellular and Systemic Insulin Resistance. *Cell.* 2016;167:973-984 e912.

169. Pang J, Rhodes DH, Pini M, Akasheh RT, Castellanos KJ, Cabay RJ, Cooper D, Perretti M, Fantuzzi G. Increased adiposity, dysregulated glucose metabolism and systemic inflammation in Galectin-3 KO mice. *PLoS One.* 2013;8:e57915.

170. Pejnovic NN, Pantic JM, Jovanovic IP, Radosavljevic GD, Milovanovic MZ, Nikolic IG, Zdravkovic NS, Djukic AL, Arsenijevic NN, Lukic ML. Galectin-3 deficiency accelerates high-fat diet-induced obesity and amplifies inflammation in adipose tissue and pancreatic islets. *Diabetes*. 2013;62:1932-1944.
171. Madani S, Hichami A, Legrand A, Belleville J, Khan NA. Implication of acyl chain of diacylglycerols in activation of different isoforms of protein kinase C. *FASEB J*. 2001;15:2595-2601.
172. Chichger H, Vang A, O'Connell KA, Zhang P, Mende U, Harrington EO, Choudhary G. PKC delta and betaII regulate angiotensin II-mediated fibrosis through p38: a mechanism of RV fibrosis in pulmonary hypertension. *Am J Physiol Lung Cell Mol Physiol*. 2015;308:L827-836.
173. Hahn HS, Marreez Y, Odley A, Sterbling A, Yussman MG, Hilty KC, Bodi I, Liggett SB, Schwartz A, Dorn GW, 2nd. Protein kinase Calpha negatively regulates systolic and diastolic function in pathological hypertrophy. *Circ Res*. 2003;93:1111-1119.
174. Chen L, Hahn H, Wu G, Chen CH, Liron T, Schechtman D, Cavallaro G, Banci L, Guo Y, Bolli R, Dorn GW, 2nd, Mochly-Rosen D. Opposing cardioprotective actions and parallel hypertrophic effects of delta PKC and epsilon PKC. *Proc Natl Acad Sci U S A*. 2001;98:11114-11119.
175. Eisinger K, Liebisch G, Schmitz G, Aslanidis C, Krautbauer S, Buechler C. Lipidomic analysis of serum from high fat diet induced obese mice. *Int J Mol Sci*. 2014;15:2991-3002.
176. Tonks KT, Coster AC, Christopher MJ, Chaudhuri R, Xu A, Gagnon-Bartsch J, Chisholm DJ, James DE, Meikle PJ, Greenfield JR, Samocha-Bonet D. Skeletal muscle and plasma lipidomic signatures of insulin resistance and overweight/obesity in humans. *Obesity (Silver Spring)*. 2016;24:908-916.
177. Li F, Jiang C, Larsen MC, Bushkofsky J, Krausz KW, Wang T, Jefcoate CR, Gonzalez FJ. Lipidomics reveals a link between CYP11B1 and SCD1 in promoting obesity. *J Proteome Res*. 2014;13:2679-2687.
178. Tulipani S, Palau-Rodriguez M, Minarro Alonso A, Cardona F, Marco-Ramell A, Zonja B, Lopez de Alda M, Munoz-Garach A, Sanchez-Pla A, Tinahones FJ, Andres-Lacueva C. Biomarkers of Morbid Obesity and Prediabetes by Metabolomic Profiling of Human Discordant Phenotypes. *Clin Chim Acta*. 2016;463:53-61.

Bibliography

179. Pickens CA, Vazquez AI, Jones AD, Fenton JJ. Obesity, adipokines, and C-peptide are associated with distinct plasma phospholipid profiles in adult males, an untargeted lipidomic approach. *Sci Rep.* 2017;7:6335.
180. Coen PM, Goodpaster BH. Role of intramyocellular lipids in human health. *Trends Endocrinol Metab.* 2012;23:391-398.
181. Del Bas JM, Caimari A, Rodriguez-Naranjo MI, Childs CE, Paras Chavez C, West AL, Miles EA, Arola L, Calder PC. Impairment of lysophospholipid metabolism in obesity: altered plasma profile and desensitization to the modulatory properties of n-3 polyunsaturated fatty acids in a randomized controlled trial. *Am J Clin Nutr.* 2016;104:266-279.
182. Ly LD, Xu S, Choi SK, Ha CM, Thoudam T, Cha SK, Wiederkehr A, Wollheim CB, Lee IK, Park KS. Oxidative stress and calcium dysregulation by palmitate in type 2 diabetes. *Exp Mol Med.* 2017;49:e291.
183. Tondera D, Grandemange S, Jourdain A, Karbowski M, Mattenberger Y, Herzig S, Da Cruz S, Clerc P, Raschke I, Merkwirth C, Ehses S, Krause F, Chan DC, Alexander C, Bauer C, Youle R, Langer T, Martinou JC. SLP-2 is required for stress-induced mitochondrial hyperfusion. *EMBO J.* 2009;28:1589-1600.
184. Tsushima K, Bugger H, Wende AR, Soto J, Jenson GA, Tor AR, McGlaufflin R, Kenny HC, Zhang Y, Souvenir R, Hu XX, Sloan CL, Pereira RO, Lira VA, Spitzer KW, Sharp TL, Shoghi KI, Sparagna GC, Rog-Zielinska EA, Kohl P, Khalimonchuk O, Schaffer JE, Abel ED. Mitochondrial Reactive Oxygen Species in Lipotoxic Hearts Induce Post-Translational Modifications of AKAP121, DRP1, and OPA1 That Promote Mitochondrial Fission. *Circ Res.* 2018;122:58-73.
185. Montaigne D, Marechal X, Coisne A, Debry N, Modine T, Fayad G, Potelle C, El Arid JM, Mouton S, Sebti Y, Duez H, Preau S, Remy-Jouet I, Zerimech F, Koussa M, Richard V, Nevriere R, Edme JL, Lefebvre P, Staels B. Myocardial contractile dysfunction is associated with impaired mitochondrial function and dynamics in type 2 diabetic but not in obese patients. *Circulation.* 2014;130:554-564.
186. Ibarrola J, Arrieta V, Sadaba R, Martinez-Martinez E, Garcia-Pena A, Alvarez V, Fernandez-Celis A, Gainza A, Santamaria E, Fernandez-Irigoyen J, Cachofeiro V, Zalba G, Fay R, Rossignol P, Lopez-Andres N. Galectin-3 downregulates antioxidant peroxiredoxin-4 in human cardiac fibroblasts: a new pathway to induce cardiac damage? *Clin Sci (Lond).* 2018.

187. Gradman AH, Alfayoumi F. From left ventricular hypertrophy to congestive heart failure: management of hypertensive heart disease. *Prog Cardiovasc Dis.* 2006;48:326-341.
188. Qian Y, Zhang Y, Zhong P, Peng K, Xu Z, Chen X, Lu K, Chen G, Li X, Liang G. Inhibition of inflammation and oxidative stress by an imidazopyridine derivative X22 prevents heart injury from obesity. *J Cell Mol Med.* 2016;20:1427-1442.
189. Xu W, Wang C, Liang M, Chen L, Fu Q, Zhang F, Wang Y, Huang D, Huang K. A20 prevents obesity-induced development of cardiac dysfunction. *J Mol Med (Berl).* 2018;96:159-172.
190. Glatz JFC, Luiken J. Dynamic role of the transmembrane glycoprotein CD36 (SR-B2) in cellular fatty acid uptake and utilization. *J Lipid Res.* 2018.
191. Zhong H, Yin H. Role of lipid peroxidation derived 4-hydroxynonenal (4-HNE) in cancer: focusing on mitochondria. *Redox Biol.* 2015;4:193-199.
192. Ikon N, Ryan RO. Barth Syndrome: Connecting Cardiolipin to Cardiomyopathy. *Lipids.* 2017;52:99-108.
193. Heerdt PM, Schlame M, Jehle R, Barbone A, Burkhoff D, Blanck TJ. Disease-specific remodeling of cardiac mitochondria after a left ventricular assist device. *Ann Thorac Surg.* 2002;73:1216-1221.
194. Nasa Y, Sakamoto Y, Sanbe A, Sasaki H, Yamaguchi F, Takeo S. Changes in fatty acid compositions of myocardial lipids in rats with heart failure following myocardial infarction. *Mol Cell Biochem.* 1997;176:179-189.
195. Han X, Yang J, Yang K, Zhao Z, Abendschein DR, Gross RW. Alterations in myocardial cardiolipin content and composition occur at the very earliest stages of diabetes: a shotgun lipidomics study. *Biochemistry.* 2007;46:6417-6428.
196. Kuhlbrandt W. Structure and function of mitochondrial membrane protein complexes. *BMC Biol.* 2015;13:89.
197. Wong HS, Dighe PA, Mezera V, Monternier PA, Brand MD. Production of superoxide and hydrogen peroxide from specific mitochondrial sites under different bioenergetic conditions. *J Biol Chem.* 2017;292:16804-16809.
198. Antoun G, McMurray F, Thrush AB, Patten DA, Peixoto AC, Slack RS, McPherson R, Dent R, Harper ME. Impaired mitochondrial oxidative phosphorylation and supercomplex assembly in rectus abdominis muscle of diabetic obese individuals. *Diabetologia.* 2015;58:2861-2866.

Bibliography

199. Quinzii CM, Lopez LC, Von-Moltke J, Naini A, Krishna S, Schuelke M, Salviati L, Navas P, DiMauro S, Hirano M. Respiratory chain dysfunction and oxidative stress correlate with severity of primary CoQ10 deficiency. *FASEB J.* 2008;22:1874-1885.
200. Yu HT, Fu XY, Liang B, Wang S, Liu JK, Wang SR, Feng ZH. Oxidative damage of mitochondrial respiratory chain in different organs of a rat model of diet-induced obesity. *Eur J Nutr.* 2017.
201. Starkov AA, Fiskum G, Chinopoulos C, Lorenzo BJ, Browne SE, Patel MS, Beal MF. Mitochondrial alpha-ketoglutarate dehydrogenase complex generates reactive oxygen species. *J Neurosci.* 2004;24:7779-7788.
202. Murphy MP. How mitochondria produce reactive oxygen species. *Biochem J.* 2009;417:1-13.
203. Ibarrola J, Sadaba R, Garcia-Pena A, Arrieta V, Martinez-Martinez E, Alvarez V, Fernandez-Celis A, Gainza A, Santamaria E, Fernandez-Irigoyen J, Cachofeiro V, Fay R, Rossignol P, Lopez-Andres N. A role for fumarate hydratase in mediating oxidative effects of galectin-3 in human cardiac fibroblasts. *Int J Cardiol.* 2018;258:217-223.
204. Lima TI, Valentim RR, Araujo HN, Oliveira AG, Favero BC, Menezes ES, Araujo R, Silveira LR. Role of NCoR1 in mitochondrial function and energy metabolism. *Cell Biol Int.* 2018;42:734-741.
205. Mouchiroud L, Eichner LJ, Shaw RJ, Auwerx J. Transcriptional coregulators: fine-tuning metabolism. *Cell Metab.* 2014;20:26-40.
206. Hoitzing H, Johnston IG, Jones NS. What is the function of mitochondrial networks? A theoretical assessment of hypotheses and proposal for future research. *Bioessays.* 2015;37:687-700.
207. Etzler JC, Bollo M, Holstein D, Deng JJ, Perez V, Lin DT, Richardson A, Bai Y, Lechleiter JD. Cyclophilin D over-expression increases mitochondrial complex III activity and accelerates supercomplex formation. *Arch Biochem Biophys.* 2017;613:61-68.
208. Fink BD, Herlein JA, Yorek MA, Fenner AM, Kerns RJ, Sivitz WI. Bioenergetic effects of mitochondrial-targeted coenzyme Q analogs in endothelial cells. *J Pharmacol Exp Ther.* 2012;342:709-719.
209. Mitchell P. Chemiosmotic coupling in energy transduction: a logical development of biochemical knowledge. *J Bioenerg.* 1972;3:5-24.

210. Ledesma A, de Lacoba MG, Rial E. The mitochondrial uncoupling proteins. *Genome Biol.* 2002;3:REVIEWS3015.
211. Armani A, Cinti F, Marzolla V, Morgan J, Cranston GA, Antelmi A, Carpinelli G, Canese R, Pagotto U, Quarta C, Malorni W, Matarrese P, Marconi M, Fabbri A, Rosano G, Cinti S, Young MJ, Caprio M. Mineralocorticoid receptor antagonism induces browning of white adipose tissue through impairment of autophagy and prevents adipocyte dysfunction in high-fat-diet-fed mice. *FASEB J.* 2014;28:3745-3757.
212. Baskaran P, Krishnan V, Ren J, Thyagarajan B. Capsaicin induces browning of white adipose tissue and counters obesity by activating TRPV1 channel-dependent mechanisms. *Br J Pharmacol.* 2016;173:2369-2389.
213. Oliver P, Pico C, Palou A. Differential expression of genes for uncoupling proteins 1, 2 and 3 in brown and white adipose tissue depots during rat development. *Cell Mol Life Sci.* 2001;58:470-476.
214. Birsoy K, Festuccia WT, Laplante M. A comparative perspective on lipid storage in animals. *J Cell Sci.* 2013;126:1541-1552.
215. Love-Gregory L, Abumrad NA. CD36 genetics and the metabolic complications of obesity. *Curr Opin Clin Nutr Metab Care.* 2011;14:527-534.
216. Serra D, Mera P, Malandrino MI, Mir JF, Herrero L. Mitochondrial fatty acid oxidation in obesity. *Antioxid Redox Signal.* 2013;19:269-284.
217. Malandrino MI, Fucho R, Weber M, Calderon-Dominguez M, Mir JF, Valcarcel L, Escote X, Gomez-Serrano M, Peral B, Salvado L, Fernandez-Veledo S, Casals N, Vazquez-Carrera M, Villarroya F, Vendrell JJ, Serra D, Herrero L. Enhanced fatty acid oxidation in adipocytes and macrophages reduces lipid-induced triglyceride accumulation and inflammation. *Am J Physiol Endocrinol Metab.* 2015;308:E756-769.
218. Draznin B. Molecular mechanisms of insulin resistance: serine phosphorylation of insulin receptor substrate-1 and increased expression of p85alpha: the two sides of a coin. *Diabetes.* 2006;55:2392-2397.
219. Shah OJ, Wang Z, Hunter T. Inappropriate activation of the TSC/Rheb/mTOR/S6K cassette induces IRS1/2 depletion, insulin resistance, and cell survival deficiencies. *Curr Biol.* 2004;14:1650-1656.
220. Rui L, Yuan M, Frantz D, Shoelson S, White MF. SOCS-1 and SOCS-3 block insulin signaling by ubiquitin-mediated degradation of IRS1 and IRS2. *J Biol Chem.* 2002;277:42394-42398.


Bibliography

221. Lowell BB, Shulman GI. Mitochondrial dysfunction and type 2 diabetes. *Science*. 2005;307:384-387.
222. Sutherland LN, Capozzi LC, Turchinsky NJ, Bell RC, Wright DC. Time course of high-fat diet-induced reductions in adipose tissue mitochondrial proteins: potential mechanisms and the relationship to glucose intolerance. *Am J Physiol Endocrinol Metab*. 2008;295:E1076-1083.
223. Wu MT, Chou HN, Huang CJ. Dietary fucoxanthin increases metabolic rate and upregulated mRNA expressions of the PGC-1alpha network, mitochondrial biogenesis and fusion genes in white adipose tissues of mice. *Mar Drugs*. 2014;12:964-982.
224. Roede JR, Jones DP. Reactive species and mitochondrial dysfunction: mechanistic significance of 4-hydroxynonenal. *Environ Mol Mutagen*. 2010;51:380-390.
225. Chrysohoou C, Panagiotakos DB, Pitsavos C, Skoumas I, Papademetriou L, Economou M, Stefanadis C. The implication of obesity on total antioxidant capacity in apparently healthy men and women: the ATTICA study. *Nutr Metab Cardiovasc Dis*. 2007;17:590-597.
226. Tavender TJ, Bulleid NJ. Molecular mechanisms regulating oxidative activity of the Ero1 family in the endoplasmic reticulum. *Antioxid Redox Signal*. 2010;13:1177-1187.
227. Kikuchi M, Doi E, Tsujimoto I, Horibe T, Tsujimoto Y. Functional analysis of human P5, a protein disulfide isomerase homologue. *J Biochem*. 2002;132:451-455.
228. Eletto D, Eletto D, Dersh D, Gidalevitz T, Argon Y. Protein disulfide isomerase A6 controls the decay of IRE1alpha signaling via disulfide-dependent association. *Mol Cell*. 2014;53:562-576.
229. Levelt E, Pavlides M, Banerjee R, Mahmood M, Kelly C, Sellwood J, Ariga R, Thomas S, Francis J, Rodgers C, Clarke W, Sabharwal N, Antoniadis C, Schneider J, Robson M, Clarke K, Karamitsos T, Rider O, Neubauer S. Ectopic and Visceral Fat Deposition in Lean and Obese Patients With Type 2 Diabetes. *J Am Coll Cardiol*. 2016;68:53-63.
230. Rossi AP, Fantin F, Zamboni GA, Mazzali G, Rinaldi CA, Del Giglio M, Di Francesco V, Barillari M, Pozzi Mucelli R, Zamboni M. Predictors of ectopic fat accumulation in liver and pancreas in obese men and women. *Obesity (Silver Spring)*. 2011;19:1747-1754.

231. Martinez-Martinez E, Jurado-Lopez R, Cervantes-Escalera P, Cachofeiro V, Miana M. Leptin, a mediator of cardiac damage associated with obesity. *Horm Mol Biol Clin Investig.* 2014;18:3-14.
232. Urbanova M, Mraz M, Durovcova V, Trachta P, Klouckova J, Kavalkova P, Haluzikova D, Lacinova Z, Hansikova H, Wenchich L, Krsek M, Haluzik M. The effect of very-low-calorie diet on mitochondrial dysfunction in subcutaneous adipose tissue and peripheral monocytes of obese subjects with type 2 diabetes mellitus. *Physiol Res.* 2017;66:811-822.
233. Zamora-Mendoza R, Rosas-Vargas H, Ramos-Cervantes MT, Garcia-Zuniga P, Perez-Lorenzana H, Mendoza-Lorenzo P, Perez-Ortiz AC, Estrada-Mena FJ, Miliar-Garcia A, Lara-Padilla E, Ceballos G, Rodriguez A, Villarreal F, Ramirez-Sanchez I. Dysregulation of mitochondrial function and biogenesis modulators in adipose tissue of obese children. *Int J Obes (Lond).* 2018;42:618-624.
234. Martinez-Martinez E, Calvier L, Rossignol P, Rousseau E, Fernandez-Celis A, Jurado-Lopez R, Laville M, Cachofeiro V, Lopez-Andres N. Galectin-3 inhibition prevents adipose tissue remodelling in obesity. *Int J Obes (Lond).* 2016;40:1034-1038.

Appendix

SCIENTIFIC REPORTS



OPEN

The role of oxidative stress in the crosstalk between leptin and mineralocorticoid receptor in the cardiac fibrosis associated with obesity

Josué Gutiérrez-Tenorio¹, Gema Marín-Royo¹, Ernesto Martínez-Martínez^{1,2}, Rubén Martín³, María Miana^{1,4}, Natalia López-Andrés², Raquel Jurado-López¹, Isabel Gallardo³, María Luaces⁵, José Alberto San Román^{6,8}, María González-Amor⁷, Mercedes Salaces^{7,8}, María Luisa Nieto^{3,8} & Victoria Cachofeiro^{1,8}

We have investigated whether mineralocorticoid receptor activation can participate in the profibrotic effects of leptin in cardiac myofibroblasts, as well as the potential mechanisms involved. The presence of eplerenone reduced the leptin-induced increase in protein levels of collagen I, transforming growth factor β , connective tissue growth factor and galectin-3 and the levels of both total and mitochondrial of superoxide anion ($O_2^{\cdot-}$) in cardiac myofibroblasts. Likewise, the MEK/ERK inhibitor, PD98059, and the PI3/Akt inhibitor, LY294002, showed a similar pattern. Mitochondrial reactive oxygen species (ROS) scavenger (MitoTempo) attenuated the increase in body weight observed in rats fed a high fat diet (HFD). No differences were found in cardiac function or blood pressure among any group. However, the cardiac fibrosis and enhanced $O_2^{\cdot-}$ -levels observed in HFD rats were attenuated by MitoTempo, which also prevented the increased circulating leptin and aldosterone levels in HFD fed animals. This study supports a role of mineralocorticoid receptor in the cardiac fibrosis induced by leptin in the context of obesity and highlights the role of the mitochondrial ROS in this process.

Extracellular matrix (ECM) accumulation is a common response of the heart to different types of damage, including obesity. The development of cardiovascular fibrosis has been repeatedly reported in obesity in experimental and clinical studies, which is frequently accompanied by co-morbidities such as hypertension and diabetes that can favour the development of cardiac fibrosis^{1–5}. Growing evidence indicates that myocardial fibrosis is one of the pivotal contributors to heart muscle dysfunction in obesity^{3,4,6}. The excessive ECM deposit due to a large number of myofibroblasts, the cell mainly responsible for fibrosis, can cause an aberrant remodelling that favours functional alterations, since a reduced relaxing capability of the heart can increase its filling pressure and contribute to diastolic dysfunction.

Multiple factors have been proposed as being responsible for the increased accumulation of collagen content in the myocardium in the context of obesity, with leptin being one of these factors^{1,7,8}. This adipokine is locally

¹Departamento de Fisiología, Facultad de Medicina, Universidad Complutense de Madrid and Instituto de Investigación Sanitaria Gregorio Marañón (IISGM), Madrid, Spain. ²Cardiovascular Translational Research, Navarrabiomed (Miguel Servet Foundation), Instituto de Investigación Sanitaria de Navarra (IdiSNA), Pamplona, Spain. ³Instituto de Biología y Genética Molecular, CSIC-Universidad de Valladolid, Valladolid, Spain. ⁴Facultad de Enfermería y Fisioterapia, Salus Infirmerum. Universidad Pontificia de Salamanca, Madrid, Spain. ⁵Servicio de Cardiología, Instituto Cardiovascular, Hospital Clínico San Carlos, Madrid, Spain. ⁶Instituto de Ciencias del Corazón (ICICOR), Hospital Clínico Universitario de Valladolid, Valladolid, Spain. ⁷Departamento de Farmacología, Facultad de Medicina, Universidad Autónoma de Madrid and Instituto de Investigación Hospital Universitario La Paz (IdiPAZ), Madrid, Spain. ⁸Ciber de Enfermedades Cardiovasculares (CIBERCV). Instituto de Salud Carlos III, Madrid, Spain. Josué Gutiérrez-Tenorio, Gema Marín-Royo, María Luisa Nieto and Victoria Cachofeiro contributed equally to this work. Correspondence and requests for materials should be addressed to V.C. (email: vcara@ucm.es)

produced in the heart in both the epicardial fat and in the myocardium and its production is up-regulated in obese rats¹. In a previous study, we have shown that the cardiac levels of leptin are associated with levels of total collagen content, collagen I and transforming growth factor (TGF)- β in diet-induced obesity in rats. Leptin is also able to stimulate the synthesis of collagen I and the profibrotic mediators TGF- β , connective transforming growth factor (CTGF) and galectin-3 through the increase of oxidative stress and the activation of PI3K/Akt in cardiac myofibroblasts from adult rats^{1,9}. Oxidative stress is characterized by the overproduction of reactive oxygen species (ROS) with the mitochondria being the main source¹⁰. Leptin seems to exert more actions at cardiac levels because elevated circulating leptin levels are associated with left ventricular hypertrophy in patients with uncomplicated obesity¹¹.

Aldosterone through binding of mineralocorticoid receptor (MR), triggers the development of cardiac fibrosis in different pathologies, and its pharmacological blockade has demonstrated reduced interstitial fibrosis in these situations^{12–14}. Different studies have demonstrated that aldosterone is inappropriately elevated in obesity, and MR antagonism improves left ventricle function and reduces circulating procollagen levels in patients with obesity without other comorbidities^{4,15}. Similarly, low doses of spironolactone showed an anti-fibrotic effect in obese rats¹⁶.

Interactions among leptin and aldosterone have been previously reported in different scenarios and at different levels. Leptin raises blood pressure and induces endothelial dysfunction via aldosterone-dependent mechanisms in obese female mice¹⁷. Regarding the fibrotic actions, it has been shown that leptin promotes cardiac fibrosis via MR-dependent mechanisms in control and leptin-deficient mice⁵. These data support a link between leptin and MR, which could result in the potentiation of the myocardial fibrosis associated with obesity. However, how or at which level these interactions occur is unknown. Therefore, the aim of this study was to investigate whether MR activation can mediate the profibrotic effects of leptin in adult cardiac myofibroblasts, the main cells involved in cardiac fibrosis¹⁸. In addition, we have explored the potential mechanisms involved in this process. For this purpose, we have performed *in vitro* and *in vivo* studies in adult cardiac myofibroblasts and in rats fed a high fat diet (HFD).

Methods

Detailed methods are available in the online-only Data Supplement.

Cell culture conditions. Cardiac fibroblasts were isolated from the heart of adult male Wistar rats and used between passages 4 and 5. All assays in the present study were done at a temperature of 37 °C, 95% sterile air and 5% CO₂ in a saturation humidified incubator. Cells were treated with leptin (100 ng/mL, BioVendor, Germany) for 24 h in the presence or absence of the MR antagonist (eplerenone 10⁻⁶ mol/L; Sigma; St Louis, MO, USA), and in the presence or absence of the inhibitors of either PI3K or MEK pathways, LY294002 (20 × 10⁻⁶ mol/L) and PD98059 (25 × 10⁻⁶ mol/L), respectively.

Animals. Male Wistar rats of 150 g (Harlan Ibérica, Barcelona, Spain) were fed either a high-fat diet (HFD, 35% fat; Harlan Teklad #TD.03307, Haslett, MI, USA; n = 16) or a standard diet (3.5% fat; Harlan Teklad #TD.2014; Haslett, MI, USA; n = 16) for 6 weeks. Half of the animals of each group received either the mitochondrial antioxidant MitoTempo (0.7 mg Kg⁻¹ day⁻¹ Sigma, Louis, MO, USA) i.p. or vehicle (saline) from the third week on. The dose used of MitoTempo was chosen from previous publication¹⁹. Animal weight was controlled every week. Food and water intake were administered at libitum and determined throughout the experimental period. Blood and heart were collected at the end of the experiment. The Animal Care and Use Committee of Universidad Complutense de Madrid and Dirección General de Medio Ambiente, Comunidad de Madrid (PROEX 242/15) approved all experimental procedures according to the Spanish Policy for Animal Protection RD53/2013, which meets the European Union Directive 2010/63/UE.

Statistical analysis. Data are expressed as mean ± SEM. Normality of distributions was verified by means of the Kolmogorov–Smirnov test. Pearson correlation analysis was used to examine association among different variables. Data were analyzed using a one-way analysis of variance, followed by a Newman–Keuls to assess specific differences among groups or conditions or unpaired Student's t-test as corresponding using GraphPad Software Inc. (San Diego, CA, USA). The predetermined significance level was p < 0.05.

Results

Mineralocorticoid receptor blockade reduces the ECM production and oxidative stress induced by leptin. As shown in Fig. 1a, eplerenone was able to reduce the collagen I production induced by leptin in cardiac myofibroblasts. Similarly, eplerenone was able to prevent the production of the profibrotic mediators involved in the collagen production induced by this adipokine: TGF- β , CTGF and galectin-3 (Fig. 1a).

Leptin increased mitochondrial superoxide anion (O₂⁻) production in both a dose- (data not shown) and a time-dependent manner (Fig. 1b) as well as total O₂⁻ (Fig. 1c) in cardiac myofibroblast. Eplerenone reduced oxidative stress in cardiac myofibroblast by reducing total (Fig. 1c) and mitochondrial O₂⁻ levels (Fig. 1d). Eplerenone alone was unable to affect any of the studied parameters (data not shown).

Likewise, leptin induced nitrosative stress in cardiac myofibroblasts, which was also diminished by the presence of eplerenone. As shown in Fig. S1a and b, cardiac myofibroblasts treated with leptin had detectable levels of intracellular nitric oxide (NO), which increased in a time-dependent manner. Untreated cells were mostly negative for the presence of NO. The presence of eplerenone abolished leptin-evoked NO production (Fig. S1c)

We also investigated whether leptin stimulation affected mitochondrial membrane potential. Leptin treatment for up to 24 h did not induce a substantial decline in Rd123 fluorescence nor in JC-1 fluorescence, indicating that

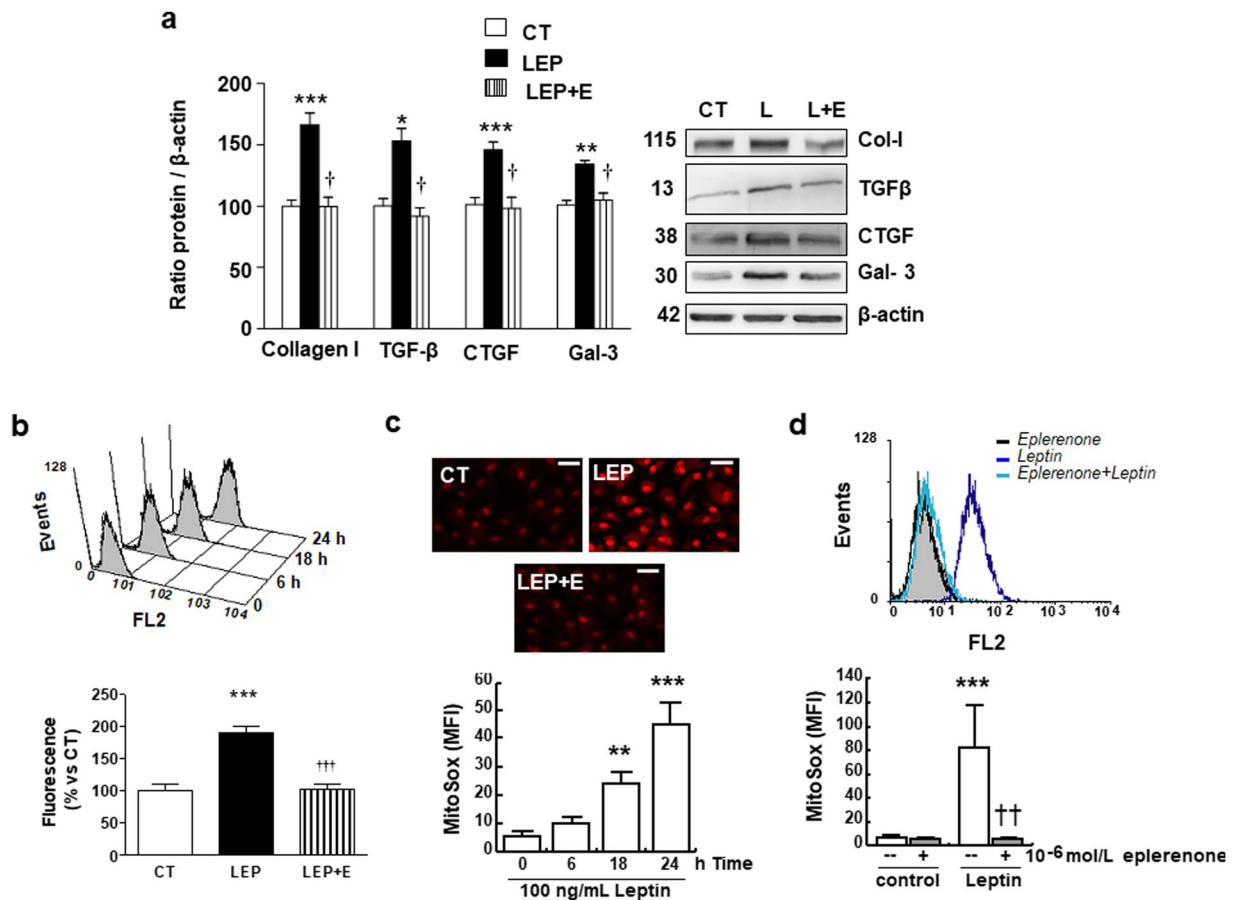


Figure 1. Impact of the mineralocorticoid receptor antagonist eplerenone on profibrotic protein factors and ROS levels in cardiac myofibroblasts. Cardiac myofibroblasts stimulated for 24 hours with leptin (100 ng/mL) in the presence (LEP) or absence (CT) of the mineralocorticoid receptor antagonist (eplerenone; 10^{-6} mol/L; L + E) were analyzed. **(a)** Protein levels of collagen type I, TGF- β , CTGF and galectin-3. **(b)** Time course of mitochondrial ROS generation in leptin-treated cells labeled with MitoSox: Representative histogram and quantification. **(c)** Representative microphotographs in cells labeled with DHE analyzed by fluorescence microscopy and quantification of total superoxide anions production induced by leptin in presence or absence of the mineralocorticoid receptor antagonist eplerenone (10^{-6} mol/L) (magnification 40X). **(d)** Mitochondrial ROS production in presence or absence of the mineralocorticoid receptor antagonist eplerenone (10^{-6} mol/L): Representative histogram and quantification. Untreated cells (solid black curves) were compared with cells treated with leptin (solid dark grey curves) or with eplerenone + leptin (open grey curves) for 24 h. Scale bar 50 μ m. Bar graphs represent the mean \pm SEM of 4 assays, in arbitrary units normalized to β -actin. * p < 0.05; ** p < 0.01; *** p < 0.001 vs. control (CT). † p < 0.05; †† p < 0.01; ††† p < 0.001 vs. leptin (LEP). Uncropped images of the blots for Fig. 2a are shown in supplementary Fig. 6.

mitochondrial membrane potential was unaffected. In contrast, and as expected, H_2O_2 exposure triggered a dramatic decrease in Rd123 and JC-1 staining (Fig. S2).

Involvement of Akt and ERK pathways in profibrotic and prooxidant effects of leptin. Leptin was able to stimulate the phosphorylation of both Akt and ERK1/2 in cardiac myofibroblasts, reaching the maximum level at 15 minutes (Fig. 2a and b). This activation shows a biphasic pattern because it was also observed 24 hours after exposure to leptin (Fig. S3). Taking into consideration that PI3K/Akt and MAPK/ERK pathways could mediate the phosphorylation of the signal transducer and activator of transcription 3 (STAT3) which regulates genes involved in ECM²⁰, we evaluated this possibility. As shown in Fig. S4a, leptin was able to stimulate the phosphorylation of STAT3 in cardiac myofibroblasts, reaching the maximum level at 30 minutes (Fig. S4a). STAT3 phosphorylation was also stimulated by leptin at 24 hours and this effect was blocked by the presence of both pathway inhibitors (LY294002 and PD98059; Fig. S4B).

Next, we determined the role of these signaling mediators in profibrotic and prooxidant effects of leptin in cardiac myofibroblasts measured in cells pretreated with the selective inhibitors of these pathways PD98059 and LY294002, respectively. Both inhibitors reduced the production of collagen type I induced by leptin (Fig. 2c), as well as that of the mediators involved in this production TGF- β , CTGF and galectin-3 (Fig. 2c). Moreover, the presence of PD98059 and LY294002 was able to reduce the production of total ROS (Fig. 2d and e).

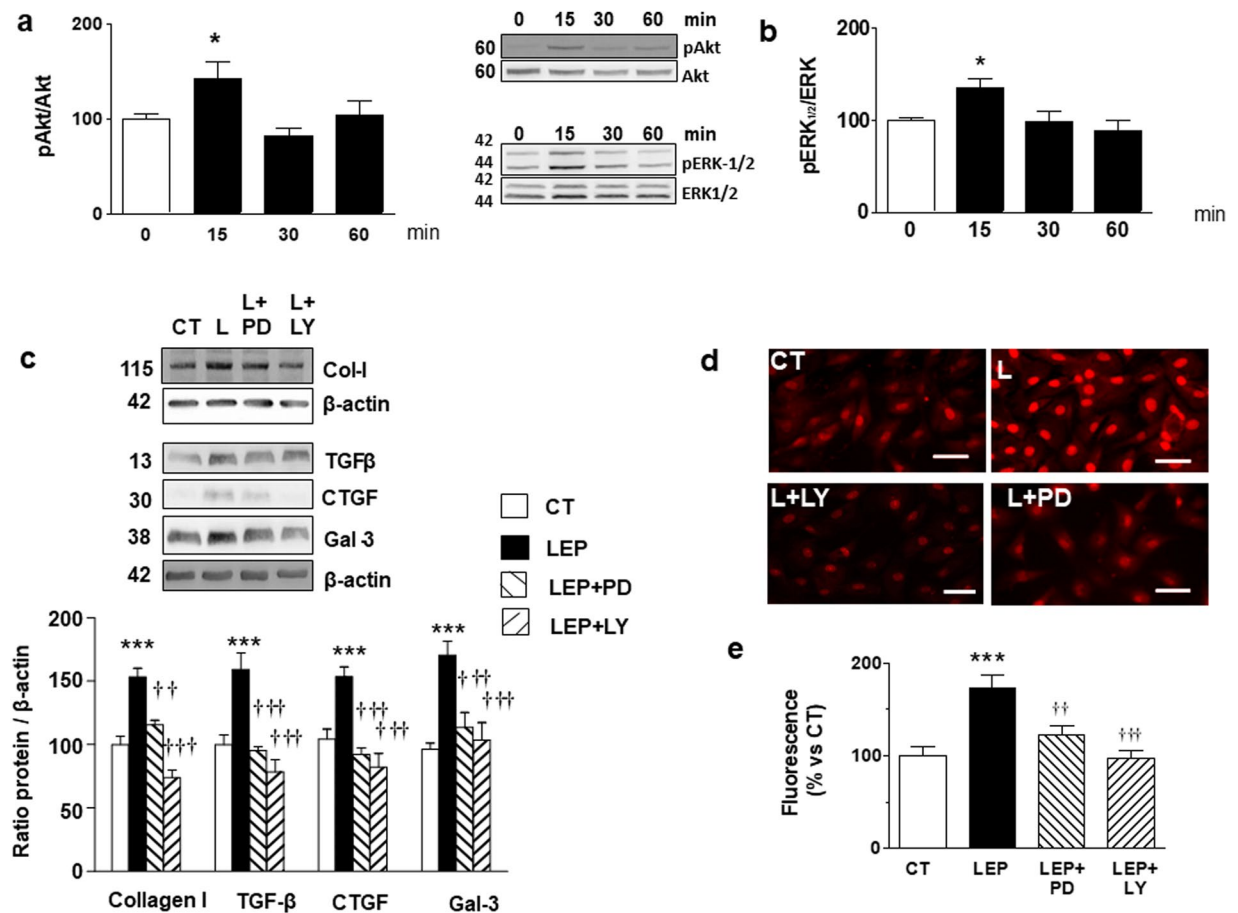


Figure 2. Effect of leptin on Akt and MEK pathways and impact of inhibition of Akt and MEK pathways on profibrotic protein factors and ROS levels in cardiac myofibroblasts. Protein levels of (a) pAkt/Akt and (b) pERK 1/2/ERK1/2 stimulated by leptin (100 ng/mL) for indicated time intervals. Cardiac myofibroblasts stimulated for 24 hours with leptin (100 ng/mL) in the presence or absence of the inhibitors of either MEK (PD98059; PD; 25×10^{-6} mol/L) or Akt (LY294002; LY; 20×10^{-6} mol/L) pathways for 24 hours. (c) Protein levels of collagen type I, TGF- β , CTGF and galectin-3. (d) Representative microphotographs in cells labeled with DHE and (e) Quantification of total superoxide anions and. Bar graphs represent the mean \pm SD of 3–4 assays in arbitrary units normalized to β -actin. * $p < 0.05$; *** $p < 0.001$ vs. control. †† $p < 0.01$; ††† $p < 0.001$ vs. leptin.

Effect of leptin in activation of EGFR. In order to determine if the activation of the receptor EGFR is involved in the effects of leptin in cardiac myofibroblasts, we examined the EGFR phosphorylation status at Tyr845 and Tyr1176 in response to 100 ng/ml of leptin at different times. Data of Fig. 3a and b show that leptin does not produce a significant effect in EGFR activation.

Interactions between mineralocorticoid receptor and leptin in the proliferation of cardiac myofibroblasts. In order to evaluate whether this interaction between MR and leptin not only involved ECM production but other actions, we explored if leptin is able to stimulate the proliferation of cardiac myofibroblasts in the presence or absence of aldosterone. Leptin alone or in the presence of aldosterone was unable to stimulate the proliferation of these cells (Fig. S5).

Mitochondrial ROS have a role in cardiac fibrosis and leptin and aldosterone levels in diet-induced obese rats. Taking into consideration that oxidative stress participates in the fibrotic effect induced by leptin and eplerenone reduced the oxidative stress induced by leptin, we evaluated whether oxidative stress is also involved in the possible interaction between MR and leptin observed *in vivo*. We also explored the effect of the administration of the mitochondrial ROS scavenger MitoTempo in rats fed an HFD. Body weight gain was expectedly significantly higher in rats fed an HFD as compared with rats fed a standard diet. This increase was smaller in animals treated with MitoTempo (Table 1). Similarly, MitoTempo reduced the increase in the body weight in obese animals (Table 1). It should be noted that the changes in body weight triggered by MitoTempo in HFD-fed rats were not consequence of a reduction in food intake (data not shown). Neither diet nor MitoTempo were able to modify systolic or diastolic function (Table 1). In addition, no differences in blood pressure levels were observed among any group along the study. Cardiac interstitial fibrosis was higher in obese animals than in

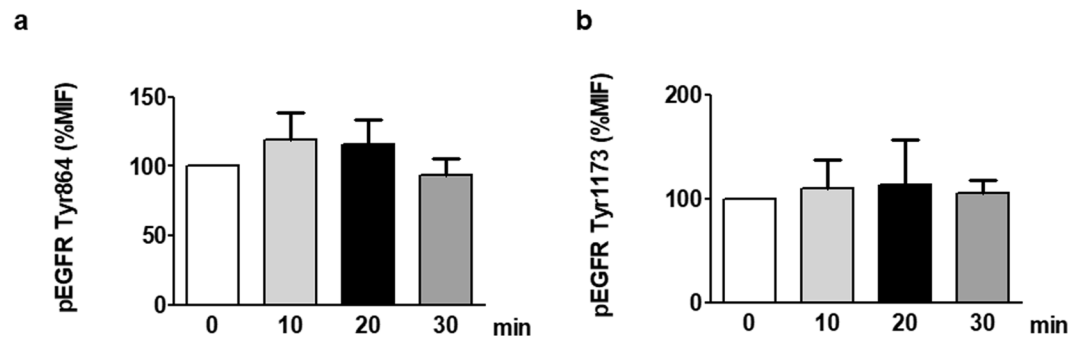


Figure 3. Effect of leptin on EGFR transactivation in cardiac myofibroblasts. EGFR phosphorylation in either Tyr864 (a) or Tyr 1173 (b) were analyzed by flow cytometry analysis in cardiac myofibroblasts stimulated with leptin (100 ng/mL) for indicated time intervals. Bar graphs represent the mean \pm SEM of 3 assays.

	CT	HFD	HFD + MT
Body Weight (g)	356.6 \pm 10.7	442.8 \pm 8.4***	397.8 \pm 9.4 **††
HW/TL (mg/cm tibia)	24.7 \pm 0.56	28.3 \pm 1*	25.9 \pm 0.7
IVT (mm)	1.51 \pm 0.12	1.38 \pm 0.5	1.4 \pm 0.06
PWT(mm)	1.46 \pm 0.1	1.37 \pm 0.06	1.45 \pm 0.06
EDD (mm)	6.88 \pm 0.43	7.21 \pm 0.23	6.81 \pm 0.11
ESD (mm)	3.40 \pm 0.36	3.98 \pm 0.27	3.75 \pm 0.3
EF (%)	86.9 \pm 2.8	79.6 \pm 3.1	78.8 \pm 3.6
FS (%)	48.5 \pm 3.2	42.3 \pm 3.3	44.4 \pm 3.8
E/A ratio	1.96 \pm 0.17	2.03 \pm 0.17	1.91 \pm 0.12
SBP (mmHg)	133.7 \pm 2.5	138.1 \pm 2.1	133.9 \pm 2.6

Table 1. Effect of the mitochondrial reactive oxygen species scavenger (MitoTempo; MT; 0.7 mg Kg⁻¹ day⁻¹) on body weight, relative heart weight, echocardiographic parameters and systolic blood pressure in rats fed a standard diet (CT) or a high fat diet (HFD). HW: heart weight; TL: tibia length; IVT: interventricular septum thickness; PWT: posterior wall thickness; EDD: end-diastolic diameter; ESD: end-systolic diameter; EF: ejection fraction; FS: fractional shortening; E/A ratio; SBP: systolic blood pressure. Data values represent mean \pm S.E.M of 8 animals. *p < 0.05; **p < 0.01; ***p < 0.001 vs. control group. ††p < 0.01 vs. HFD group.

controls (Fig. 4a and b). These levels were correlated with those of leptin ($r = 0.8003$, $p < 0.001$) and aldosterone ($r = 0.6630$, $p < 0.01$). The increase in cardiac fibrosis observed in HFD was prevented by the administration of MitoTempo. This antioxidant also prevented the altered cardiac O₂⁻ production in heart observed in HFD animals (Fig. 4c and d). In fact, cardiac ROS and fibrosis levels correlated with each other ($r = 0.6634$, $p < 0.01$).

Leptin levels were expectedly higher in obese animals than in controls, which were reduced in those animals treated with MitoTempo (Fig. 4e). Aldosterone plasma levels show a similar pattern to those observed with leptin (Fig. 4f). In fact, a correlation was observed between both leptin and aldosterone levels ($r = 0.6229$, $p < 0.01$). In addition, both leptin ($r = 0.6237$; $p < 0.05$) and aldosterone levels ($r = 0.7861$, $p < 0.001$) were correlated with those of cardiac ROS. The administration of MitoTempo did not modify any of the evaluated parameters in control animals (data not shown).

Discussion

The purpose of this study was to investigate the involvement of MR in the ECM production induced by leptin in cardiac myofibroblasts, which participates in the cardiac fibrosis associated with obesity¹. We herein report that the MR antagonist eplerenone prevents the increase in collagen I synthesis induced by this adipokine. Eplerenone also reduced oxidative stress, TGF- β , CTGF and galectin-3 levels which are involved in the ECM production induced by leptin^{1,7,8}. These results might suggest that the cardiac fibrotic effect of leptin could involve MR activation through oxidative stress-dependent pathway which activates the down-stream mediators by the activation of PI3K/Akt and MAPK/ERK pathways. Likewise, the *in vivo* data also show that the administration of a mitochondrial ROS scavenger in rats fed an HFD reduced cardiac fibrosis, as well as leptin and aldosterone plasma levels, supporting that there is an association among fibrosis, oxidative stress, leptin, and MR in obese normotensive rats. These data could help to understand the complex scenario involved in the development of cardiac fibrosis in the context of obesity.

The present data suggests an interaction between leptin and MR, which seems to be relevant in the development of cardiac fibrosis in the context of obesity in which both play a significant role^{1,4,5,7,21,22}. This affirmation is based on two facts: First, the presence in the incubation media of eplerenone reduced the increase in collagen type I induced by leptin in cardiac myofibroblasts, the main cells involved in cardiac fibrosis¹⁸. Second,

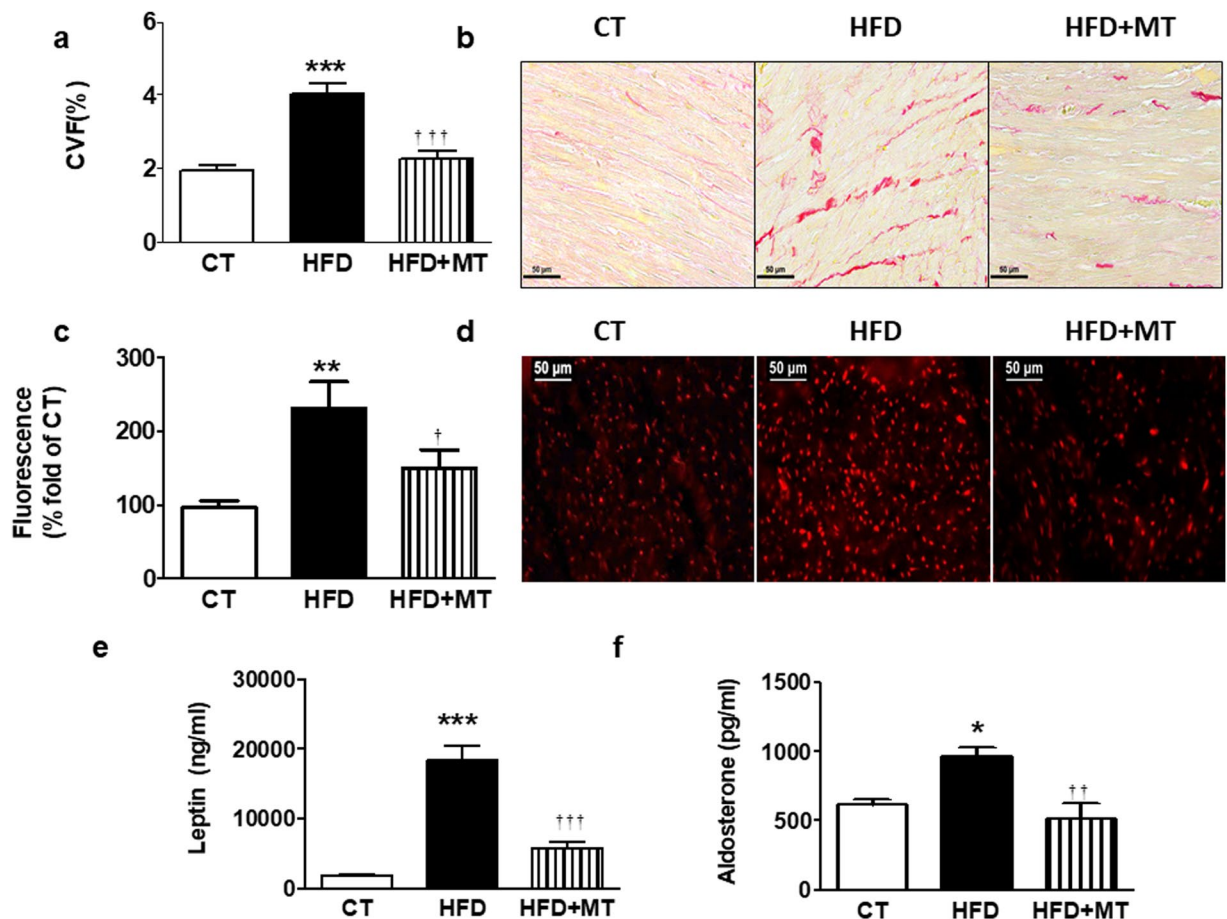


Figure 4. Impact of a mitochondrial ROS scavenger on cardiac fibrosis and ROS levels and plasma leptin and aldosterone levels in control and obese rats. Heart from rats fed a standard diet (CT) or a high fat diet (HFD) treated with the mitochondrial ROS scavenger (MitoTempo; MT; $0.7 \text{ mg Kg}^{-1} \text{ day}^{-1}$) were analyzed. **(a)** Quantification of collagen volume fraction (CVF). **(b)** Representative microphotographs of myocardial sections staining with picosirius red examined by light microscopy (magnification 40X). **(c)** Quantification of superoxide anions production and **(d)** representative microphotographs of myocardial sections labeled with DHE analyzed by fluorescence microscopy (magnification 40X). Plasma levels of leptin **(e)** and aldosterone **(f)** of the same animals. Bar graphs represent the mean \pm SEM of 6–8 animals. Scale bar: $50 \mu\text{m}$. * $p < 0.05$; ** $p < 0.01$; *** $p < 0.001$ vs. control group. † $p < 0.05$; †† $p < 0.01$; ††† $p < 0.001$ vs. HFD group.

epplerone prevented the production of the end effectors of leptin-induced ECM production (TGF- β , CTGF or galectin-3) in these cells¹. In addition, a correlation between aldosterone levels and total cardiac collagen was observed in normotensive animals fed an HFD in the presence of high leptin levels. Moreover, the reduction of cardiac fibrosis induced by the mitochondrial ROS scavenger MitoTempo in animals fed an HFD was accompanied by a reduction in both leptin and aldosterone plasma levels. We have previously reported the role of oxidative stress in the fibrotic effect induced by leptin in cardiac and vascular fibrosis^{1,23}. Therefore, the data suggest that leptin through ROS production can facilitate MR activation, which can mediate ECM production induced by this adipokine. In fact, this interaction seems to be more complex because eplerone was able to reduce oxidative stress induced by leptin independently of its origin or nature (total ROS, nitro-oxidative species or mitochondrial ROS) in cardiac myofibroblasts, supporting the notion that there exists a vicious circle between oxidative stress and MR.

It is necessary to mention that we cannot exclude the possibility that the reduction in body weight gain, which was not consequence of a reduction in food intake, elicited by MitoTempo in HFD animals could also be partially responsible for the reduction in cardiac fibrosis and in leptin and aldosterone levels observed in the treated group. A similar finding has been reported with another mitochondrial ROS scavenger (MitoQ) in obese rats^{24,25}. However, MitoQ was able to reduce cardiac fibrosis in a model of cardiac toxicity in rats without body weight change²⁶ or reduced Akt activation in rat cardiac myocyte²⁷. Total antioxidant capacity in the diet has been found to be inversely related to central adiposity, metabolic and oxidative stress bio-markers, and risk for cardiovascular diseases²⁸. Therefore, it could be proposed that the observed effect on body weight could also be a consequence of the antioxidant capacity of MitoTempo. Given that changes in food intake were not observed further investigation focusing on lipid absorption, metabolism and/or accumulation are required to understand the underlying mechanisms involved in the slimming effect.

Consistent with previous studies in different conditions^{23,29–34}, leptin stimulates PI3K/Akt, STAT-3 and MAPK/ERK signaling mediators in cardiac myofibroblasts that seem to be involved in the ECM production in cardiac myofibroblasts caused by this adipokine. This affirmation is based on the fact that the presence of their inhibitors blocked the synthesis of collagen I and the downstream–mediators (TGF- β , CTGF and galectin-3) induced by leptin. Therefore, taking into consideration that phosphorylation of PI3K/Akt and MAPK/ERK is involved in the fibrotic effects of both leptin and mineralocorticoid receptor activation^{32,34–37}, these data suggest that PI3K/Akt and MAPK/ERK can act as common signaling mediators for both factors, regulating downstream events which lead to the production of end effectors, including TGF- β , CTGF and galectin-3, and which finally lead to the synthesis of ECM in cardiac myofibroblasts. The possible interaction between leptin and MR signaling pathways leading to PI3K/Akt and MAPK/ERK activation may occur at several different stages and their understanding warrants a more detailed analysis

The EGFR family and its ligands serve as a switchboard for the regulation of multiple cellular processes, including fibrosis. EGFR transactivation in cardiac cells has been observed following stimulation with leptin after MR activation, and its action has been implicated in cardiac remodelling^{38–41}. EGFR transactivation is also involved in ROS generation, induced by high concentrations of glucose in rat cardiomyocytes⁴² and supporting that transactivation of EGFR plays a central role in mediating cardiac damage. However, our data does not support the phosphorylation of EGFR as a signaling which engages in leptin–mineralocorticoid receptor crosstalk in ECM production in adult cardiac myofibroblasts.

In summary, our data show that the cardiac fibrotic effect of leptin could involve the MR activation through oxidative stress-dependent pathway which activates the PI3K/Akt and MAPK/ERK pathways and consequently the production of end effectors, including TGF- β , CTGF and galectin-3, which are mainly responsible for the final synthesis of ECM in cardiac fibroblasts. These findings will all together aid in understanding the crosstalk among these factors in the production of ECM, which plays a role in the development of cardiac remodelling in the context of obesity and support the relevance of mitochondrial oxidative stress in this process. Therefore, the study highlights the complexity of the molecular mechanisms involved in the development of myocardial fibrosis associated with obesity.

References

- Martinez-Martinez, E. *et al.* Leptin induces cardiac fibrosis through galectin-3, mTOR and oxidative stress: potential role in obesity. *J Hypertens* **32**, 1104–1114; discussion 1114, <https://doi.org/10.1097/HJH.000000000000149> (2014).
- Eschaliier, R. *et al.* Features of cardiac remodeling, associated with blood pressure and fibrosis biomarkers, are frequent in subjects with abdominal obesity. *Hypertension* **63**, 740–746, <https://doi.org/10.1161/HYPERTENSIONAHA.113.02419> (2014).
- Cavalera, M., Wang, J. & Frangogiannis, N. G. Obesity, metabolic dysfunction, and cardiac fibrosis: pathophysiological pathways, molecular mechanisms, and therapeutic opportunities. *Transl Res* **164**, 323–335, <https://doi.org/10.1016/j.trsl.2014.05.001> (2014).
- Kosmala, W., Przewlocka-Kosmala, M., Szczepanik-Osadnik, H., Mysiak, A. & Marwick, T. H. Fibrosis and cardiac function in obesity: a randomised controlled trial of aldosterone blockade. *Heart* **99**, 320–326, <https://doi.org/10.1136/heartjnl-2012-303329> (2013).
- Huby, A. C. *et al.* Adipocyte-Derived Hormone Leptin Is a Direct Regulator of Aldosterone Secretion, Which Promotes Endothelial Dysfunction and Cardiac Fibrosis. *Circulation* **132**, 2134–2145, <https://doi.org/10.1161/CIRCULATIONAHA.115.018226> (2015).
- Martinez-Martinez, E. *et al.* Galectin-3 Participates in Cardiovascular Remodeling Associated With Obesity. *Hypertension* **66**, 961–969, <https://doi.org/10.1161/HYPERTENSIONAHA.115.06032> (2015).
- Zibadi, S., Cordova, F., Slack, E. H., Watson, R. R. & Larson, D. F. Leptin's regulation of obesity-induced cardiac extracellular matrix remodeling. *Cardiovasc Toxicol* **11**, 325–333, <https://doi.org/10.1007/s12012-011-9124-0> (2011).
- Leifheit-Nestler, M. *et al.* Importance of leptin signaling and signal transducer and activator of transcription-3 activation in mediating the cardiac hypertrophy associated with obesity. *J Transl Med* **11**, 170, <https://doi.org/10.1186/1479-5876-11-170> (2013).
- Martinez-Martinez, E. *et al.* The lysyl oxidase inhibitor (beta-aminopropionitrile) reduces leptin profibrotic effects and ameliorates cardiovascular remodeling in diet-induced obesity in rats. *J Mol Cell Cardiol* **92**, 96–104, <https://doi.org/10.1016/j.yjmcc.2016.01.012> (2016).
- Murphy, M. P. How mitochondria produce reactive oxygen species. *Biochem J* **417**, 1–13, <https://doi.org/10.1042/BJ20081386> (2009).
- Perego, L. *et al.* Circulating leptin correlates with left ventricular mass in morbid (grade III) obesity before and after weight loss induced by bariatric surgery: a potential role for leptin in mediating human left ventricular hypertrophy. *J Clin Endocrinol Metab* **90**, 4087–4093, <https://doi.org/10.1210/jc.2004-1963> (2005).
- Calvier, L. *et al.* The impact of galectin-3 inhibition on aldosterone-induced cardiac and renal injuries. *JACC Heart Fail* **3**, 59–67, <https://doi.org/10.1016/j.jchf.2014.08.002> (2015).
- Capuano, A. *et al.* Mineralocorticoid receptor antagonists in heart failure with preserved ejection fraction (HFpEF). *Int J Cardiol* **200**, 15–19, <https://doi.org/10.1016/j.ijcard.2015.07.038> (2015).
- Brown, K. *et al.* Mineralocorticoid Receptor Antagonism in Acute Heart Failure. *Curr Treat Options Cardiovasc Med* **17**, 402, <https://doi.org/10.1007/s11936-015-0402-1> (2015).
- Kosmala, W. *et al.* A randomized study of the beneficial effects of aldosterone antagonism on LV function, structure, and fibrosis markers in metabolic syndrome. *JACC Cardiovasc Imaging* **4**, 1239–1249, <https://doi.org/10.1016/j.jcmg.2011.08.014> (2011).
- Bender, S. B. *et al.* Mineralocorticoid receptor antagonism treats obesity-associated cardiac diastolic dysfunction. *Hypertension* **65**, 1082–1088, <https://doi.org/10.1161/HYPERTENSIONAHA.114.04912> (2015).
- Huby, A. C., Otvos, L. Jr & Belin de Chantemele, E. J. Leptin Induces Hypertension and Endothelial Dysfunction via Aldosterone-Dependent Mechanisms in Obese Female Mice. *Hypertension* **67**, 1020–1028, <https://doi.org/10.1161/HYPERTENSIONAHA.115.06642> (2016).
- Travers, J. G., Kamal, F. A., Robbins, J., Yutzey, K. E. & Blaxall, B. C. Cardiac Fibrosis: The Fibroblast Awakens. *Circ Res* **118**, 1021–1040, <https://doi.org/10.1161/CIRCRESAHA.115.306565> (2016).
- Martinez-Revelles, S. *et al.* Reciprocal relationship between reactive oxygen species and cyclooxygenase-2 and vascular dysfunction in hypertension. *Antioxid Redox Signal* **18**, 51–65, <https://doi.org/10.1089/ars.2011.4335> (2013).
- Heldsinger, A., Grabauskas, G., Song, I. & Owyang, C. Synergistic interaction between leptin and cholecystokinin in the rat nodose ganglia is mediated by PI3K and STAT3 signaling pathways: implications for leptin as a regulator of short term satiety. *J Biol Chem* **286**, 11707–11715, <https://doi.org/10.1074/jbc.M110.198945> (2011).
- Essick, E. E. & Sam, F. Cardiac hypertrophy and fibrosis in the metabolic syndrome: a role for aldosterone and the mineralocorticoid receptor. *Int J Hypertens* **2011**, 346985, <https://doi.org/10.4061/2011/346985> (2011).

22. Lastra, G. & Sowers, J. R. Obesity and cardiovascular disease: role of adipose tissue, inflammation, and the renin-angiotensin-aldosterone system. *Horm Mol Biol Clin Invest* **15**, 49–57, <https://doi.org/10.1515/hmbci-2013-0025> (2013).
23. Martínez-Martínez, E. *et al.* The potential role of leptin in the vascular remodeling associated with obesity. *Int J Obes (Lond)* **38**, 1565–1572, <https://doi.org/10.1038/ijo.2014.37> (2014).
24. Feillet-Coudray, C. *et al.* The mitochondrial-targeted antioxidant MitoQ ameliorates metabolic syndrome features in obesogenic diet-fed rats better than Apocynin or Allopurinol. *Free Radic Res* **48**, 1232–1246, <https://doi.org/10.3109/10715762.2014.945079> (2014).
25. Hallek, M., Levi, F., Haen, E. & Emmerich, B. [The significance of chronopharmacology for oncology]. *Onkologie* **12**, 230–238 (1989).
26. Chandran, K. *et al.* Doxorubicin inactivates myocardial cytochrome c oxidase in rats: cardioprotection by Mito-Q. *Biophys J* **96**, 1388–1398, <https://doi.org/10.1016/j.bpj.2008.10.042> (2009).
27. Song, J. *et al.* Activation of PI3Kgamma/Akt pathway increases cardiomyocyte HMGB1 expression in diabetic environment. *Oncotarget* **7**, 80803–80810, <https://doi.org/10.18632/oncotarget.13096> (2016).
28. Hermsdorff, H. H. *et al.* Dietary total antioxidant capacity is inversely related to central adiposity as well as to metabolic and oxidative stress markers in healthy young adults. *Nutr Metab (Lond)* **8**, 59, <https://doi.org/10.1186/1743-7075-8-59> (2011).
29. Niu, L. *et al.* Leptin stimulates alpha1(I) collagen expression in human hepatic stellate cells via the phosphatidylinositol 3-kinase/Akt signalling pathway. *J Steroid Biochem Mol Biol* **149**, 1265–1272, <https://doi.org/10.1111/j.1478-3231.2007.01582.x> (2007).
30. Tong, K. M. *et al.* Leptin induces IL-8 expression via leptin receptor, IRS-1, PI3K, Akt cascade and promotion of NF-kappaB/p300 binding in human synovial fibroblasts. *Cell Signal* **20**, 1478–1488, <https://doi.org/10.1016/j.cellsig.2008.04.003> (2008).
31. Wen, R. *et al.* Leptin exerts proliferative and anti-apoptotic effects on goose granulosa cells through the PI3K/Akt/mTOR signaling pathway. *J Steroid Biochem Mol Biol* **149**, 70–79, <https://doi.org/10.1016/j.jsbmb.2015.01.001> (2015).
32. Maymo, J. L. *et al.* Regulation of placental leptin expression by cyclic adenosine 5'-monophosphate involves cross talk between protein kinase A and mitogen-activated protein kinase signaling pathways. *Endocrinology* **151**, 3738–3751, <https://doi.org/10.1210/en.2010-0064> (2010).
33. Caricilli, A. M. *et al.* Topiramate treatment improves hypothalamic insulin and leptin signaling and action and reduces obesity in mice. *Endocrinology* **153**, 4401–4411, <https://doi.org/10.1210/en.2012-1272> (2012).
34. Wang, L., Shao, Y. Y. & Ballock, R. T. Leptin Antagonizes Peroxisome Proliferator-Activated Receptor-gamma Signaling in Growth Plate Chondrocytes. *PPAR Res* **2012**, 756198, <https://doi.org/10.1155/2012/756198> (2012).
35. Tsai, C. F., Yang, S. F., Chu, H. J. & Ueng, K. C. Cross-talk between mineralocorticoid receptor/angiotensin II type 1 receptor and mitogen-activated protein kinase pathways underlies aldosterone-induced atrial fibrotic responses in HL-1 cardiomyocytes. *Int J Cardiol* **169**, 17–28, <https://doi.org/10.1016/j.ijcard.2013.06.046> (2013).
36. Zhu, C. J. *et al.* The mineralocorticoid receptor-p38MAPK-NFkappaB or ERK-Sp1 signal pathways mediate aldosterone-stimulated inflammatory and profibrotic responses in rat vascular smooth muscle cells. *Acta Pharmacol Sin* **33**, 873–878, <https://doi.org/10.1038/aps.2012.36> (2012).
37. Huang, L. L., Nikolic-Paterson, D. J., Ma, F. Y. & Tesch, G. H. Aldosterone induces kidney fibroblast proliferation via activation of growth factor receptors and PI3K/MAPK signalling. *Nephron Exp Nephrol* **120**, e115–122, <https://doi.org/10.1159/000339500> (2012).
38. Beltowski, J. & Jazmroz-Wisniewska, A. Transactivation of ErbB receptors by leptin in the cardiovascular system: mechanisms, consequences and target for therapy. *Curr Pharm Des* **20**, 616–624 (2014).
39. Schreier, B. *et al.* Loss of epidermal growth factor receptor in vascular smooth muscle cells and cardiomyocytes causes arterial hypotension and cardiac hypertrophy. *Hypertension* **61**, 333–340, <https://doi.org/10.1161/HYPERTENSIONAHA.112.196543> (2013).
40. Grossmann, C. *et al.* Aldosterone-induced EGFR expression: interaction between the human mineralocorticoid receptor and the human EGFR promoter. *Am J Physiol Endocrinol Metab* **292**, E1790–1800, <https://doi.org/10.1152/ajpendo.00708.2006> (2007).
41. Forrester, S. J. *et al.* Epidermal Growth Factor Receptor Transactivation: Mechanisms, Pathophysiology, and Potential Therapies in the Cardiovascular System. *Annu Rev Pharmacol Toxicol* **56**, 627–653, <https://doi.org/10.1146/annurev-pharmtox-070115-095427> (2016).
42. Liang, D. *et al.* EGFR inhibition protects cardiac damage and remodeling through attenuating oxidative stress in STZ-induced diabetic mouse model. *J Mol Cell Cardiol* **82**, 63–74, <https://doi.org/10.1016/j.yjmcc.2015.02.029> (2015).

Acknowledgements

We thank Avelina Hidalgo, Roberto Cañadas, Blanca Martínez, and Virginia Peinado for their technical help and Anthony DeMarco for his help in editing the article. This work was supported by Instituto de Salud Carlos III-Fondo Europeo de Desarrollo Regional (FEDER) (PI15/01060; RD12/0042/0024, RD12/0042/0026 and RD12/0042/0033, CIBERCV; Miguel Servet contract CP13/00221) a way to build Europe. Ministerio de Economía y Competitividad (SAF2012-34460 and SAF2016-81063), the FPI Program del Gobierno de Castilla y León (co-funded by FSE) and COST ADMIRE network (BM1301).

Author Contributions

J.G.T. performed experiments and data analysis and helped to write the manuscript, G.M.R. performed data analysis and helped to write the manuscript, E.M.M. performed experiments and data analysis and helped to write the manuscript, R.M. performed experiments and data analysis, M.M. performed experiments and data analysis and helped to write the manuscript, N.L.A. contributed to discussion and the writing of the manuscript, R.J.L. performed experiments and data analysis, I.G. performed experiments and data analysis, M.L. performed experiments and data analysis and helped to write the manuscript, J.A.S.R. contributed to discussion and the writing of the manuscript, M.G.A. performed experiments and data analysis, M.S. contributed to discussion and the writing of the manuscript, M.L.N. designed the study, performed experiments and data analysis and wrote the manuscript, V.C. designed the study, performed experiments and data analysis and wrote the manuscript.

Additional Information

Supplementary information accompanies this paper at <https://doi.org/10.1038/s41598-017-17103-9>.

Competing Interests: The authors declare that they have no competing interests.

Publisher's note: Springer Nature remains neutral with regard to jurisdictional claims in published maps and institutional affiliations.



Open Access This article is licensed under a Creative Commons Attribution 4.0 International License, which permits use, sharing, adaptation, distribution and reproduction in any medium or format, as long as you give appropriate credit to the original author(s) and the source, provide a link to the Creative Commons license, and indicate if changes were made. The images or other third party material in this article are included in the article's Creative Commons license, unless indicated otherwise in a credit line to the material. If material is not included in the article's Creative Commons license and your intended use is not permitted by statutory regulation or exceeds the permitted use, you will need to obtain permission directly from the copyright holder. To view a copy of this license, visit <http://creativecommons.org/licenses/by/4.0/>.

© The Author(s) 2017



ORIGINAL ARTICLE

The impact of obesity in the cardiac lipidome and its consequences in the cardiac damage observed in obese rats



Gema Marín-Royo^a, Ernesto Martínez-Martínez^a, Beatriz Gutiérrez^b,
Raquel Jurado-López^a, Isabel Gallardo^b, Olimpio Montero^c,
M^a Visitación Bartolomé^{d,g}, José Alberto San Román^{e,g}, Mercedes Salaices^{f,g},
María Luisa Nieto^{b,g,1}, Victoria Cachofeiro^{a,g,*,1}

^a Departamento de Fisiología, Facultad de Medicina, Universidad Complutense de Madrid and Instituto de Investigación Sanitaria Gregorio Marañón (IiSGM), Spain

^b Instituto de Biología y Genética Molecular, CSIC-Universidad de Valladolid, Spain

^c Centro de Desarrollo Biotecnológico, CSIC, Valladolid, Spain

^d Departamento de Oftalmología y Otorrinolaringología, Facultad de Psicología, Universidad Complutense, Madrid, Spain

^e Instituto de Ciencias del Corazón (ICICOR), Hospital Clínico Universitario de Valladolid, Valladolid, Spain

^f Departamento de Farmacología, Facultad de Medicina, Universidad Autónoma de Madrid and Instituto de Investigación Hospital Universitario La Paz (IdiPAZ), Spain

^g Ciber de Enfermedades Cardiovasculares (CIBERCV), Instituto de Salud Carlos III, Madrid, Spain

Received 9 May 2017; accepted 6 July 2017

Available online 30 August 2017

KEYWORDS

Lipid profiling;
Obesity;
Cardiac remodeling;
Fibrosis

Abstract

Aims: To explore the impact of obesity on the cardiac lipid profile in rats with diet-induced obesity, as well as to evaluate whether or not the specific changes in lipid species are associated with cardiac fibrosis.

Methods: Male Wistar rats were fed either a high-fat diet (HFD, 35% fat) or standard diet (3.5% fat) for 6 weeks. Cardiac lipids were analyzed using by liquid chromatography-tandem mass spectrometry.

Results: HFD rats showed cardiac fibrosis and enhanced levels of cardiac superoxide anion (O_2^*), HOMA index, adiposity, and plasma leptin, as well as a reduction in those of cardiac glucose transporter (GLUT 4), compared with control animals. Cardiac lipid profile analysis showed a significant increase in triglycerides, especially those enriched with palmitic, stearic, and arachidonic acid. An increase in levels of diacylglycerol (DAG) was also observed. No changes in cardiac levels of diacyl phosphatidylcholine, or even a reduction in total levels of diacyl phosphatidylethanolamine, diacyl phosphatidylinositol, and sphingomyelins (SM) was observed in HFD, as compared with control animals. After adjustment for other variables (oxidative stress,

* Corresponding author.

E-mail address: vcara@ucm.es (V. Cachofeiro).

¹ These authors contributed equally to this work.

RESEARCH ARTICLE

Inhibition of galectin-3 ameliorates the consequences of cardiac lipotoxicity in a rat model of diet-induced obesity

Gema Marín-Royo^{1,*}, Isabel Gallardo^{2,*}, Ernesto Martínez-Martínez¹, Beatriz Gutiérrez², Raquel Jurado-López¹, Natalia López-Andrés³, Josué Gutiérrez-Tenorio¹, Eduardo Rial⁴, María Visitación Bartolomé^{5,6}, María Luisa Nieto^{2,6,‡} and Victoria Cachofeiro^{1,6,‡,§}

ABSTRACT

Obesity is accompanied by metabolic alterations characterized by insulin resistance and cardiac lipotoxicity. Galectin-3 (Gal-3) induces cardiac inflammation and fibrosis in the context of obesity; however, its role in the metabolic consequences of obesity is not totally established. We have investigated the potential role of Gal-3 in the cardiac metabolic disturbances associated with obesity. In addition, we have explored whether this participation is, at least partially, acting on mitochondrial damage. Gal-3 inhibition in rats that were fed a high-fat diet (HFD) for 6 weeks with modified citrus pectin (MCP; 100 mg/kg/day) attenuated the increase in cardiac levels of total triglyceride (TG). MCP treatment also prevented the increase in cardiac protein levels of carnitine palmitoyl transferase IA, mitofusin 1, and mitochondrial complexes I and II, reactive oxygen species accumulation and decrease in those of complex V but did not affect the reduction in ¹⁸F-fluorodeoxyglucose uptake observed in HFD rats. The exposure of cardiac myoblasts (H9c2) to palmitic acid increased the rate of respiration, mainly due to an increase in the proton leak, glycolysis, oxidative stress, β -oxidation and reduced mitochondrial membrane potential. Inhibition of Gal-3 activity was unable to affect these changes. Our findings indicate that Gal-3 inhibition attenuates some of the consequences of cardiac lipotoxicity induced by a HFD since it reduced TG and lysophosphatidyl choline (LPC) levels. These reductions were accompanied by amelioration of the mitochondrial damage observed in HFD rats, although no improvement was observed regarding insulin resistance. These findings increase the interest for Gal-3 as a potential new target for therapeutic intervention to prevent obesity-associated cardiac lipotoxicity and subsequent mitochondrial dysfunction.

KEY WORDS: Galectin-3, Insulin resistance, Lipotoxicity, Mitochondria, Obesity, Oxidative stress

¹Departamento de Fisiología, Facultad de Medicina, Universidad Complutense de Madrid and Instituto de Investigación Sanitaria Gregorio Marañón (IISGM), Madrid 28040, Spain. ²Instituto de Biología y Genética Molecular, CSIC-Universidad de Valladolid, Valladolid 47003, Spain. ³Cardiovascular Translational Research, Navarrabiomed (Miguel Servet Foundation), Instituto de Investigaciones Sanitarias de Navarra (IdiSNA), Pamplona 31008, Spain. ⁴Centro de Investigaciones Biológicas, CSIC, Madrid 28040, Spain. ⁵Departamento de Oftalmología y Otorrinolaringología, Facultad de Psicología, Universidad Complutense, Madrid 28223, Spain. ⁶Ciber de Enfermedades Cardiovasculares (CIBERCv). Instituto de Salud Carlos III, Madrid 28029, Spain.

*These authors contributed equally to this work

‡These authors contributed equally to this work

§Author for correspondence (vcara@ucm.es)

 V.C., 0000-0001-6959-6293

This is an Open Access article distributed under the terms of the Creative Commons Attribution License (<http://creativecommons.org/licenses/by/3.0>), which permits unrestricted use, distribution and reproduction in any medium provided that the original work is properly attributed.

Received 20 September 2017; Accepted 29 December 2017

INTRODUCTION

Obesity is a chronic disease characterized by excessive accumulation of adipose tissue and lipids forming ectopic fat deposits in different tissues, including the heart (Abdurrachim et al., 2014; French et al., 2016; Ghosh et al., 2011). This excessive accumulation of lipid in the heart – termed cardiac lipotoxicity – can trigger cellular alterations since lipids are important regulators of cardiac function through their role in membrane structure, transport, signaling and as substrate for β -oxidation for obtaining energy in the mitochondria (Cedars et al., 2009; Lim et al., 2011). Cardiac lipotoxicity not only involves an excessive accumulation of intramyocellular triglycerides (TGs) in the heart but also changes in different lipid classes, as well as in their fatty acid composition, thereby facilitating the formation of active lipid mediators which affect metabolism and cardiac function, in part by altering mitochondrial function (Bugger and Abel, 2008; Elezaby et al., 2015; Lucas et al., 2016; Wang et al., 2015).

A common additional feature of the obese heart is impaired insulin signaling, which represents an adaptation of the heart to an excess of calories, which promotes the development of diabetic cardiomyopathy (Guo and Guo, 2017; Jia et al., 2016; Riehle and Abel, 2016). This condition not only alters cardiac metabolism but also increases myocardial oxygen consumption, reduces cardiac efficiency by affecting mitochondrial function and increases oxidative stress with the mitochondria being the main source of reactive oxygen species (ROS) (Boudina et al., 2007; Elezaby et al., 2015; McMurray et al., 2016).

Galectin-3 (Gal-3) is a member of a β -galactoside-binding lectin family produced in the heart and whose expression is upregulated in obesity (Martínez-Martínez et al., 2014). Its role as a central mediator of cardiovascular fibrosis and the inflammatory processes present in different pathological situations, including obesity, has been demonstrated (Martínez-Martínez et al., 2014, 2015b). In addition, the potential role of Gal-3 as a regulator of cardiac oxidative stress which can facilitate the development of fibrosis has been suggested since it is able to upregulate Nox4 expression in cardiac fibroblasts (He et al., 2017). In addition, we have reported Gal-3 to be a mediator of leptin-induced ROS production in the heart of obese rats (Martínez-Martínez et al., 2014, 2015b). However, information regarding the role of Gal-3 in the metabolic consequences of obesity is not well established since it has exhibited roles of being both mediator and preventer of metabolic disorders (Martínez-Martínez et al., 2016; Menini et al., 2016). Therefore, the aim of this study was to explore the potential contribution of Gal-3 to the metabolic disturbances associated with obesity. In addition, we have explored whether its participation is, at least partially, acting on mitochondrial damage. To address this issue, we analyzed the effect of the specific Gal-3 inhibitor modified citrus pectin (MCP) (Martínez-Martínez et al., 2015b) by using an animal model

of diet-induced obesity and cultured cardiomyoblasts stimulated by palmitic acid.

RESULTS

Consequences of Gal-3 activity inhibition on body weight, cardiac function and fibrosis, and blood pressure in rats that had been fed a high-fat diet

Animals that are fed a high-fat diet (HFD) show an increase in body weight, cardiac hypertrophy and interstitial fibrosis, although no changes in cardiac function or blood pressure, when compared to control rats (Martinez-Martinez et al., 2015b) after 6 weeks of HFD intake. Gal-3 protein expression was upregulated in hearts of HFD rats, and MCP treatment reduced the increase in total cardiac collagen content without modifying either body weight or cardiac hypertrophy (Martinez-Martinez et al., 2015b). MCP did not affect any of these parameters in control animals (Martinez-Martinez et al., 2015b). Therefore, and to simplify the data, only rats fed on a standard diet (CT), and on HFD or HFD+MCP are presented in the results.

Effect of Gal-3 activity inhibition on cardiac glucose use and insulin resistance in HFD-fed rats

Next, we addressed whether upregulation of Gal-3 is involved in the changes of glucose use observed in obese rats. Therefore, PET studies were performed to assess their use of cardiac glucose. Representative examples of PET images (Fig. 1A,B) revealed that uptake of fluorine-18 (^{18}F)-tagged fluorodeoxyglucose (FDG) in the heart was higher in the control group than in obese animals. Administration of MCP did not increase myocardial ^{18}F -FDG uptake. Similarly, dietary addition of MCP did not affect the increase of the homeostatic model assessment (HOMA) index in obese rats (Fig. 1C).

Consequences of Gal-3 activity inhibition on cardiac lipid profile in HFD-fed rats

As expected, obese animals showed an increase in total TG content in the heart (Fig. 2A), mainly due to an accumulation of TGs enriched with palmitic acid (16:0) and, to a lesser extent, TGs enriched with stearic acid (18:0) and arachidonic acid (20:4)

(Fig. 2B). In fact, obese animals showed an overall increase (4-fold; $P<0.001$) in TGs enriched with saturated fatty acids, although no significant changes were observed in the amounts of polyunsaturated fatty acids (data not shown). Treatment with MCP was able to reduce this rise observed in animals that were fed an HFD (Fig. 2A-B). An increase in the only type of ceramide (Cer) detected (Cer d18:1/16:0) was observed in HFD rats as compared with control animals (Fig. 2C). However, a reduction in the levels of total sphingomyelin (SM) was observed in HFD-fed animals as compared with control animals (Fig. 2D), a consequence of the decrease in the majority of the eight species of SM detected. MCP treatment was unable to revert this SM reduction (Fig. 2C,D). A negative correlation was observed between levels of total SM and Cer ($r=-0.5274$; $P=0.0433$). In addition, a correlation was found between Cer and ^{18}F -FDG cardiac uptake levels ($r=-0.668$; $P=0.0065$) and also between total SM levels and those of ^{18}F -FDG cardiac uptake ($r=0.6220$; $P=0.0175$). A similar correlation was found between the HOMA index and Cer levels ($r=0.6299$; $P=0.012$). Given that phosphatidyl choline (PC) and lysophosphatidyl choline (LPC) are involved in various diseases and because altered levels of LPC in the serum is considered to be a specific metabolic trait associated with obesity (Li et al., 2014; Tulipani et al., 2016), we focused on the types of PC and LPC found in the hearts of HFD rats. No significant differences were observed in the levels of total PC in the hearts of CT and HFD rats. About 56 types of PC were detected in hearts from CT rats, and their expression pattern was very similar to those observed in the heart of the HFD group (data not shown). However, an increase was found in the level of total LPC in HFD compared to CT animals (Fig. 2E). This increase was mainly due to the rise in those types of LPC enriched with stearic acid – LPC (18:0), or arachidonic acid – LPC (20:4) (Fig. 2F). The levels of detected LPC (16:0), LPC (18:2), LPC (18:3), LPC (22:5) and LPC (22:6) were not affected by the HFD. Treatment with MCP was able to prevent the increase in total LPC levels and in those enriched with stearic (18:0) or arachidonic (20:4) acids in HFD rats (Fig. 2E,F). Total LPC levels were correlated to those TGs enriched with palmitic acid ($r=0.6841$; $P=0.0048$). The increase in TGs was associated with higher levels of

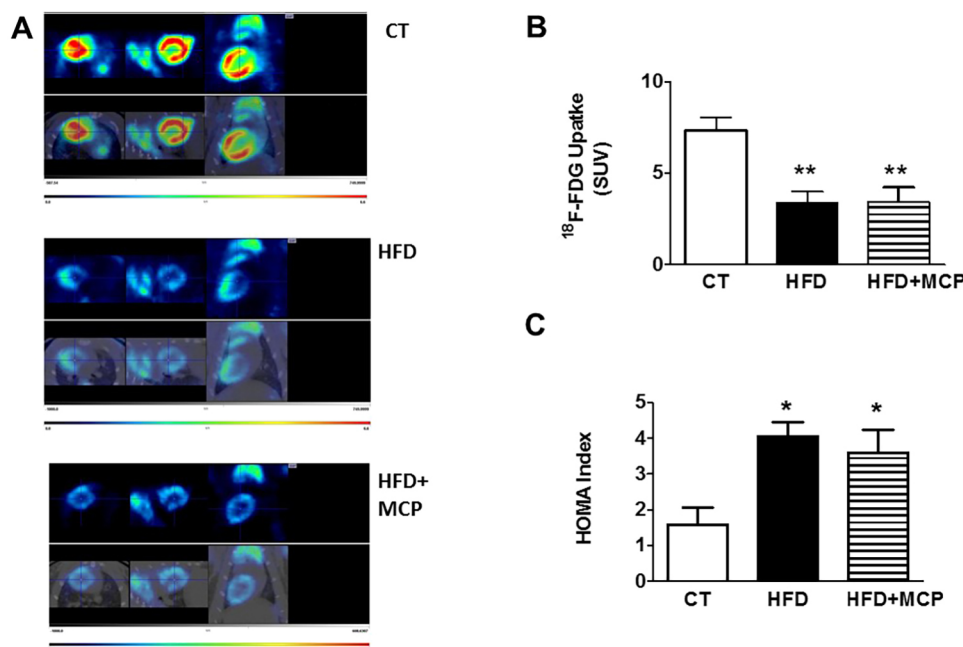


Fig. 1. Impact of Gal-3 inhibition on cardiac ^{18}F -FDG-uptake and the HOMA index in obese rats. (A) Representative photographs of ^{18}F -Fluorodeoxyglucose (FDG) PET/CT scans of the heart from rats fed a standard diet (CT) or a high fat diet (HFD) treated with vehicle or with MCP, the inhibitor of Gal-3 activity (100 mg/kg/day) in coronal, sagittal and *trans*-axial views scaled to SUV. (B) Quantification in SUV units. (C) HOMA index of the different experimental groups. Bar graphs represent the mean \pm s.e.m. of 6-8 animals. * $P<0.05$; ** $P<0.01$ control group.

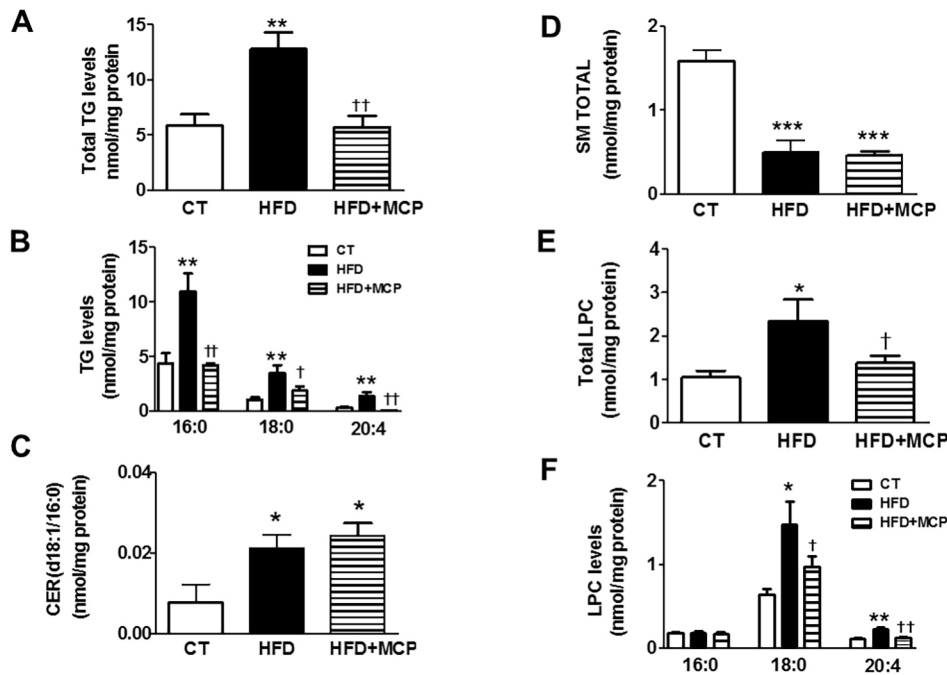


Fig. 2. Effects of Gal-3 inhibition on lipid species in heart from control and obese rats. Rats were fed a standard diet (CT) or a high fat diet (HFD) and treated with control vehicle or with the Gal-3 activity inhibitor MCP (100 mg/kg/day). Cardiac levels of (A) total TGs, (B) the three main types of TG, (C) ceramide (Cer), (D) total sphingomyelins (SM), (E) total lyso phosphatidylcholine (LPC), (F) the three main types of LPC. Bar graphs represent the mean \pm s.e.m. of 6-8 animals. * P <0.05; ** P <0.01; *** P <0.001 vs control group. † P <0.05; †† P <0.01; ††† P <0.001 vs HFD group.

CPT1A, the enzyme that controls the entry of long-chain fatty acyl CoA into mitochondria (Fig. 3A). Treatment with the inhibitor of Gal-3 was able to normalize CPT1A levels in HFD rats (Fig. 3A).

Consequences of inhibition of Gal-3 activity on cardiac mitochondria dynamic in HFD-fed rats

Considering the accumulation of fatty acids in the mitochondria of obese animals, we explored the consequences of this accumulation on

the mitochondrial dynamics. To this end, we evaluated the levels of two proteins, mitofusin 1 and DRP1, involved in the process of fusion and fission. As shown in Fig. 3B, the protein levels of mitofusin 1 are higher in obese animals than in controls. MCP treatment was able to reduce these high levels. By contrast, levels of the fission marker DRP1 were unaffected by either obesity or Gal-3 inhibition (data not shown). In addition, obese animals showed an increase in mitochondrial oxidative stress in response to MitoSOX (red

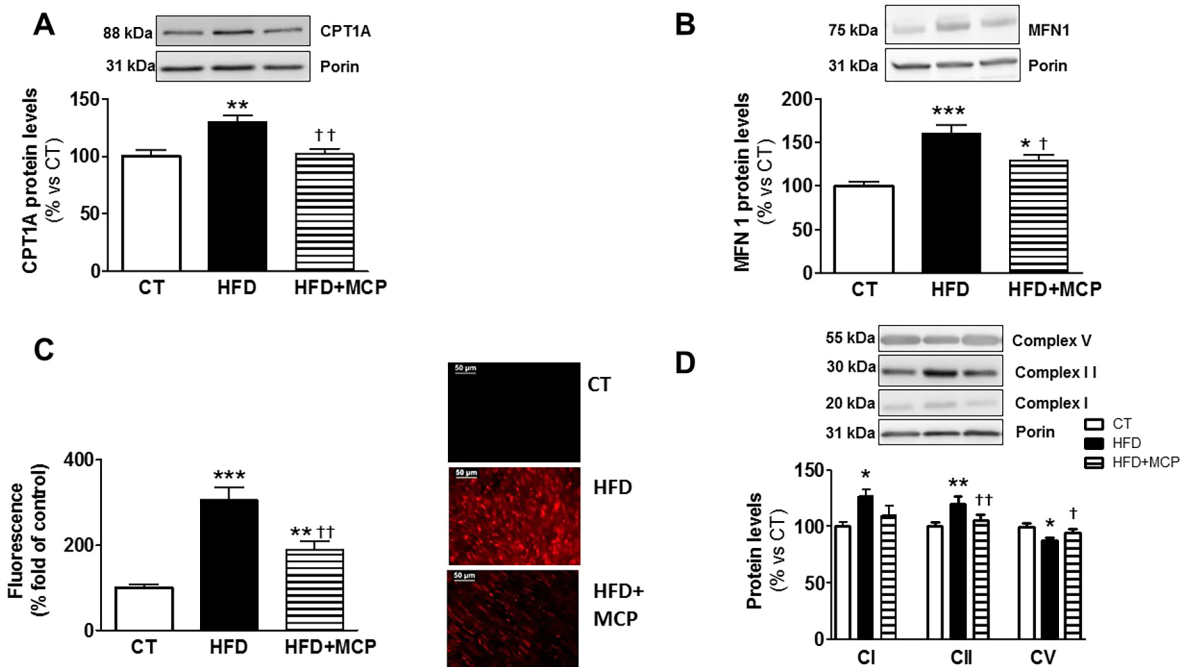


Fig. 3. Impact of Gal-3 inhibition on proteins and superoxide anion production in hearts from control and obese rats. Hearts from rats fed a standard diet (CT) or a high fat diet (HFD) treated with vehicle or with the inhibitor of Gal-3 activity (modified citrus pectin; MCP; 100 mg/kg/day) were analyzed. Protein expression of (A) carnitine palmitoyl transferase IA (CPT1A), (B) mitofusin 1 (MFN1), (D) for mitochondrial complexes I (subunit NDUFB8), II (30 kDa) and V (alpha subunit) are presented. (C) Representative microphotographs (magnification \times 40) of cardiac sections labeled with MitoSOX and quantification of superoxide anions in heart. Bar graphs represent the mean \pm s.e.m. of 6-8 animals normalized to porin. Scale bars: 50 μ m. * P <0.05; ** P <0.01 vs control group. † P <0.05; †† P <0.01 vs HFD group.

mitochondrial superoxide indicator) as indicated by more-intense fluorescence staining in the heart of the obese animals compared with control animals (Fig. 3C). A correlation was found between levels of mitochondrial ROS, and levels of total TGs (Table 1) and of TGs enriched with stearic or arachidonic acid (Table 1). We also evaluated the protein levels of the components of mitochondrial respiratory chain complexes. As shown in Fig. 3D, obesity exerts a different impact on different complexes since obese animals show an increase in complexes I and II, and a decrease in complex V, the ATP synthase. No changes were observed in the levels of complexes III and IV (Fig. S1). MCP treatment was able to reverse these changes.

Effect of palmitic acid on mitochondrial function in rat cardiomyoblasts – consequences of Gal-3 activity inhibition

Taking the observed accumulation of palmitic acid into consideration, we decided to explore its effects on mitochondrial function by using cultured rat cardiomyoblasts. Fig. S2 shows that palmitic acid was unable to affect cell viability at the doses used (100 $\mu\text{mol/l}$, 200 $\mu\text{mol/l}$ and 300 $\mu\text{mol/l}$). Next, we performed a ‘mitochondrial stress test’ in order to evaluate the mitochondrial bioenergetics caused by palmitic acid. The general scheme of the stress test is shown in Fig. S3A. Palmitic acid caused a modest and dose-dependent increase in the basal rate of respiration (Fig. S3A) and was paralleled by a dose-dependent increase of the extracellular acidification rate (ECAR) signal, indicating that palmitic acid is lowering the OXPHOS efficiency due to its uncoupling capabilities (Fig. S3B). Indeed, the proton leakage rate (Fig. S3C) was significantly increased in the palmitic acid-treated cells. The presence of MCP did not significantly alter the cellular energetics induced by palmitic acid (200 $\mu\text{mol/l}$; Fig. 4A-C). Additionally, as shown in Fig. S4A,B, the presence of palmitic acid for 24 h was able to reduce Rhodamine 123 staining in rat cardiomyoblasts in a dose-dependent manner, thereby reinforcing the idea that the increase in proton leak due to fatty acid uncoupling causes a reduction in the mitochondrial potential membrane. The presence of MCP did not alter the decrease in Rhodamine 123 staining caused by palmitic acid (200 $\mu\text{mol/l}$; Fig. 4D). Likewise, the presence of triacsin C – the inhibitor of acyl-CoA synthase – was unable to modify the effect induced by palmitic acid (Fig. S4C). In addition, palmitic acid was able to increase mitochondrial ROS production in a dose-dependent manner, as suggested by an increase in MitoSOX-induced fluorescence in palmitic acid-treated cells relative to that of vehicle-treated cells (Fig. S5A-B). The presence of MCP did not significantly alter the fluorescence intensity induced by MitoSOX in cells treated with palmitic acid (200 $\mu\text{mol/l}$; Fig. 4E). This was accompanied by a dose-dependent reduction in staining with the fluorochrome 10-N-nonyl-Acridin Orange (NAO), indicating an increase in the levels of oxidized cardiolipins (Fig. S6). Finally, palmitic acid was able to increase the β -oxidation in a time-

dependent manner (Fig. S7). The presence of MCP did not significantly alter this effect induced by palmitic acid (Fig. 4F).

DISCUSSION

The role of Gal-3 as a central mediator of cardiovascular fibrosis and the inflammatory processes present in different pathological situations has been amply demonstrated (Calvier et al., 2013, 2015; Martinez-Martinez et al., 2014, 2015a,b). We here report for the first time that Gal-3 can modulate some of the metabolic consequences of obesity, since the inhibitor of Gal-3 activity MCP reduced cardiac lipotoxicity and ameliorated the mitochondrial damage observed in the heart of obese rats.

Our present data show a significant increase in TG levels in the heart of normotensive obese animals, confirming previous clinical and experimental studies (Kroon et al., 2017; Shimabukuro et al., 2013). This increase was mainly a consequence of the rise in the levels of TGs enriched with saturated (16:0, 18:0) and polyunsaturated (20:4) fatty acids. We have also found an increase in LPC levels, mainly of those enriched with fatty acids 20:4 and 18:0. A similar increase has been reported for circulating LPC levels in obese patients and in experimental models of obesity (Eisinger et al., 2014; Li et al., 2014; Tonks et al., 2016). It should be noted, however, that reductions have been reported in other studies, which may be the result of varying LPC fatty acid composition (Li et al., 2014; Tulipani et al., 2016; Wahl et al., 2012) and suggests a more-complex effect of obesity in this lipid class. In contrast, PC profiles were not affected in HFD rats. Therefore, our data support the idea that cardiac lipotoxicity involves not only variations in the type of lipid but is also due to differences in their fatty acid composition.

Neither TG nor LPC levels seem to be major determinants of the altered cardiac glucose use observed in HFD animals because no correlation was found amongst these parameters. In addition, treatment with MCP was able to normalize both cardiac TG and LPC levels without altering the abnormal ^{18}F -FDG cardiac uptake. These data confirm previous observations that found no link between either TG or LPC circulating levels and insulin resistance in the context of obesity (Coen and Goodpaster, 2012; del Bas et al., 2016; Eisinger et al., 2014; Tulipani et al., 2016). However, the reduced cardiac SM levels observed in HFD rats might participate in the cardiac insulin resistance observed in these animals since a direct correlation between levels of SM and ^{18}F -FDG uptake was observed, confirming previous data (Denimal et al., 2016; Tonks et al., 2016). In agreement with this observation, we have found that cardiac SM levels are independent predictors of GLUT4 cardiac levels in HFD (Marin-Royo et al., 2017). In addition, and considering the role of Cer in the pathogenesis of diabetes (Galadari et al., 2013), our data here support the participation of this lipid class, whose levels were increased in response to a HFD and associated with increased cardiac levels of ^{18}F -FDG uptake. Cer levels result from both *de novo* synthesis as well as hydrolysis of SM, suggesting a link between both lipids; in fact, a negative correlation was found between them. A variety of potential mechanisms – oxidative stress, changes in mitochondrial function and endoplasmic reticulum stress – might underlie these effects (Fucho et al., 2017; Petersen and Shulman, 2017; Yazici and Sezer, 2017).

Our present study shows an increase of mitochondrial oxidative stress in the heart of normotensive obese animals, which was accompanied by some mitochondrial alterations: an increase in CPT1A, mitofusin 1, and respiratory chain complexes I and II, as well as a reduction of complex V. These alterations suggest that changes occur not only in the context of mitochondrial machinery but also in that of mitochondrial morphology. This is in agreement

Table 1. Association between the levels of mitochondrial ROS and those of lipids in the hearts of control and obese rats

Mitochondrial ROS levels	<i>r</i>	<i>P</i> value
Total TGs	0.6523	0.0045
TG (16:0)	0.7941	0.0002
TG (18:0)	0.555	0.03
TG (20:4)	0.7719	0.0007
Total LPC	0.8996	<0.0001
LPC (18:0)	0.9031	<0.0001
LPC (20:4)	0.7509	0.0013

TGs, triglycerides; LPC, lysophosphatidylcholine; *r*, correlation coefficient obtained using a linear regression model.

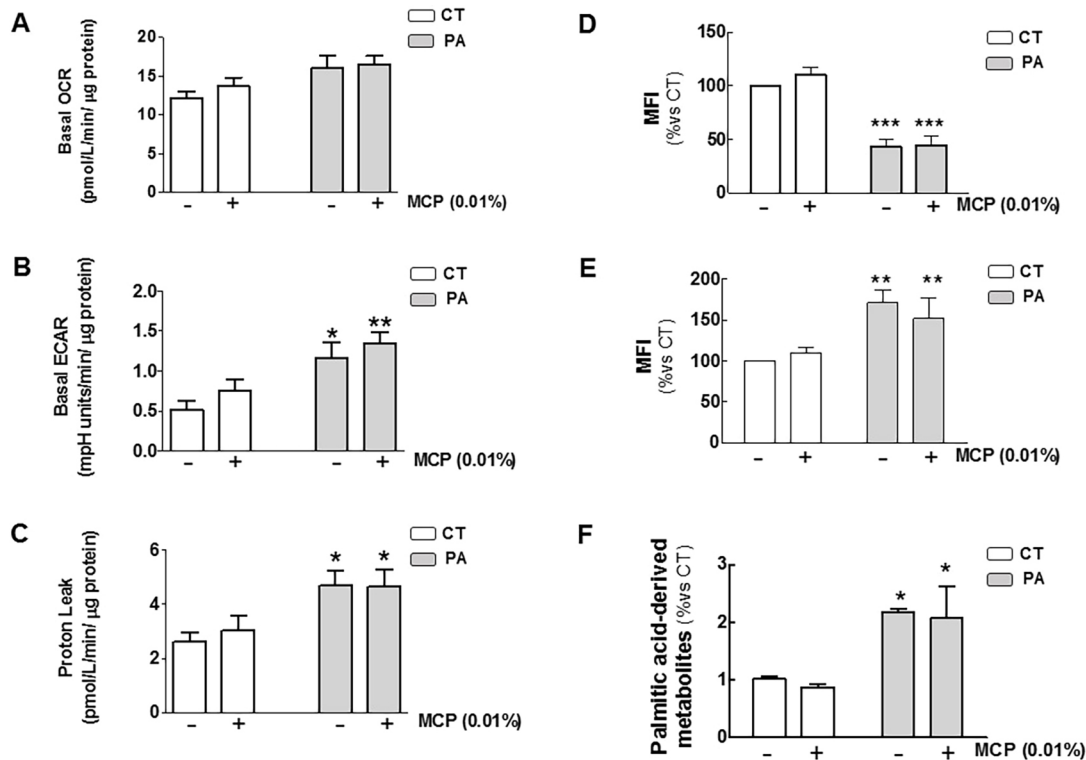


Fig. 4. Effects of Gal-3 inhibition on mitochondrial function, glycolysis, membrane potential, ROS production and β -oxidation in palmitic-acid-treated H9c2 cells. (A) Basal respiration expressed as oxygen consumption rate (OCR). (B) Basal glycolysis expressed as extracellular acidification rate (ECAR). (C) Proton leak respiration expressed as OCR. (D) Quantification of flow cytometry analysis of mitochondrial membrane potential in cells stained with Rhodamine 123 expressed as mean fluorescence intensity (MFI). (E) Quantification of flow cytometry analysis of mitochondrial superoxide anions in cells labeled with MitoSOX expressed as MFI, (F) Quantification of β -oxidation in cardiac myoblasts treated for 24 h with palmitic acid (200 μ M) in the presence of absence inhibitor of Gal-3 activity (modified citrus pectin; MCP; 0.01%). Error bars represent the mean \pm s.e.m. of four assays. ** P <0.01; *** P <0.001 vs vehicle-treated cells (CT).

with the concept that mitochondrial dysfunction is one mechanism that participates in the cardiac damage associated with obesity, as mitochondria play a central role in the energy production essential in maintaining cardiac activity (Mercer et al., 2010; Wang et al., 2015). The fact that treatment with MCP reduced oxidative stress and normalized the levels of CPT1A, mitofusin 1 and respiratory chain complexes further supports this role. In fact, connections between oxidative stress, lipotoxicity and mitochondrial dysfunction has been suggested (Mercer et al., 2010; Schulze et al., 2016; Wang et al., 2015). Supporting this concept, we have found a correlation between the cardiac levels of TGs and LPC, and those of mitochondrial ROS in MCP-treated and untreated HFD rats. In addition, we have observed that palmitic acid, the most elevated fatty acid in TGs (the main cardiac energetic reservoir of HFD rats) was able to stimulate mitochondrial ROS production in H9c2 cells, confirming previous observations (Miller et al., 2005).

An increase in ROS can be the consequence of either an increase in oxidative metabolism or a reduction in antioxidant capacity (Cheng et al., 2017; Vakifahmetoglu-Norberg et al., 2017). Apart from the main contributors to mitochondrial ROS production, complex I and complex III, several oxidoreductases located in mitochondrial membrane can produce superoxide at significant rates during oxidation of fatty acids (Andreyev et al., 2015; Brand, 2010). This oxidant environment can disturb mitochondrial membrane phospholipids, including cardiolipins, as evident by the significant reduction in NAO fluorescence. The peroxidized cardiolipin generated changes in the physico-chemical properties of the mitochondrial membrane that, in turn, could be altering mitochondrial bioenergetics since cardiolipins play a central role

in normal function and structure of the inner mitochondrial membrane (Birk et al., 2014; Paradies et al., 2014). In fact, this could explain the observed increase in mitofusin 1, which suggests an increase in mitofusion, a process that represents an adaptive pro-survival response against stress (Tondera et al., 2009).

The increase in the proton leak in H9c2 cells stimulated by palmitic acid suggests a reduced efficiency of the oxidative phosphorylation. The increase observed in the β -oxidation of H9c2 cells in the same conditions could be explained as a compensatory mechanism for the oxidative phosphorylation reduction. This process might occur in the heart of obese animals since the decreased ATP synthase levels observed in these animals was accompanied by an increase in CPT1A involved in the mitochondrial uptake of fatty acids, an essential step for the β -oxidation in the mitochondria. However, the compensatory increase in glycolysis induced by palmitic acid in H9c2 in order to maintain ATP levels are adequate to meet the energy demands of the cell, although anaerobic ATP production might be limited in obese animals because the glucose uptake of the heart is reduced. We found that palmitic acid was able to reduce mitochondrial membrane potential independently of its transformation into acyl-CoA because inhibition of triacsin C, the enzyme involved in this step, had no effect. Indeed, it has previously been reported that fatty acids have a protonophoric activity that are likely to be mediated by the adenine nucleotide translocator (ANT) (Ash and Merry, 2011).

Our data show that the Gal-3 activity inhibitor is able to prevent some of the changes observed in the cardiac lipid profile in obese animals and, thus, supports a role of Gal-3 in cardiac lipotoxicity. In fact, addition of MCP was able to reduce the excessive accumulation

of TGs and LPC. The exact mechanism through which Gal-3 participates in cardiac lipotoxicity is unclear, although its ability to produce an oxidant environment that can, finally, affect mitochondrial activity, might be an option. In support of this concept is the observation that Gal-3 colocalizes with ATP synthase in the inner membrane of mitochondria and has an inhibitory effect on ATP synthase in human colon cancer cells (Kim et al., 2008). Interestingly, MCP does not protect against palmitic acid-induced mitochondrial dysfunction in H9c2 cells *in vitro*, thus, suggesting that the beneficial effect induced by MCP in obese animals is a consequence of Gal-3 inhibition and not that of other actions of this drug, since Gal-3 production was not induced by palmitic acid being present in the cells (data not shown).

By contrast, MCP did not affect glucose homeostasis. In fact, MCP did not modify the levels of SM and Cer – that are related to insulin resistance – further supporting the lack of effect Gal-3 has in glucose homeostasis in our model. By contrast, a recent study has shown that, in mice, administration of Gal-3 is associated with insulin resistance, and that Gal-3 inhibition, pharmacologically or genetically, causes glucose intolerance in HFD animals for 8 weeks (Li et al., 2016). However, this role has not been supported by previous data that have shown that Gal-3 knockout mice that had been fed a HFD for 12 or 18 weeks present a dysregulated glucose metabolism (Pang et al., 2013; Pejnovic et al., 2013). Therefore, the specific role of Gal-3 as a player in metabolic disorders needs further investigation.

In summary, to understand the mechanisms that underlying the damage associated with cardiac lipotoxicity in the context of obesity is crucial. Our present data suggest a role of Gal-3 in this damage, draw a more-complex scenario for the actions of Gal-3 that, in obese animals, is overexpressed in the heart, and seems to modulate some of the consequences of cardiac lipotoxicity. However, further work to demonstrate its specific role in mitochondrial function will help to clarify the underlying mechanism and might also come up with new approaches in the management of obesity-related heart damage.

MATERIALS AND METHODS

Animal model

Male Wistar rats of 150 g (Harlan Ibérica, Barcelona, Spain) were fed either a high-fat diet (HFD) containing 35% fat [Envigo (formerly Harlan) Teklad global rodent diet number, TD.03307, MN; $n=16$] or a standard diet (CT) containing 3.5% fat (Harlan Teklad number, TD.2014, MN; $n=16$) for 6 weeks. For the same period the Gal-3 activity inhibitor MCP (100 mg/kg per day), was supplied to half of each group in the drinking water. The Animal Care and Use Committee of Universidad Complutense de Madrid approved all experimental procedures according to the Spanish Policy for Animal Protection RD53/2013, which meets the European Union Directive 2010/63/UE.

In vivo PET-CT imaging to study uptake of ^{18}F -fluorodeoxyglucose in the heart

Myocardial metabolic activity was evaluated by means of a small-animal dedicated dual scanner (Albira PET/CT scanner, Bruker NMI, Valencia Spain). One week before the end of the experiment, animals were starved for 18 h, followed by intraperitoneal injection with ^{18}F -fluorodeoxyglucose [FDG; 12.99 ± 0.04 MBq in 0.2 ml NaCl (0.9%); Instituto Tecnológico PET, Madrid, Spain]. Twenty min later, rats underwent PET and computed tomography (CT) scanning under isoflurane anesthesia. The acquired PET and CT images were then reconstructed by, respectively, using maximum-likelihood (ML) expectation-maximization (EM) [ML-EM] and filtered-back projection algorithms. In order to account for the weight difference in rats and the [^{18}F] doses of injected FDG, we calculated the standardized uptake value (SUV). The semi-quantitative SUV measurement is the most widely used in [^{18}F] FDG PET studies of both small animals and humans (Byrnes et al., 2014; Deleye et al., 2014). The software used was PMOD 3.6 (PMOD Technologies Ltd., Zurich, Switzerland).

To quantify the metabolic activity the CT image of the heart from each animal was registered to its corresponding PET image. Then a three-dimensional region of interest (ROI) was drawn on the fused PET/CT image to measure the metabolic activity of the entire left ventricle. These steps were carried out by using PMOD 3.0. SUV was obtained as an index of regional metabolic activity. The SUV parameter was calculated as a ratio of the ROI radioactivity concentration (kBq/ml) measured by the scanner and the administered dose (kBq) was decay-corrected at the time of the injection, divided by the body weight (g).

Isolation of cardiac mitochondria

Cardiac mitochondria were isolated as reported previously (Doerrier et al., 2016). Frozen hearts were placed into and washed with cold homogenization medium containing 0.075 mol/l sucrose, 1 mmol/l EDTA, 10 mmol/l Tris-HCl pH 7.4. Briefly, heart tissue was homogenized (1:10 w/v) at 800 rpm in a homogenizer (T 10 basic Ultra-turrax, Ika-Werke; Germany). The homogenates were centrifuged at 1300 g for 5 min at 4°C to remove nuclei and debris. Supernatants were separated and centrifuged at 12,000 g for 10 min at 4°C. The resulting pellets were suspended in homogenization medium and centrifuged twice at 14,400 g for 3 min at 4°C to wash the mitochondrial fraction. Mitochondrial pellets were stored at -80°C until use. Protein concentration was determined using the Bradford method.

Western blotting

Mitochondrial proteins were separated by SDS polyacrylamide electrophoresis (PAGE) and transferred to Hybond-c Extra nitrocellulose membranes (Hybond-P; Amersham Biosciences, Piscataway, NJ). Membranes were probed with primary antibody against the mitochondrial complex (Mitoprofile Total OXPHOS – CI subunit NDUFB8, CII-30 kDa, CIII-Core protein 2, CIV subunit I and the CV alpha subunit, ab110413, Abcam, Cambridge, UK; dilution 1/1000), carnitine palmitoyl transferase I (CPT1A, ab128568, Abcam, Cambridge; dilution 1/1000), dynamin-1-like protein (DRP1, ab56788, Abcam, Cambridge; dilution 1/1000), mitofusin 1 (MFN1, ab57602, Abcam, Cambridge; dilution 1/1000) and porin (ab15895, Abcam, Cambridge; dilution 1/1000) as a mitochondrial protein loading control. Signals were detected using the ECL system (Amersham Pharmacia Biotech). Results are expressed as an n-fold increase over the values of the control group in densitometric arbitrary units.

Measurement of mitochondrial ROS production

For detection of mitochondrial ion O_2^- production, cardiac sections (6 μm) were incubated with MitoSOXTM (red mitochondrial superoxide indicator; 5 $\mu\text{mol/l}$) for 10 min at 37°C. MitoSOX Red reagent is a live-cell permeant probe and is rapidly and selectively targeted to the mitochondria. Once in the mitochondria, MitoSOX Red reagent is oxidized by superoxide and exhibits red fluorescence. MitoSOX Red reagent is readily oxidized by superoxide but not by other reactive oxygen species (ROS) – or reactive nitrogen species (RNS) – generating systems. The oxidation product becomes highly fluorescent upon binding to nucleic acids. Fluorescent signals were viewed using a fluorescent laser scanning microscope (40 \times objective in Leica DMI 3000 microscope).

Quantitative analysis of O_2^- production was performed by using an image analyzer (LEICA Q550 IWB). Three sections per animal were quantified and averaged for each experimental condition. The mean fluorescence densities in the target region were analyzed. Results are expressed as an n-fold increase over the values of the control group in arbitrary units.

Lipidomic analysis

Methanol:chloroform (1:2) cardiac extracts were divided into two aliquots. One was evaporated to dryness and the pellet was resuspended in 250 μl of acetone:propanol:ethanol (3:4:3) and used to measure triglyceride (TG) content. The other aliquot was evaporated to dryness and the pellet re-suspended in 200 μl methanol:water (9:1) and used to measure phospholipids (PPLs). Extracts were kept at -80°C until analysis.

TG compounds were eluted at a flow rate of 0.4 ml/min using a gradient as follows: initial, 100% A; 3 min, 100% A; 6 min, 98% A; 8 min, 98% A; 9.5 min, 95% A; 11 min, 95% A; 16 min, 100% A, and this was kept isocratic for 2 min to recover initial pressure before next injection. Solvents

A and B were methanol:acetonitrile:isopropanol (Met:ACN:IPr 30:30:40, v/v/v) and ACN:IPr (3:7, v/v), respectively, both 0.1% NH₄OH (25%). To avoid the carry-over, which was calculated to be 12% for unsaturated TGs and 5% for saturated TGs, methanol was injected and an entire chromatographic run was performed, with an additional one performed after five samples were injected. An extract volume of 7.5 µl was injected into chromatographic columns. Mass spectrometric analysis was performed in positive mode (ESI+), using the following parameters: capillary, 0.8 kV; sampling cone, 15 V; source temperature, 90°C; desolvation temperature, 280°C; cone gas, 40 l/h; and desolvation gas, 700 liters/h. Data were acquired with the software Mass Lynx at a rate of 5 scans/s within the range 0–18 min, and m/z 100–1200 Da for the low-energy function and m/z 100–900 Da for the high-energy function (MS^E method, trap collision energy 30 V). LC and MS methods were optimized by using the commercial standards TG (18:2/18:2) and TG (16:0/16:0/16:0). These standards were also used to draw calibration curves for quantification.

PPLs compounds were eluted at a flow rate of 0.35 ml/min using a gradient as follows: initial, 100% A; 1 min, 100% A; 2.5 min, 20% A; 4 min, 20% A; 5.5 min, 0.1% A; 8.0 min, 0.1% A; 10 min, 100% A, and this was kept isocratic for 2 min to recover initial pressure before the following injection. Solvents were (A) methanol:water:formic acid (Met:H₂O:FA 50:50:0.5, v/v/v) and (B) Met:ACN:FA (59:40:0.5, v/v/v), both with 5 mmol/l ammonium formate. Methanol was injected every five samples and an entire chromatographic run was performed in order to clean the system for possible carry-over (<1%). An extract volume of 7.5 µl was injected. Mass spectrometer parameters were fitted as follows: capillary, 0.9 kV; sampling cone, 18 V; source temperature, 90°C; desolvation temperature, 320°C; cone gas, 45 l/h; and desolvation gas, 900 l/h. Data were acquired with the software MassLynx at a rate of 5 scans/s within the range 0–12 min and 100–1200 Da m/z for the low-energy function, and 50–900 Da m/z for the high-energy function (MS^E method, trap collision energy 30 V), with ionization in positive mode (ESI+) for detection of diacylphosphatidylcholines (PCs), ceramides (Cer) and sphingomyelins (SM). External commercial standards PC (10:0/10:0) were used for method optimization and quantification.

Up to three different chromatograms were manually checked for mass spectral peak identification where possible. Within each chromatographic point, m/z values with an intensity ≥700 were checked for this in order to afford a defined chromatographic peak (Extracted Ion Chromatogram, EIC); if positive, the elemental composition tool was then used to determine all the possible chemical compositions (C_nH_mO_pN_sP_rS_t) that were compatible with the isotopic distribution (M, M+1, M+2 and M+3 peaks) of a given m/z value.

Using LipidMaps, Metlin, CheBI, LipidBank and KEGG databases, a particular elemental composition was searched for possible known compounds. Where possible, acyl chains were aimed at being identified by data from the high-energy function (fragmentation). To assess the specific location of each acyl chain at the positions sn-1 or sn-2 of the glycerol backbone is not possible by using this methodology; thus, the most-current structure is indicated. The chromatographic peak area from the EIC of every m/z value detected, whether or not having been identified, was quantified using the QuanLynx application.

Chromatograms and mass spectra of all samples were processed with a MarkerLynx method in order to search for differential features (retention time m/z) amongst sample groups. Five injections of methanol were used as blanks to determine features prone to rejection. Only features that appeared in at least 66% of the samples were accepted. Sets of about 1650 features for data in negative mode and about 2109 features for data in positive mode were detected using the MarkerLynx application. They were checked manually to remove all the features that were present in the blanks. The array resulting from this process, which is comprised of samples and features as independent variables, and the feature signal intensity as dependent variable was submitted to multivariate statistical analysis using the Extended Statistics application that is available with the instrument software; this application is licensed from part of the statistical software SIMCA+ from Umetrics Ltd. (Sweden).

Cell culture

Cells of the H9c2 rat cardiomyoblast cell line (Merck, Darmstadt, Germany) were maintained in Dulbecco's modified Eagle's medium (DMEM; Merck, Darmstadt, Germany) supplemented with 25 mmol/l glucose, 1 mmol/l

pyruvate and 2 mmol/l L-glutamine. Cells were cultured according to the manufacturer's instructions and were used until passages 20–22. Cells were stimulated with 100, 200 or 300 µmol/l of palmitate – with bovine serum albumin (BSA) as a carrier – conjugated to 10% free fatty acids (FFA)-free BSA for 24 h for the different analyses in order to choose the dose appropriate for performing the experiments. The dose of 200 µmol/l was finally used in all analyses in the presence or absence of MPC (0.01%), which was added before incubation with the palmitic acid.

Measurements of cellular respiration and estimation of the rate of glycolysis

An XF24-3 extracellular flux analyzer (Seahorse Biosciences, North Billerica, MA) was used to determine the bioenergetic profile of the H9c2 cardiac myoblasts. 40×10³ cells/well were seeded in Seahorse XF24 plates and stimulated for 24 h with palmitate-BSA conjugated in 10% FFA-free BSA in the presence or absence of MCP. For the XF24-3 assays, DMEM used initially (see above) was replaced with fresh DMEM supplemented with 5.5 mmol/l glucose, 1 mmol/l pyruvate and 10 mmol/l L-glutamine, stimuli were added again and cells incubated at 37°C in a CO₂-free incubator for 1 h. Subsequently, the oxygen consumption rate (OCR) and extracellular acidification rate (ECAR), a proxy for lactate production, were recorded to assess the mitochondrial respiratory activity and glycolytic activity, respectively. After four measurements under basal conditions, cells were treated sequentially with 1 µmol/l oligomycin, 0.6 µmol/l carbonyl cyanide p-(trifluoromethoxy)phenylhydrazone (FCCP) and 0.4 µmol/l FCCP with three consecutive determinations under each condition that were averaged during data evaluation. At the end of the run, 1 µmol/l rotenone and 1 µmol/l antimycin A were added to determine the mitochondria-independent oxygen consumption and the value subtracted from all OCR measurements. ATP turnover was estimated from the difference between the basal and the oligomycin-inhibited respiration, and maximum respiratory capacity was the rate in the presence of the uncoupler FCCP. Protein concentration in each well was determined using the BCA method and results were normalized according to protein content. Experiments were repeated four times with similar results.

Viability assay

H9c2 cell proliferation was evaluated by using the Promega kit (Madison, WI), Cell Titer 96[®] Aqueous One Solution Cell Proliferation Assay, according to the manufacturer's recommendations. Briefly, cells were seeded in 96-well plates and serum-starved for 24 h. Cells were then stimulated with 100, 200 or 300 µmol/l of palmitate-BSA or 20% of fetal bovine serum (FBS). After 24 h of incubation, formazan product formation was assayed by recording the absorbance at 490 nm in a 96-well plate reader (OD value). Formazan is measured as an assessment of the number of metabolically active cells and expressed in percentages relative to unstimulated cells.

Fatty acid oxidation assay

H9c2 myoblasts were seeded on six-well plates, grown until semi-confluence and serum-starved overnight. Then, cells were incubated with ³H-Palmitate (0.25 µCi/ml) for 1 h at 37°C, and washed three times with 0.5% BSA-PBS to remove any unincorporated and surface-bound fatty acid. Subsequently, cells were pre-treated with 5 µmol/l of triacsin C for 30 min at 37°C and stimulated with 200 µmol/l of palmitate-BSA. After 6 h of incubation at 37°C, DMEM was removed from the plates and total cellular lipids were extracted according to the method of Bligh and Dyer (Bligh and Dyer, 1959). The incorporation of ³H-palmitate into total lipids as well as the radioactivity present in the aqueous phase corresponding to ³H-soluble metabolites (taken as measure of fatty acid β oxidation) were assayed for radioactivity by liquid scintillation counting.

Measurement of mitochondrial superoxide anion production and mitochondrial inner transmembrane potential detection

For detection of mitochondrial ion O₂⁻ production, H9c2 myoblasts were stimulated at 37°C with 200 µmol/l palmitate-BSA in the absence or presence of MCP (0.01%). Thereafter, cells were washed and loaded with 5 µmol/l MitoSOX[™] Red for 30 min, at 37°C. The fluorescent signal

was analyzed by recording FL2 fluorescence in a Gallius™ flow cytometer (Beckman Coulter).

To evaluate the mitochondrial transmembrane potential ($\Delta\psi_m$), H9c2 myoblasts were incubated with 4 $\mu\text{mol/l}$ of Rhodamine 123 for 15 min at 37°C. Stained cells were washed with serum-free medium and stimulated with the indicated doses with palmitate-BSA for 24 h at 37°C. After treatment, cells were washed with PBS and changes in fluorescence were monitored using flow cytometry analysis. In some experiments, before incubation with 200 $\mu\text{mol/l}$ of palmitate-BSA, H9c2 cells were pretreated for 30 min with 3 $\mu\text{mol/l}$ of Triacsin C, an inhibitor of long fatty acid acyl-CoA synthetase (Sigma, St Louis, MO) or with the indicated dose of MCP. Experiments were repeated at least three times. Cells were also visualized on a Leica TCS SP5 X confocal microscope with a $\times 40$ objective.

Measurement of mitochondrial cardiolipin by using NAO

10-N-nonyl-Acridin Orange (NAO; Invitrogen, Carlsbad, CA) is a fluorochrome that binds to intact mitochondrial cardiolipin and it is independent of the mitochondrial membrane potential over a physiologically relevant range (Maftah et al., 1989; Petit et al., 1992). Decreases in the fluorescence of NAO in cells have been reported to reflect the peroxidation of intracellular cardiolipin because the dye loses its affinity for peroxidized cardiolipin (Nomura et al., 2000).

H9c2 cells were treated with 100, 200 or 300 $\mu\text{mol/l}$ of palmitic acid conjugated to BSA for 24 h at 37°C. Afterwards, cells were stained with 5 $\mu\text{mol/l}$ of NAO for 15 min at 37°C in dark. Cells were then washed with PBS and NAO fluorescence intensity was analyzed by recording FL1 fluorescence in a Gallius™ flow cytometer (Beckman Coulter). Cells were also visualized on a Leica TCS SP5 X confocal microscope with a $\times 40$ objective. The cells were excited using 488 nm and emission of NAO was measured beyond 585 nm. Nuclei of cells were stained with DAPI as a counter stain. Experiments were repeated at least three times.

Statistical analysis

Continuous variables are expressed as mean \pm s.e.m. Normality of distributions was verified by means of the Kolmogorov–Smirnov test. One-way ANOVA was used and followed by Tukey test. Either Pearson or Spearman correlation analysis was used to examine association among different variables according to whether they are normally distributed. A value of $P < 0.05$ was used as the cutoff value for defining statistical significance. Data analysis was performed using the statistical program SPSS version 22.0 (SPSS Inc, Chicago, IL).

Acknowledgements

We thank Avelina Hidalgo, Blanca Martínez, Virginia Peinado, Roberto Cañadas and Alma Astudillo for their technical help and Anthony DeMarco for his help in editing the article. We thank Olimpio Montero for his help in the lipidomic analysis.

Competing interests

The authors declare no competing or financial interests.

Author contributions

Conceptualization: V.C., E.M.-M., R.J.-L., N.L.-A., E.R., M.V.B., M.L.N.; Methodology: V.C., G.M.-R., I.G., E.M.-M., B.G., R.J.-L., N.L.-A., J.G.-T., E.R., M.V.B., M.N.; Software: V.C., E.M.-M., B.G., R.J.-L., N.L.-A., E.R., M.L.N.; Validation: V.C., G.M.-R., B.G., R.J.-L., N.L.-A., J.G.-T., E.R., M.L.N.; Formal analysis: V.C., G.M.-R., I.G., E.M.-M., B.G., R.J.-L., N.L.-A., J.G.-T., E.R., M.V.B., M.L.N.; Investigation: V.C., G.M.-R., I.G., E.M.-M., B.G., R.J.-L., N.L.-A., J.G.-T., M.V.B., M.L.N.; Resources: V.C., G.M.-R., N.L.-A., M.L.N.; Data curation: V.C., G.M.-R., I.G., E.M.-M., R.J.-L., N.L.-A., J.G.-T., M.V.B., M.L.N.; Writing - original draft: V.C., G.M.-R., E.M.-M., N.L.-A., E.R., M.V.B., M.L.N.; Writing - review & editing: V.C., N.L.-A., E.R., M.L.N.; Visualization: V.C., G.M.-R., E.M.-M., M.L.N.; Supervision: V.C., R.J.-L., M.L.N.; Project administration: V.C.; Funding acquisition: V.C.

Funding

This work was supported by Instituto de Salud Carlos III – European Regional Development Fund (Fondo Europeo de Desarrollo Regional) [grant number: PI15/01060; CIBERCV] a way to build Europe. Ministerio de Economía y Competitividad [grant numbers: SAF2012-34460 and SAF2016-81063], the FPI Program del Gobierno de Castilla y León (co-funded by FSE). NL-A was supported

by a Miguel Servet grant CP13/00221 from the Instituto de Salud Carlos III – European Regional Development Fund (Fondo Europeo de Desarrollo Regional), a way to build Europe, Fondo de Investigaciones Sanitarias [PI15/02160].

Supplementary information

Supplementary information available online at <http://dmm.biologists.org/lookup/doi/10.1242/dmm.032086.supplemental>

References

- Abdurrachim, D., Ciapaite, J., Wessels, B., Nabben, M., Luiken, J. J. F. P., Nicolay, K. and Prompers, J. J. (2014). Cardiac diastolic dysfunction in high-fat diet fed mice is associated with lipotoxicity without impairment of cardiac energetics in vivo. *Biochim. Biophys. Acta* **1842**, 1525-1537.
- Andreyev, A. Y., Tsui, H. S., Milne, G. L., Shmanai, V. V., Bekish, A. V., Fomich, M. A., Pham, M. N., Nong, Y., Murphy, A. N., Clarke, C. F. et al. (2015). Isotope-reinforced polyunsaturated fatty acids protect mitochondria from oxidative stress. *Free Radic. Biol. Med.* **82**, 63-72.
- Ash, C. E. and Merry, B. J. (2011). The molecular basis by which dietary restricted feeding reduces mitochondrial reactive oxygen species generation. *Mech. Ageing Dev.* **132**, 43-54.
- Birk, A. V., Chao, W. M., Bracken, C., Warren, J. D. and Szeto, H. H. (2014). Targeting mitochondrial cardiolipin and the cytochrome c/cardiolipin complex to promote electron transport and optimize mitochondrial ATP synthesis. *Br. J. Pharmacol.* **171**, 2017-2028.
- Bligh, E. G. and Dyer, W. J. (1959). A rapid method of total lipid extraction and purification. *Can. J. Biochem. Physiol.* **37**, 911-917.
- Boudina, S., Sena, S., Theobald, H., Sheng, X., Wright, J. J., Hu, X. X., Aziz, S., Johnson, J. I., Bugger, H., Zaha, V. G. et al. (2007). Mitochondrial energetics in the heart in obesity-related diabetes: direct evidence for increased uncoupled respiration and activation of uncoupling proteins. *Diabetes* **56**, 2457-2466.
- Brand, M. D. (2010). The sites and topology of mitochondrial superoxide production. *Exp. Gerontol.* **45**, 466-472.
- Bugger, H. and Abel, E. D. (2008). Molecular mechanisms for myocardial mitochondrial dysfunction in the metabolic syndrome. *Clin. Sci. (Lond.)* **114**, 195-210.
- Byrnes, T. J. D., Xie, W., Al-Mukhailed, O., D'Sa, A., Novruzov, F., Casey, A. T. H., House, C. and Bomanji, J. B. (2014). Evaluation of neck pain with (18)F-NaF PET/CT. *Nucl. Med. Commun.* **35**, 298-302.
- Calvier, L., Miana, M., Reboul, P., Cachofeiro, V., Martínez-Martínez, E., de Boer, R. A., Poirier, F., Lacolley, P., Zannad, F., Rossignol, P. et al. (2013). Galectin-3 mediates aldosterone-induced vascular fibrosis. *Arterioscler. Thromb. Vasc. Biol.* **33**, 67-75.
- Calvier, L., Martínez-Martínez, E., Miana, M., Cachofeiro, V., Rousseau, E., Sádaba, J. R., Zannad, F., Rossignol, P. and López-Andrés, N. (2015). The impact of galectin-3 inhibition on aldosterone-induced cardiac and renal injuries. *JACC Heart Fail* **3**, 59-67.
- Cedars, A., Jenkins, C. M., Mancuso, D. J. and Gross, R. W. (2009). Calcium-independent phospholipases in the heart: mediators of cellular signaling, bioenergetics, and ischemia-induced electrophysiologic dysfunction. *J. Cardiovasc. Pharmacol.* **53**, 277-289.
- Cheng, J., Nanayakkara, G., Shao, Y., Cueto, R., Wang, L., Yang, W. Y., Tian, Y., Wang, H. and Yang, X. (2017). Mitochondrial proton leak plays a critical role in pathogenesis of cardiovascular diseases. *Adv. Exp. Med. Biol.* **982**, 359-370.
- Coen, P. M. and Goodpaster, B. H. (2012). Role of intramyocellular lipids in human health. *Trends Endocrinol. Metab.* **23**, 391-398.
- del Bas, J. M., Caimari, A., Rodríguez-Naranjo, M. I., Childs, C. E., Paras Chavez, C., West, A. L., Miles, E. A., Arola, L. and Calder, P. C. (2016). Impairment of lysophospholipid metabolism in obesity: altered plasma profile and desensitization to the modulatory properties of n-3 polyunsaturated fatty acids in a randomized controlled trial. *Am. J. Clin. Nutr.* **104**, 266-279.
- Deleay, S., Verhaeghe, J., Wyffels, L., Dedeurwaerdere, S., Stroobants, S. and Staelens, S. (2014). Towards a reproducible protocol for repetitive and semi-quantitative rat brain imaging with (18) F-FDG: exemplified in a memantine pharmacological challenge. *Neuroimage* **96**, 276-287.
- Denimal, D., Nguyen, A., Pais de Barros, J.-P., Bouillet, B., Petit, J.-M., Vergès, B. and Duveillard, L. (2016). Major changes in the sphingophospholipidome of HDL in non-diabetic patients with metabolic syndrome. *Atherosclerosis* **246**, 106-114.
- Doerrier, C., García, J. A., Volt, H., Díaz-Casado, M. E., Luna-Sánchez, M., Fernández-Gil, B., Escames, G., López, L. C. and Acuña-Castroviejo, D. (2016). Permeabilized myocardial fibers as model to detect mitochondrial dysfunction during sepsis and melatonin effects without disruption of mitochondrial network. *Mitochondrion* **27**, 56-63.
- Eisinger, K., Liebisch, G., Schmitz, G., Aslanidis, C., Krautbauer, S. and Buechler, C. (2014). Lipidomic analysis of serum from high fat diet induced obese mice. *Int. J. Mol. Sci.* **15**, 2991-3002.
- Elezaby, A., Sverdlov, A. L., Tu, V. H., Soni, K., Luptak, I., Qin, F., Liesa, M., Shirinai, O. S., Rimer, J., Schaffer, J. E. et al. (2015). Mitochondrial remodeling

- in mice with cardiomyocyte-specific lipid overload. *J. Mol. Cell. Cardiol.* **79**, 275-283.
- French, S. S., Chester, E. M. and Demas, G. E.** (2016). Timing of maternal immunization affects immunological and behavioral outcomes of adult offspring in siberian hamsters (phodopus sungorus). *J. Exp. Zool A Ecol. Genet. Physiol.* **325**, 377-389.
- Fucho, R., Casals, N., Serra, D. and Herrero, L.** (2017). Ceramides and mitochondrial fatty acid oxidation in obesity. *FASEB J.* **31**, 1263-1272.
- Galadari, S., Rahman, A., Pallichankandy, S., Galadari, A. and Thayyullathil, F.** (2013). Role of ceramide in diabetes mellitus: evidence and mechanisms. *Lipids Health Dis.* **12**, 98.
- Ghosh, S., Sulistyoningrum, D. C., Glier, M. B., Verchere, C. B. and Devlin, A. M.** (2011). Altered glutathione homeostasis in heart augments cardiac lipotoxicity associated with diet-induced obesity in mice. *J. Biol. Chem.* **286**, 42483-42493.
- Guo, C. A. and Guo, S.** (2017). Insulin receptor substrate signaling controls cardiac energy metabolism and heart failure. *J. Endocrinol.* **233**, R131-R143.
- He, J., Li, X., Luo, H., Li, T., Zhao, L., Qi, Q., Liu, Y. and Yu, Z.** (2017). Galectin-3 mediates the pulmonary arterial hypertension-induced right ventricular remodeling through interacting with NADPH oxidase 4. *J. Am. Soc. Hypertens* **11**, 275-289.e2.
- Jia, G., DeMarco, V. G. and Sowers, J. R.** (2016). Insulin resistance and hyperinsulinaemia in diabetic cardiomyopathy. *Nat. Rev. Endocrinol.* **12**, 144-153.
- Kim, D. W., Kim, K. H., Yoo, B. C., Hong, S. H., Lim, Y. C., Shin, Y. K. and Park, J. G.** (2008). Identification of mitochondrial F(1)F(0)-ATP synthase interacting with galectin-3 in colon cancer cells. *Cancer Sci.* **99**, 1884-1891.
- Kroon, T., Baccega, T., Olsén, A., Gabriellsson, J. and Oakes, N. D.** (2017). Nicotinic acid timed to feeding reverses tissue lipid accumulation and improves glucose control in obese Zucker rats[S]. *J. Lipid Res.* **58**, 31-41.
- Li, F., Jiang, C., Larsen, M. C., Bushkofsky, J., Krausz, K. W., Wang, T., Jefcoate, C. R. and Gonzalez, F. J.** (2014). Lipidomics reveals a link between CYP1B1 and SCD1 in promoting obesity. *J. Proteome Res.* **13**, 2679-2687.
- Li, P., Liu, S., Lu, M., Bandyopadhyay, G., Oh, D., Imamura, T., Johnson, A. M., Sears, D., Shen, Z., Cui, B. et al.** (2016). Hematopoietic-derived galectin-3 causes cellular and systemic insulin resistance. *Cell* **167**, 973-984.e12.
- Lim, H.-Y., Wang, W., Wessells, R. J., Ocorr, K. and Bodmer, R.** (2011). Phospholipid homeostasis regulates lipid metabolism and cardiac function through SREBP signaling in *Drosophila*. *Genes Dev.* **25**, 189-200.
- Lucas, E., Vila-Bedmar, R., Arcones, A. C., Cruces-Sande, M., Cachofeiro, V., Mayor, F. Jr. and Murga, C.** (2016). Obesity-induced cardiac lipid accumulation in adult mice is modulated by G protein-coupled receptor kinase 2 levels. *Cardiovasc. Diabetol.* **15**, 155.
- Maftah, A., Petit, J. M., Ratinaud, M.-H. and Julien, R.** (1989). 10-N nonyl-acridine orange: a fluorescent probe which stains mitochondria independently of their energetic state. *Biochem. Biophys. Res. Commun.* **164**, 185-190.
- Marin-Royo, G., Martinez-Martinez, E., Gutierrez, B., Jurado-Lopez, R., Gallardo, I., Montero, O., Bartolome, M. V., Roman, J. A. S., Salaces, M., Nieto, M. L. et al.** (2017). The impact of obesity in the cardiac lipidomic and its consequences in the cardiac damage observed in obese rats. *Clin. Investig. Arterioscler.*
- Martinez-Martinez, E., Jurado-Lopez, R., Valero-Munoz, M., Bartolome, M. V., Ballesteros, S., Luaces, M., Briones, A. M., Lopez-Andres, N., Miana, M. and Cachofeiro, V.** (2014). Leptin induces cardiac fibrosis through galectin-3, mTOR and oxidative stress: potential role in obesity. *J. Hypertens.* **32**, 1104-1114; discussion 1114.
- Martinez-Martinez, E., Calvier, L., Fernández-Celis, A., Rousseau, E., Jurado-López, R., Rossoni, L. V., Jaisser, F., Zannad, F., Rossignol, P., Cachofeiro, V. et al.** (2015a). Galectin-3 blockade inhibits cardiac inflammation and fibrosis in experimental hyperaldosteronism and hypertension. *Hypertension* **66**, 767-775.
- Martinez-Martinez, E., López-Andres, N., Jurado-López, R., Rousseau, E., Bartolomé, M. V., Fernández-Celis, A., Rossignol, P., Islas, F., Antequera, A., Prieto, S. et al.** (2015b). Galectin-3 participates in cardiovascular remodeling associated with obesity. *Hypertension* **66**, 961-969.
- Martinez-Martinez, E., Ibarrola, J., Calvier, L., Fernandez-Celis, A., Leroy, C., Cachofeiro, V., Rossignol, P. and Lopez-Andres, N.** (2016). Galectin-3 blockade reduces renal fibrosis in two normotensive experimental models of renal damage. *PLoS One* **11**, e0166272.
- McMurray, F., Patten, D. A. and Harper, M.-E.** (2016). Reactive oxygen species and oxidative stress in obesity-recent findings and empirical approaches. *Obesity (Silver Spring)* **24**, 2301-2310.
- Menini, S., Iacobini, C., Blasetti Fantauzzi, C., Pesce, C. M. and Pugliese, G.** (2016). Role of galectin-3 in obesity and impaired glucose homeostasis. *Oxid. Med. Cell Longev.* **2016**, 9618092.
- Mercer, J. R., Cheng, K.-K., Figg, N., Gorenne, I., Mahmoudi, M., Griffin, J., Vidal-Puig, A., Logan, A., Murphy, M. P. and Bennett, M.** (2010). DNA damage links mitochondrial dysfunction to atherosclerosis and the metabolic syndrome. *Circ. Res.* **107**, 1021-1031.
- Miller, T. A., LeBrasseur, N. K., Cote, G. M., Trucillo, M. P., Pimentel, D. R., Ido, Y., Ruderman, N. B. and Sawyer, D. B.** (2005). Oleate prevents palmitate-induced cytotoxic stress in cardiac myocytes. *Biochem. Biophys. Res. Commun.* **336**, 309-315.
- Nomura, K., Imai, H., Koumura, T., Kobayashi, T. and Nakagawa, Y.** (2000). Mitochondrial phospholipid hydroperoxide glutathione peroxidase inhibits the release of cytochrome c from mitochondria by suppressing the peroxidation of cardiolipin in hypoglycaemia-induced apoptosis. *Biochem. J.* **351**, 183-193.
- Pang, J., Rhodes, D. H., Pini, M., Akasheh, R. T., Castellanos, K. J., Cabay, R. J., Cooper, D., Perretti, M. and Fantuzzi, G.** (2013). Increased adiposity, dysregulated glucose metabolism and systemic inflammation in Galectin-3 KO mice. *PLoS One* **8**, e57915.
- Paradies, G., Paradies, V., De Benedictis, V., Ruggiero, F. M. and Petrosillo, G.** (2014). Functional role of cardiolipin in mitochondrial bioenergetics. *Biochim. Biophys. Acta* **1837**, 408-417.
- Pejnovic, N. N., Pantic, J. M., Jovanovic, I. P., Radosavljevic, G. D., Milovanovic, M. Z., Nikolic, I. G., Zdravkovic, N. S., Djukic, A. L., Arsenijevic, N. N. and Lukic, M. L.** (2013). Galectin-3 deficiency accelerates high-fat diet-induced obesity and amplifies inflammation in adipose tissue and pancreatic islets. *Diabetes* **62**, 1932-1944.
- Petersen, M. C. and Shulman, G. I.** (2017). Roles of diacylglycerols and ceramides in hepatic insulin resistance. *Trends Pharmacol. Sci.* **38**, 649-665.
- Petit, J.-M., Maftah, A., Ratinaud, M.-H. and Julien, R.** (1992). 10N-nonyl acridine orange interacts with cardiolipin and allows the quantification of this phospholipid in isolated mitochondria. *Eur. J. Biochem.* **209**, 267-273.
- Riehle, C. and Abel, E. D.** (2016). Insulin signaling and heart failure. *Circ. Res.* **118**, 1151-1169.
- Schulze, P. C., Drosatos, K. and Goldberg, I. J.** (2016). Lipid use and misuse by the heart. *Circ. Res.* **118**, 1736-1751.
- Shimabukuro, M., Kozuka, C., Taira, S., Yabiku, K., Dagvasumberel, M., Ishida, M., Matsumoto, S., Yagi, S., Fukuda, D., Yamakawa, K. et al.** (2013). Ectopic fat deposition and global cardiometabolic risk: new paradigm in cardiovascular medicine. *J. Med. Invest.* **60**, 1-14.
- Tondera, D., Grandemange, S., Jourdain, A., Karbowski, M., Mattenberger, Y., Herzig, S., Da Cruz, S., Clerc, P., Raschke, I., Merkwirth, C. et al.** (2009). SLP-2 is required for stress-induced mitochondrial hyperperfusion. *EMBO J.* **28**, 1589-1600.
- Tonks, K. T., Coster, A. C. F., Christopher, M. J., Chaudhuri, R., Xu, A., Gagnon-Bartsch, J., Chisholm, D. J., James, D. E., Meikle, P. J., Greenfield, J. R. et al.** (2016). Skeletal muscle and plasma lipidomic signatures of insulin resistance and overweight/obesity in humans. *Obesity (Silver Spring)* **24**, 908-916.
- Tulipani, S., Palau-Rodriguez, M., Miñarro Alonso, A., Cardona, F., Marco-Ramell, A., Zonja, B., Lopez de Alda, M., Muñoz-Garach, A., Sanchez-Pla, A., Tinahones, F. J. et al.** (2016). Biomarkers of morbid obesity and prediabetes by metabolomic profiling of human discordant phenotypes. *Clin. Chim. Acta* **463**, 53-61.
- Vakifahmetoglu-Norberg, H., Ouchida, A. T. and Norberg, E.** (2017). The role of mitochondria in metabolism and cell death. *Biochem. Biophys. Res. Commun.* **482**, 426-431.
- Wahl, S., Yu, Z., Kleber, M., Singmann, P., Holzapfel, C., He, Y., Mittelstrass, K., Polonikov, A., Prehn, C., Römisch-Margl, W. et al.** (2012). Childhood obesity is associated with changes in the serum metabolite profile. *Obes. Facts* **5**, 660-670.
- Wang, X., West, J. A., Murray, A. J. and Griffin, J. L.** (2015). Comprehensive metabolic profiling of age-related mitochondrial dysfunction in the high-fat-fed ob/ob mouse heart. *J. Proteome Res.* **14**, 2849-2862.
- Yazici, D. and Sezer, H.** (2017). Insulin resistance, obesity and lipotoxicity. *Adv. Exp. Med. Biol.* **960**, 277-304.

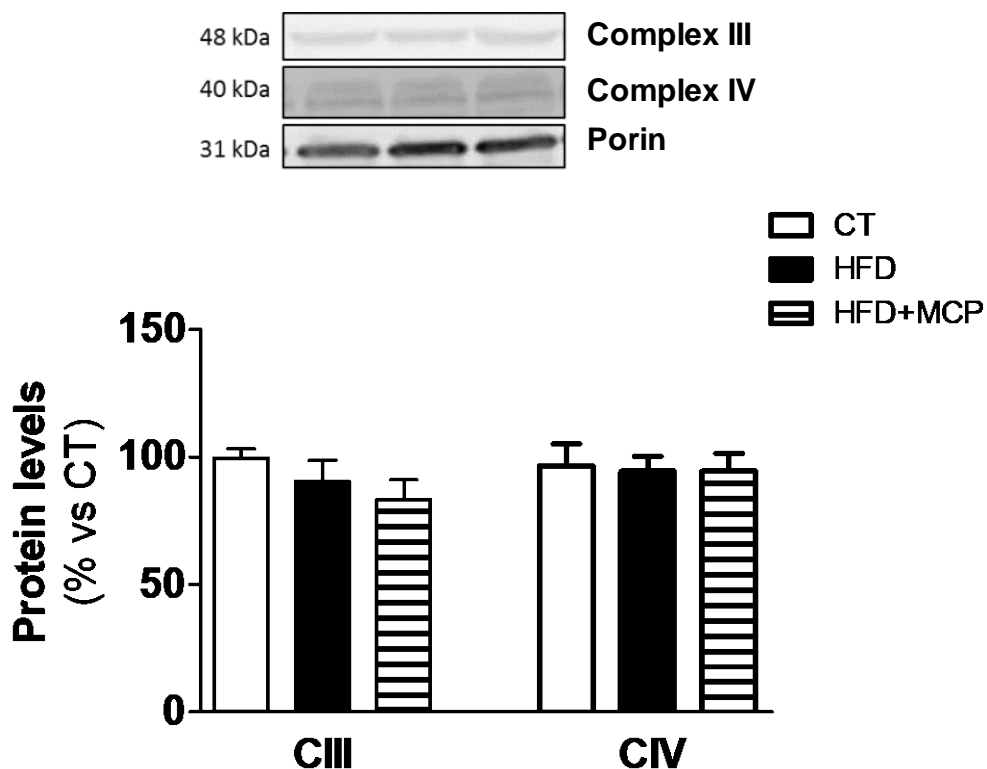


Figure S1. Impact of Gal-3inhibition on protein in heart from control and obese rats. Heart from rats fed a standard diet (CT) or a high fat diet (HFD) treated with vehicle or with the inhibitor of Gal-3 activity (Modified citrus pectin; MCP; 100 mg/Kg/day) were analyzed. Protein expression of subunits 2 and 1 from, respectively, mitochondrial complexes III and IV are presented. Bar graphs represent the mean \pm SEM of 6-8 animals normalized to porin.

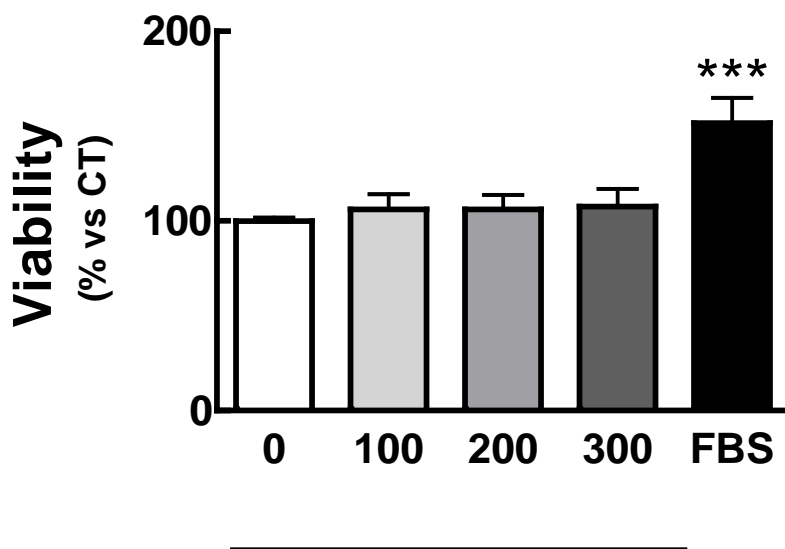


Figure S2. Effects of palmitic acid on the viability in H9c2 cells. Cardiac myoblasts were stimulated with palmitic acid (100-300 $\mu\text{mol/L}$) or 20 % of fetal bovine serum (FBS) for 24 hours. Viability was determined by an MTT assay. Data are expressed as percent of unstimulated cells. Values are mean \pm SEM of three assays. *** p <0.001 vs. vehicle treated cells.

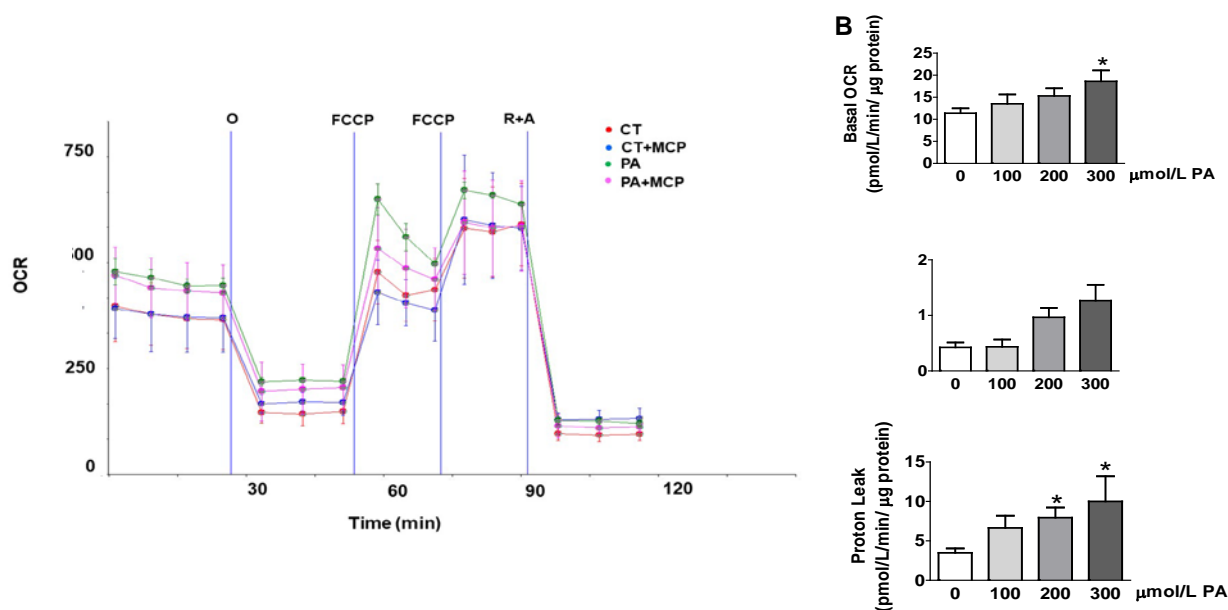


Figure S3. Effects of palmitic acid on mitochondrial function and glycolysis in H9c2 cells. (A) Representative mitochondrial respiratory profile from a XF Mitochondrial Stress Test. Oxygen consumption rate (OCR) was measured under basal conditions followed by the sequential addition (vertical lines) of oligomycin (O; 1 $\mu\text{mol/L}$); FCCP carbonyl cyanide p-(trifluoromethoxy) phenylhydrazone (0.6 $\mu\text{mol/L}$), FCCP (0.4 $\mu\text{mol/L}$); R+A, 1 μM rotenone plus 1 $\mu\text{mol/L}$ antimycin A as indicated. H9c2 myoblasts were treated for 24 hours with palmitic acid (PA; 200 $\mu\text{mol/L}$) in the presence of absence inhibitor of Gal-3 activity (Modified citrus pectin; MCP; 0.01%). Each data point represents an OCR measurement as mean \pm SEM ($n = 5$). (B) Basal respiration expressed as oxygen consumption rate (OCR), (C) Basal glycolysis expressed as extracellular acidification rate (ECAR), (D) proton leak respiration expressed as OCR in cardiac myoblasts treated for 24 hours with palmitic acid (PA; 100-300 $\mu\text{mol/L}$). Bar graphs represent the mean \pm SEM of 4 assays. * $p < 0.05$ vehicle treated cells (CT).

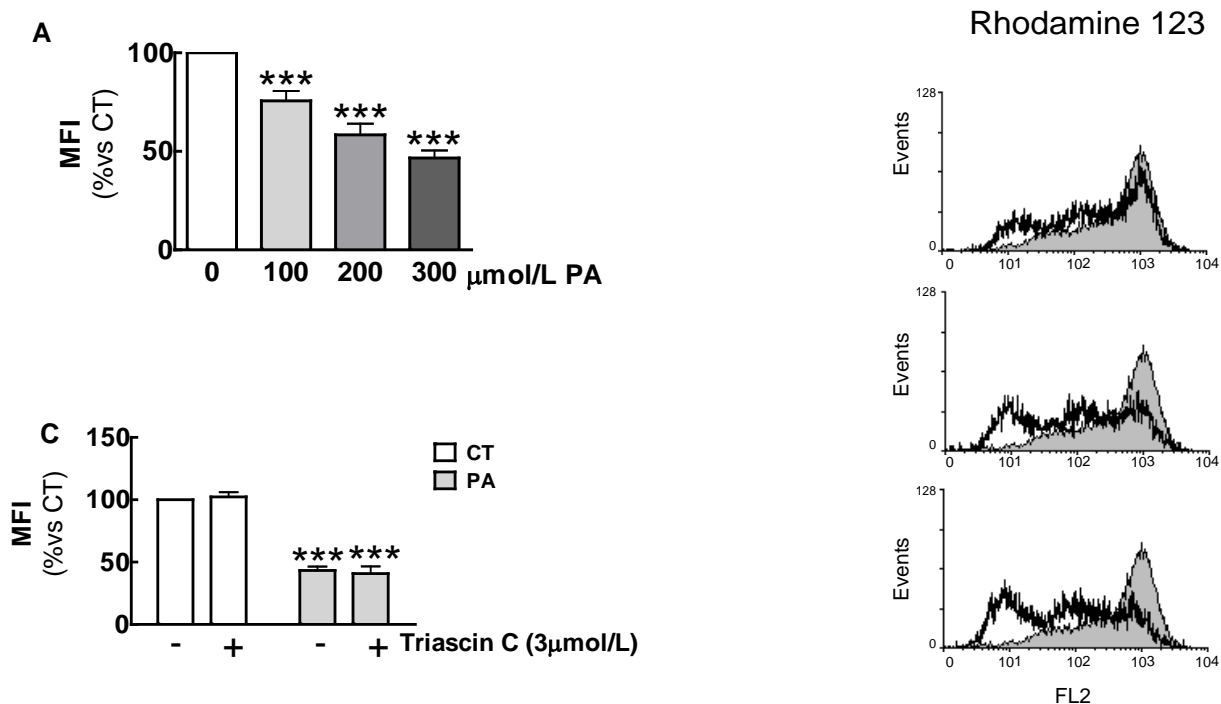


Figure S4. Effects of palmitic acid on mitochondrial membrane potential in H9c2 cells.

(A) Quantification of flow cytometry analysis of mitochondrial membrane potential in cardiac myoblasts stained with Rhodamine 123 treated for 24 hours with palmitic acid (PA; 100-300 μmol/L) and expressed as mean fluorescence intensity (MFI), **(B)** Representative histogram, untreated cells (solid curves) were compared with stimulated cells (open curves), **(C)** Flow cytometry analysis of mitochondrial membrane potential in cardiac myoblasts stained with Rhodamine 123 treated for 24 hours with palmitic acid (200 μmol/L) in the presence of absence of the inhibitor of long fatty acyl CoA synthetase, Triascin C (3 μmol/L) and expressed a MFI. Bar graphs represent the mean ± SEM of 3 assays. ***p<0.001 vehicle treated cell.

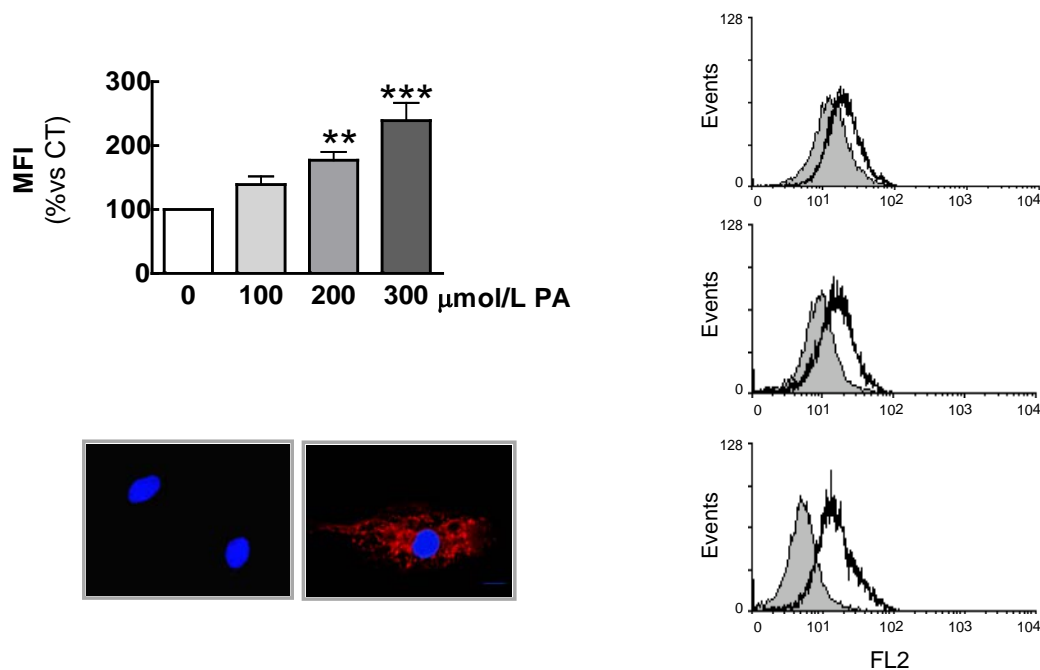


Figure S5. Effects of palmitic acid on ROS production in H9c2 cells. (A) Quantification of flow cytometry analysis of mitochondrial superoxide anions in cardiac myoblasts labeled with MitoSox and treated for 24 hours with palmitic acid (PA; 100-300 μmol/L) and expressed as mean fluorescence intensity (MFI), (B) Representative histogram, untreated cells (solid curves) were compared with stimulated cells (open curves), (C) Representative microphotographs showing H9c2 cells labeled with MitoSox. Nuclei of cells were co-stained with DAPI. Bar graphs represent the mean \pm SEM of 3 assays. ** $p < 0.01$; *** $p < 0.001$ vehicle treated cell.

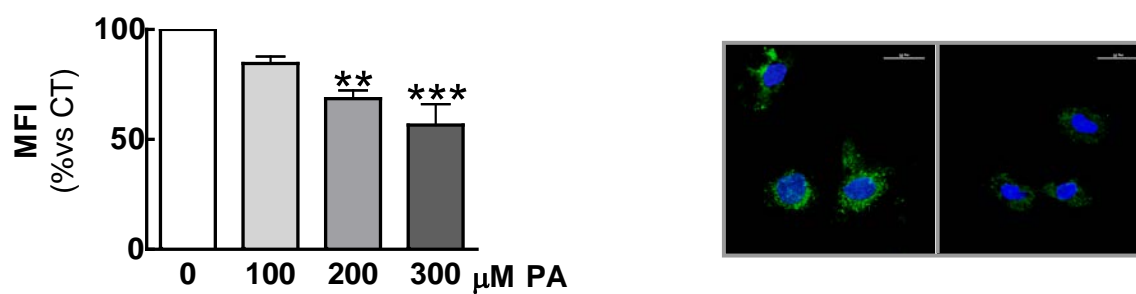


Figure S6. Effects of palmitic acid on cardiolipin oxidation in H9c2 cells. (A) Quantification of flow cytometry analysis of cardiolipin oxidation levels in cardiac myoblasts stained with 10-Nony acridine orange treated for 24 hours with palmitic acid (PA;100-300 μmol/L) and expressed as mean fluorescence intensity (MFI). **(B)** Representative microphotographs showing H9c2 cells labeled with 10-Nony acridine orange. Nuclei of cells were co-stained with DAPI. Representative microphotographies. Bar graphs represent the mean \pm SEM of 3 assays. ** $p < 0.01$; *** $p < 0.001$ vehicle treated cell.

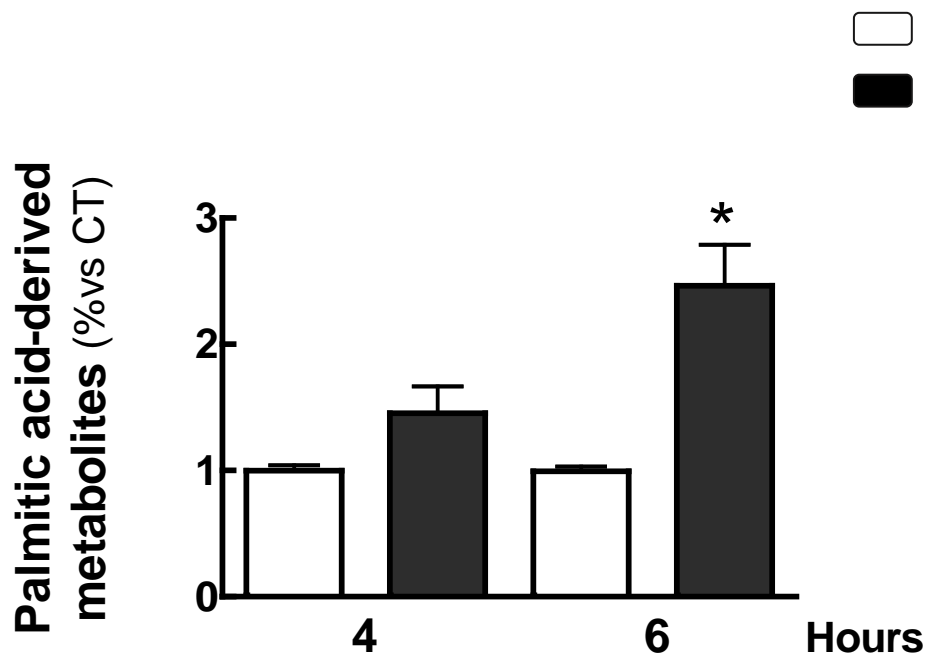


Figure S7. Effects of palmitic acid on β -oxidation in H9c2 cells. Quantification of on β -oxidation in cardiac myoblasts treated for 4 or 6 hours with palmitic acid (PA; 200 μ mol/L) and expressed as palmitic acid hydrosoluble derived metabolites. Bar graphs represent the mean \pm SEM of 3 assays. * $p < 0.05$ vehicle treated cell.



Hypertension

Manuscript Submission and Peer Review System

Disclaimer: The manuscript and its contents are confidential, intended for journal review purposes only, and not to be further disclosed.

URL: <http://hype-submit.aha-journals.org>

Title: **THE IMPACT OF CARDIAC LIPOTOXICITY ON CARDIAC FUNCTION AND MIRNAS SIGNATURE IN OBESE AND NON-OBESE RATS WITH MYOCARDIAL INFARCTION**

Manuscript number: HYPE201811779

Author(s): Victoria Cachofeiro, Universidad Complutense

Gema Marín-Royo, Universidad Complutense

Adriana Ortega-Hernandez, Laboratorio en Biología Vasculard, Hospital Clínicod San Carlos-IdISSC, Madrid, Spain.

Ernesto Martinez-Martinez, Departamento de Fisiología, Facultad de Medicina, Universidad Complutense de Madrid and Instituto de Investigación Sanitaria Gregorio Marañón (IiSGM), Madrid, Spain

Raquel Jurado-López, Universidad Complutense

Novelty and significance

What Is New?

- Cardiac lipotoxicity is a feature observed not only in the context of obesity but also is associated with MI although cardiac lipid profile is different in non-obese and obese rats with MI.
- Triglycerides levels are independently associated with fibrosis supporting the relevance of cardiac lipotoxicity on the functional consequences of MI.
- Myocardial infarction is associated with a specific miRNA signature which was further modified by the presence of obesity.
- miRNAs circulating levels were associated with different lipid species.

What Is Relevant?

- This study provides a new view of the complexity of the changes that occur in response to MI which include cardiac lipotoxicity. Lipid accumulation could affect heart function by modulating miRNAs.

Summary

This study demonstrates that the MI is associated with an excessive accumulation of lipids in the heart of non-obese and obese rats at mitochondrial level. This was accompanied by a specific miRNA signature which was further modified by the presence of obesity and it was associated with different lipid species. Therefore, it helps to understand the complexity of the mechanisms involved in response to MI in which cardiac lipotoxicity could play a role in its functional consequences.

Mineralocorticoid receptor and leptin: a dangerous liaison in the obese heart

Gema Marin-Royo¹, María Luaces², Victoria Cachofeiro¹, Ernesto Martínez-Martínez¹

¹ *Departamento de Fisiología, Facultad de Medicina, Universidad Complutense de Madrid and Instituto de Investigación Sanitaria Gregorio Marañón (IiSGM), Madrid, Spain.* ² *Servicio de Cardiología, Instituto Cardiovascular, Hospital Clínico San Carlos, Madrid, Spain.*

Abstract

Obesity is characterized by a low grade inflammatory state, as well as a prooxidant environment which can trigger an excessive extracellular cellular matrix accumulation, and which in turn promotes an aberrant remodelling with functional alterations. These modifications contribute to the diastolic dysfunction observed in obese patients. Multiple factors have been proposed as being responsible for cardiac damage in the context of obesity, including aldosterone/mineralocorticoid receptor and leptin. Aldosterone exerts proinflammatory, prooxidant and profibrotic actions, which can play a key role in the development of cardiac damage associated with different pathologies, through binding of mineralocorticoid receptor (MR). Moreover, its pharmacological blockade has demonstrated to improve these situations. Different studies have demonstrated that aldosterone is inappropriately elevated in obesity and MR antagonism improves left ventricle function and reduces circulating procollagen levels in patients with obesity without other comorbidities. Leptin is locally produced in the heart in both the epicardial fat and in the myocardium and its production is up-regulated in obesity. This adipokine is a proinflammatory, prooxidant and profibrotic factor that can participate in the cardiac damage associated with obesity. Interactions among leptin and aldosterone have previously been reported in different scenarios and at different levels, supporting a link between leptin and MR and which could result in the potentiation of the cardiac damage associated with obesity. Therefore, the aim of this review is to discuss whether MR activation can mediate the deleterious effects of leptin in the heart in the context of obesity, as well as the potential mechanisms involved in this process.

85. Hall, J.E., J.M. do Carmo, A.A. da Silva, Z. Wang & M.E. Hall (2015) Obesity-induced hypertension: interaction of neurohumoral and renal mechanisms. *Circ Res* 116(6): 991-1006.
86. Hall, J.E., D.A. Hildebrandt & J. Kuo (2001) Obesity hypertension: role of leptin and sympathetic nervous system. *Am J Hypertens* 14(6 Pt 2): 103S-115S.
87. Huby, A.C., et al. (2015) Adipocyte-Derived Hormone Leptin Is a Direct Regulator of Aldosterone Secretion, Which Promotes Endothelial Dysfunction and Cardiac Fibrosis. *Circulation* 132(22): 2134-2145.
88. Xue, B., et al. (2016) Leptin Mediates High-Fat Diet Sensitization of Angiotensin II-Elicited Hypertension by Upregulating the Brain Renin-Angiotensin System and Inflammation. *Hypertension* 67(5): 970-976.
89. Natarajan, R., S. Ploszaj, R. Horton & J. Nadler (1989) Tumor necrosis factor and interleukin-1 are potent inhibitors of angiotensin-II-induced aldosterone synthesis. *Endocrinology* 125(6): 3084-3089.
90. Belin de Chantemele, E.J., J.D. Mintz, W.E. Rainey & D.W. Stepp (2011) Impact of leptin-mediated sympatho-activation on cardiovascular function in obese mice. *Hypertension* 58(2): 271-279.
91. Huby, A.C., L. Otvos, Jr. & E.J. Belin de Chantemele (2016) Leptin Induces Hypertension and Endothelial Dysfunction via Aldosterone-Dependent Mechanisms in Obese Female Mice. *Hypertension* 67(5): 1020-1028.
92. Hofmann, A., et al. (2017) Elevated Steroid Hormone Production in the db/db Mouse Model of Obesity and Type 2 Diabetes. *Horm Metab Res* 49(1): 43-49.

